SEBASTIAN MARTIN KRAFT

MULTI-DIMENSIONAL DYNAMICS OF AN ELASMOBRANCH ASSEMBLAGE IN A MARINE PARK

2024

SEBASTIAN MARTIN KRAFT

MULTI-DIMENSIONAL DYNAMICS OF AN ELASMOBRANCH ASSEMBLAGE IN A MARINE PARK

Doutoramento em Ciências do Mar, da Terra e do Ambiente,

Ramo Ciências do Mar

Trabalho efetuado sob a orientação de:

Dr. David Maria Aguiar Abecasis

Prof. Dr. Johann Mourier

2024

Multi-dimensional dynamics of an elasmobranch assemblage in a marine park

Declaration of authorship of the work

I declare to be the author of this work, which is original and unpublished. Authors and works consulted are duly cited in the text and appear in the list of references included.

Declaração de autoria do trabalho

Declaro ser a autora deste trabalho, que e original e inédito. Autores e trabalhos consultados estão devidamente citados no texto e constam da listagem de referências incluída.

Sebastian Martin Kraft

Support

This study received support from the “la Caixa” Foundation (ID 100010434), grant number LCF/BQ/DI20/11780001. This study also received funding from the INFORBIOMARES project (POSEUR-03-2215-FC-000047), and from the Fundação para a Ciência e a Tecnologia (FCT) projects UIDB/04326/2020, UIDP/04326/2020 and LA/P/0101/2020. Dr. David Abecasis also acknowledges FCT support through the transitional norm DL57/2016/CP1361/CT0036.

Acknowledgements

Getting to where I am today is a dream long in the making, and in this process, I have been accompanied by many people I hold dear. They also helped me see through moving across the ocean to a new life, a pandemic, and a PhD. It would not have been the same without all of these people, and there is a bit of all of them in this work.

To begin, I want to thank my supervisor Dr. David Abecasis and co-supervisor Dr. Johann Mourier, for their support, patience, and guidance throughout the development of this project. Dr. David Abecasis and Dr. Alex Winkler also helped me greatly during my integration into CCMAR and the country. These amazing people taught me a lot, and working with them has been a privilege.

I want to thank my loved family, who have nurtured this side of me since I first showed interest in the ocean. They went to the extreme of finishing my application to the PhD while I was uncommunicated in the Antarctic Peninsula for three weeks just to make sure everything was correctly submitted. Even though they are far away, they have always made sure I feel their care and affection.

I also would not be where I am without the dear friends life has thrown at me. Leaving my family and friends behind was a very hard thing to do, but this also made me realize that the world is full of friends yet to be met. I had the fortune of not having my bonds affected by distance, and of building wonderful new relationships here. Thank you all for the laughs, support, and shared time.

Finally, I want to thank people that, although some I did not meet, helped in several ways during this project. I want to thank Juliano Macedo for the operation of his vessel and trammel nets during some of our sampling trips; Joffrey Baeyaert for tagging, deploying, and maintaining receivers; my lab mates Dr. Alex Winkler and Lucas Martínez-Ramírez for their help in servicing receivers, fishing and tagging; C. Robert Priester and the “Flipper Divers” dive center for servicing receivers; and my lab mate Miguel Gandra for helping me when data analysis became too *aRduous* of a task.

Thank you.

Gracias.

Obrigado.

Danke.

Abstract

Elasmobranchs are marine predators with important ecological and economical roles throughout the world. Many of these species are also vulnerable to anthropogenic impacts, particularly to overfishing. Elasmobranchs are mostly captured as bycatch of other more profitable fisheries and have been historically undermanaged. Presently, overfishing threatens a large proportion of these species with extinction. Marine protected areas (MPAs) are a common management strategy used to protect species and habitats by controlling or prohibiting anthropogenic activities within a delimited area. A critical aspect for their success is the use of reliable information on the movement ecology of species. Nevertheless, elasmobranchs are rarely included in MPA planification as frequently no information on their spatial ecology is available. A common method of collecting this information is passive acoustic telemetry, which allows the long-term tracking of multiple individuals. In this study, a literature review on common methods to analyse acoustic telemetry data was done to guide research efforts. Then, the movement patterns of *Dasyatis pastinaca*, *Rostroraja alba* and *Raja clavata* were studied in the Luiz Saldanha Marine Park by assessing residency, area use, activity, and depth, and evaluating the contribution of spatial data to the conservation of elasmobranchs. Diverse movement patterns were observed, some species-specific, like seasonal residency, and others common to the three species, like diel changes in activity. Finally, fine scale associations and aggregations of *D. pastinaca* were explored using social network analysis, relating this to the conservation of the species. Although *D. pastinaca* likely receives the overall lowest amount of protection, demographic differences in *Rostroraja alba* and *Raja clavata* suggest protection may be unevenly distributed among conspecifics of these species, favouring immature and male individuals, respectively. These results represent important contributions to the understanding of these species' spatial ecology and to the management of elasmobranchs of coastal areas.

Keywords: Area-based conservation, batoids, management, marine protected area, passive acoustic telemetry, spatial ecology.

Resumo

Os elasmobrânquios são um grupo de predadores marinhos distribuídos por todos os oceanos do mundo, onde desempenham importantes funções ecológicas e económicas. A maioria destas espécies também caracteriza-se por ter estratégias de história de vida k, exibindo longos períodos de vida, maturação sexual tardia e investindo muita energia na produção de poucos descendentes. Os elasmobrânquios são principalmente capturados como capturas acessórias nas pescarias de outros peixes ósseos de maior valor económico e, devido ao seu valor inferior em relação a estes últimos, historicamente não têm sido geridos de forma adequada. São mantidos a bordo principalmente pela sua carne e barbatanas, sendo consumidos localmente ou comercializados. Em consequência do aumento da atividade de pesca a nível mundial, a sobrepesca deixou uma grande parte dos elasmobrânquios ameaçados de extinção.

Como resposta a estes efeitos negativos, as áreas marinhas protegidas (AMP) constituem uma estratégia de gestão espacial comummente utilizada para proteger as espécies e os habitats, através do controlo ou da proibição de atividades antropogénicas numa área delimitada. Dado o estatuto explicitamente espacial das AMP, para o seu sucesso é fundamental possuir informação fiável sobre os movimentos das espécies a proteger. No entanto, os elasmobrânquios raramente são incluídos no planeamento das AMP e, quando o são, a informação sobre a sua ecologia espacial frequentemente não está disponível.

Um método comum para a recolha desta informação é a telemetria acústica passiva. Este método baseia-se na implantação de transmissores acústicos em indivíduos da(s) espécie(s) em estudo, libertando-os em seguida e monitorizando os seus movimentos através de recetores acústicos distribuídos pela área de estudo. Esta técnica permite o seguimento de vários indivíduos e a obtenção de grandes quantidades de dados.

Em Portugal, a pesca de elasmobrânquios é uma atividade muito comum, o que coloca o país entre os com maiores descargas da Europa. À semelhança da situação mundial, em consequência da falta de regulamentação das pescarias que os capturam e da sobre-exploração, os desembarques de elasmobrânquios em Portugal diminuíram para metade nas últimas décadas. Este facto levou ao estabelecimento de vários regulamentos e ações que procuram contrariar esta consequência, incluindo a implementação de AMPs.

Esta tese centrou-se na utilização da telemetria acústica para o estudo da ecologia espacial de elasmobrânquios e na utilização de esta informação para melhorar a gestão da

sua proteção no contexto das AMP. Como primeiro passo, foi desenvolvida uma revisão dos principais métodos existentes para a análise desse tipo de dados, com foco na residência e no uso do espaço e as vantagens, desvantagens e características gerais de cada método. Este trabalho bibliográfico foi transformado num guia e publicado para ajudar os investigadores que procuram realizar estudos como o deste projeto e precisam de encontrar métodos que se adaptem aos seus dados, desenho e questões de estudo.

De seguida, foram estudados os padrões de movimento de três espécies de raias no Parque Marinho Luiz Saldanha (PMLS), um AMPs costeira na península de Setúbal e uma das AMPs mais importantes de Portugal. A *Dasyatis pastinaca*, uma espécie vivípara da família Dasyatidae, e duas espécies da família Rajidae: *Rostroraja alba*, uma raia de grande tamanho e Criticamente Ameaçada, e *Raja clavata*, um dos elasmobrânquios mais importantes comercialmente em Portugal e no mundo. Com estes dados também foi avaliada a contribuição desta área protegida para a conservação destas espécies. Através da avaliação da sua residência, áreas utilizadas, atividade e uso de profundidade, foram observados vários padrões de movimento. Alguns destes foram específicos de cada espécie, como o padrão de movimento sazonal entre o PMLS e o estuário de Sado de *D. pastinaca*, e outros comuns a todas, como o incremento de atividade durante o crepúsculo e a noite em comparação com o dia.

De entre as três espécies, a *D. pastinaca* apresentou a menor residência média, devido à sua marcada presença sazonal. Esta espécie permaneceu no PMLS durante os meses mais frios e migrou para o estuário do Sado durante a primavera e o verão, provavelmente para se reproduzir e dar à luz. Adicionalmente, os indivíduos de *D. pastinaca* que foram detetados no PMLS antes e depois da migração mostraram utilizar áreas semelhantes e associações entre indivíduos durante ambos os períodos, indicando um nível de reutilização do espaço. A deteção de associações preferenciais entre indivíduos indica que este padrão parece ser pelo menos parcialmente mediado por fatores sociais.

Por outro lado, a *Rostroraja alba* e a *Raja clavata* apresentaram índices de residência mais elevados e estáveis ao longo de todo o ano. No entanto, a área onde se localiza o PMLS parece ser dominada por indivíduos imaturos de *Rostroraja alba* e por machos de *Raja clavata*, o que pode indicar diferenças demográficas na proteção dessas espécies. Os resultados relativos a *Rostroraja alba* sugerem que esta área pode ser uma zona de maternidade para os juvenis da espécie, que são áreas de grande importância para a proteção de espécies. As três espécies apresentaram um padrão diário semelhante com

um aumento da atividade à noite e ao crepúsculo em comparação com o dia e, em geral, também se verificou um aumento da área de utilização e uma menor profundidade média em comparação com o dia. Estes padrões podem indicar um maior risco de captura durante a noite e o crepúsculo, uma vez que uma maior mobilidade aumenta a probabilidade de encontrar artes de pesca passivas, como redes de tresmalhe e palangres, tipicamente utilizadas pelos pescadores da zona.

Por fim, os resultados obtidos nesta tese são importantes para serem considerados no plano de gestão do PMLS, pois revelaram diferenças importantes na ecologia espacial de cada espécie, que se podem traduzir em diferenças específicas de proteção. Os resultados também são uma importante fonte de comparação para outras AMP costeiras semelhantes. Contribuições importantes foram feitas para o estudo da ecologia espacial de estas espécies. No caso de *D. pastinaca*, este é o primeiro estudo sobre a sua ecologia espacial com recurso a telemetria acústica, e no caso da *Rostroraja alba*, apenas havia dados preliminares para alguns indivíduos e necessita urgentemente de dados precisos sobre os seus movimentos para melhorar o seu estado de conservação. Finalmente, o trabalho contribuiu para resultados preliminares existentes sobre *Raja clavata*, melhorando a compreensão dos movimentos desta espécie a nível local, o que é importante para a gestão da pesca da sua população local e do sul da Europa.

Palavras-chave: Área marinha protegida, conservação, elasmobrânquios, gestão, ecologia espacial, telemetria acústica passiva

Table of contents

Index of Figures

Chapter 1

Chapter 2

Chapter 5

Chapter 6

Index of Tables

Chapter 2

Chapter 3

Chapter 4

Chapter 5

Chapter 6

List of abbreviations

3D-KUD	Three-dimensional Kernel Utilisation Distribution
AIC	Akaike Information Criterion
AKDE	Autocorrelated kernel density estimator
$AKDE_C$	Area-corrected autocorrelated kernel density estimator
a-LoCoH	Adaptive Local Convex Hull
ANOVA	Analysis of variance
ATT	Animal Tracking Toolbox
BA	Buffer area
BBMM	Brownian Bridge Movement Model
BRB	Biased random bridge kernel method
B-SSM	Bayesian state-space model
CDMA	Code Division Multiple Access
CHP	Characteristic hull polygons
COA	Centre of activity
CRAN	Comprehensive R Archive Network
CTR	Continuous time residence
CV	Coefficient of Variation
dBBMM	Dynamic Brownian Bridge Movement Model
DOP	Dilution of precision
doy	day of the year
DST	Data storage tag
DW	Disc width
edf	Estimated degrees of freedom
EU	European Union
F	Female
FAO	Food and Agriculture Organization
FPA	Fully protected area
GAMM	General Additive Mixed Model
GIS	Geographic Information System
GLMM	General Linear Mixed-Effects Model
HDOP	Horizontal dilution of precision
HPE	Horizontal Position Error
HR-VPS	High Residence Vemco Positioning System
ICNF	Institute for Nature Conservation and Forests
ID	Identification
IID	Independent and identically distributed
IOR	Index of reuse
I_R	Residency index
IUCN	International Union for Conservation of Nature
I_{WR}	Weighted residency index
kHz	kilohertz
k-LoCoH	k-nearest neighbour Local Convex Hull

km2	Square kilometres
k-NNCH	k-nearest neighbour convex hull
KUD	Kernel Utilisation Distribution
LoCoH	Local Convex Hull
LSMP	Luiz Saldanha Marine Park
m	Meter
M	Male
MBP	Maximum Blanking Period
MCP	Minimum Convex Polygon
min	Minutes
MKDE	Movement-based kernel density estimation
MPA	Marine Protected Area
MSHC	Minimum spurious hole covering
n	number
NA	Network analysis
OU	Ornstein-Uhlenbeck process
OUF	Ornstein-Uhlenbeck Foraging process
OU-SSM	Ornstein–Uhlenbeck state-space model
PBSN	Proximity-based social network
PDF	Probability density function
PPA	Partially protected area
PSAT	Pop-up satellite tag
RI	Reliability index
r-LoCoH	Fixed radius Local Convex Hull
RM-ANOVA	Repeated measures ANOVA
s	Seconds
SE	Standard error
SRI	Simple Ratio Index
SSM	State-space model
SST	Sea surface temperature
TAC	Total Allowable Catch
TDOA	Time difference-of-arrival
TGDE	Time-geographic density estimation
TL	Total length
T-LoCoH	Time Local Convex Hull
TOA	Time of arrival
TSD	Time-scaled distance
UD	Utilisation Distribution
VPS	Vemco Positioning System
VUE	Vemco User Environment
wAKDEC	Optimally weighted, area-corrected autocorrelated kernel density estimator
YAPS	Yet Another Positioning Solver

List of acronyms

a	Defined maximum cumulative distance	r	Radius
C	Coordinate	s	Dimensionless scaling parameter
%	Percentage	T_{max}	Upper recording time limit
cm	Centimetres	v_{max}	Theoretical maximum velocity
$\bar{C}_{\Delta t}$	Coordinate average weighted over time difference	w	Sliding window
D_d	Days detected	X_i	X coordinate
D_H	Habitat-specific diffusion coefficients	$\bar{X}_{\Delta t}$	X coordinate weighted over time difference
D_i	Detection interval	$\bar{X}_{\Delta t}$	X coordinate weighted over time difference
D_t	Total days detected	y_A	Number of detections of individual A
h	Smoothing factor or bandwidth	y_{A+B}	Number of detections of individuals A and B at different receivers
h_{max}	Highest smoothing factor value	y_B	Number of detections of individual B
h_{min}	Lowest smoothing factor value	Y_i	Y coordinate
k	k number of nearest neighbours	$\bar{Y}_{\Delta t}$	Y coordinate weighted over time difference
m	margin size	Δt	Time difference
n°	Number	σ^2_m	Brownian motion variance parameter

Chapter 1

General Introduction

Luiz Saldanha Marine Park

1.1 General Introduction

1.1.1 Elasmobranchs

Elasmobranchs (sharks, rays and skates) are a subclass of cartilaginous fishes currently composed of over 1130 species (Weigmann, 2017, 2016). Their long evolutionary history places them as the most distinct group among all major jawed vertebrates, with each species accumulating an average of 26 million years of unique evolutionary history (Stein et al., 2018). Elasmobranchs have adapted to diverse ecological niches in virtually all aquatic ecosystems, from tropical waters in low latitudes (White and Sommerville, 2010), to the Arctic and Antarctic (Ebert and Winton, 2010) and even freshwater systems (Ebert et al., 2013; Rosa et al., 2010), spanning from shallow coastal areas to open ocean (Stevens, 2010; White and Sommerville, 2010) and depths below 1000 meters (Kyne and Simpfendorfer, 2010).

Elasmobranchs commonly have some of the slowest-paced life histories among vertebrates. Although there are exceptions, they are generally considered as long-lived species of slow growth, late maturity and high energetic investment in developing few offspring (Ebert et al., 2008; Frisk et al., 2001). An extreme example of their longevity is the Greenland shark (*Somniosus microcephalus*), with an estimated lifespan of at least 272 years and age of maturity of 156 years based on radiocarbon dating of eye lens nuclei (Nielsen et al., 2016). Similarly, gestation periods can last from around two months to over three years as in *Chlamydoselachus anguineus* (Tanaka et al., 1990), while many are close to or over a year in duration (Tokunaga et al., 2022).

1.1.2 Roles of elasmobranchs

Throughout their evolution, elasmobranchs became one of the dominant groups of marine predators, playing an important role in the top-down control of animal populations (Dedman et al., 2024). Species in this group usually have a medium to high trophic level (Navia et al., 2017), with some that even feed on other elasmobranchs (Flowers et al., 2019; Strong et al., 1990). In addition to direct predation, elasmobranchs also exert indirect effects through their presence, like anti-predator responses. This non-lethal effect is largely understudied, but thought to be at least as important as direct predation (Creel and Christianson, 2008). For example, green sea turtles (*Chelonia mydas)* and dugongs (*Dugong dugon*) can alter their feeding behaviour in the presence of tiger sharks (*Galeocerdo cuvier*) (Heithaus et al., 2007; Wirsing et al., 2007).

Elasmobranchs also represent an essential source of income and nourishment for many people, supporting the livelihoods of numerous coastal settlements worldwide (Jaiteh et al., 2017). These species are traded mostly for their meat and fins, which are consumed or commercialized (Jaiteh et al., 2017), and to a lesser degree used to obtain a variety of products from their cartilage, skin, liver and teeth (Jaiteh et al., 2017; Vannuccini, 1999). Although targeted elasmobranch fisheries exist in some parts of the world, most of catches derive from bycatch in other more profitable fisheries. For example, several oceanic species of sharks are captured in longline fisheries targeting tuna and swordfish, while many shark and ray species are captured by coastal and deep-sea trawling operations (Oliver et al., 2015).

1.1.3 Overfishing and population declines

As a response to the worldwide increasing demand of food and growing economic interests in fishing, fishing activity underwent a steep rise, going from total catches of around 20 million tons in the early 1950s to 91 million tons during 2022 (FAO, 2024). This brought many negative consequences, such as the collapse of various fisheries (e.g. Dickey-Collas et al., 2010; Hutchings and Myers, 1994), marked declines in biomass of numerous species (Christensen et al., 2003), and local extinctions and shifts in community structure (McCain et al., 2016).

Elasmobranchs currently face the effects of anthropogenic stressors such as pollution, loss and degradation of habitats, climate change, and especially overfishing (Dulvy et al., 2014; Stevens et al., 2000). According to recent assessments, overfishing is the main threat to elasmobranch species (Dulvy et al., 2021). Moreover, the damage to their populations may be underestimated because elasmobranch bycatch has historically been highly underreported (Bonfil, 1994). For example, species catch records are often aggregated (Dent and Clarke, 2015) and several elasmobranchs, most notably skates in the Rajidae family, have been managed as mixed-species stocks (Agnew et al., 2000; Curtis and Sosebee, 2015; Dulvy et al., 2000; Hogan et al., 2013). In some regions like the North Sea, catch limits have been set for several stocks and species of skates, which have been exceeded to double the recommended limit (Batsleer et al., 2024). These practices mask population declines of some species even if the aggregated landing data suggests stability in catches (Dulvy et al., 2000). In turn, all these factors hinder the

species-specific management of elasmobranchs and perpetuate unsustainable fishing practices (Hogan et al., 2013).

As a consequence of sustained high fishing pressure and lack of regulations, global landings of elasmobranchs have greatly declined in recent decades (Davidson et al., 2016; Dent and Clarke, 2015; Worm et al., 2013). Some areas have undergone changes in species composition (Agnew et al., 2000; Dulvy et al., 2000), while sharp population declines or even local extinctions have also been recorded (Casey and Myers, 1998; Dulvy et al., 2000). Examples of some of the most extreme consequences are the disappearance of *Dipturus batis* from the Irish Sea, believed to be the first documentation of a fish being brought to near extinction by commercial fishing (Brander, 1981), and even the possible extinction of *Carcharhinus obsolerus*, a species described from individuals in a museum collection (White et al., 2019).

1.1.4 Conservation and management: importance of movement studies

Several management strategies have been employed to tackle the consequences of overfishing and other anthropogenic stressors. These include direct changes to the fishing activity in the form of species and gear restrictions, catch quotas, size limits, and temporal bans. Other common actions are spatial bans, among which a frequently implemented method is the establishment of marine protected areas (MPAs), defined as "clearly defined geographical space, recognized, dedicated and managed, through legal or other effective means, to achieve the long-term conservation of nature with associated ecosystem services and cultural values" (Dudley, 2008). This way, MPAs provide spatial refuge to marine life and habitats within a delimited area by excluding or managing fishing and other human activities (Bohnsack, 1998). The reported benefits of this method are several, such as improvements in areas like fisheries, human well-being, economics, development of scientific knowledge, and conservation and management (Ban et al., 2019; Lester et al., 2009). In turn, because of their multidimensional influence, designing and managing MPAs is a complex process that integrates many areas and connects social, economic and scientific aspects (Grorud-Colvert et al., 2021; Ruiz-Frau et al., 2015). Therefore, the success of an MPA also depends on the accomplishment of the goals set for each of these parts (Simpfendorfer et al., 2011). Among the biological and fisheries-related benefits are increases in fish abundance, biodiversity, biomass and body size (Abecasis et al., 2015; Gell and Roberts, 2003; Roberts et al., 2005; Tetreault and Ambrose, 2007), and MPAs have been regarded as pivotal in the successful management of many fisheries (Green et

al., 2014; Roberts et al., 2005). Furthermore, these positive outcomes may extend beyond an MPA's boundaries, for example by promoting the net emigration of individuals (i.e., spillover) and by egg and larval dispersal, also called recruitment subsidy (Cudney-Bueno et al., 2009; Pérez-Ruzafa et al., 2008; Russ and Alcala, 2011).

In this context, an MPA's effectiveness will be directly influenced by how much of an animal's movements it encompasses (Afonso et al., 2011; Kramer and Chapman, 1999; Villegas-Ríos et al., 2021). However, establishing large MPAs without knowledge of the movements of the species sought to protect does not guarantee their success, as this will depend on the species' spatial ecology (Lee et al., 2014). Overall, species or populations that benefit mostly from MPAs tend to have smaller body size, higher residency or more sedentary habits, thus remaining more time in the area under protection (Gell and Roberts, 2003; Kramer and Chapman, 1999; Lee et al., 2014). Small MPAs may suffice for many site-attached reef fishes and even for large sized species in some cases (e.g., Afonso et al., 2011; Bryars et al., 2012). However, other species may be more vagile and also use additional sites outside of the protected area's boundaries. In these cases, obtaining information on movement habits is essential because isolated MPAs will likely not be as successful as a network of well-connected MPAs (Heupel et al., 2015; MacKeracher et al., 2019). This also aids species that show migratory plasticity, where some individuals in a population are more prone to migrate while others show stronger residency (Abecasis et al., 2014a; Carlisle et al., 2019), promoting biomass build-up and stimulating spillover (Gell and Roberts, 2003), and in addition, shelters migration routes (Lipcius et al., 2003). This way, it is critical to identify areas of higher vulnerability that are key to the survival of species, like spawning sites (Rhodes et al., 2012), nursery areas (Martins et al., 2018), feeding areas (Ashe et al., 2010) and biological corridors (Chapman et al., 2005; Olds et al., 2012). This highlights the importance of understanding animal movement has in spatial conservation and management strategies like MPAs (Allen and Singh, 2016).

However, despite the importance of information on the spatial ecology of elasmobranchs, this is still scarcely available when compared to economically more important bony fishes (Matley et al., 2021), particularly for batoids (Siskey et al., 2019). In fact, most of the existing area-based protection measures that have been established to protect elasmobranchs were implemented with little or even no information on their movement ecology (Hyde et al., 2022). This can have unwanted consequences that undermine the goals of the MPA, including poor enclosure of their home ranges

(MacKeracher et al., 2019), inefficient or wasteful utilization of resources (Ferraro and Pattanayak, 2006), and overestimating an MPA's protection (Agardy et al., 2011).

Although elasmobranchs have shown positive results under area-based conservation measures in some instances (Karlovic et al., 2021; Lavender et al., 2021; Le Port et al., 2012), the protection MPAs provide to them is generally considered moderate or insufficient (Dwyer et al., 2020; MacKeracher et al., 2019). In this sense, estimating the contribution of MPAs to the protection of elasmobranchs is a task that remains to be more thoroughly conducted (Davidson and Dulvy, 2017; MacKeracher et al., 2019), ideally by obtaining long-term data of their movements (Knip et al., 2012). This task is particularly pressing considering the imperiled conservation status of many of these species (Dulvy et al., 2021).

1.1.5 Passive acoustic telemetry

A method commonly used to collect data on the movement of fish is passive acoustic telemetry (Hussey et al., 2015; Matley et al., 2021). For this approach, an acoustic transmitter or tag is internally or externally attached to an individual to remotely monitor its movements using acoustic receivers (Heupel et al., 2006). Internal attachment requires a small incision in the peritoneal cavity, into which the tag is inserted. The incision is then sutured, and the animal is released after ensuring it has recovered from the procedure. Each tag emits a uniquely coded signal that is detected and logged by receivers along with additional information (like depth or temperature) depending on the tag model.

To obtain this information, receivers must be retrieved and brought on board to download the data, replacing them with another receiver to ensure the continuous surveillance of the study area and avoid gaps in the data (Figure 1.1).

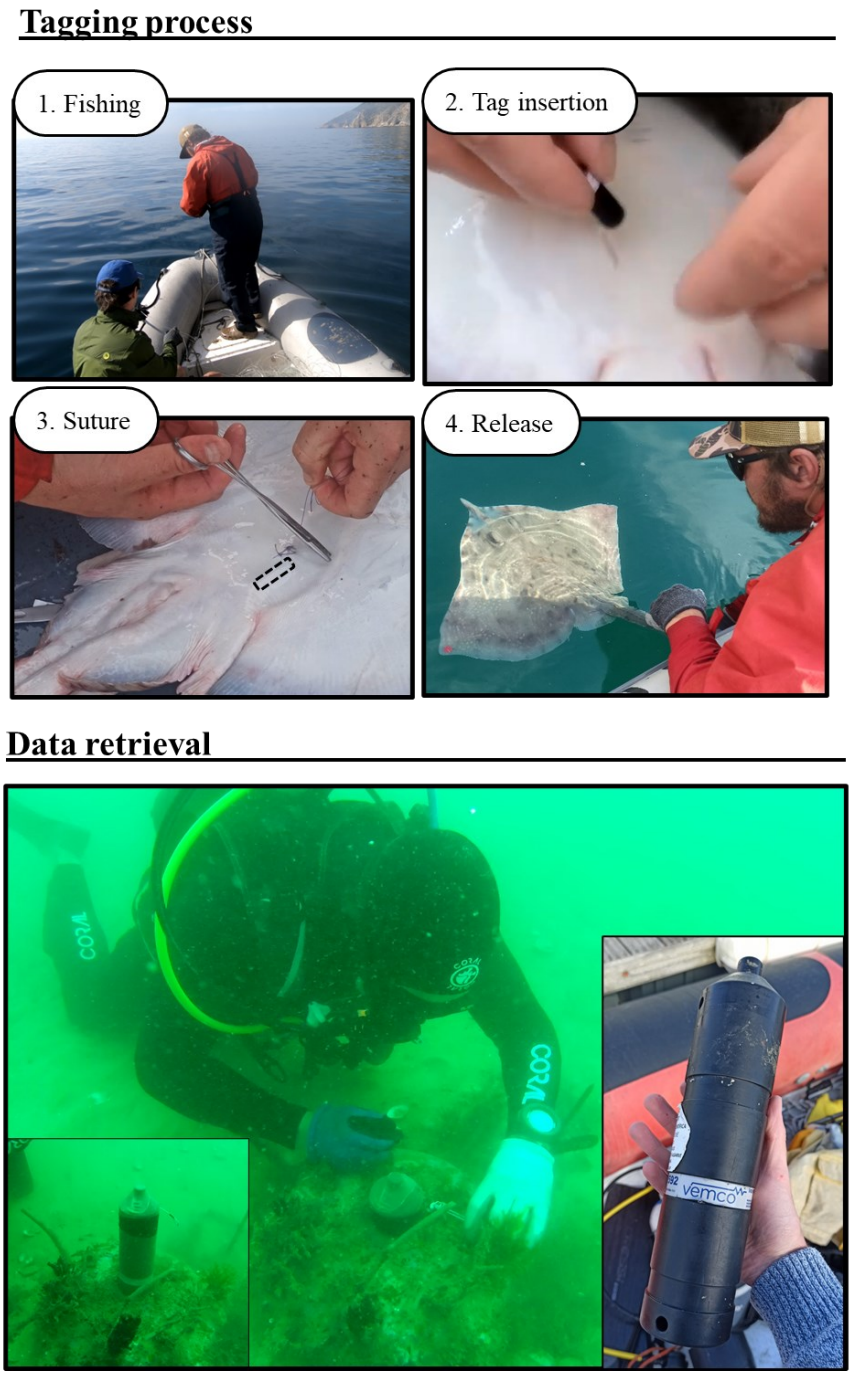

Figure 1.1: Illustration of the tagging process and the collection of data performed in this study. First, individuals were captured using trammel nets or longlines (longline pictured). Each animal was brought on board to collect biological data (species, sex, size) and for tagging. A small incision of 2 cm was made in the peritoneal cavity (pictured) to insert the tag. The incision was then sutured (approximate location of tag shown with dashed contour). Posteriorly, the tagged animal was returned to the water and held to wait for its recovery before release. In the large frame below, a receiver change done by SCUBA diving can be seen. The large image shows a diver securing an Innovasea VR2W receiver to its station. The smaller insert on the left shows the same receiver before being inserted, and the inserted image to the right shows a receiver during while data was downloaded on board via Bluetooth.

To survey the site of interest, receivers are placed at fixed known locations to form one or more acoustic arrays. Once in place, the tagged individual must stay within detection range of a receiver for a time that is long enough to allow a successful detection of the tag's signal (Figure 1.2). A tag's detection probability decreases with distance from the receiver, and is influenced by the physical and chemical properties of water (e.g., turbidity, salinity), physical characteristics of the study area (bathymetry, bottom type), obstacles to the propagation of signals (rock outcrops, large algae), background noise (motorized vessels, waves, sounds of animal origin) and time since deployment (battery life and biofouling on receivers) (Heupel et al., 2006; Huveneers et al., 2016; Kessel et al., 2014). Detection range is also highly variable across studies and over time within a same study (Heupel et al., 2006), and is commonly evaluated before conducting a study (Kessel et al., 2014).

Technological advances in recent decades have enabled researchers to continuously collect detailed, long-term data from multiple individuals in an automated and progressively cheaper way (Hussey et al., 2015). Such datasets can provide more precise estimates of animal movement (Chevis et al., 2017) and highlight areas that can be critical to conservation efforts of migratory species that shorter observation periods would otherwise overlook (Chevis et al., 2017; Martin et al., 2007; Siskey et al., 2019). In fact, this kind of technology has allowed an improved understanding of the complexity of space use patterns in elasmobranchs (Hunter et al., 2005; Siskey et al., 2019). For example, more precise home range estimations have been obtained, and previously unnoticed seasonal migrations and ontogenetic changes in migration patterns have been detected (Siskey et al., 2019). Similarly, passive acoustic telemetry has also progressed our understanding of the social and aggregation habits of elasmobranchs in the wild, providing unprecedented insights in an environment in which it is inherently difficult to conduct such studies (Jacoby et al., 2016). Compared to more traditional methods (like visual surveys), passive acoustic telemetry does not rely on visibility conditions and diver autonomy to monitor associations, and provides an uninterrupted and long-term monitoring of multiple tagged individuals (Krause et al., 2011). Social behaviours and aggregations can also underlie their distribution and movement patterns (Jacoby et al., 2016, 2010) and therefore are important to consider for conservation and management strategies (Jacoby et al., 2012; Mourier et al., 2018).

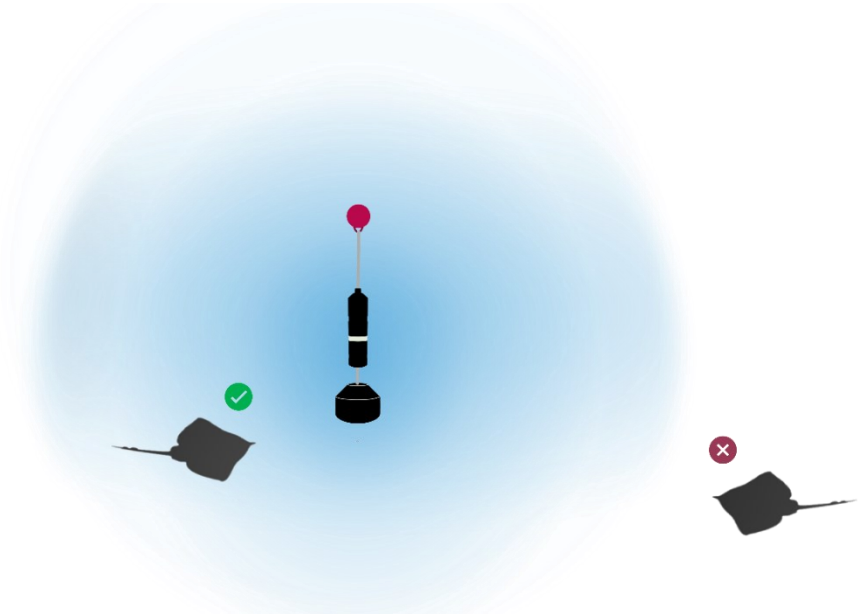

Figure 1.2: Schematic representation of an Innovasea VR2W acoustic receiver and its detection range (blue sphere, not to scale). Also depicted are the successful detection of a tagged skate within detection range (green check mark) and a failed detection of another tagged skate outside of detection range (red cross).

1.1.6 Portugal and the Luiz Saldanha Marine Park

Portuguese fisheries have landed large amounts of elasmobranchs, estimated at a total annual mean between 2229 and 4504 tonnes over the last 30 years (Alves et al., 2020); not including unreported catches and discards at sea. This is an important economic activity for the country, as Portugal ranks 16th worldwide and third in Europe in elasmobranch landings between 2000 and 2011 (Dent and Clarke, 2015). In Portugal, elasmobranchs are mainly captured as by-catch by the artisanal fleet and trawlers in other more valuable fisheries (Bordalo-Machado et al., 2004; Figueiredo et al., 2007). Batoids are the largest component of elasmobranch catches in these fisheries with one family, Rajidae, composes 48% of elasmobranch landings in continental waters (Directorate General for Natural Resources, 2017). This fishing activity is known to involve over 1000 vessels, 80% of which are under 10 m in length, indicating the high social importance of batoids in the fishing community (Serra-Pereira et al., 2018). However, the capture of elasmobranchs in Portugal is also under-regulated. For example, a high proportion of skates is landed with no species identification, usually labeled under more general categories such as *Raja* spp. (Alves et al., 2020). These multi-species fisheries can simultaneously target up to 8 skate species according to some estimates (Bordalo-Machado et al., 2004). Skates may also be discarded at sea or skinned before landing to

avoid penalties for capturing of prohibited species (Silva et al., 2021). As a result of their underregulated capture and overexploitation (Correia et al., 2016; Correia and Smith, 2003), landings of elasmobranchs have halved from approximately 4500 tonnes in 1986 to 2229 tonnes in 2017 (Alves et al., 2020).

In turn, this prompted the establishment of several regulations to manage elasmobranchs over the years, many at the European Union level. One example is total allowable catches (TACs), which are established yearly or for a period of a few years, after which the quotas are revised and modified following scientific, technical, and economic counseling before renewing them. The newest TACs to date were published in January 2024 and established the quotas for 2024, 2025 and 2026, which includes fishing zone or stock-specific quotas for elasmobranchs (Regulamento [UE] 2024/257). Other established regulations include the ban of capturing, retaining, and landing of some species in specific regions. Some examples of endangered species under this regulation in mainland Portugal's waters are the Critically Endangered *Dipturus batis* complex (IUCN, 2021), the Endangered *Raja undulata* (IUCN, 2009) (although this was later modified in 2015 and 2016), and the Critically Endangered *Rostroraja alba* (IUCN, 2015; Serra-Pereira et al., 2018). Species-specific landings have been required since 2009 for several species of Rajiformes (EC, 2009), and temporal bans were also established for some skates, like the prohibition of the targeted capture of *Raja* spp. and *Leucoraja* spp. in May and June, as well as a minimum landing size of 52 cm (Serra-Pereira et al., 2018). Similar measures were established for *Raja undulata*, namely a capture ban from May to July and minimum and maximum landing sizes of 78 cm and of 97 cm, respectively (Serra-Pereira et al., 2018).

Additionally, spatial protection measures for marine environments have also been implemented along the Portuguese coast. Various classes of spatial protection exist (natural parks, natural reserves, protected landscapes, and natural monuments), and these can be of national or regional scope. These areas are part of the National Network of Protected Areas (RNAP) and are state regulated under the jurisdiction of the Institute for Nature Conservation and Forests (ICNF) and the Directorate-General for Natural Resources, Safety and Maritime Services (DGRM). Although none of these were established with the express objective of protecting elasmobranchs, a few studies have suggested that some batoid species may receive adequate protection (Cabral, 2014; Martínez-Ramírez et al., 2021; Sousa et al., 2018).

One of the most studied marine protected areas in Portugal is the Luiz Saldanha Marine Park (LSMP) (e.g., Abecasis et al., 2014b; Cabral, 2014; Horta e Costa et al., 2013b, 2013a; Martínez-Ramírez et al., 2021; Sousa et al., 2019, 2018), found on the southern coastline of the Setúbal peninsula (Figure 1.3). It is part of the Arrábida Natural Park and is included in the European Union's network of nature protection areas (Natura 2000). This coastal MPA was designated in 1998 with the aim of protecting the local marine biodiversity and habitats, and to sustain the livelihoods of the local fishers.

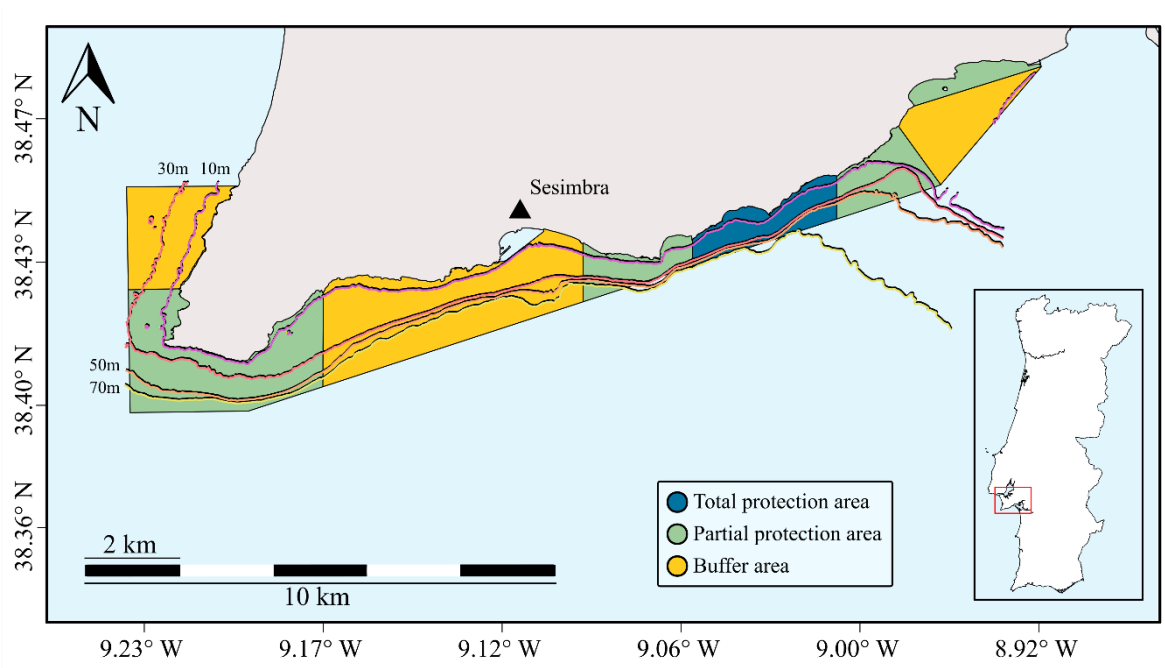

Figure 1.3: Map of the Luiz Saldanha Marine Park, in the tip of the Setúbal peninsula. The three protection levels found in the marine park and isobaths are shown and colour-coded.

The LSMP was first established in 2005 after its designation in 1998, which was followed by a transition phase to sequentially implement the existing design (Horta e Costa et al., 2013b). During this time, restrictions were progressively increased until the LSMP reached its full implementation in 2009 (Horta e Costa et al., 2013b). Currently, the LSMP extends over 38 km of coastline and covers an area of 53 km^2 and is organised into three different protection levels: a total protection area -or marine reserve- of 4.3 km^2, four partial protection areas that cover a total of 21 km^2 and three complementary protection areas or buffer areas of a combined 28 km^2. The total protection area has the highest restrictions: access is denied for all activities other than research or education and all types of fishing are banned. In the partial protection areas, only octopus traps and

jigging are allowed beyond 200 m from the coastline. Finally, in the buffer areas, recreational angling and fishing using traditional gear is allowed for licensed vessels under seven meters in length.

Two studies have conducted scientific fishing surveys to assess the LSMP's reserve effect on soft bottom fish species, including elasmobranchs (Martínez-Ramírez et al., 2021; Sousa et al., 2018). Generally positive results were seen in the measured responses (biomass, abundance, individual size), but variation among species and studies was also noted. For example, Sousa et al. (2018) found an increase in biomass, abundance and size for *Raja clavata* and *Rostroraja alba*, while Martínez-Ramírez et al. (2021) found a significant increase in biomass and abundance for *Raja clavata* and in biomass for *Rostroraja alba* after the implementation of the reserve. An increase in size of *Raja clavata* was also noted, but it was not statistically significant (Martínez-Ramírez et al., 2021). Similarly, only one of these studies found a positive reserve effect (Sousa et al., 2018). Martinez-Ramirez et al. (2021) suggested there was no reserve effect, which was attributed in part to the slow life history traits of these species and concluded that a noticeable reserve effect might take a longer time than for other faster-reproducing species. Reserve effect could also be hindered by factors like non-compliance, which can increase if benefits are perceived to be lower compared to before an MPA's implementation (Martínez-Ramírez et al., 2021; Sousa et al., 2018).

Despite the positive results that have been found for some elasmobranchs, no data on their movement ecology was available to inform the design and implementation process of the LSMP, which only became available after two preliminary studies (Cabral, 2014; Sousa et al., 2019). In turn, this prompts the need for results based on long-term data and more individuals, in order to better contextualize the protection provided by the LSMP to these species and to support its adaptive management to improve its contribution to conservation in the future.

1.1.7 Thesis outline

In this context, the objective of this study centred on improving our understanding of the movement patterns of batoids, a poorly studied and heavily fished group of elasmobranchs. In addition to improving our knowledge on the spatial ecology of batoids, this data is needed to estimate the protection provided by coastal MPAs like the LSMP, and to inform management and conservation efforts around these species (Knip et al., 2012). For this, a passive acoustic telemetry array installed in the LSMP was used to

collect long-term data on three species of batoids commonly found in this area. The first species was *Dasyatis pastinaca* (Dasyatidae, Myliobatiformes). The English common name of this species is common stingray and in Portugal it is known as *uge* or *ratão*. It is the only live-bearing species of the three included in this thesis and for which no previous acoustic telemetry data was available. The second species was *Rostroraja alba* (Rajidae, Rajiformes), known in English as white skate and in Portugal as *raia-taigora*. The relevance of this large-bodied skate lies in its classification as Critically Endangered by the International Union for Conservation of Nature, IUCN, which emphasizes the need for information on its movement patterns. Finally, the last species was *Raja clavata* (Rajidae, Rajiformes), known as thornback ray in English and *raia-lenga* in Portuguese. This species is among the most widely captured elasmobranchs in Portugal and the world, and therefore it is of high economic importance, but local information on its movement patterns was not available. The data collected on these species was analyzed using several metrics and approaches, and the work done for these tasks was structured as follows:

1) **Chapter 1:** General Introduction. The objective of this chapter was to contextualize the study, including a description of the most important concepts to be used and a characterization of the fisheries status of elasmobranchs in the world and in Portugal. The study site, the Luiz Saldanha Marine Park, was also introduced. The fundaments for the development of this thesis are presented by describing the importance of elasmobranchs, the risks they face, and the efforts being conducted to address these risks, with a focus on MPAs. The status of protection measures for elasmobranchs in Portugal was also provided.

2) **Chapter 2:** In this chapter, the methodological framework that will be used in the following sections of the thesis was presented. Some of the methodologies used to analyse passive acoustic telemetry data were reviewed, including their characteristics, limitations, and applications. This bibliographic work focused mostly on describing methods used for estimating of residency and space use, two of the most common metrics in movement ecology studies. The information was presented as a guide for researchers. This chapter has already been published in a peer reviewed scientific journal.

3) **Chapter 3:** In this first species-specific chapter, data on 31 individuals of *Dasyatis pastinaca* was collected and analysed to study the residency, space use, and activity of the species. The main finding of this work was the identification of a strong seasonal migratory pattern between the LSMP and the Sado estuary, for which conservation measures were proposed. The role of MPAs and protected corridors in the conservation of species that present these patterns were discussed. This chapter has already been published in a peer reviewed scientific journal.

4) **Chapter 4:** The second species-specific chapter focused on the Critically Endangered *Rostroraja alba*. In this work, the movement patterns of 30 individuals were studied. Mostly juvenile individuals were captured and tagged, which together with previous catch data suggest the presence of a nursery area. The implications of these results were discussed in the context of protecting species during vulnerable stages of their development.

5) **Chapter 5:** The third and last species-specific chapter focused on *Raja clavata*, a species that is among the most captured and most economically relevant elasmobranchs. Thirty-five individuals were tagged and their residency, space use, depth and activity were evaluated. The seasonal and daily dynamics of *R. clavata* in the LSMP, the noted bias towards males, and the likely unequal protection of individuals by the LSMP were discussed.

6) **Chapter 6:** This chapter focused on exploring the long-term acoustic telemetry data collected to study intraspecific aggregations and association patternsof *Dasyatis pastinaca*. The spatiotemporal distribution of aggregations was studied using co-detections at receivers, and associations among individuals were studied using social network analysis. The non-randomness and long-term stability of associations, fine-scale space use and site fidelity were discussed in the frame of the migratory nature of this species, and the conservation implications were addressed.

7) **Chapter 7:** General conclusions. The main objective of this chapter was to summarize the most important findings of the previous chapters in the context of the Luiz Saldanha Marine Park and other coastal MPAs, reflect on the findings, discuss identified limitations, and propose ideas for future endeavours.

1.2 References

Abecasis, D., Afonso, P., Erzini, K., 2014a. Can small MPAs protect local populations of a coastal flatfish, *Solea senegalensis*? Fisheries Management and Ecology 21, 175–185. https://doi.org/10.1111/fme.12061

Abecasis, D., Afonso, P., Erzini, K., 2014b. Combining multispecies home range and distribution models aids assessment of MPA effectiveness. Marine Ecology Progress Series 513, 155–169. https://doi.org/10.3354/meps10987

Abecasis, D., Horta e Costa, B., Afonso, P., Gonçalves, E.J., Erzini, K., 2015. Early reserve effects linked to small home ranges of a commercial fish, *Diplodus sargus*, Sparidae. Marine Ecology Progress Series 518, 255–266. https://doi.org/10.3354/meps11054

Afonso, P., Fontes, J., Santos, R.S., 2011. Small marine reserves can offer long term protection to an endangered fish. Biological Conservation 144, 2739–2744. https://doi.org/10.1016/j.biocon.2011.07.028

Agardy, T., Di Sciara, G.N., Christie, P., 2011. Mind the gap: Addressing the shortcomings of marine protected areas through large scale marine spatial planning. Marine Policy 35, 226–232. https://doi.org/10.1016/j.marpol.2010.10.006

Agnew, D.J., Nolan, C.P., Beddington, J.R., Baranowski, R., 2000. Approaches to the assessment and management of multispecies skate and ray fisheries using the Falkland Islands fishery as an example. Canadian Journal of Fisheries and Aquatic Sciences 57, 429–440. https://doi.org/10.1139/f99-264

Allen, A.M., Singh, N.J., 2016. Linking Movement Ecology with Wildlife Management and Conservation. Frontiers in Ecology and Evolution 3, 155. https://doi.org/10.3389/fevo.2015.00155

Alves, L.M.F., Correia, J.P.S., Lemos, M.F.L., Novais, S.C., Cabral, H., 2020. Assessment of trends in the Portuguese elasmobranch commercial landings over three decades (1986–2017). Fisheries Research 230, 105648. https://doi.org/10.1016/j.fishres.2020.105648

Ashe, E., Noren, D.P., Williams, R., 2010. Animal behaviour and marine protected areas: incorporating behavioural data into the selection of marine protected areas for an endangered killer whale population. Animal Conservation 13, 196–203. https://doi.org/10.1111/j.1469-1795.2009.00321.x

Ban, N.C., Gurney, G.G., Marshall, N.A., Whitney, C.K., Mills, M., Gelcich, S., Bennett, N.J., Meehan, M.C., Butler, C., Ban, S., Tran, T.C., Cox, M.E., Breslow, S.J., 2019. Well-being outcomes of marine protected areas. Nature Sustainability 2, 524–532. https://doi.org/10.1038/s41893-019-0306-2

Batsleer, J., Griffiths, C.A., Bleeker, K., Johnston, G., Cardinale, M., Lorance, P., 2024. Comparisons of landings to scientific advice indicate overshooting within the common TAC for skates and rays in the Northeast Atlantic. ICES Journal of Marine Science fsae008. https://doi.org/10.1093/icesjms/fsae008

Bohnsack, J.A., 1998. Application of marine reserves to reef fisheries management. Austral Ecology 23, 298–304. https://doi.org/10.1111/j.1442-9993.1998.tb00734.x

Bonfil, R., 1994. Overview of world elasmobranch fisheries, FAO fisheries technical paper. FAO, Rome.

Bordalo-Machado, P., Serrano-Gordo, L., Figueiredo, I., 2004. Skate and ray species composition in mainland Portugal from the commercial landings. Aquatic Living Resources 17, 231–234. https://doi.org/10.1051/alr:2004015

Brander, K., 1981. Disappearance of common skate *Raia batis* from Irish Sea. Nature 290, 48–49. https://doi.org/10.1038/290048a0

Bryars, S., Rogers, P., Huveneers, C., Payne, N., Smith, I., McDonald, B., 2012. Small home range in southern Australia's largest resident reef fish, the western blue groper (*Achoerodus gouldii*): implications for adequacy of no-take marine protected areas. Marine and Freshwater Research 63, 552. https://doi.org/10.1071/MF12016

Cabral, S., 2014. *Raja* spp. spatial dynamics in the Arrábida Marine Park (Master's Thesis). Universidade do Algarve.

Carlisle, A.B., Tickler, D., Dale, J.J., Ferretti, F., Curnick, D.J., Chapple, T.K., Schallert, R.J., Castleton, M., Block, B.A., 2019. Estimating Space Use of Mobile Fishes in a Large Marine Protected Area With Methodological Considerations in Acoustic Array Design. Frontiers in Marine Science 6, 256. https://doi.org/10.3389/fmars.2019.00256

Casey, J.M., Myers, R.A., 1998. Near extinction of a large, widely distributed fish. Science 281, 690–692. https://doi.org/10.1126/science.281.5377.690

Chapman, D.D., Pikitch, E.K., Babcock, E., Shivji, M.S., 2005. Marine Reserve Design and Evaluation Using Automated Acoustic Telemetry: A Case-study Involving Coral Reef-associated Sharks in the Mesoamerican Caribbean. Marine Technology Society Journal 39, 42–55. https://doi.org/10.4031/002533205787521640

Chevis, M.G., Godley, B.J., Lewis, J.P., Jackson Lewis, J., Scales, K.I., Graham, R.T., 2017. Movement patterns of juvenile hawksbill turtles *Eretmochelys imbricata* at a Caribbean coral atoll: long-term tracking using passive acoustic telemetry. Endangered Species Research 32, 309–319. https://doi.org/10.3354/esr00812

Christensen, V., Guenette, S., Heymans, J.J., Walters, C.J., Watson, R., Zeller, D., Pauly, D., 2003. Hundred-year decline of North Atlantic predatory fishes. Fish Fisheries 4, 1–24. https://doi.org/10.1046/j.1467-2979.2003.00103.x

Correia, J.P., Morgado, F., Erzini, K., Soares, A.M.V.M., 2016. Elasmobranch landings in the Portuguese commercial fishery from 1986 to 2009. Arquipélago. Life and Marine Sciences 33, 81–109.

Correia, J.P.S., Smith, M.F.L., 2003. Elasmobranch landings for the Portuguese commercial fishery from 1986 to 2001. Marine Fisheries Review 65, 32–40.

Creel, S., Christianson, D., 2008. Relationships between direct predation and risk effects. Trends in Ecology & Evolution 23, 194–201. https://doi.org/10.1016/j.tree.2007.12.004

Cudney-Bueno, R., Lavín, M.F., Marinone, S.G., Raimondi, P.T., Shaw, W.W., 2009. Rapid Effects of Marine Reserves via Larval Dispersal. PLOS ONE 4, 1–7. https://doi.org/10.1371/journal.pone.0004140

Davidson, L.N.K., Dulvy, N.K., 2017. Global marine protected areas to prevent extinctions. Nature Ecology & Evolution 1, 0040. https://doi.org/10.1038/s41559-016-0040

Davidson, L.N.K., Krawchuk, M.A., Dulvy, N.K., 2016. Why have global shark and ray landings declined: improved management or overfishing? Fish and Fisheries 17, 438–458. https://doi.org/10.1111/faf.12119

Dedman, S., Moxley, J.H., Papastamatiou, Y.P., Braccini, M., Caselle, J.E., Chapman, D.D., Cinner, J.E., Dillon, E.M., Dulvy, N.K., Dunn, R.E., Espinoza, M., Harborne, A.R., Harvey, E.S., Heupel, M.R., Huveneers, C., Graham, N.A.J., Ketchum, J.T., Klinard, N.V., Kock, A.A., Lowe, C.G., MacNeil, M.A., Madin, E.M.P., McCauley, D.J., Meekan, M.G., Meier, A.C., Simpfendorfer, C.A., Tinker, M.T., Winton, M., Wirsing, A.J., Heithaus, M.R., 2024. Ecological roles and importance of sharks in the Anthropocene Ocean. Science 385, adl2362. https://doi.org/10.1126/science.adl2362

Dent, F., Clarke, S., 2015. State of the global market for shark products. FAO Fisheries and Aquaculture Technical Paper No. 590. FAO, Rome.

Dickey-Collas, M., Nash, R.D.M., Brunel, T., van Damme, C.J.G., Marshall, C.T., Payne, M.R., Corten, A., Geffen, A.J., Peck, M.A., Hatfield, E.M.C., Hintzen, N.T., Enberg, K., Kell, L.T., Simmonds, E.J., 2010. Lessons learned from stock collapse and recovery of North Sea herring: a review. ICES Journal of Marine Science 67, 1875–1886. https://doi.org/10.1093/icesjms/fsq033

Dudley, N. (Ed.), 2008. Guidelines for Applying Protected Area Management Categories. IUCN, Gland, Switzerland.

Dulvy, N.K., Fowler, S.L., Musick, J.A., Cavanagh, R.D., Kyne, P.M., Harrison, L.R., Carlson, J.K., Davidson, L.N., Fordham, S.V., Francis, M.P., Pollock, C.M., Simpfendorfer, C.A., Burgess, G.H., Carpenter, K.E., Compagno, L.J., Ebert, D.A., Gibson, C., Heupel, M.R., Livingstone, S.R., Sanciangco, J.C., Stevens, J.D., Valenti, S., White, W.T., 2014. Extinction risk and conservation of the world's sharks and rays. eLife 3, e00590. https://doi.org/10.7554/eLife.00590

Dulvy, N.K., Metcalfe, J.D., Glanville, J., Pawson, M.G., Reynolds, J., 2000. Fishery stability, local extinctions, and shifts in community structure in skates. Conservation Biology 14, 283–293. https://doi.org/10.1046/j.1523-1739.2000.98540.x

Dulvy, N.K., Pacoureau, N., Rigby, C.L., Pollom, R.A., Jabado, R.W., Ebert, D.A., Finucci, B., Pollock, C.M., Cheok, J., Derrick, D.H., Herman, K.B., Sherman, C.S., VanderWright, W.J., Lawson, J.M., Walls, R.H.L., Carlson, J.K., Charvet, P., Bineesh, K.K., Fernando, D., Ralph, G.M., Matsushiba, J.H., Hilton-Taylor, C., Fordham, S.V., Simpfendorfer, C.A., 2021. Overfishing drives over one-third of all sharks and rays toward a global extinction crisis. Current Biology 31, 4773-4787.e8. https://doi.org/10.1016/j.cub.2021.08.062

Dwyer, R.G., Krueck, N.C., Udyawer, V., Heupel, M.R., Chapman, D., Pratt, H.L., Garla, R., Simpfendorfer, C.A., 2020. Individual and Population Benefits of Marine Reserves for Reef Sharks. Current Biology 30, 480-489.e5. https://doi.org/10.1016/j.cub.2019.12.005

Ebert, D., Winton, M., 2010. Chondrichthyans of High Latitude Seas, in: Sharks and Their Relatives II, Marine Biology. CRC Press, pp. 115–158. https://doi.org/10.1201/9781420080483-c3

Ebert, D.A., Compagno, L.J.V., Cowley, P.D., 2008. Aspects of the reproductive biology of skates (Chondrichthyes: Rajiformes: Rajoidei) from southern Africa. ICES Journal of Marine Science 65, 81–102. https://doi.org/10.1093/icesjms/fsm169

Ebert, D.A., Fowler, S.L., Compagno, L.J.V., Dando, M., 2013. Sharks of the world: a fully illustrated guide.

EC, 2009. Council Regulation (EC) No 43/2009 of 16 January 2009 fixing for 2009 the fishing opportunities and associated conditions for certain fish stocks and groups of fish stocks, applicable in Community waters and, for Community vessels, in waters where catch limitations are required.

FAO, 2024. The State of World Fisheries and Aquaculture 2024 – Blue Transformation in action. Rome. https://doi.org/10.4060/cd0683en

Ferraro, P.J., Pattanayak, S.K., 2006. Money for Nothing? A Call for Empirical Evaluation of Biodiversity Conservation Investments. PLoS Biol 4, e105. https://doi.org/10.1371/journal.pbio.0040105

Figueiredo, I., Moura, T., Bordalo-Machado, P., Neves, A., Rosa, C., Serrano Gordo, L., 2007. Evidence for temporal changes in ray and skate populations in the Portuguese coast (1998–2003) – its implications in the ecosystem. Aquatic Living Resources 20, 85–93. https://doi.org/10.1051/alr:2007019

Flowers, K., Heithaus, M., Papastamatiou, Y.P., 2019. Buried in the sand: Uncovering the ecological roles and importance of ray. Fish and Fisheries 00, 1–23. https://doi.org/10.1111/faf.12508

Frisk, M.G., Miller, T.J., Fogarty, M.J., 2001. Estimation and analysis of biological parameters in elasmobranch fishes: a comparative life history study. Canadian Journal of Fisheries and Aquatic Sciences 58, 969–981. https://doi.org/10.1139/f01-051

Gell, F.R., Roberts, C.M., 2003. Benefits beyond boundaries: the fishery effects of marine reserves. Trends in Ecology & Evolution 18, 448–455. https://doi.org/10.1016/S0169-5347(03)00189-7

Green, A.L., Fernandes, L., Almany, G., Abesamis, R., McLeod, E., Aliño, P.M., White, A.T., Salm, R., Tanzer, J., Pressey, R.L., 2014. Designing Marine Reserves for Fisheries Management, Biodiversity Conservation, and Climate Change Adaptation. Coastal Management 42, 143–159. https://doi.org/10.1080/08920753.2014.877763

Grorud-Colvert, K., Sullivan-Stack, J., Roberts, C., Constant, V., Horta E Costa, B., Pike, E.P., Kingston, N., Laffoley, D., Sala, E., Claudet, J., Friedlander, A.M., Gill, D.A., Lester, S.E., Day, J.C., Gonçalves, E.J., Ahmadia, G.N., Rand, M., Villagomez, A., Ban, N.C., Gurney, G.G., Spalding, A.K., Bennett, N.J., Briggs, J., Morgan, L.E., Moffitt, R., Deguignet, M., Pikitch, E.K., Darling, E.S., Jessen, S., Hameed, S.O., Di Carlo, G., Guidetti, P., Harris, J.M., Torre, J., Kizilkaya, Z., Agardy, T., Cury, P., Shah, N.J., Sack, K., Cao, L., Fernandez, M., Lubchenco, J., 2021. The MPA Guide: A framework to achieve global goals for the ocean. Science 373, eabf0861. https://doi.org/10.1126/science.abf0861

Heithaus, M.R., Frid, A., Wirsing, A.J., Dill, L.M., Fourqurean, J.W., Burkholder, D., Thomson, J., Bejder, L., 2007. State-dependent risk-taking by green sea turtles mediates top-down effects of tiger shark intimidation in a marine ecosystem. J Anim Ecology 76, 837–844. https://doi.org/10.1111/j.1365-2656.2007.01260.x

Heupel, M.R., Semmens, J.M., Hobday, A.J., 2006. Automated acoustic tracking of aquatic animals: scales, design and deployment of listening station arrays. Marine and Freshwater Research 57, 1. https://doi.org/10.1071/MF05091

Heupel, M.R., Simpfendorfer, C.A., Espinoza, M., Smoothey, A.F., Tobin, A., Peddemors, V., 2015. Conservation challenges of sharks with continental scale migrations. Frontiers in Marine Science 2. https://doi.org/10.3389/fmars.2015.00012

Horta e Costa, B., Batista, M.I., Gonçalves, L., Erzini, K., Caselle, J.E., Cabral, H.N., Gonçalves, E.J., 2013a. Fishers' Behaviour in Response to the Implementation of a Marine Protected Area. PLoS ONE 8, e65057. https://doi.org/10.1371/journal.pone.0065057

Horta e Costa, B., Erzini, K., Caselle, J., Folhas, H., Gonçalves, E., 2013b. 'Reserve effect' within a temperate marine protected area in the north-eastern Atlantic (Arrábida Marine Park, Portugal). Marine Ecology Progress Series 481, 11–24. https://doi.org/10.3354/meps10204

Hunter, E., Buckley, A.A., Stewart, C., Metcalfe, J.D., 2005. Migratory behaviour of the thornback ray, *Raja clavata*, in the southern North Sea. Journal of the Marine Biological Association of the United Kingdom 85, 1095–1105. https://doi.org/10.1017/S0025315405012142

Hussey, N.E., Kessel, S.T., Aarestrup, K., Cooke, S.J., Cowley, P.D., Fisk, A.T., Harcourt, R.G., Holland, K.N., Iverson, S.J., Kocik, J.F., Mills Flemming, J.E., Whoriskey, F.G., 2015. Aquatic animal telemetry: A panoramic window into the underwater world. Science 348, 1255642–1255642. https://doi.org/10.1126/science.1255642

Hutchings, J.A., Myers, R.A., 1994. What Can Be Learned from the Collapse of a Renewable Resource? Atlantic Cod, *Gadus morhua*, of Newfoundland and Labrador. Canadian Journal of Fisheries and Aquatic Sciences 51, 2126–2146. https://doi.org/10.1139/f94-214

Huveneers, C., Simpfendorfer, C.A., Kim, S., Semmens, J.M., Hobday, A.J., Pederson, H., Stieglitz, T., Vallee, R., Webber, D., Heupel, M.R., Peddemors, V., Harcourt, R.G., 2016. The influence of environmental parameters on the performance and detection range of acoustic receivers. Methods in Ecology and Evolution 7, 825–835. https://doi.org/10.1111/2041-210X.12520

Hyde, C.A., Notarbartolo di Sciara, G., Sorrentino, L., Boyd, C., Finucci, B., Fowler, S.L., Kyne, P.M., Leurs, G., Simpfendorfer, C.A., Tetley, M.J., Womersley, F., Jabado, R.W., 2022. Putting sharks on the map: A global standard for improving shark area-based conservation. Frontiers in Marine Science 9, 968853. https://doi.org/10.3389/fmars.2022.968853

IUCN, 2021. Dipturus batis: Ellis, J., McCully-Philipps, S.R., Sims, D., Derrick, D., Cheok, J. & Dulvy, N.K.: The IUCN Red List of Threatened Species 2021: e.T203364219A203375487. https://doi.org/10.2305/IUCN.UK.2021-2.RLTS.T203364219A203375487.en

IUCN, 2015. Ellis, J., Morey, G & Walls, R. 2015. *Rostroraja alba*. The IUCN Red List of Threatened Species 2015: e.T61408A48954174.

IUCN, 2009. *Raja undulata*: Coelho, R., Bertozzi, M.,Ungaro. N. & Ellis, J.: The IUCN Red List of Threatened Species 2009: e.T161425A5420694.

Jacoby, D.M.P., Busawon, D.S., Sims, D.W., 2010. Sex and social networking: the influence of male presence on social structure of female shark groups. Behavioral Ecology 21, 808–818. https://doi.org/10.1093/beheco/arq061

Jacoby, D.M.P., Croft, D.P., Sims, D.W., 2012. Social behaviour in sharks and rays: analysis, patterns and implications for conservation: Shark social behaviour. Fish and Fisheries 13, 399–417. https://doi.org/10.1111/j.1467-2979.2011.00436.x

Jacoby, D.M.P., Papastamatiou, Y.P., Freeman, R., 2016. Inferring animal social networks and leadership: applications for passive monitoring arrays. Journal of The Royal Society Interface 13, 20160676. https://doi.org/10.1098/rsif.2016.0676

Jaiteh, V.F., Loneragan, N.R., Warren, C., 2017. The end of shark finning? Impacts of declining catches and fin demand on coastal community livelihoods. Marine Policy 82, 224–233. https://doi.org/10.1016/j.marpol.2017.03.027

Karlovic, T.C., Gomes, R.R., Paiva, P.C., Babcock, E.A., Dias, J.F., 2021. Functionality and Effectiveness of Marine Protected Areas in Southeastern Brazilian Waters for Demersal Elasmobranchs. Frontiers in Marine Science 8, 694846. https://doi.org/10.3389/fmars.2021.694846

Kessel, S.T., Cooke, S.J., Heupel, M.R., Hussey, N.E., Simpfendorfer, C.A., Vagle, S., Fisk, A.T., 2014. A review of detection range testing in aquatic passive acoustic telemetry studies. Rev Fish Biol Fisheries 24, 199–218. https://doi.org/10.1007/s11160-013-9328-4

Knip, D.M., Heupel, M.R., Simpfendorfer, C.A., 2012. Evaluating marine protected areas for the conservation of tropical coastal sharks. Biological Conservation 148, 200–209. https://doi.org/10.1016/j.biocon.2012.01.008

Kramer, D.L., Chapman, M.R., 1999. Implications of fish home range size and relocation for marine reserve function. Environmental Biology of Fishes 55, 65–79. https://doi.org/10.1023/A:1007481206399

Krause, J., Wilson, A.D.M., Croft, D.P., 2011. New technology facilitates the study of social networks. Trends in Ecology & Evolution 26, 5–6. https://doi.org/10.1016/j.tree.2010.10.004

Kyne, P.M., Simpfendorfer, C.A., 2010. Deepwater Chondrichthyans, in: Sharks and Their Relatives II, Marine Biology. CRC Press, pp. 37–113. https://doi.org/10.1201/9781420080483-c3

Lavender, E., Aleynik, D., Dodd, J., Illian, J., James, M., Wright, P.J., Smout, S., Thorburn, J., 2021. Movement patterns of a Critically Endangered elasmobranch (*Dipturus intermedius*) in a Marine Protected Area. Aquatic Conservation: Marine and Freshwater Ecosystems aqc.3753. https://doi.org/10.1002/aqc.3753

Le Port, A., Lavery, S., Montgomery, J.C., 2012. Conservation of coastal stingrays: seasonal abundance and population structure of the short-tailed stingray *Dasyatis*

brevicaudata at a Marine Protected Area. ICES Journal of Marine Science 69, 1427–1435. https://doi.org/10.1093/icesjms/fss120

Lee, K.A., Huveneers, C., Macdonald, T., Harcourt, R.G., 2014. Size isn't everything: movements, home range, and habitat preferences of eastern blue gropers (*Achoerodus viridis*) demonstrate the efficacy of a small marine reserve: do small reserves protect eastern blue gropers? Aquatic Conservation: Marine and Freshwater Ecosystems 25, 174–186. https://doi.org/10.1002/aqc.2431

Lester, S., Halpern, B., Grorud-Colvert, K., Lubchenco, J., Ruttenberg, B., Gaines, S., Airamé, S., Warner, R., 2009. Biological effects within no-take marine reserves: a global synthesis. Marine Ecology Progress Series 384, 33–46. https://doi.org/10.3354/meps08029

Lipcius, R.N., Stockhausen, W.T., Seitz, R.D., Geer, P.J., 2003. Spatial dynamics and value of a marine protected area and corridor for the blue crab spawning stock in Chesapeake Bay. Bulletin of Marine Science 72, 453–469.

MacKeracher, T., Diedrich, A., Simpfendorfer, C.A., 2019. Sharks, rays and marine protected areas: A critical evaluation of current perspectives. Fish and Fisheries 20, 255–267. https://doi.org/10.1111/faf.12337

Martin, T.G., Chadès, I., Arcese, P., Marra, P.P., Possingham, H.P., Norris, D.R., 2007. Optimal Conservation of Migratory Species. PLoS ONE 2, e751. https://doi.org/10.1371/journal.pone.0000751

Martínez-Ramírez, L., Priester, C.R., Sousa, I., Erzini, K., Abecasis, D., 2021. Reserve effect of a small North-East Atlantic marine protected area (Arrábida, Portugal) on soft-sediment fish species. Aquatic Conservation: Marine and Freshwater Ecosystems 31, 1584–1595. https://doi.org/10.1002/aqc.3577

Martins, A., Heupel, M., Chin, A., Simpfendorfer, C., 2018. Batoid nurseries: definition, use and importance. Marine Ecology Progress Series 595, 253–267. https://doi.org/10.3354/meps12545

Matley, J.K., Klinard, N.V., Barbosa Martins, A.P., Aarestrup, K., Aspillaga, E., Cooke, S.J., Cowley, P.D., Heupel, M.R., Lowe, C.G., Lowerre-Barbieri, S.K., Mitamura, H., Moore, J.-S., Simpfendorfer, C.A., Stokesbury, M.J.W., Taylor, M.D., Thorstad, E.B., Vandergoot, C.S., Fisk, A.T., 2021. Global trends in aquatic animal tracking with acoustic telemetry. Trends in Ecology & Evolution S0169534721002470. https://doi.org/10.1016/j.tree.2021.09.001

McCain, J.S.P., Cull, D.J., Schneider, D.C., Lotze, H.K., 2016. Long-term shift in coastal fish communities before and after the collapse of Atlantic cod (*Gadus morhua*). ICES Journal of Marine Science 73, 1415–1426. https://doi.org/10.1093/icesjms/fsv216

Mourier, J., Lédée, E., Guttridge, T., Jacoby, D., 2018. Network Analysis and Theory in Shark Ecology - Methods and Applications, in: Carrier, J., Heithaus, M., Simpfendorfer, C. (Eds.), Shark Research Emerging Technologies and Applications for the Field and Laboratory. CRC Press, Boca Raton, USA, pp. 337–356.

Navia, A.F., Mejía-Falla, P.A., López-García, J., Giraldo, A., Cruz-Escalona, V.H., 2017. How many trophic roles can elasmobranchs play in a marine tropical network? Marine and Freshwater Research 68, 1342. https://doi.org/10.1071/MF16161

Nielsen, J., Hedeholm, R.B., Heinemeier, J., Bushnell, P.G., Christiansen, J.S., Olsen, J., Ramsey, C.B., Brill, R.W., Simon, M., Steffensen, K.F., Steffensen, J.F., 2016. Eye lens radiocarbon reveals centuries of longevity in the Greenland shark (*Somniosus microcephalus*). Science 353, 702–704. https://doi.org/10.1126/science.aaf1703

Olds, A.D., Connolly, R.M., Pitt, K.A., Maxwell, P.S., 2012. Habitat connectivity improves reserve performance: Connectivity improves reserve performance. Conservation Letters 5, 56–63. https://doi.org/10.1111/j.1755-263X.2011.00204.x

Oliver, S., Braccini, M., Newman, S.J., Harvey, E.S., 2015. Global patterns in the bycatch of sharks and rays. Marine Policy 54, 86–97. https://doi.org/10.1016/j.marpol.2014.12.017

Pérez-Ruzafa, A., Martín, E., Marcos, C., Zamarro, J.M., Stobart, B., Harmelin-Vivien, M., Polti, S., Planes, S., García-Charton, J.A., González-Wangüemert, M., 2008. Modelling spatial and temporal scales for spill-over and biomass exportation from MPAs and their potential for fisheries enhancement. Journal for Nature Conservation 16, 234–255. https://doi.org/10.1016/j.jnc.2008.09.003

Rhodes, K.L., McIlwain, J., Joseph, E., Nemeth, R.S., 2012. Reproductive movement, residency and fisheries vulnerability of brown-marbled grouper, *Epinephelus fuscoguttatus* (Forsskål, 1775). Coral Reefs 31, 443–453. https://doi.org/10.1007/s00338-012-0875-2

Roberts, C.M., Hawkins, J.P., Gell, F.R., 2005. The role of marine reserves in achieving sustainable fisheries. Philosophical Transactions of the Royal Society B: Biological Sciences 360, 123–132. https://doi.org/10.1098/rstb.2004.1578

Rosa, R.S., Charvet-Almeida, P., Diban Quijada, C.C., 2010. Biology of the South American Potamotrygonid Stingrays, in: Sharks and Their Relatives II, Marine Biology. CRC Press, pp. 241–282. https://doi.org/10.1201/9781420080483-c4

Ruiz-Frau, A., Possingham, H.P., Edwards-Jones, G., Klein, C.J., Segan, D., Kaiser, M.J., 2015. A multidisciplinary approach in the design of marine protected areas: Integration of science and stakeholder based methods. Ocean & Coastal Management 103, 86–93. https://doi.org/10.1016/j.ocecoaman.2014.11.012

Russ, G.R., Alcala, A.C., 2011. Enhanced biodiversity beyond marine reserve boundaries: The cup spillith over. Ecological Applications 21, 241–250. https://doi.org/10.1890/09-1197.1

Serra-Pereira, B., Maia, C., Lagarto, N., Figueiredo, I., 2018. A investigação realizada no IPMA de suporte ao aconselhamento científico para a gestão de espécies de raias (No. 21).

Silva, P.M., Teixeira, C.M., Pita, C., Cabral, H.N., França, S., 2021. Portuguese Artisanal Fishers' Knowledge About Elasmobranchs—A Case Study. Frontiers in Marine Science 8, 684059. https://doi.org/10.3389/fmars.2021.684059

Simpfendorfer, C.A., Heupel, M.R., White, W.T., Dulvy, N.K., 2011. The importance of research and public opinion to conservation management of sharks and rays: a synthesis. Marine and Freshwater Research 62, 518. https://doi.org/10.1071/MF11086

Siskey, M.R., Shipley, O.N., Frisk, M.G., 2019. Skating on thin ice: Identifying the need for species-specific data and defined migration ecology of Rajidae spp. Fish and Fisheries 20, 286–302. https://doi.org/10.1111/faf.12340

Sousa, I., Baeyaert, J., Gonçalves, J.M.S., Erzini, K., 2019. Preliminary insights into the spatial ecology and movement patterns of a regionally critically endangered skate (*Rostroraja alba*) associated with a marine protected area. Marine and Freshwater Behaviour and Physiology 52, 283–299. https://doi.org/10.1080/10236244.2019.1705805

Sousa, I., Gonçalves, J.M.S., Claudet, J., Coelho, R., Gonçalves, E.J., Erzini, K., 2018. Soft-bottom fishes and spatial protection: findings from a temperate marine protected area. PeerJ 6, e4653. https://doi.org/10.7717/peerj.4653

Stein, R.W., Mull, C.G., Kuhn, T.S., Aschliman, N.C., Davidson, L.N.K., Joy, J.B., Smith, G.J., Dulvy, N.K., Mooers, A.O., 2018. Global priorities for conserving the evolutionary history of sharks, rays and chimaeras. Nat Ecol Evol 2, 288–298. https://doi.org/10.1038/s41559-017-0448-4

Stevens, J., 2010. Epipelagic Oceanic Elasmobranchs, in: Sharks and Their Relatives II, Marine Biology. CRC Press, pp. 3–35. https://doi.org/10.1201/9781420080483-c1

Stevens, J.D., Bonfil, R., Dulvy, N.K., Walker, P.A., 2000. The effects of fishing on sharks, rays, and chimaeras (Chondrichthyans), and the implications for marine ecosystems. ICES Journal of Marine Science 57, 476–494. https://doi.org/10.1006/jmsc.2000.0724

Strong, W.R., Snelson, F.F., Gruber, S.H., 1990. Hammerhead Shark Predation on Stingrays: An Observation of Prey Handling by *Sphyrna mokarran*. Copeia 1990, 836. https://doi.org/10.2307/1446449

Tanaka, S., Shiobara, Y., Hioki, S., Abe, H., Nishi, G., Yano, K., Suzuki, K., 1990. The reproductive biology of the frilled shark, *Chlamydoselachus anguineus*, from Suruga Bay, Japan. https://doi.org/10.11369/jji1950.37.273

Tetreault, I., Ambrose, R.F., 2007. Temperate marine reserves enhance targeted but not untargeted fishes in multiple no-take MPAs. Ecological Applications 17, 2251–2267. https://doi.org/10.1890/06-0161.1

Tokunaga, S., Watanabe, Y.Y., Kawano, M., Kawabata, Y., 2022. Factors affecting gestation periods in elasmobranch fishes. Biology Open 11, bio059270. https://doi.org/10.1242/bio.059270

Vannuccini, S., 1999. Shark utilization, marketing and trade, FAO fisheries technical paper. FAO, Rome.

Villegas-Ríos, D., Claudet, J., Freitas, C., Moland, E., Thorbjørnsen, S.H., Alonso-Fernández, A., Olsen, E.M., 2021. Time at risk: Individual spatial behaviour drives effectiveness of marine protected areas and fitness. Biological Conservation 263, 109333. https://doi.org/10.1016/j.biocon.2021.109333

Weigmann, S., 2017. Reply to Borsa (2017): Comment on ‘Annotated checklist of the living sharks, batoids and chimaeras (Chondrichthyes) of the world, with a focus on biogeographical diversity by Weigmann (2016)’: reply to Borsa’s comment on Weigmann (2016). Journal of Fish Biology 90, 1176–1181. https://doi.org/10.1111/jfb.13234

Weigmann, S., 2016. Annotated checklist of the living sharks, batoids and chimaeras (Chondrichthyes) of the world, with a focus on biogeographical diversity: annotated global checklist of chondrichthyes. Journal of Fish Biology 88, 837–1037. https://doi.org/10.1111/jfb.12874

White, W., Sommerville, E., 2010. Elasmobranchs of Tropical Marine Ecosystems, in: Sharks and Their Relatives II, Marine Biology. CRC Press, pp. 159–239. https://doi.org/10.1201/9781420080483-c4

White, W.T., Kyne, P.M., Harris, M., 2019. Lost before found: A new species of whaler shark *Carcharhinus obsolerus* from the Western Central Pacific known only from historic records. PLoS ONE 14, e0209387. https://doi.org/10.1371/journal.pone.0209387

Wirsing, A.J., Heithaus, M.R., Dill, L.M., 2007. Fear factor: do dugongs (*Dugong dugon*) trade food for safety from tiger sharks (*Galeocerdo cuvier*)? Oecologia 153, 1031–1040. https://doi.org/10.1007/s00442-007-0802-3

Worm, B., Davis, B., Kettemer, L., Ward-Paige, C.A., Chapman, D., Heithaus, M.R., Kessel, S.T., Gruber, S.H., 2013. Global catches, exploitation rates, and rebuilding options for sharks. Marine Policy 40, 194–204. https://doi.org/10.1016/j.marpol.2012.12.034

Chapter 2

Residency and space use estimation methods based on acoustic telemetry data

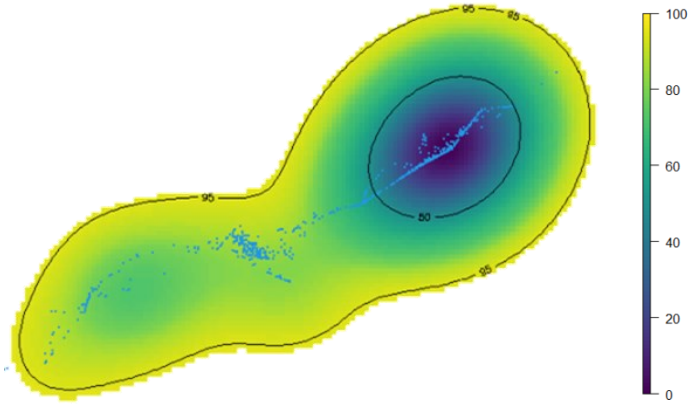

Kernel Utilization Distribution

Chapter published as:

Kraft, S., Gandra, M., Lennox, R.J., Mourier, J., Winkler, A.C., Abecasis, D., 2023. Residency and space use estimation methods based on passive acoustic telemetry data. Movement Ecology 11, 12. https://doi.org/10.1186/s40462-022-00364-z

Abstract

Acoustic telemetry has helped overcome many of the challenges faced when studying the movement ecology of aquatic species, allowing to obtain unprecedented amounts of data. This has made it into one of the most widely used methods nowadays. Many ways to analysing acoustic telemetry data have been made available and deciding on how to analyse the data requires considering the type of research objectives, relevant properties of the data (e.g., resolution, study design, equipment), habits of the study species, researcher experience, among others. To ease this decision process, here we showcase some of the methods used to 1) estimate pseudo-positions and positions from raw acoustic telemetry data, 2) estimate residency and 3) estimate two-dimensional home and occurrence range using geometric or hull-based methods and density-distribution methods, a network-based approach, and three-dimensional methods. We also provide examples of some of these using real data. With this work, we intend to provide the necessary background for researchers to select the method(s) that better fit their research objectives when using acoustic telemetry data.

Keywords: Home range, Range distribution, Movement ecology, Biotelemetry, Data analysis

2.1 Introduction

Movement is a central and complex component of animal life (Nathan et al., 2008). Many metrics have been developed to quantify movement. Two of the most common measurements are residency and space use, like core and home range areas. Residency can be defined as an individual's preference for an area where it decides to stay over a specified and usually extended period, and is mostly occupied uninterruptedly (Chapman et al., 2015). Nevertheless, brief departures from this area can occur and are considered part of resident behaviour. Animals can also display site fidelity if, despite being absent for a long time they return to the same area, which is different from the brief forays to other places mentioned before (Chapman et al., 2015). The duration of this absence is not a fixed value and is allowed to vary, but is generally expected to be similar or longer than the residency in said area (Chapman et al., 2015). Finally, how we define residency can therefore be also adapted to a specific time frame defined by the analyst. The concept of residency, which prompts familiarity with the distribution of resources in a defined area, is tightly related to home range (Piper, 2011).

Although there is no universal definition for the concept of home range (Powell, 2000), one of the most frequently cited ones is that of Burt (1943):
"*that area traversed by the individual in its normal activities of food gathering, mating, and caring for young. Occasional sallies outside the area, perhaps exploratory in nature, should not be considered as in part of the home range*." […] "*The size of the home range may vary with sex, possibly age, and season.*"

Home range estimation is an attempt at quantifying an animal's relationship with its environment and is a challenging task (Powell, 2000). This is commonly done by modelling space use to evaluate how an animal occupies space and is influenced by environmental and biotic factors (Kie et al., 2010; Powell and Mitchell, 2012; Sanderson, 1966). Conventionally, two levels (or isopleths) of space use are reported, the core or 50% area (Ewer, 1968), which refers to the most frequently visited part of a range that contains the features most important to the individual, and the home range or 95% area (Jennrich and Turner, 1969), which fits the traditional definition of home range. However, despite vast technological improvements in acoustic telemetry, no existing technique allows recording continuous long-term data without gaps or errors, and home range should be studied using methods that include these sources of uncertainty (Kie et al., 2010). Examples of this are location error and the variation in detection range of acoustic

receivers (hereon “receivers”), gaps from irregular or spaced out sampling, and missing data resulting from technical errors like code collisions, loss of receivers, battery failure, among others (Kessel et al., 2014b; Melnychuk, 2012; Payne et al., 2010). Home range estimation methods need to be objective, repeatable, and make biological sense (Powell, 2000). Disagreement about what measurements satisfy these criteria has led to the development of several methods over the years, and new ones are regularly emerging. The approach of most home range estimators can be classified into two general categories: they can be either geometric, which is based on constructing hulls to outline the animal’s home range and lack a probabilistic basis, or statistical, some of which use utilization distributions, which describes the intensity of use given to different areas by an animal (Fleming et al., 2015).

The study of movement ecology in aquatic environments has been historically challenging, however, acoustic telemetry has helped overcome this and is one of the most widely used methods nowadays (Hussey et al., 2015). A passive acoustic telemetry setup is commonly composed of three main elements: receivers, acoustic transmitters (hereon, transmitters or tags), and individuals we wish to study. Each individual is fitted with a transmitter that emits a uniquely coded signal. When a tagged animal comes into the detection range of a receiver, the emitted signal is picked up and stored, along with the time and date of detection and any additional information the specific tag model might collect, such as pressure, temperature, or acceleration. To collect this information receivers are deployed at known locations to create a detection array throughout an area of monitoring interest. Receivers in these configurations usually have overlapping detection ranges for position estimation purposes, to monitor all movements in an area, or to act as gates to detect of crossing movements (Heupel et al., 2006). Some systems can be adequately covered by a comprehensive network of receivers with overlapping detection ranges, which allow triangulation or multilateralization of the acoustic signals to calculate a position and derive a path, which is a special case of acoustic telemetry providing precise positions. The main advantages of acoustic telemetry are the ability to constantly and simultaneously monitor many active tags, and its cost-effectiveness considering a running array’s low maintenance effort and the amount of data it can provide (Heupel et al., 2006).

Like any methodology, it also has some limitations that should be accounted for. Detections cannot be recorded in areas out of the detection range of the receivers, which can bias the estimated area use of the tagged animal if it is present in areas where it cannot

be detected. The fate of undetected animals with active tags is in most cases undetermined, as it can be attributed to different reasons, e.g., Klinard and Matley, (2020). Additionally, while the successful detection of a tag on a receiver confirms its presence within detection range, the distance from the receiver, and the position of the animal, are unobserved. Finally, the detection ranges of receivers fluctuate unpredictably in four dimensions with environmental noise, water stratification resulting from temperature and salinity gradients, and other environmental factors (Kessel et al., 2014b; Payne et al., 2010).

This review showcases some of the estimators of position, residency, and space use with a focus on their application to data derived from passive acoustic telemetry systems. This way, we hope to provide background to guide a more thorough selection of the method(s) that better fit specific research objectives in acoustic telemetry. Some of the described methods were tested using a sample of tracking data from thornback rays (*Raja clavata*) and a common stingray (*Dasyatis pastinaca*). These data sets were used to illustrate the output of some of the methods and in some instances to show differences between them. However, it must be noted that since real life data is being used, not all differences described for each method might be noticeable in the figures.

2.2 Methods

The search for literature where residency, position, and home range estimation methods were described and/or applied was performed using Google Scholar. The methods for each of these three categories (position, residency, and space use estimation) were looked for with a set of keywords that were used in varying combinations. Some keywords were used in all searches (either “acoustic telemetry”, “acoustic tracking”, or “acoustic monitoring” with “estimation”) which were used in combination with words exclusive to each of the three search categories. The keywords exclusive to residency were “residence”, “residency”, “index”, and “site fidelity”; those exclusive to position estimation were “positioning” and “fine scale”; while the exclusive words for the home range search were “home range”, “contour area”, “core area”, and “home range area”. Additional literature was also drawn from the citations in the manuscripts found using Google Scholar.

2.3 Abacus plots

Abacus plots or calendar plots are an informative and simple way to undertake initial explorations of acoustic telemetry data and obtain a general idea of the residency of each animal, and even dispersion in some cases. The frequency and spread of detections can be visualized over time like a chronogram, which can provide an idea of how many times each individual was detected, their permanence in the study area and coarse movement patterns among receivers or areas in the array. In an abacus plot, time is displayed on the X-axis and the Y-axis represents either receivers or tagged individuals on individual lines, over which detections are represented as dots (Figure 2.1). However, this provides no information about the spatial configuration of the array. For linear systems such as rivers, longitude or latitude may be replaced by receiver number to generate a spatial abacus plot. Otherwise, a best practice would be to sort receivers by some spatial metric such as distance from a point of interest. Single-individual plots feature the receivers at which each animal was detected, showing the movement across receivers, while plots with more than one animal separately present each animal's cumulative detections. This latter format trades detailed information of movement between receivers for a more general view by condensing all detections into a single figure.

More information can be added in many ways to facilitate the identification of patterns. Detections can be colour-coded to include spatial or temporal data, dot size can be set to represent the number of detections in a day, or when receivers are displayed on the Y-axis dot size can represent the number of different tags detected within a defined time window. Spatial information can be included by coding detections according to receivers or sub-arrays of a particular subsection of the full array at which the animal was detected. Colour coding can follow seasons or day/night regimes and will ultimately depend on the time range of the data. Finally, both spatial and temporal information can be combined for example by colour coding detections by area and shading the background with different colours to reflect seasons of the year or time of day. These plots can also be used to identify unusual detection patterns, for example in the event of capture by fishing or post-surgical mortality or tag loss (Klinard and Matley, 2020; Tickler et al., 2019), even in the absence of predation or accelerometer tags to support it (Green et al., 2021; Weinz et al., 2020).

2.4 Residency estimation

2.4.1 Residency index

The residency index (I_R) has two forms. The total number of days the animal was detected (D_d) can be divided by either (1) detection interval, the number of days between first and last detection (D_i) or (2) monitoring or study interval, the total number of monitoring days in the study (time between tagging date and last monitoring day) (D_t) (Eq. 1). The resulting value fluctuates from 0 (no residency) to 1 (full residency) (Afonso et al., 2008). Residency can be calculated at any spatial or temporal scale, as D_d can correspond from the entire array to individual receivers. Similarly, data can be partitioned into timeframes to calculate seasonal or monthly residency. This residency index can be adapted to represent other time frames, like the number of hours in which at least one detection was made per day.

Eq. 1 $\quad (1.1)\ I_R = \frac{D_d}{D_i} \qquad (1.2)\ I_R = \frac{D_d}{D_t}$

Both forms of the residency index can be interpreted differently and present some considerations (Cochran et al., 2019). In equation 1.1, using D_i accounts for tag loss, which ensures the calculation includes the period for which one knows the animal was alive and the tag operational. It represents a maximum residency value (Cochran et al., 2019). The approach of equation 1.2 is more conservative and gives a minimum residency value. The study period duration D_t is used to estimate the index and assumes that throughout it the animal was alive and detectable when in range.

However, equation 1.1 can in some cases overestimate residency. When a short detection interval is obtained (first and last detection days are close to each other), a high residency index for that period is obtained. Unless it was the objective, this approach can be troublesome when the study period (D_t) is much longer. Similar residency values can be obtained for two individuals detected with a similar consistency in the study area but over two very different time intervals (Cochran et al., 2019). For example, similar values can be obtained by an individual detected 4 days over a period of 5 days and an individual detected 48 days over 60 days, however, the latter was present for a much longer time when considering the duration of the study period.

On the other hand, residency values estimated using equation 1.2 can be biased upwards for animals that were tagged later during the study (Cochran et al., 2019). Similarly, the absence of detections is assumed to be because the animal is out of detection range, without considering alternative scenarios that can lead to a cessation in detections.

The occurrence of events that lead to changes in detection patterns, like fishing or predation, can be assessed by observing individual detection plots (Green et al., 2021; Klinard and Matley, 2020; Tickler et al., 2019; Weinz et al., 2020). For example, an individual would suddenly cease transmitting after being fished, while suffering predation can produce a change in the detection pattern to reflect the movement of the predator. On the other hand, a different pattern is produced after events that result in the animal/tag to remain static on the bottom, e.g., natural mortality, partial/failed predation, fishing discard, tag loss. In this case, only the receiver(s) covering that area can detect the tag, so it stops being detected elsewhere. A static tag's detection frequency can also increase on account of being permanently within detection range. If these situations are unaccounted for, the real residency values can be artificially modified (e.g., increased by a static tag on the bottom).

2.4.2 Weighted residency index

The weighted residency index (I_{WR}) is composed of two fractions (Eq. 2) and ranges from 0 to 1. The first fraction corresponds to D_d divided by D_t, which is weighted by a second fraction, the period between first and last detections (D_i) divided by D_t (Lino, 2012). This formula can also represent residency at various spatial levels by adjusting D_d to represent the detections obtained at the chosen scale.

$$\text{Eq. 2} \qquad I_{WR} = \frac{D_d}{D_t} x \frac{D_i}{D_t}$$

If the tag lifetime is shorter than the total monitoring period, the value of D_t should be replaced with the tag lifetime (Abecasis et al., 2013). I_{WR} is sometimes preferred over I_R calculated as eq. 1.1 because it tends to reflect residency more accurately, for example, not overestimating cases of individuals with few but consecutive detections (Lino, 2012). This index is also more robust to periods without detections, which can arise for example from difficulties during receiver replacement (Lino, 2012).

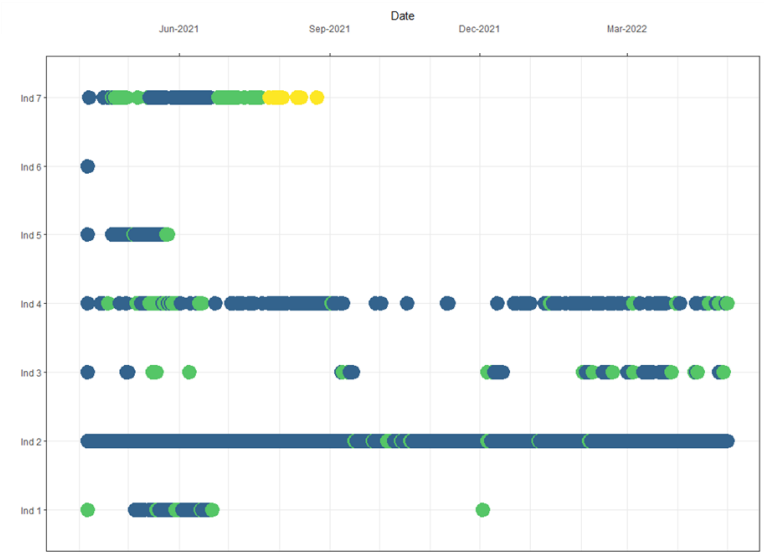

	D_d	D_i	D_t	I_R (eq. 1.1)	I_R (eq. 1.2)	I_{WR}
Ind 7	**75**	**141**	**393**	**0.53**	**0.19**	**0.07**
Ind 6	**1**	**1**	**393**	**1.00**	**0.00**	**0.00**
Ind 5	**36**	**50**	**393**	**0.72**	**0.09**	**0.01**
Ind 4	**150**	**391**	**393**	**0.38**	**0.38**	**0.38**
Ind 3	**62**	**389**	**393**	**0.16**	**0.16**	**0.16**
Ind 2	**393**	**393**	**393**	**1.00**	**1.00**	**1.00**
Ind 1	**48**	**242**	**393**	**0.20**	**0.12**	**0.08**

Figure 2.1: Abacus plot showing the detection patterns of seven *Raja clavata* individuals from 06/04/2021 to 03/05/2022. Their respective days detected (D_d), detection interval (D_i), monitoring/study period (D_t), and residency indices calculated with the three described fractions are also shown: I_R as eq.1 (D_d/D_i).; I_R as eq. 2 (D_d/D_i); and I_{WR} = (D_d/D_t) x (D_i/D_t). Colours illustrate how different arrays or different sections in the same array can be colour-coded to add extra information to the plot.

2.4.3 Continuous Time Residence

Detections are discrete events or samples of animal movement, which are continuous in time. Continuous time residence (CTR) calculates residency as a continuous event as well, while also considering the effects of small temporal scale biases and movement behaviour (Capello et al., 2015). Small scale bias can be caused by environmental noise, obstacles, transmission intervals between signals, and collisions in signal propagation. Accounting for these aspects can prevent, for example, assuming an individual is absent when its presence is masked by external factors. Similarly, at larger temporal scales this method also considers that animals that consistently reside within a particular area can still engage in natural behaviours that lead out of detection range (e.g., diel movement patterns). The goal is to avoid wrongly interpreting an apparent absence as a true absence product of the temporal scale at which residency is being measured (Capello et al., 2015).

This CTR approach generalizes the method by Ohta and Kakuma, (2005) of calculating residency as the continuous presence without absences longer than 24 hours around fish aggregating devices. Instead of using 24 hours, the period is defined by applying a statistical procedure to the data, also considering the previous knowledge of

the researcher(s) (Capello et al., 2015). This predefined period is called Maximum Blanking Period (MBP) (Soria et al., 2009), the maximum time allowed to pass between two consecutive detections before assuming the individual left the area. CTR is then interpreted as a time frame during which an individual was detected without being absent for longer than the MBP (Soria et al., 2009). In this interpretation, an ongoing CTR is composed of a series of successive detections separated by a time < MBP and ends when the time between a detection and the next one is > MBP, or when the second detection occurs in a place out of the study area. Both events mark the last detection of an ongoing CTR, and also the first detection in the next CTR (i.e., the detection that ended the CTR) (Capello et al., 2015). The MBP should always have a high enough extension to ensure a tag is detected even if a signal collision occurs (Soria et al., 2009), and the optimal value will depend on the research question and the species. MBP is determined by following a statistical analysis akin to constructing a survival curve, which reflects the probability of the CTR being interrupted by one of the two cases mentioned above. For this, the data is analysed using incremental [1:N] MBP values (N should be higher than the timescale of interest), yielding several CTRs. The objective is to determine the optimal MBP after which the survival curves stabilize. This indicates the timescale at which the confounding elements no longer influence the estimation of residency times and the MBP value that should be used in the calculation of CTR (Capello et al., 2015).

Some examples of MBP values studies have used can be divided into fine-scale CRTs, which have MBPs from 20 minutes to one hour and have been used in studies on bull sharks and tunas (Forget et al., 2020; Govinden et al., 2013; Mourier et al., 2021; Soria et al., 2019; Véras et al., 2020) and large-timescale CRTs with an MBP of 24 hours, mostly applied to studies on residency of tunas around fish aggregating devices, e.g. (Govinden et al., 2021; Pérez et al., 2020; Véras et al., 2020). Such differences highlight the importance of the research question in defining the MBP. Similarly, the time between two consecutive CRTs is defined as large-scale and fine-scale continuous absence time (CAT), respectively (Capello et al., 2015; Govinden et al., 2021). This approach to estimating residence has also applications in social network analysis using automated telemetry systems, e.g., (Shizuka et al., 2022). This residency estimate can be obtained using the log rank statistical test (Harrington and Fleming, 1982), implemented in the *survival* R package (Therneau, 2015), e.g., (Baidai et al., 2020; Tolotti et al., 2020).

2.5 Pseudo-position estimation from passive acoustic telemetry data

Generally, a successful tag detection is a confirmation that the individual carrying it was within the detection range of a receiver, which is accompanied by a date and time stamp. However, the positions associated with these detections are usually as precise as the detection range of the receiver. Overcoming the lack of fine-scale precision of passive acoustic telemetry is therefore a mandatory first step when using most space use estimators. Locations of greater accuracy also permit an improved view into the position of the tagged animals around critical areas, such as marine protected area borders, or while engaging in behaviours of interest that might have taken place, like spawning, feeding, or refuging. Position estimation methods that use the raw data to obtain more precise position estimates for this end have been developed (triangulation or trilateralization methods), and some will be described in the following section. Before this, it needs to be noted that in the same way a tag can go undetected despite being within detection range, false-positive detections can also happen. These occur when a receiver detects a signal with a tag ID code that was generated from the collision of two or more tags and their frequency, among other reasons, depends on the number of tags simultaneously within range of the receiver (Simpfendorfer et al., 2015). A false detection can produce a code tag ID that is either different or identical to a code tag ID in the study. Cases where there is no match with a deployed transmitter, are straightforward to detect and exclude, yet these might correspond to a tag of a different study. False code tag IDs identical to one of the tags deployed for the study are harder to detect. False detections do not occur frequently (Simpfendorfer et al., 2015), however, ways of filtering them out exist. For example, this can be done by removing single detections within a defined timeframe, using maximum speed estimates of the study animal (Heupel et al., 2010), or custom estimates of precision (Smith, 2013).

2.5.1 Center of activity

A center of activity (COA) **(**Simpfendorfer et al., 2002) is a point on a two-dimensional plane whose X and Y coordinates represent the weighted average position of the group of locations, during a given time, used to estimate it (Hayne, 1949). Therefore, rather than a precise location in time, a COA is an average position over a defined period (Δt) selected by the analyst. The detection probability of a transmitter is assumed to increase linearly with proximity to a receiver, as does the number of times the transmitter

is detected during Δt. Importantly, as an average position, a COA can represent a location where the animal never actually was. Weighted means are obtained either with an arithmetic (Eq. 3.1) or harmonic approach (Eq. 3.2) and the following variables: number of receivers in the array (n); the number of receptions at the *i*th receiver during Δt (R_i); the X coordinate (X_i) and Y coordinate (Y_i) of the i^{th} receiver. The original paper reports separate equations for each X and Y coordinate, here these should replace the general "coordinate" variable (C) depending on which weighted mean is being calculated. This in turn yields the weighted mean for each coordinate ($\bar{X}_{\Delta t}$ and $\bar{Y}_{\Delta t}$, both represented here by $\bar{C}_{\Delta t}$).

Eq. 3.1 $$\bar{C}_{\Delta t} = \frac{\sum_{i=1}^{n} R_i C_i}{\sum_{i=1}^{n} R_i}$$

Eq. 3.2 $$\bar{C}_{\Delta t} = \frac{\sum_{i=1}^{n} R_i}{\left(\sum_{i=1}^{n} \left(\frac{1}{\sum_{i=1}^{n} R_i C_i}\right)\right)}$$

This method is sensitive to the selection of Δt, therefore it requires evaluation before performing calculations, taking into consideration factors such as signal emission frequency, animal activity (rate of movement, speed), and external interferences from topography and vegetation (Simpfendorfer et al., 2002). Too brief windows will not contain sufficient detections to obtain an estimate, while protracted periods can result in excessive movement by the tracked animal, which affects the precision of the activity center as well as the number of positions generated for analysis (Simpfendorfer et al., 2002). However, vast quantities of locations are normally obtained with acoustic telemetry because tag transmissions delays tend to be about 90-180 s, so a low sample size could potentially become an issue in the event of analyzing small subsets of the total data (Boyle et al., 2009). Simpfendorfer et al., (2002) also recommend that receivers should have overlapping detection ranges, arranged in a grid of triangles, squares, or hexagons. Users should be aware that the spatial configuration of receivers will dramatically affect the COA calculation and further testing of this method is recommended to provide more explicit advice on how to proceed for subsequent analysis. Position estimation using COA is a widely used method in passive acoustic telemetry. Users may wish to use pseudo-positions to replace the need for actual positions for methods such as kernel density estimation that require them. Calculation of the COA can be obtained using R packages like *V-Track*'s Animal Tracking Toolbox (ATT) (Campbell et al., 2012; Udyawer et al., 2018), however, users can easily calculate this metric by simply grouping detections by individual ID and a time window and calculating the mean longitude and latitude. Figure 2.2 illustrates the 30-minute COAs obtained from the *Dasyatis pastinaca* sample dataset that will be used in the paper.

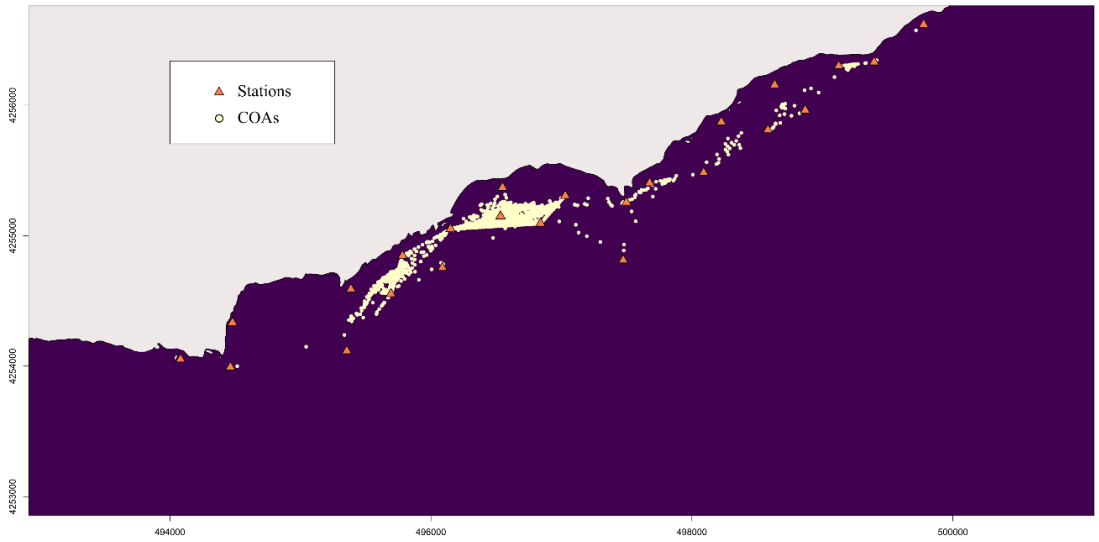

Figure 2.2: Centers of activity (COAs) obtained for the *Dasyatis pastinaca* dataset, using a period of Δt = 30 minutes (each yellow circle) from the sample dataset collected by a coastal acoustic receiver array (orange triangles). Land is grey and water is dark blue.

Hedger et al., (2008) evaluated the local polynomial regression or Freidman's SuperSmoother (Friedman, 1984) as a non-parametric alternative to the weighted mean COA. An advanced method of calculating COA has been developed by Winton et al., (2018) using the Bayesian spatial point process (SPP) model that also allows accounting for the variation of detection probability over time, yet the authors acknowledge that the computational expense of the method may make it inaccessible to many users. Detections of a tagged animal are viewed as samples of an underlying spatial process that depends on (therefore is biased by) the observation process, which is composed of the position and detection range of the receivers used to detect the tags. Receiver- and time-related variations in detection probability can be included in the SPP model, by integrating data from stationary test tags in the study area. Including this information improves the model, as it can reveal otherwise overlooked fine-scale movements. These characteristics make it a more computationally demanding process than the mean weighted COA, however, it is comparatively less biased, especially when including data on variation in detection probability. Detections that are only recorded by peripheral receivers in the array (i.e., from individuals present in the area but not within the array) are also used, and lower errors are obtained for position estimations in these areas. COAs can be estimated with the SPP model using the R package *TelemetrySpace* (Winton et al., 2018). An important

difference between this method of estimating pseudo-positions and the triangulation-based methods in the following section is the area where a calculated pseudo-position/position can be found. COA-based estimation can only place a calculated pseudo-position within the area confined by the array, while triangulation-based methods can allocate them to areas out of receiver range, although with lower precision (Smith, 2013).

2.6 Triangulation or trilateralization

2.6.1 Proprietary positioning systems

2.6.1.1 Vemco (now Innovasea) Positioning System

The Vemco Positioning System (VPS) is a fine-scale positioning system that estimates positions by using omnidirectional receivers and fixed synchronizing transmitters, or sync tags (Espinoza et al., 2011; Smith, 2013). Such high-resolution tracking systems have allowed greater detail in residency and home range estimation, and also to venture into other areas such as behavioural studies, as shown by (Orrell and Hussey, 2022).

Synchronization tags that transmit at fixed intervals are placed at known locations to help synchronize receivers and are deployed either over each receiver (Piraino and Szedlmayer, 2014; Smith, 2013) or in a way that one sync tag's detection range encompasses receivers in the aforementioned groups of three (Espinoza et al., 2011). Positions are estimated based on hyperbolic positioning or time difference-of-arrival (TDOA). The difference in detection time between pairs of receivers indicates which receiver detected it first, and how much time passed until it was detected by the second receiver, which is used to calculate the distance of the tag to each receiver. Distance difference and receiver positions are used to obtain an approximate location for the transmission in a hyperbolic position system. VPS calculates one basic position for every possible group of three receivers that detected a given transmission, which is then combined to calculate a synthesized position (Smith, 2013). Positional error is expressed as Horizontal Position Error (HPE), a relative unitless estimate of error sensitivity used to retain the highest quality estimated positions (Espinoza et al., 2011; Roy et al., 2014), which is not comparable across studies because calibration is specific to each study (Smith, 2013). Higher HPE means a calculated position is more sensitive to measurement errors, hence, a lower HPE is preferred (Piraino and Szedlmayer, 2014; Smith, 2013). The

accuracy estimation of calculated positions requires stationary transmitters at known locations to compare with (Smith, 2013). Even though high-resolution of positions are obtained with systems like VPS or PinPoint, the data may still need to be filtered before analyzing it as suggested by some authors (e.g., Meckley et al., 2014; Roy et al., 2014). For example, filtering VPS data by the HPE can greatly reduce the positioning error in the dataset (Meckley et al., 2014; Roy et al., 2014).

More recently, Innovasea introduced high residence (HR) tags and receivers, which can be combined into an HR-VPS system that operates at 180 kHz (Guzzo et al., 2018), allowing to simultaneously monitor a higher number of tags. Such characteristics are ideal when many animals aggregate because of migratory, reproductive, feeding, or geographic reasons (Guzzo et al., 2018). However, it must be noted that frequencies above 100 kHz are greatly attenuated by salt water (Ainslie and McColm, 1998), which affects transmitter efficiency. Vemco/Innovasea developed the software Vemco User Environment (VUE)[1], which centralized many tasks. Among these, it is used to collect, organize, and visualize the data, also allowing to run some initial analyses. VUE is also used for tasks like receiver clock synchronization and memory clearing. From here, data sets can be exported to be used in other programs.

2.6.1.2 Thelma PinPoint Positioning System

PinPoint[2] is a service provided by Thelma Biotel (Trondheim, Norway) that can operate in two and three dimensions, depending on whether the tags are equipped with depth sensors. For this method, receivers in the array are ideally organized in equilateral triangles to maintain the same distance and angle between neighbouring receivers. Thelma runs a service that provides the best deployment configuration of the receivers in the array to obtain the best coverage of the study area.

Like other high precision positioning systems, PinPoint uses time difference of arrival to calculate fish positions, with synchronized clocks and temperature sensors in the receivers. Error sensitivity in the calculation of positions (horizontal dilution of precision, HDOP) is estimated by Thelma (as Innovasea's HPE). This is done by placing a grid of points around the receiver array, for each of which the signal travel time to reach each receiver is calculated. Then a random time error is added to each position, yielding simulated travel times which are replicated several times with a new random error for

[1] https://support.vemco.com/s/downloads
[2] http://www.thelmabiotel.com/service/pinpoint/

every grid point. The deviation between these calculated positions and the known position is then referred to as HDOP. Higher HDOP values indicate higher error sensitivity (Muñoz et al., 2020).

Thelma also developed the software ComPort[3] to upload the data, visualize it in several ways, and do preliminary explorations. This software can also be used to configure receivers and manage the data in an SQLite database, allowing to clean and filter it, for example, to remove false detections before analysing it with software such as R. Filtering can be done using the HDOP, commonly defined as being proportional to a location error's standard deviation, with higher HDOP values indicating greater variance (Misra and Enge, 2006).

2.6.2 Open-source positioning systems

2.6.2.1 Lotek Code Division Multiple Access

The Lotek MAP acoustic telemetry system is based on the Code Division Multiple Access (CDMA) technology, used to enhance GPS precision and to provide many users simultaneous use of a cellular network also used in acoustic telemetry (Cote et al., 1998). Central receivers are used to monitor, clock-synchronize, and store the information of additional hydrophones. CDMA systems also achieve higher sampling rates (faster pulse bursts), better code discrimination in cases of high noise environments, multipath signals (detections that did not travel in a straight line between tag and receiver) or overlapping signals, and lower signal-to-noise ratio threshold, meaning signal power does not need to be much stronger than noise power. Moreover, signal output appears to be less affected by distance compared to other tags (Biesinger et al., 2013). These characteristics allow to simultaneously monitor a higher number of transmitters compared to pulse-position coding (Cooke et al., 2005). CDMA telemetry can provide data at a broad arrange of spatial (across a study area to sub-meter) and temporal scales (seasonal to seconds) (Hanson et al., 2007). For example, this suits studies of fish activity near boundaries, like in an existing or proposed reserve (Cooke et al., 2005), giving the method applicability in conservation and management. This system uses hyperbolic triangulation to position tags, which requires a theoretical minimum of three receivers to simultaneously detect a tag to calculate a two-dimensional location (Niezgoda et al., 2002).

[3] http://www.thelmabiotel.com/software/

More control and insight into the data filtering process and quality checks are possible as these are done by the researcher using the company's software to manage information, estimate transmitter positions, and evaluate performance, unlike with VPS (Biesinger et al., 2013). This process filters out position estimates that fall in areas known to be inaccessible to the animal (e.g., a fish on land), that arise from impossible movements like excessively fast speeds, or are of insufficient precision. This is performed using two measures, dilution-of-precision (DOP) and reliability index (RI). DOP predicts precision levels for a given receiver array design and maps the results. On the other hand, the RI is indicative of the effective contribution of all receivers to a calculated position (Niezgoda et al., 2002). During the study design, mathematical modelling, DOP, and RI are used to maximize the position estimate precision, allowing to objectively predict data quality and select an appropriate array design (Niezgoda et al., 2002). Such high-frequency acoustic systems are generally thought to be less efficient in the marine environment compared to fresh water, but field tests have proven them to be useful when studying species of small home range size (Aspillaga et al., 2021).

2.6.2.2 Yet Another Positioning Solver

Many manufacturers obtain estimate positions and their associated errors using methods that are commonly unknown to the researchers, resulting in lower control over the analysis process and hindered comparability across studies (Baktoft et al., 2017, 2019). Yet Another Positioning Solver, or YAPS (Baktoft et al., 2017), is one of the newest fine-scale positioning estimators and uses time of arrival calculations to position tags in a receiver grid. The implementation seeks to maximize the utilization of data in a transparent and open source way that applies to all acoustic telemetry brands and indeed to any acoustic signal that can be multilateralized among stations (Baktoft et al., 2017, 2019). An associated R package, *yaps* (Baktoft et al., 2019), is available on CRAN and in ongoing development on GitHub[4].

The workhorse of YAPS is the synchronization model, which relies on the user to create a list of data frames including the receiver locations with corresponding sync tags (sync tags are assumed to be attached to each receiver) and sync tag detection data. The synchronization tag detections within the network will determine the suitability of the design for triangulating animal positions in the next step. The sync model residuals can

[4] http://github.com

be evaluated by the user and tuned to optimize performance. The synchronization model is then applied to the remainder of the data such that receivers are operating on the same clock and times of arrival at receivers are exact.

Once the receivers are synchronized, the analyst can generate time of arrival estimates and fit the yaps function to the data, typically in chunks separated into one individual per day. Instead of using time-differences of arrival (TDOA) to obtain position estimates as other position estimators (*e.g.,* VPS), YAPS directly uses each location's time of arrival (TOA) at each receiver, which allows taking fuller advantage of the data. YAPS does not require a signal to be detected by at least three receivers, avoiding information loss by discarding detections. Additionally, instead of operating like a point-by-point positioning model that calculates each position separately, YAPS calculates tracks directly, fitting a movement model to the raw detection data (Baktoft et al., 2017). A state-space model is applied to the TOA data, composed of 1) a process model and 2) an observational model. The process model describes the system's dynamics and the transmitters' coordinates over time, assuming a random walk between transmissions. Estimations are performed for transmission time (i.e., time of signal emission), transmitter coordinates, and speed of sound (Baktoft et al., 2017). The latter, and arrival time at a receiver, are used to calculate the time of signal emission. The observational model relates unobserved processes to the data. It calculates distances between the transmitter position at the time of signal emission and the position of all receivers, relating the observed time of the signal. Finally, residuals between observed and predicted times of transmission arrival are defined, accounting for detections from multipath propagation. A Maximum Likelihood analysis selects the track with the lowest error (Baktoft et al., 2017).

An advantage of YAPS is that the inclusion of a movement model fitted to the raw TOA data yields biologically sound position estimates (Baktoft et al., 2017). Compared to VPS, YAPS has been shown to yield more position estimates per track, to better correct reflected signals and model fish behaviour when the fish are not within the acoustic array but still within range, and to be more robust in highly reflective environments (Vergeynst et al., 2020b). However, since a movement model is directly applied to the raw data, YAPS requires a minimum number of total transmissions, unlike point-by-point estimators (Baktoft et al., 2017; Vergeynst et al., 2020a). YAPS also requires receivers to be synchronized before analysing the data, which is simultaneously done for all receivers, allowing to reduce the amount of error compared to approaches like sequential

synchronization (Baktoft et al., 2019). A critical factor for the performance of YAPS is knowing when the next signal will be emitted, and constant intervals or known random intervals significantly improve the accuracy of position estimates over unknown random intervals, as some manufacturers operate (Vergeynst et al., 2020a). When ping sequences are not known, a random burst interval is set as default. YAPS should be iterated so that each fish day is run multiple times with the best fit, determined by the $obj value returned from the output. The user may determine how many runs are optimal, but 5-20 could be sufficient, with up to 50 for difficult tracks (Baktoft, personal communication). Poor data may never fit and will have to be discarded. Despite its advantages, YAPS is time-demanding and requires considerable work and expertise on the part of the analyst along with access to sufficient computing resources (Vergeynst et al., 2020b). Although guidelines have been developed (Baktoft et al., 2019), receiver array synchronization has proven to be challenging for many users (Baktoft et al., 2019; Vergeynst et al., 2020b).

2.6.3 Accuracy

The accuracy of the position estimates obtained with triangulation-based systems is much higher than that of COA-based methods. A table compiling the accuracy of the former is available in the supplementary material of Manicacci et al. (2022).

2.7 Geometric, hull-based estimators

2.7.1 Minimum Convex Polygon

Minimum Convex Polygons (MCP) (Mohr, 1947) are among the first home range estimation methods, which represent a two-dimensional maximum area estimate for a group of locations obtained by tracing the smallest polygon possible using only the exterior points and interior angles under 180° (Figure 2.3.a). Polygons may be drawn using raw detections that represent the receiver coordinates or based on calculated pseudo-positions or positions. Because of their simplicity, MCPs are fast to compute and have been widely used for decades, which has provided much comparative material (Laver and Kelly, 2008; Nilsen et al., 2008). Polygons, and MCPs in particular, are sometimes used to estimate the maximum area used by an animal (Nilsen et al., 2008). The International Union for the Conservation of Nature currently applies it as a proxy to calculate the maximum extent of occurrence, a measure of extinction risk (IUCN, 2012).

Using MCP in these assessments has been thought to ensure there is consistency among comparisons (Joppa et al., 2016), although alternative methods that deal better with range discontinuities and are not biased with increasing sample size have been proposed, such as α-hulls (Burgman and Fox, 2003). The polygon-based approach has been said to be too simple and fails to correctly characterize and predict the distribution of species, e.g. (Peterson, 2017; Peterson et al., 2016) while others support their use, especially in data-poor situations, e.g. (Pimm et al., 2017).

Yet, MCPs present several drawbacks (Grueter et al., 2009; Powell, 2000) and some even advise against their use (Laver and Kelly, 2008). Only considering the outermost locations dismisses all internal data points and the information these might convey, and an even use of the area within the polygon is assumed (Powell, 2000). This precludes detecting heterogeneities in animal movement like preferred and unused areas, and boundaries to movement. MCPs are sensitive to habitat shape, location error, and distribution of sampling effort in space and time (Burgman and Fox, 2003), extreme location points from sporadic forays into adjacent areas (Grueter et al., 2009), and non-compliance with location independence, which results in the underestimation of home range (Swihart and Slade, 1985a). In acoustic telemetry, MCP dimensions will be limited by the array design, as areas excluded from receiver coverage cannot be included in the polygon, which may dramatically misestimate the dimensions of the polygon in a way that misinforms the ecology of the animal. Some of these shortcomings can be addressed in a few ways. Constructing MCPs using 95% of the data that form the smallest polygon reduces the inclusion of rarely or not visited areas and accounts for the sensitivity to extreme locations (Fashing et al., 2007; Powell, 2000). Creating monthly or seasonal polygons can be a more biologically-sound approximation to space use (Grueter et al., 2009). Finally, since MCPs are prone to sample size bias, communicating details about this in the study can help to produce more comparable results (Börger et al., 2006; Burgman and Fox, 2003; Fashing et al., 2007; Nilsen et al., 2008; Worton, 1987).

2.7.2 Characteristic hull polygons

The characteristic hull polygons (CHPs) method (Downs and Horner, 2009) is a hull construction approximation based on the characteristic shapes algorithm (Duckham et al., 2008). CHPs are obtained by creating triangles by Delaunay triangulation of neighbouring points, which favours the construction of more regularly shaped triangles. Home range estimates are obtained by removing the triangles with the largest perimeters

and retraining 95% of the smallest triangles. Other features like area can be used as a sorting criterion, but perimeter allows to eliminate the slenderer triangles with exceptionally acute angles that normally form at the boundaries of the used area. An MCP equivalent is obtained if no triangles are removed (Downs and Horner, 2009). Point distribution of the data is better represented using Delauney triangles than with MCPs, as the former method can build non-convex hulls and more complex shapes (Downs and Horner, 2009; Duckham et al., 2008) (Figure 2.3.b). CHPs can also have "holes" and be composed of disjoint polygons, which can accommodate distribution patterns of animals that avoid certain areas. CHP are fairly robust to sample size variations and to inhomogeneous point distributions (Downs et al., 2012) and do not overestimate areas of use like MCP (Downs and Horner, 2009; Olsen et al., 2011). However, they perform relatively worse when home ranges have a concave, or convex shape compared to linear, disjoint or perforated, but this could be related to the process of removing triangles (Downs and Horner, 2009). Despite its advantages, CHP are not as studied and frequently used as MCP (Downs and Horner, 2009; Quinton, 2016). The Delaunay triangulation required for producing CHP can be implemented in many GIS softwares (Downs and Horner, 2009; Duckham et al., 2008), such as standard functions in ArcGIS[5] (ESRI, Inc., requires subscription purchase) e.g., (Downs et al., 2012; Olsen et al., 2011) and also QGIS[6] (free and open-source). In the former, the hot spot analysis with rendering spatial statistical tool can be used as a more objective way of selecting triangles (José-Domínguez et al., 2015).

2.7.3 Local Convex Hull (LoCoH) methods

The k-LoCoH or k-nearest neighbour convex hull (k-NNCH) is an extension of the MCP in which space use is estimated by constructing local convex hulls around each point using its *k*-1 closest neighbours, akin to small MCPs. The obtained hulls are then ordered from smallest to largest and merged to create area isopleths that contain a proportion of the data (e.g., 50%, 95%) and utilization distributions (UDs) from the proportion of points contained in each local convex hull. This approximation allows to better account for boundaries produced by geographic features or other factors (Getz and Wilmers, 2004), but can take much longer to compute, increasing exponentially with the

[5] https://www.arcgis.com/index.html
[6] https://www.qgis.org/en/site/

size of the data (adehabitatHR manual, Calenge (2006)). Selecting the number of nearest neighbours (*k*) is user-defined and is a crucial step that follows the minimum spurious hole covering (MSHC) rule. Low *k* values generate coverings that contain "holes" that disappear as *k* increases. In real landscapes, such "holes" (or unused areas) can be produced by features like cliffs, mountains, lakes, and water edges, which represent restrictions to movement. Following this rule, the smallest *k*-value that produces a convex hull reconstruction with a shape that matches the study area of known topology (*i.e.,* known location of "holes") is selected. If the topology is unknown, large features can be identified to guide this process (Getz and Wilmers, 2004). Because LoCoH draws the kernel shape directly from the data, it tends to perform better close to boundaries than MCP and kernel-based methods (Getz and Wilmers, 2004; Lichti and Swihart, 2011; Scull et al., 2012). By not including unused areas, LoCoH methods are less prone to type I errors (to include unused areas in the estimate) than the aforementioned methods, although, in turn, this can increase the risk of type II errors (exclusion of used areas) (Lichti and Swihart, 2011; Ryan et al., 2006).

Two variations of k-LoCoH exist, the *fixed radius* r-LoCoH and the *adaptive* a-LoCoH (Getz et al., 2007; Getz and Wilmers, 2004) (Figure 2.3.c, 2.3.c2). They differ in the calculation process and sorting method of local hulls, but overall operate in the same way (Getz et al., 2007). The r-LoCoH uses all points within a radius *r* from a root point, resulting in hulls of similar size but may differ in the contained number of points. This is used to sort circles in descending order (hull area as the second criterion). On the other hand, a-LoCoH creates circles of variable size around root points of radius size depending on the cumulative distance from the root point to its nearest neighbours until it is equal or as close to the defined maximum cumulative distance (*a*). This way areas with higher point density (or of higher use) will have more points at shorter distances from the root point, resulting in smaller convex hulls, and vice versa. This can be used to identify range edges where points can concentrate, like shorelines or cliff edges (Getz et al., 2007). If the topology of the study area is known and unused areas can be identified, the MSHC rule can be followed to select *r* and *a* (Getz et al., 2007). Of the three, a-LoCoH is the best performing method (Getz et al., 2007; Scull et al., 2012), as it is more reliable in the absence of topological information, while r-LoCoH usually performs the poorest.

However, because movement information is ignored, UD estimates can be of lower resolution and present home range boundary biases compared to methods that include it (Benhamou, 2011; Benhamou and Cornélis, 2010). This drawback is addressed

by the Time Local Convex Hull (T-LoCoH) (Lyons et al., 2013), which integrates both temporal and spatial dimensions to serially correlates points in the construction of local hulls. The inclusion of timestamps during nearest neighbour selection and local hull sorting allows separating spatially proximate but temporally distant locations and local hulls. The nearest neighbour selection follows the time-scaled distance (TSD) metric, which transforms time into a third distance axis using a maximum theoretical velocity (v_{max}) and the dimensionless scaling parameter *s*. v_{max} can be drawn from biological studies, statistical models (Long and Nelson, 2012), or the maximum segment velocity in the data (Lyons et al., 2013). The elapsed time between two consecutive locations and v_{max} is used to obtain a theoretical maximum traveled distance (Lyons et al., 2013). The parameter *s* controls the importance of time in the modelling of space use: a higher value gives time more weight and setting *s* to 0 renders it equivalent to k-LoCoH. The value of *s* is subjective, yet it can be determined following guidelines (Lyons et al., 2013), and a more objective approach based on cross-validation has also been proposed to select both *s* and *k* (Dougherty et al., 2017).

Compared to hulls created without considering time, isopleths from TSD hulls better identify temporal changes in movement patterns and spatially overlapping but temporally differentiated resources. Unlike the Brownian bridge-based methods (covered later), which integrate time with a segment-based approach, TSD is calculated for all possible pairs of points (Lyons et al., 2013). As a result, points that are close in space, yet occurred in separate time frames are "pushed" away by this time-distance axis. In turn, the obtained local hulls share similar traits, as they also are local in space and time and the boundaries of resource patches that spatially overlap but are used at different times are preserved (Lyons et al., 2013). Local hulls created using the TSD method can be used to estimate the level of directionality in movement and time-use. The type of movement (*e.g.,* more sinuous, or linear) can be estimated by assessing hull elongation metrics to identify possible transit areas or of low resource value, while calculating time spent in an area (duration of use) and rate of revisitation an area has can be used to infer the type of use an animal gives to it (Lyons et al., 2013). Finally, local hulls can be sorted following one of several hull metrics (e.g. area, perimeter/area ratio, revisitation rate, duration of visit, date of root point) and combined to obtain isopleths that highlight different types of information depending on the objectives of the analysis (Lyons et al., 2013).

2.8 Density distribution probabilistic estimators

2.8.1 Kernel Utilization Distribution

Before describing this method, the concepts of Utilization Distribution (UD) and bandwidth or smoothing factor (*h*) need to be defined.

2.8.1.1 Utilization Distribution

This concept refers to the use of the observed location data points of an animal to create a two-dimensional relative frequency distribution in an area over a specific time (Van Winkle, 1975). UDs, therefore, allow the description of space use in terms of a probabilistic model to represent the probable location of an animal on a plane, which is used to estimate metrics such as home range (Van Winkle, 1975; Worton, 1989). UD is directly influenced by the smoothing factor or bandwidth used in kernel methods (Worton, 1989).

2.8.1.2 Smoothing factor or bandwidth

It is the standard deviation of the kernel, the extent to which a location is allowed to influence the home range estimation or the distance over which it is allowed to influence the total density estimate. It is central to kernel analyses, as it can have significant effects on results (Kie, 2013; Powell, 2000; Seaman and Powell, 1996; Wand and Jones, 1995). Its 1) value and the 2) number of bandwidths are user-defined.

1) Value: a higher smoothing factor (*h*) widens the UD over each data point and allows more distant points to have greater influence, increasing the overall home range size (Powell, 2000; Seaman and Powell, 1996; Worton, 1989). Higher *h* also smooths out sampling errors (for instance, related to telemetry error) and eliminates details at finer scales, retaining only the most notorious features (Powell, 2000; Seaman and Powell, 1996; Worton, 1989). Contrarily, a smaller *h* provides greater detail at small scales, yet tends to be more sensitive to measurement error (Powell, 2000; Worton, 1989). No universal method to determine the optimal *h* value exists (Worton, 1989), but several ways exist to determine it, like least-square cross-validation, reference bandwidth, ad-hoc choice of *h*, its variation $h_{\text{ad hoc}}$, direct plug-in, and solve the-equation (Eidous et al., 2010; Kie, 2013; Worton, 1989). In some instances, bandwidth is selected manually based on information about detection range in the array (March et al., 2010). Bandwidth can also be altered if space use estimates result smaller, separate isopleths, but having them form a single, continuous area makes more biological sense (Kie, 2013; Wand and Jones,

1995). This can be done using an ad-hoc smoothing parameter, which seeks the reference bandwidth value just before space use fractures or gaps appear (Berger and Gese, 2007; Kie, 2013).

2) *h* can either be fixed (one value for *h* is used) or vary according to point density. The former is also called global bandwidth and will result in a fixed-kernel analysis, while the latter is also known as local bandwidth and results in an adaptive-kernel analysis (Worton, 1989). Kie (2013) presents a detailed analysis of how bandwidth selection, sample size, and fixed- and adaptive-kernel estimates interact. The use of a fixed or a variable kernel has long been debated, yet studies have shown that the selection of one over the other does not influence bias and type I and II errors as much as the choice of h (Kie, 2013).

2.8.1.3 Kernel Utilization Distribution

Kernel utilization distribution (KUD) (Worton, 1989) is a non-parametric statistical method regarded as one of the most popular and best-known estimators in use (Laver and Kelly, 2008; Powell, 2000). KUD calculates the area of probability of finding an individual, similar to sampling a distribution of occurrence, by placing a kernel or probability density function (PDF) over each data point. Kernels can be visualized as a three-dimensional "hill" (Worton, 1989), whose shape and width (*h*) are user-defined (Powell, 2000; Worton, 1989). Kernel shape does not influence the results as significantly as the smoothing factor (Epanechnikov, 1969). Once parameters are defined and kernels are in place, a grid is positioned over the area to calculate estimates of density by averaging the densities of all kernels that overlap at each grid intersection (Worton, 1989) (Figure 2.3.d, 2.3.d2).

KUD is a straightforward method to estimate home range and has much supporting statistical literature, yet it presents important caveats. Locations are assumed to be uncorrelated, or independent of each other and identically distributed (IID) (Worton, 1987). While a sufficiently spaced-out sampling complies with this, it is unlikely to be the case with the high-rate samplings of acoustic telemetry. The inherent autocorrelation of movement data has been regarded as a valuable source of biologically relevant information (Cushman et al., 2005), and not meeting this assumption can result in biased results like underestimated home range sizes (Fleming et al., 2015; Swihart and Slade, 1985a). Since the PDF is applied in all directions around a point, areas that are not part of the animal's home range can be included, like areas around narrow trails whose

dimensions greatly differ from the selected bandwidth (Powell and Mitchell, 2012) or over impenetrable barriers. Other bias sources are sample size (Hemson et al., 2005), especially overestimation at low effective sample size (Girard et al., 2002), and point pattern shape (Downs and Horner, 2008). KUD is implemented in packages like *adehabitatHR* (Calenge, 2006), *ks* (Chacón and Duong, 2018), and *amt* (Signer et al., 2019).

2.8.2 Autocorrelated Kernel Density Estimation

The group of autocorrelated kernel density estimation (AKDE) methods is the generalized version of the Gaussian reference function KDE which addresses commonly encountered biases during space use estimation. Nowadays three methods exist, the AKDE (Fleming et al., 2015), area-corrected AKDE ($AKDE_C$) (Fleming and Calabrese, 2017), and optimally weighted $AKDE_C$ ($wAKDE_C$) (Fleming et al., 2018). AKDEs incorporate autocorrelation into range estimation, tackling KDE's assumption of IID data and space use underestimation. This and the associated confidence interval that is provided have improved accuracy in comparison (Noonan et al., 2019). Location independence, and avoiding underestimating home ranges, requires using a sampling periodicity that is above the autocorrelation timescale, or at least equal to the home range crossing time (the time it takes for an individual to cross the linear extent of its home range), which can vary greatly by species (Fleming et al., 2015). This means that given the same number of locations in one autocorrelated and one uncorrelated dataset, the former contains an overestimated sample and less positional information. To have similar positional information and be as informative, autocorrelated data would need to be larger and span for a much longer period (Fleming et al., 2015). Moreover, autocorrelation becomes stronger with more frequent sampling (Swihart and Slade, 1985a), which is mostly the case with acoustic telemetry. To explicitly include autocorrelation in home range estimation, AKDE requires the selection of a movement model that includes autocorrelation in the analysis and then uses a Gaussian reference function to calculate bandwidth. Currently, available movement models are an IID process with uncorrelated locations and velocities, Ornstein-Uhlenbeck (OU) process with correlated locations and uncorrelated velocities (Uhlenbeck and Ornstein, 1930), and an Ornstein-Uhlenbeck Foraging (OUF) process of correlated locations and velocities (Fleming et al., 2014a, 2014b).

AKDE's use of the Gaussian reference function creates a positive bias in area estimation, which is adjusted by the area-corrected AKDE ($AKDE_C$) (Fleming and Calabrese, 2017). It calculates the level of oversmoothing and corrects it to create improved area estimates, especially at low effective sample sizes where positive bias is strongest. As a result, the contour of the calculated areas is drawn towards where the data points are higher in density under all autocorrelation movement models (Fleming and Calabrese, 2017).

More recently, (Fleming et al., 2018) introduced the optimally weighted $AKDE_C$ ($wAKDE_C$) which optimizes estimates by correcting time-related sampling biases, *i.e.,* irregularly collected or missing data (Figure 2.3.e). Such issues can arise from equipment malfunction, signal loss related to habitat interference (common in aquatic environments), or behaviour, among others. This way the importance of the areas an individual visits is appropriately levelled by upweighting under-sampled areas and downweighting over-sampled areas (Fleming et al., 2018). Additionally, similar to Fleming and Calabrese, (2017), this approximation improves home range estimations from evenly sampled but small effective sample size data (Fleming et al., 2018). AKDE is included in the R package *continuous-time movement modeling* (*ctmm*) (Calabrese et al., 2016) and in the point-and-click graphical interface *ctmmweb* (Calabrese et al., 2021). Guidelines for the use of these estimators and the correction of the biases here described are compiled into a document that includes an R script (Silva et al., 2021)[7].

2.8.3 State-Space Models

Essentially, a state-space model (SSM) analyses movement data and integrates error correction, the calculation of metrics, and statistical analysis by combining 1) an observational model to statistically describe the sampling process and 2) a process or movement model, which relates to the description of the dynamics of movement in space and time. As a Hidden Markov Model with discrete hidden behavioural states, this method is useful to use movement data to infer behavioural modes and estimate the probability of being in a given behavioural state (Patterson et al., 2008).

The Ornstein–Uhlenbeck SSM (OU-SSM) (Pedersen and Weng, 2013) is a SSM adapted to estimate home range using acoustic telemetry data in which the observation model describes the probability of a receiver detecting a tagged animal. At a given time,

[7] https://ecoisilva.github.io/AKDE_minireview/code/AKDE_R-tutorial.html

each station in a receiver array will either record the presence or absence of a tracked individual, information which is used by the detection function to model positions and compared to other non-mechanistic methods (Hedger et al., 2008; Simpfendorfer et al., 2002) presents improvements in the estimation process (Pedersen and Weng, 2013). This function computes the most likely position of the animal at a given time by combining the presence/absence information from all receivers in the array, for which changes in detection probability over time can be accounted for (Pedersen and Weng, 2013). As a function of distance, at the time of successful detection, the likelihood of an animal's position is higher closer to the receiver that detected it. The detection function also incorporates positional information on undetected individuals, assuming they are more likely to be found in areas farther from the receiver (Pedersen and Weng, 2013).

Changes in detection probability over time produced by environmental interference, for example, day/night cycle, seasons, or temperature, can also be integrated into the model by collecting reference data at the study site. Not accounting for this can lead to misinterpretation of results (for example unaccounted diel change in detection range can be wrongly interpreted as the animal leaving during what is a period of reduced detection capability), however, this is not straightforward to incorporate (Pedersen and Weng, 2013).

Additionally, the movement model characterizes the dynamics of the tracked animal through space and time. The OU-SSM model implements a OU process (Blackwell, 1997), a modification of a continuous random walk model. It considers a fixed point of attraction that introduces a movement bias towards it, which can biologically be considered as the home range center and makes it suitable for studying species that are normally monitored with acoustic arrays (Pedersen and Weng, 2013). Furthermore, the SSM optimizes the position estimation at a given time by taking the information provided by other points that are proximate in time, obtaining a range of possible positions given a maximum speed. The SSM is applied as a spatial hidden Markov Model (Pedersen et al., 2011; Pedersen and Weng, 2013), with discrete hidden states (in this case, locations) generated by an unobserved Markov process. In a Markov process, the probability of a future state (the next location) is only dependent on its current and past state. This stochastic process can be of first-order, depending only on the current state, or of higher order, depending on the previous state or more (Patterson et al., 2008).

Later a Bayesian SSM (B-SSM) was introduced (Alós et al., 2016). The observational model calculates the detection probabilities based on the distance between

animals and receivers, also considering the effect of environmental factors (Alós et al., 2016). The process model or movement model is based on the OU-SSM (Pedersen and Weng, 2013) and, rather than an upgrade, is proposed as a Bayesian alternative to the frequentist approach of the OU-SSM (Alós et al., 2016). This combines existing knowledge (as prior probabilities) and data-derived information through maximum likelihood, to obtain the posterior distribution of the movement parameters and movement path (Alós et al., 2016). Positions are estimated by considering the previous position and the following movement parameters: position of the home range center at a given time (r^H), speed at which the individual moves in a fractal movement path of infinite distance covered at infinite speed through its home range or exploration rate of the home range in min^{-1} (k), and size of the circular home range (radius, r). The Bayesian SSM is computationally more demanding than frequentist SSMs, however, the R package *Template Model Builder* (Albertsen et al., 2015), fits SSM models to movement data and can compensate for this (Alós et al., 2016). Additionally, the supporting information of the manuscript includes code that can be used in R to estimate movement parameters (home range behaviour) and positions with acoustic tracking data (Alós et al., 2016).

2.8.4 Brownian bridge movement model

Brownian bridge movement model (BBMM, Figure 2.3.f) interprets data as a collection of consecutive, known locations and models a time-structured path to reconstruct the expected track the animal traversed (Bullard, 1999; Horne et al., 2007). By accounting for autocorrelation, BBMM can provide biologically more meaningful results compared to KUD (Horne et al., 2007) and is less sensitive to irregular sampling because it considers time differences between locations (Kranstauber et al., 2012). Animal tracks are commonly modelled with a random walk, which is a stochastic process of random and discrete steps (*i.e.,* composed of integers) taken on a space. Brownian bridges are based on diffusion-based Brownian motion, which is like a random walk but occurs on a space and time continuum and is conditioned at the beginning and the end by a pair of known, consecutive locations (Horne et al., 2007). Path modelling between successive locations is done using a Brownian bridge function that consists of a probability of occurrence calculated along the path traced by the animal (Horne et al., 2007). The probability distribution spreads in the direction of movement instead of in every direction as in KUD. This way using time-ordered location points allows to link areas of frequent use, while areas that the animal does not use can be excluded (Horne et al., 2007). The

model includes the animal's mobility as the Brownian motion variance parameter (σ^2_m), which is related to the animal's speed and represents the area an animal could use between locations. Using a single value for this parameter simplifies calculations, however, allowing it to vary would better reflect different behaviours of an animal, as the parameter relates to its movement which can naturally vary over time (Horne et al., 2007). The location data of each animal is used to independently calculate one σ^2_m value for their respective track (Horne et al., 2007).

The BBMM's robustness in identifying movement paths is reduced with increasing time intervals between locations, as the assumption of random movement is weakened by increasing location error in the data and mobility (*i.e.,* behaviour) (Horne et al., 2007). Additionally, the assumption of purely diffusive movements might not effectively estimate home range and habitat preferences in all cases because it dismisses biologically meaningful information that might be behind changes in movement patterns (Benhamou, 2011). Diffusive movement best suits animals that continuously move in a constant environment, *i.e.,* with no home range and with randomly distributed resources (Benhamou, 2011). Therefore, the movement of an animal between two locations very distant in time may be more accurately modelled as a biased random walk rather than a purely diffusive random walk such as that of the BBMM (Horne et al., 2007). Importantly, because the probability distribution here computed is constrained by these pairs of locations at both ends, the BBMM and the next two Brownian bridge models are occurrence or trajectory estimators rather than home range estimators in the strict sense (Fleming et al., 2016, 2015). Therefore, the path of the animal during the monitoring period is modelled, which does not involve a range prediction into the future (Fleming et al., 2015).

2.8.5 Biased random bridge kernel method

The main difference between the advective-diffusive or biased random bridge kernel method (BRB) and the previously described BBMM is that the latter purely includes diffusive movements, making it less suitable to estimate home ranges (Benhamou, 2011). The BBMM also assumes a constant animal mobility value, which dismisses behavioural changes in movement, for example, changes in speed, direction, and permanence in preferred areas (Benhamou, 2011). As opposed to the BBMM, the advective component is allowed to vary between bridges but must be constant within each one (Benhamou, 2011).

The BRB uses the movement-based kernel density estimation (MKDE) to calculate BRB-based UDs (Benhamou and Cornélis, 2010), which allow flexibility in the animal's movement and more accurately estimate home range. This method focuses on active UDs and not on global UDs (which include resting phases) by assuming that space use intensity is proportional to activity time spent. This also results in differences regarding the way the smoothing extends over space. KDE UDs extend in all directions around a location point, while MKDE's active UDs distribute probability density along a track between pairs of observed locations by interpolating positions between them (creating new points between two observed ones) (Benhamou and Cornélis, 2010). To ensure that the animal was between the two observed points and not elsewhere in its home range during the time elapsed between them, an upper recording time limit (*Tmax*) is used to identify data points that are too distant in time to be safely considered correlated, which get no locations interpolated between them and are filtered out for the calculations of BRB (Benhamou, 2011; Benhamou and Cornélis, 2010). These positions of high uncertainty would be included by the BBMM (Benhamou, 2011). *Tmax* is used to apply a variable smoothing factor to all observed and interpolated locations, assigning the lowest smoothing factor value (h_{min}) to the recorded positions and the highest (h_{max}) to the interpolated position found at the midpoint of the largest segment (*i.e.,* of size *Tmax*). Therefore, the longer the time between an interpolated and a recorded position, the higher h or uncertainty of the position. Habitat-specific diffusion coefficients (D_H) can be identified by calculating the diffusion coefficient of all track segments in the same habitat type. This can be included in the MKDE by assigning habitat-specific h_{max} and allowing to differentiate, for example, preferred habitat types from others the tracked animal traverses faster. The MKDE also addresses the boundary biases typically found in traditional kernel density estimators, by modeling boundaries as contiguous straight segments and correcting them via boundary-based coordinate transformations (Benhamou and Cornélis, 2010). BRB is available in the R package *adehabitatHR* (Calenge, 2006) (Figure 2.3.g).

2.8.6 Dynamic Brownian bridge movement model

The Dynamic Brownian bridge movement model (dBBMM) (Kranstauber et al., 2012) extends the BBMM by combining it with a method for identifying significant changes in the movement pattern similar to the likelihood-based behavioural change point analysis (Gurarie et al., 2009) (Figure 2.3.h). The dBBMM, therefore, allows the

Brownian motion variance parameter σ^2m to change across an animal's path, which is fixed in the BBMM, improving UD estimation and allowing to infer behavioural changes along an animal's track (Kranstauber et al., 2012). This process takes subsets of location points and evaluates for breakpoints or changes in the motion variance parameter. For this, a sliding window of w locations in size is placed on a subset of locations, and a margin size (m) of at least three locations is left on each end of the window, which is not used in the estimation. First, a single σ^2m value is calculated for the whole window, which is then split into all possible pairs of segments. Additional pairs of σ^2m values are then calculated for each split window. Then Bayesian information criterion values are calculated for each model and the case with the lowest value is selected. If the case of a single σ^2m is favoured, the value is assigned to the entire window. If a behavioural break is favoured, the calculated σ^2m values for each split window are assigned to the respective track segment on each side of the break (Kranstauber et al., 2012). Sliding this window across the track produces several σ^2m values for each segment, which are averaged to obtain one value per segment (Kranstauber et al., 2012). Then, UDs are calculated as in the BBMM (Horne et al., 2007), but more realistic estimations of space use are obtained because a flexible σ^2m is less biased, for example by not overestimating UDs during resting phases (Kranstauber et al., 2012). The selection of w and m is done by the researcher(s) and should follow biologically grounded criteria, although the authors provide some guidelines (Kranstauber et al., 2012). Increasing w improves the robustness of the variation parameter calculation, giving more stable estimates, albeit reducing sensitivity to short-term changes in σ^2m. On the other hand, increasing m allows to detect weaker breakpoints, but the larger margins reduce the number of locations to detect breakpoints (Kranstauber et al., 2012). The variation of σ^2m can be used to infer the animal's behaviour (Kranstauber et al., 2012), for example, to identify circadian or seasonal patterns in habitat use from fine-scale movement variations (Byrne et al., 2014; Kranstauber et al., 2012). The dBBMM offers an automated process to analyse behavioural changes on a track without requiring external information to classify them (which can be laborious and at times not possible), making it a more objective and repeatable process (Kranstauber et al., 2012). However, the simplicity of using σ^2m to detect behavioural changes (turning angles, speed, step length) has the disadvantage that it can potentially assign similar σ^2m to very different behavioural states, which needs to be considered during the interpretation of results (Kranstauber et al., 2012). The dBBMM performed better than the BBMM at estimating home ranges with irregular sampling

schemes and the variable UD allowed not to overestimate space use during resting phases or assign unrealistically high confidence intervals to migration segments (Kranstauber et al., 2012). It has also been shown to perform better than MCP and fixed KUD under low-resolution sampling (Silva et al., 2020).

2.9 Time-geographic density estimation

Time-geographic density estimation (TGDE) (Downs, 2010) combines time geography, the study of the movement of objects over time (Hägerstrand, 1970; Miller, 2005), with statistical density estimation to generate a continuous probability density surface for a moving object over a fixed time interval (Downs, 2010). TGDE uses three elements to analyse movement over space and time: control points, space-time paths, and space-time prisms. Control points are the observed locations with their corresponding timestamp, and space-time paths of a moving object are created by tracing a straight line between adjacent control points. Finally, space-time paths are used to construct space-time prisms or potential path areas (PPA), which encompass the total space that was accessible to the animal during the trajectory between the two control points. This is calculated using -and constrained by- the location in space of the two control points (as start and end locations for all simulated paths), the time elapsed between them, and the specified maximum velocity. A two-dimensional space-time prism is called a geo-ellipse, the equivalent of KUD's kernel, but is centered on the path rather than on each location (Downs, 2010). Similarly, densities can be estimated in a similar way to KUD, as geo-ellipses are constructed using a function that calculates the space-use probability distribution. This function can be uniform (all areas in the geo-ellipse weight equally) or of linear decay (intensity is weighted and decreases with distance from the control points and space-time path) (Downs, 2010), among other possibilities (Downs et al., 2018, 2011). A KDE bandwidth equivalent is obtained by setting the intensity of use to 0 beyond the boundaries of the geo-ellipse, where it is assumed impossible for the animal to have been. This is estimated using the maximum distance travelled in each geo-ellipse, calculated using the specified maximum velocity and time between the two control points, and, unlike KDE's arbitrarily chosen bandwidth, can be confidently estimated if the animal's properties are known (Downs, 2010). If velocity is kept constant, a fixed-velocity TGDE is obtained, and if it is allowed to vary, it results in an adaptive-velocity TGDE (Downs et al., 2018). The latter is better suited for home range analysis because it

allows velocity to match the animal's activity, i.e., when in rest vs. in active movement (Downs et al., 2018).

TGDE is mainly sensitive to the geo-ellipse function, temporal tracking intervals, sampling scheme, and defined maximum velocity (Downs et al., 2011). The selection of the geo-ellipse function determines how the intensity of use will be distributed, however, its effect on the results is more limited (Downs et al., 2011). Areas with more intense sampling have less uncertainty between locations, and therefore space use areas are drawn closer to the space-time path, whereas areas with more sparse sampling have broader density surfaces as an outcome of larger sampling gaps (Downs, 2010; Downs et al., 2011). Finally, the user-defined maximum velocity can have considerable effects (Downs, 2010; Downs et al., 2011). A higher maximum velocity will allow the PPA to reach farther from the space-time path, thus creating larger geo-ellipses and estimates of space-use (Downs et al., 2011) and also increasing bias (Downs et al., 2018). Nevertheless, lower velocities are not always the best choice (Downs et al., 2011). This value can be either theoretical or an observed maximum speed and its suitability can be evaluated by checking if all control points fall within the complete PPA or if only a small proportion falls outside the 95% isopleth (Downs et al., 2011). The TGDE process results in a continuous probability density surface of the animal's spatial position, from which core area and home range isopleths can be drawn (Downs et al., 2011). TGDE works in analogous ways to KDE, however, TGDE is based on movement trajectories from autocorrelated locations and generally performs better in simulations (Downs et al., 2018). Other advantages are the exclusion of inaccessible areas, considering uncertainty in spatial position during unsampled periods, objective smoothing based on the animal's velocity, and correct incorporation of uneven sampling intervals.

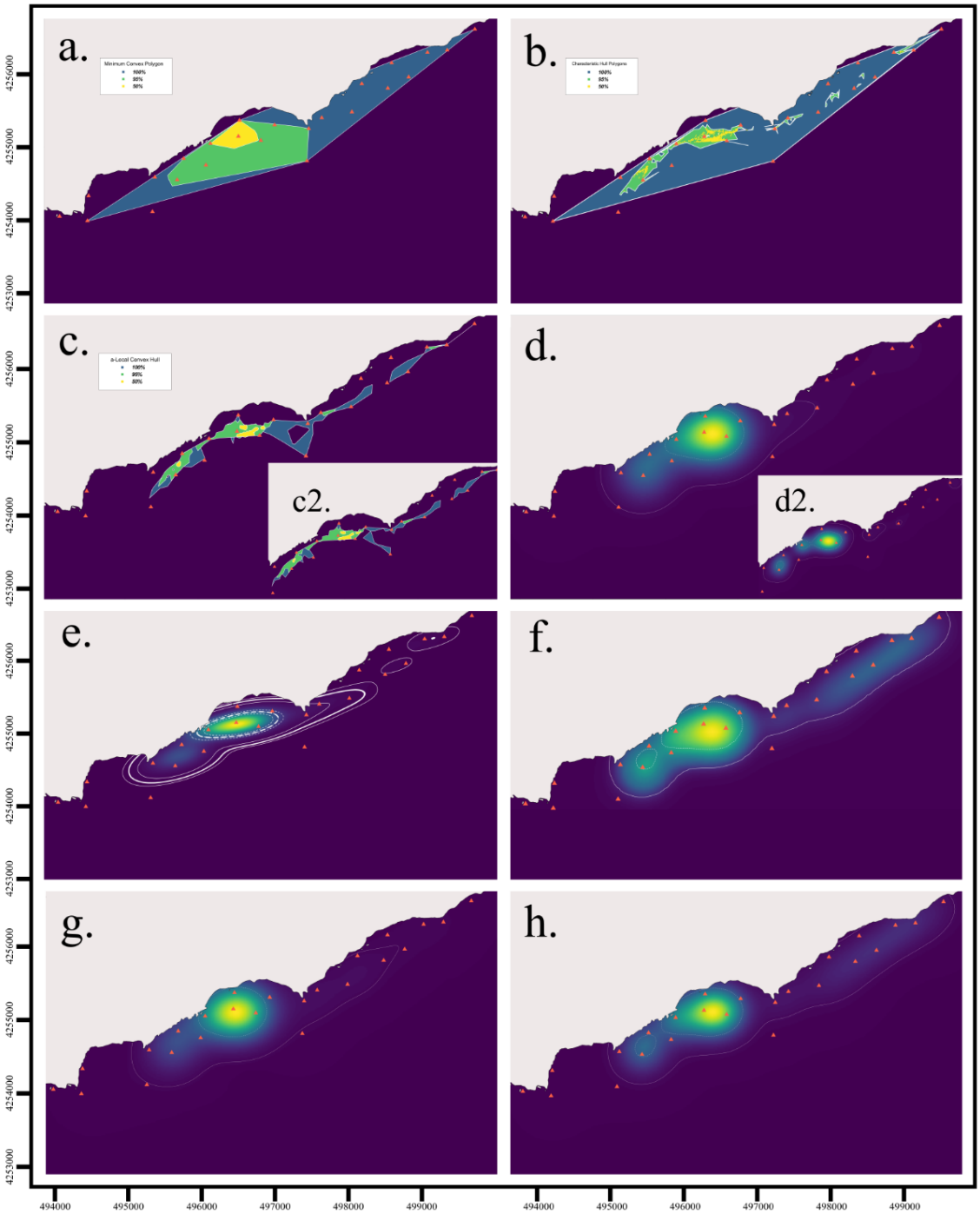
a.
b.
c.
c2.
d.
d2.
e.
f.
g.
h.
4256000
4255000
4254000
4253000
494000
495000
496000
497000
498000
499000

Figure 2.3: Examples of space use estimation using some of the methods described in this paper. Land is grey and water is dark blue. a) Minimum Convex Polygon at 100% (blue), 95% (green) and 50% (yellow; b) Characteristic Hull Polygons at the 100% (blue), 95% (green) and 50% (yellow) isopleths. Note the 100% CHP is equal to the 100% MCP. The estimations at lower percentage levels (95% and 50%) differ from their MCP counterparts because of how each method constructs polygons. Discontinuous area estimates and highly irregular shapes can occur depending on the characteristics of the real-life data used; c) a-Local Convex Hull using a value of a = 600 m, with the 100% isopleth in blue, 95% isopleth in green and 50% in yellow. The inserted picture shows another example using a value of a = 1000 m: d) Kernel Utilisation Distribution estimation method using sample data at the 95% (solid white line) and 50% (dotted white line) isopleths using a fixed bandwidth of h=250. The inserted picture shows another example using reference bandwidth h_{ref} = 116 to highlight the effect of bandwidth selection; e) Optimally weighted $AKDE_C$ ($wAKDE_C$) range estimation with confidence intervals using an anisotropic OU movement model. The 50% core area (bold dashed line), 95% home range (bold solid line) and their respective confidence intervals (thinner dotted and solid lines) are shown; f) Brownian Bridge Movement Model at the 95% (solid white line) and 50% (dotted white line) isopleths, using a location error of 250 m; g) Biased Random Bridge kernel method at the 95% (solid white line) and 50% (dotted white line) isopleths, using a diffusion parameter of D = 4.44, L_{min} of 50 m, a minimum smoothing parameter of h=250; h) Dynamic Brownian Bridge Movement Model at the 95% (solid white line) and 50% (dotted white line) isopleths, using a location error of 250 m, margin size m=11, and window size w=31. Images a) to d) and g) were created using the R package *adehabitatHR*, e) using the R package *ctmm* following the R script provided by Silva et al., (2021), f) using the Animal Tracking Toolbox in the R package V-Track, and h) using the R package *move*. All images were posteriorly edited for publication.

2.10 Network analysis-based home range estimation

Network analysis (NA) is a part of graph theory applied in many disciplines to describe relationships between discrete objects (West, 2001). Networks are formed using two basic units: nodes (the objects), and edges, which are links between pairs of nodes. Nodes are commonly used to represent two types of objects when using acoustic telemetry data. Nodes can represent receivers and edges the movement of tagged individuals between them, forming spatial networks, and nodes can also represent individuals and edges the interactions between them, which produces social networks (Jacoby et al., 2012, 2012b). Network's nodes and edges can be constructed with different complexity, and the most adequate representation will depend on several factors like the research question or the quality of the data. Simpler networks can be unweighted, in which only the presence or absence of a connection between nodes is shown by the presence or absence of an edge, or weighted, where an edge's thickness is proportional to the frequency of connection between nodes. Edges can additionally be directed, which indicates the direction of

interaction, *i.e.*, whether a connection is inbound or outbound at a given node (Jacoby and Freeman, 2016). The structural importance of the elements in a network is described using centrality metrics. Some of the most common ones are node degree, or the number of edges connecting to a node; node strength, used to measure the sum of all connection weights at a node (Barrat et al., 2004); closeness, which uses shortest-path distances to describe how central a node's position is in network space (the lower the sum of its edges or pathways connecting to other nodes, the higher the closeness) (Urban et al., 2009); eigenvector, which indicates how well connected a node is to other well-connected nodes (Bodin et al., 2011), and betweenness, which describes the contribution of a node to the connectivity between nodes in a network, or the number of times the node occurs in the shortest paths between all pairs of nodes (Fortuna et al., 2009). Such metrics can be included in the network by adjusting the size of nodes and/or using a coloured scale, for example as depicted in (Heupel et al., 2019; Jacoby et al., 2012; Mourier et al., 2021). If a spatial representation of the network is required, it can be obtained by plotting receiver positions on a map of the study site (Finn et al., 2014).

Networks can be constructed to answer specific questions, for example by grouping receivers by habitat or other environmental properties (e.g., depth) to study topics such as habitat use frequency, and movement patterns between areas of interest (Espinoza et al., 2015; Heupel et al., 2019). Other types of tests like removal analyses can be made, where the importance of an area or individual and the effect of isolation are evaluated (Espinoza et al., 2015; Mourier et al., 2017). On the other hand, networks that simultaneously depict two types of objects are called bipartite and, while not spatial in nature, are useful to represent associations between nodes of different classes (Dale and Fortin, 2010). In these representations, edges exclusively link nodes of different classes (Dale and Fortin, 2010), for example connecting nodes that represent individuals to nodes representing receivers based on their visitation patterns (Finn et al., 2014).

Importantly, the network constructions hitherto mentioned are static because they aggregate data across time and assume edges to be permanent associations. However, the temporal dynamics of space use and sociality can be represented using dynamic networks, for which centrality metrics are also calculated (Blonder et al., 2012; Jacoby and Freeman, 2016). A type of dynamic network is the time-aggregated network, which uses a pre-defined time window that "slides" across the temporal axis of the data. This way, all movements encompassed by each window are collapsed into one network, creating a sequence of temporally ordered networks. Such constructions allow examining dynamic

processes by assessing changes in network topography (Blonder et al., 2012). What type of network to use will depend on the data and research question (Farine, 2018).

Compared to probability distribution estimators such as KUD, one of the major differences with NA is that the latter uses a network of nodes to examine movement between receivers and does not require the calculation of UDs. Instead, metrics akin to KUD's core areas (called core use receivers) and 95% isopleths ranges (general use receivers) are estimated. This can be advantageous when position estimates are not obtainable from the data, as results are similar to those of UD-based methods (Lédée et al., 2015). Network analysis also allows looking into movement within the array, identifying movement pathways across nodes, and highlighting paths that are more heavily transited or connect relevant areas (Lédée et al., 2015). The randomness in the network is also tested by developing specific null models, e.g. (Croft et al., 2011; Farine and Whitehead, 2015; Lusseau et al., 2008). Like other methods, NA and its associated centrality metrics also have limitations and can be subject to bias. For example, the design of the array needs to be accounted for in the analysis, as receiver positions in the array can influence their centrality, e.g., receivers on the edge of the array are less likely to be connected than those from the center. Other considerations include that movement is three-dimensional and usually convoluted but is represented as a straight line in a network (such a simplification is also true for most space use estimators); a low number of nodes (low receiver coverage); receiver distribution; detection range of receivers and tags; and the temporal scale of movement is generally ignored (Mourier et al., 2018).

Despite the applicability of NA to the study of space use using acoustic telemetry, not only in ecology but also in management and conservation (Galpern et al., 2011; Jacoby et al., 2012b, 2012a), its use has been scarce compared to traditional home range estimators (Lédée et al., 2015). Network analysis can be conducted in the R environment with the R packages *sna* (Butts, 2013), *igraph* (Csardi and Nepusz, 2006), and *tnet* (Opsahl, 2009). Similarly, advances to facilitate the inclusion of time in NA have been proposed, by providing guidelines to analyse the temporal succession of network motif patterns (Pasquaretta et al., 2021) or by applying a moving window approach (Bonnell and Vilette, 2021) using the bespoke R package *netTS* [8].

As mentioned before, neighbouring receivers with overlapping detection ranges are often used to calculate positions/pseudo-positions for space use estimation. However,

[8] netTS: https://github.com/tbonne/netTS

for spatial NA generally non-overlapping detection ranges are used, e.g., as in (Jacoby et al., 2012a; Lédée et al., 2015). Simultaneous (i.e., "duplicate") detections at adjacent receivers are avoided with this configuration, as this can impact the centrality metrics. This presents a challenge when the goal is to both study space use and use NA using the same acoustic array. Two ways to work around this can be followed: either to modify the data to eliminate the overlap, or to create occupation pixels based on calculated positions/pseudo-positions before NA (Bastille-Rousseau et al., 2018; Pasquaretta et al., 2021). To eliminate the overlap, the receivers connected by overlapping detection ranges can be combined into one node, e.g., as Stehfest et al., (2014) did when creating receiver "curtains" to cover a passage. Alternatively, a subset of receivers can be selected, e.g., as done by Papastamatiou et al., (2020), which requires careful consideration as it implies subjective data selection and could greatly alter the study design.

On the other hand, maintaining the overlapping receivers implies working with positions or pseudo-positions, and requires transforming raw movement data into a format that can be automatically analysed with network metrics. For this, the animal coordinates that make up the trajectory can be rasterized on a spatial grid, whose cells will become nodes and the movement between them the edges (Bastille-Rousseau et al., 2018; Pasquaretta et al., 2021) (Figure 2.4). Different grid resolutions affect the topological structure of the resulting network, which can be evaluated by using a range of grid resolutions to build and compare several networks to find the optimal resolution (Pasquaretta et al., 2021).

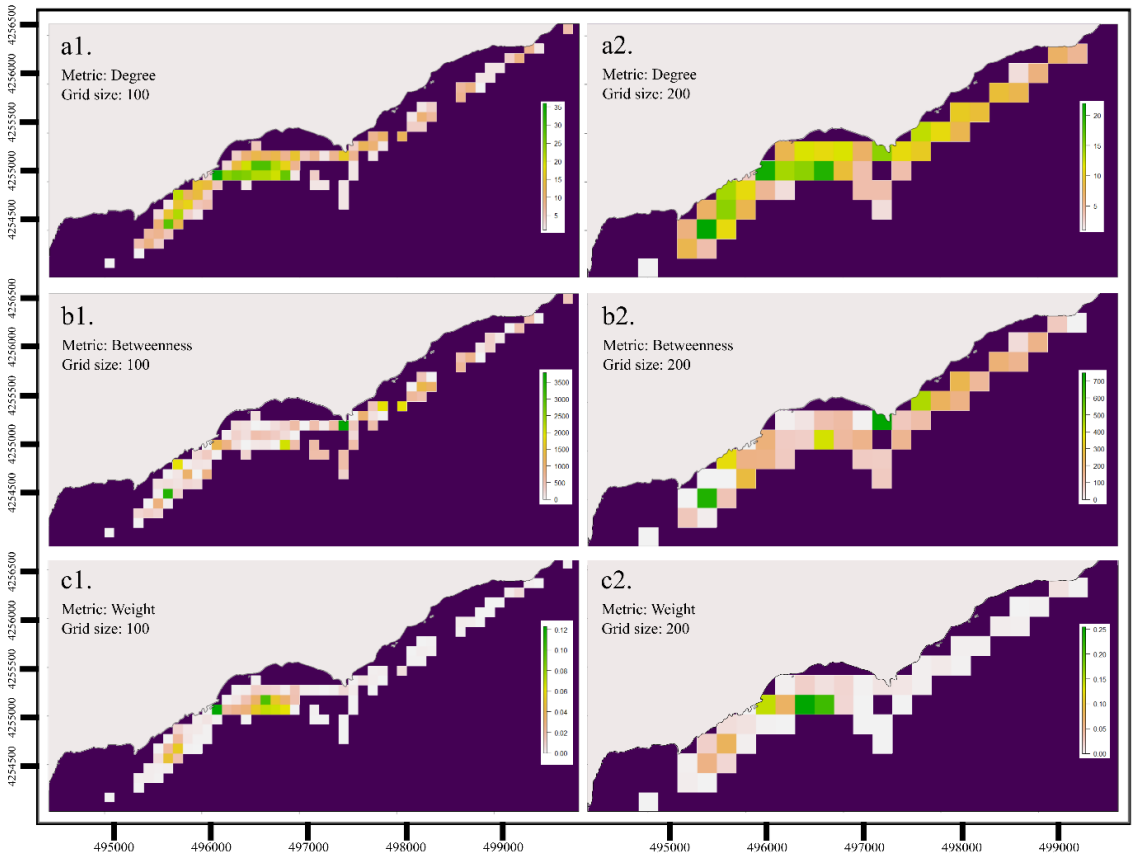

Figure 2.4: Examples of a spatial network created using a trajectory based on COA data. Shown are three centrality metrics (degree, betweenness, and weight) using two grid resolutions (100 and 200), highlighting the influence of grid resolution on network metrics. Degree: number of different pixels a pixel is connected to; Betweenness: number of shortest paths going through a pixel relative to the total number of shortest paths (the importance of a pixel in the organization of flows in the network); weight: number of locations within a pixel. To investigate space use, degree can act as a measure of connectedness, indicating spatial hubs where most movements depart from or/and arrive to; betweenness is a measure of connectivity and indicates bridge patterns in the network (i.e., corridors), and weight is a measure of residency or relocation density. The trajectory was created with adehabitatLT, the network metrics with moveNT. Image edited posteriorly for publication using Inkscape 1.1.

2.11 Three-dimensional KUD

Most movement ecology studies explore space use in two dimensions (Laver & Kelly, 2008) and, when data on vertical movements (depth) are collected, they are generally analysed separately from horizontal movements. This precludes examining space use in the same number of dimensions aquatic animals usually move, which would be more complete and produce a more realistic understanding of their movements (Simpfendorfer et al., 2012). Three-dimensional position estimates operate by adding a third dimension to the calculation of pseudo-positions using COAs (Simpfendorfer et al.,

2012), or any method described above. For example, a basic 3D position using VPS is calculated in a process similar to the 2D equivalent, which locates the intersection of a set of hyperboloids (each one constructed by tracing a line with a constant range difference between pairs of receivers of known position) and a plane (defined by transmitter depth). The most common method of estimating space use volume is a three-dimensional version of KUD (3D-KUD) available in the R package *ks* (Duong, 2007). To build a 3D-KUD, first, a three-dimensional cube is created and gridded. This results in a cube in space that contains a user-defined number of three-dimensional pixels known as voxels. A density estimate is then calculated for each voxel, for which a bandwidth value is selected. Utilization distributions can then be visualized at different isopleths, like 50% 3D-KUD and 95% 3D-KUD. As in two-dimensional KUD estimation, under-or oversmoothing are consequences that can arise from inappropriate bandwidth selection (Cooper et al., 2014). Sample code to estimate 50% and 95% 3D-KUDs is available in the Appendix of (Simpfendorfer et al., 2012) and (Cooper et al., 2014).

Considering that marine species live and move in three dimensions, this approach can be a better fit which offers more ways to explore and analyse the data (Lee et al., 2017; Udyawer et al., 2015). 3D-KUD estimation can include three-dimensional topography (Aspillaga et al., 2019). A movement-based 3D space use estimator using Brownian bridges was also developed to estimate UDs (Tracey et al., 2014), based on the *raster* (Hijmans and van Etten, 2012) and *Rcpp* (Eddelbuettel and François, 2011) R packages. Finer insights into space use of animals can be obtained compared to two-dimensional methods, like a fuller understanding of diel movement patterns (Udyawer et al., 2015), differences in home range size relating to intraspecific differences such as sex (Lee et al., 2017), the role environmental factors such as thermoclines can have as barriers (Aspillaga et al., 2017), and the susceptibility of animals to certain types of fishing gear (Simpfendorfer et al., 2012). Additionally, estimating range overlap in 2D space can be prone to overestimation, as including a vertical dimension (depth) has shown that overlap can be reduced, like animals in the same location might be at different depths (Charles et al., 2017; Cooper et al., 2014; Simpfendorfer et al., 2012).

This approach, although a more realistic reflection of animal movement, is also more complex to implement and implies greater challenges. To date, 3D space use estimation has not been as widely used as its 2D counterpart for reasons such as a historical lack of suitable analytical tools (Simpfendorfer et al., 2012). Also, tags equipped with pressure sensors are required, information which is measured at the time

of signal emission and sent along with the signal ID to estimate tag depth. Usually, receiver depth is also required. However, recently improved statistical analyses and capacity to improve movement data exploration render it a central part of future research (Udyawer et al., 2015).

2.12 Discussion

Technological advances and the increased complexity and refinement of analytical methods have provided unprecedented insight into the study of animal movement in aquatic environments using acoustic telemetry (Hussey et al., 2015). However, quantifying a complex and continuous phenomenon is a challenging task. In the study of animal movement, a common objective is to estimate space use, for which several methods exist, some of which have been described here (Figure 2.5).

These methods are commonly analysed using the R software (R Core Team, 2020), a free, open-source software in which research can be conducted in a reproducible way. It runs on all common operating systems and has a growing community constantly developing and updating bespoke code packages (Table 2.1). Further reading can be found in the review by Joo et al., (2020) on R packages to analyse movement data, although not limited to estimation methods that use acoustic telemetry data. However, there is no perfect, all-purpose estimator because there is no perfect way of measuring space use and all methods have different properties and caveats (Kie et al., 2010; Powell, 2000). Therefore, this decision process is not an easy task, as many factors must be considered. The suitability of each option depends on their particular characteristics and a combination of factors such as the research questions, properties of the data like gaps, resolution and monitoring time, study design and equipment, study species, and researcher experience (Carlisle et al., 2019; Fieberg and Börger, 2012; Laver and Kelly, 2008; Nathan et al., 2022; Scull et al., 2012; Signer and Fieberg, 2021). The performance of estimators can be compared, for example, using the standardised workflow in the *amt* R package by Signer and Fieberg, (2021) that compares some of the most commonly used home range estimators (MCP, LoCoH, KDE and AKDE).

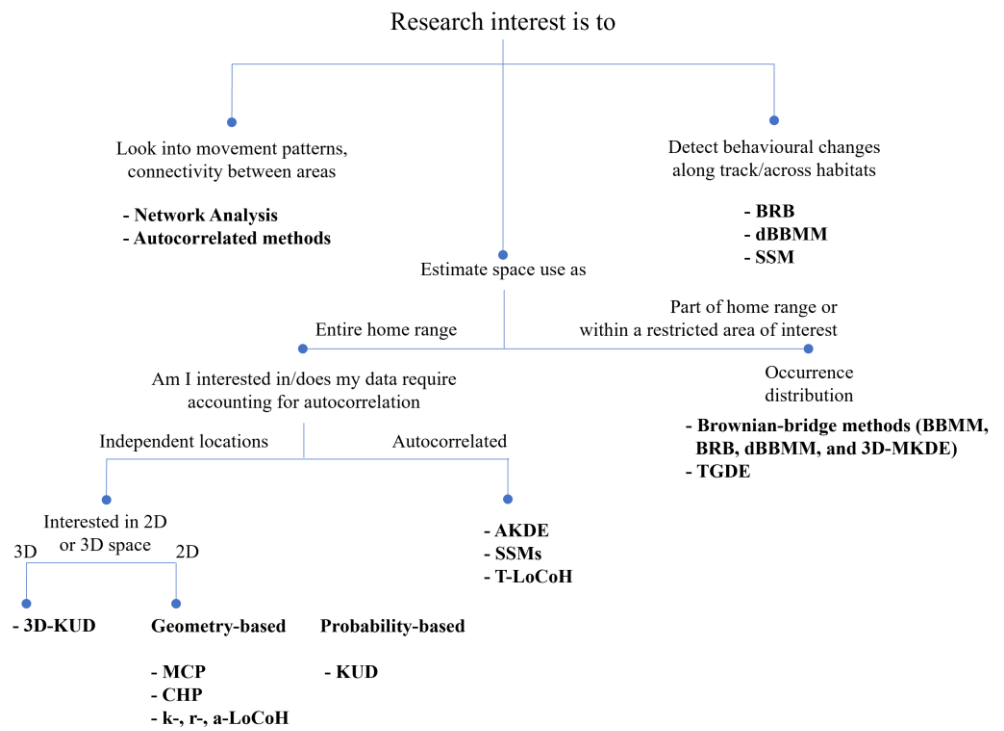

Figure 2.5: Decision tree with the described space use estimation methods, organized considering some of the questions they might be used to answer. BRB = Biased Random Bridges; dBBMM = dynamic Brownian Bridge Movement Model; SSM = State-Space Model; 3D-MKDE = Three-dimensional movement-based Kerned Density Estimation; TGDE = Time-Geography Density Estimation; 3D-KDE = Three-dimensional Kernel Utilization Distribution; MCP = Minimum Convex Polygon; k-, r-, a-LoCoH = Local Convex Hull methods; KUD = Kernel Utilization Distribution; AKDE = autocorrelated Kerned Density Estimation; T-LoCoH = Time Local Convex Hulls.

The most traditional estimators such as MCP and KUD are commonly favoured (Laver and Kelly, 2008) over newer, likely better-suited ones for a variety of reasons (Signer and Fieberg, 2021). The higher familiarity and more frequent use of the former might convey a greater sense of confidence and preclude from considering others. For most researchers, these reasons might at least presently exceed the analytical advantages offered by newer methods, which might appear too complex and of higher operational costs. For example, the wide application of SSMs in ecology had been impeded by computational limitations until some time ago (Patterson et al., 2008), while three-dimensional methods, despite offering a more realistic estimation of the movement of animals (Simpfendorfer et al., 2012), have their more extensive application hindered by the higher implementation costs and required analytical power. However, several of the newer, more complex methods offer guidelines and even R code to analyse data, for

example for AKDEs (Silva et al., 2021), B-SSM (Alós et al., 2016), dBBMM[9,10], and 3D-KUDs (Cooper et al., 2014; Simpfendorfer et al., 2012).

One of the most important factors affecting an estimator's efficiency is its compatibility with the question(s) driving the study and deciding on a method should be done with this in consideration. A table of key steps and considerations was provided by Fieberg and Börger, (2012), as the properties of an estimation method can help highlight the aspects of the data that are of interest. For example, SSMs (Patterson et al., 2008) and the Brownian bridge-based methods BRB and dBBMM are useful to explore behavioural changes in movement (Silva et al., 2020, 2018). Brownian bridge-based methods allow for studying changes in movement patterns and space use over different timescales (diel, seasons) or across different habitats (to forage, travel, rest) (Gurarie et al., 2009; Johnson et al., 2008; Morales et al., 2004). Identifying movement trajectories inside the activity space, which traditional kernel analyses do only superficially (Lédée et al., 2015) is better done using methods that construct trajectories by including the time of locations in addition to their spatial distribution, like T-LoCoH and Brownian bridge-based methods. This approach enables the creation of paths and connecting areas that are important to the animal.

Network analysis provides a different approach to this type of question, allowing for the exploration of movement patterns, detect important pathways and assess associations between individuals and habitat types inside the acoustic array, improving the understanding of space use and therefore a valuable analytical complement to probability density-based methods (Dale and Fortin, 2010; Lédée et al., 2015). Network analysis can provide metrics for each receiver that can be compared across time or among individuals (provided receivers have non-overlapping detection ranges). Network analysis also provides an alternative approximation to the estimation of core areas and home ranges while lacking area biases such as positive bias from boundary crossing and the need of calculating pseudo-positions (Lédée et al., 2015). Nevertheless, this method is not as commonly applied as others, greatly reducing across-studies comparisons (Lédée et al., 2015).

[9] R package *RSP* vignettes: http://127.0.0.1:12148/session/Rvig.512c13945f85.html for which data is prepared using actel (Flávio and Baktoft, 2021): https://CRAN.R-project.org/package=actel
[10] R- package move vignettes: https://cran.r-project.org/web/packages/move/vignettes/browseMovebank.html

Table 2.1: Table of available R packages that implement the described methods for positioning, residency, and space use estimation. Other software alternatives are also mentioned.

Method	adehabitatHR	actel	amt	BBMM	ctmm	fishtrack3d	glatos	igraph	ks	mkde	move	moveNT	netTS	raster	Rcpp	rhr	RSP	sna	survival	tlocoh	tnet	VTrack	wildlifeTG	yaps	Other sources
Abacus plots							•															•			
Residence/Weighted residence index		•					•															•			
Continuous Time Residence																			•						
Center of activity																						•			Group detections by individual ID and a time window; calculating mean longitude and latitude
Vemco/Innovasea VPS																									Position estimation done by the company
Thelma Biotel PinPoint																									Position estimation done by the company
Lotek Code Division Multiple Access																									Position estimation done by researcher using Lotek's positioning software
Yet Another Positioning Solver																								•	
Minimum Convex Polygon	•		•													•						•			GIS packages and software (ArcGIS, QGIS)
Characteristic hull polygons	•																								
Local Convex Hull method family	•		•													•				•		•			
Kernel Utilization Distribution	•		•						•							•									
Autocorrelated Kernel Density Estimator family			•		•																				Point-and-click graphical interface: https://ctmm.shinyapps.io/ctmmweb/
Ornstein–Uhlenbeck State-Space Model																									Sample code in Appendix S2 of Pedersen & Weng (2013)
Bayesian State-Space Modelling																									Sample code in Appendix S1 of Alós et al. (2016)
Brownian bridge movement model	•			•												•						•			
Biased random bridge kernel method	•																								
Dynamic Brownian bridge movement model											•						•								
Time-geographic density estimation																							•		
Network analysis-based home range estimation									•			•	•					•			•				
Three-dimensional KUD						•				•															
Movement-based 3D KDE														•	•										
Movement-based KDE										•															
Installation source	CRAN	CRAN		CRAN	CRAN	a	b	CRAN	CRAN	c	CRAN	CRAN	d	CRAN	CRAN	e	f	CRAN	CRAN	g	CRAN	h	i	CRAN	
User guides	1	2			4	5					6	7				8	9		10			11			
R package reference	Calenge (2006)	Flávio and Baktoft (2021)	Signer et al. (2019)	Nielson et al. (2013)	Calabrese et al. (2016)	Aspillaga (2019)	Holbrook et al. (2020)	Csardi and Nepusz (2006)	Duong (2007)	Tracey et al. (2014)	Kranstauber et al. (2021)	Bastille-Rousseau et al. (2018)	https://github.com/tbonne/netTS	Hijmans & van Etten (2012)	Eddelbuettel & François (2011)	Signer & Balkenhol (2015)	Niella et al. (2020)	Butts (2013)	Therneau (2015)	Kranstauber et al. (2018)	Opsahl (2009)	Udyawer et al. (2018)	Calabrese et al. (2016)	Baktoft et al. (2019)		

a. GitHub (https://rdrr.io/github/aspillaga/fishtrack3d/)
b.GitLab (https://gitlab.oceantrack.org/GreatLakes/glatos/-/wikis/installation-instructions)
c.Removed from the CRAN repository and archived: https://cran.r-project.org/src/contrib/Archive/mkde/
d. GitHub (https://github.com/tbonne/netTS)
e. R-Forge (https://rdrr.io/rforge/rhr/)
f. GitHub (https://rdrr.io/github/YuriNiella/RSP/)
g. R-Forge (https://rdrr.io/rforge/tlocoh/)
h. GitHub (development version: https://github.com/RossDwyer/VTrack)
i. GitHub (https://github.com/jedalong/wildlifeTG)

1. https://cran.r-project.org/web/packages/adehabitatHR/vignettes/adehabitatHR.pdf
2. typing "browseVignettes("actel")" in R / https://CRAN.R-project.org/package=actel;
3. Signer & Fieberg (2021);
4. https://github.com/aspillaga/fishtrack3d/blob/master/vignettes/modelling_ud3d.Rmd;
5. https://ecoisilva.github.io/AKDE_minireview/code/AKDE_R-tutorial.html;
6. https://cran.r-project.org/web/packages/move/vignettes/move.html;
7. Supporting information (https://esajournals.onlinelibrary.wiley.com/action/downloadSupplement?doi=10.1002%2Feap.1697&file=eap1697-sup-0002-AppendixS2.pdf)
8. http://www.spamwell.net/index.php;
9. typing "browseVignettes("RSP")" in R/http://127.0.0.1:24834/session/Rvig.17a035e11a3a.html;
10. Vignettes in https://CRAN.R-project.org/package=survival ;
11. https://vinayudyawer.github.io/ATT/docs/ATT_Vignette.html

Accounting for boundaries to movement might be important in some study areas, like when the receiver array is placed in rivers, fjords, or in proximity to coastlines, where large overlaps between space use estimates and land might occur, leading to the overestimation of space use. Limits to movement can also have biological origins such as territorial behaviours (Benhamou and Cornélis, 2010). A common approach to remove densities estimated over unusable areas is to manually clip this portion of the area estimate after space use estimation, redistribute the density so it sums to 1 again and redraw the utilization boundaries. Alternatively, estimators that produce area estimates with less overlap can be favoured over others. Polygon-based methods like CHP and LoCoH-based methods present advantages over MCP and KUD because they accommodate boundaries and holes inside the estimated area (Downs and Horner, 2007; Getz et al., 2007). Similarly, among probability density estimators, movement-based methods generally deal better with barriers than the traditional KUD estimator because of the way density is modelled to fit the movement of the animal. Additionally, some R packages allow accounting for boundaries by explicitly including one during modelling. Examples of this are *adehabitatHR* (Calenge, 2006), which allows creating a SpatialLines object to define an impenetrable barrier, *RSP* (Niella et al., 2020), which requires a shapefile with the topography of the study site to estimate the shortest path between consecutive detections, and in 3D-KUD methods (Aspillaga et al., 2019).

Similarly, not all methods are equally suited to estimate home range. This will depend not only on the estimator but also on other factors such as the properties of the data and study design. Brownian bridge models are not true home range estimators but occurrence or trajectory estimators (Fleming et al., 2016, 2015). They model probability distribution between successive pairs of locations and do not perform range prediction into the future, creating a trajectory with an associated uncertainty of where the animal was during the monitoring period (Fleming et al., 2015). This approach suits situations where the entire home range is most likely not being recorded, such as when the interest lies in characterizing space use during a restricted time frame and/or inside a limited area.

Furthermore, following Burt's (1943) definition of home range, it is important to ensure the extent of the animal's home range is covered during the tracking period (Noonan et al., 2019). The time it takes for an individual to cover its home range can vary greatly (Cooper, 1978) depending on the species, size, behaviour, or other characteristics, therefore it is crucial to adjust the monitoring period accordingly. Such range resident behaviour can be tested by constructing a variogram that seeks asymptotes in the extent of space use over time (Calabrese et al., 2016; Fleming et al., 2014a; Signer and Balkenhol, 2015). The time needed to reach

asymptotic space use can be variable, for example depending on the species, e.g. (Carlisle et al., 2019).

If no asymptote is reached, home range estimation might not be the appropriate method to analyse the data set. This can occur for example if the animal is transiting through the study area instead of remaining, being only briefly within detection range or because the monitoring period is too short, or the acoustic array only partially covers the actual home range. In such scenarios, the use of occurrence estimators (i.e., to answer the question "where has the animal been during the tracking period?") might better fit the data (Fleming et al., 2015).

If the extent of the animal's home range is effectively covered, whether the estimator operates under the assumption of IID or autocorrelation is important to consider (Laver and Kelly, 2008; Noonan et al., 2019; Signer and Balkenhol, 2015). Independent data points are obtained by sampling at intervals that are large enough to ensure they are not autocorrelated, which is habitually over timescales greater than the time an individual needs to cross its linear home range. The number of such locations in a dataset is referred to as effective sample size. Larger effective sample sizes are preferred, so the study duration should ideally span for much longer than the home range crossing time (Fleming and Calabrese, 2017; Noonan et al., 2019). This differs from (and is sometimes confounded with) absolute sample size, which is the total number of locations in a data set regardless of the sampling frequency (Fleming and Calabrese, 2017; Noonan et al., 2019). The time of statistical independence (time interval after which two subsequent locations are statistically independent) (Swihart and Slade, 1985b) can be tested, for example, with the R package *rhr* (Signer and Balkenhol, 2015).

However, autocorrelation is an intrinsic property of animal movement (Fleming and Calabrese, 2017; Noonan et al., 2019) and most studies do not include it (Laver and Kelly, 2008). Moreover, the assumption of IID is incompatible with (most) movement data sets, because autocorrelation intensifies with an increasing sampling frequency (De Solla et al., 1999; Swihart and Slade, 1985b), which is especially relevant when working with acoustic telemetry data (Hussey et al., 2015). Modern acoustic telemetry techniques allow the collection of data at very high frequencies, so the number of locations corresponds to the absolute sample size (Fleming and Calabrese, 2017; Noonan et al., 2019). Traditional home range estimators usually assume independent data points, like most polygon-based methods and KDE, hence movement data obtained with acoustic telemetry is incongruous with this underlying assumption.

A way to comply with this assumption is to coarsen the sampling period to space out locations in time to be considered independent (Fleming et al., 2015). However, removing data

to fulfil this assumption results in tremendous amounts of data loss, and subsampling tracking data is generally not recommended (Signer & Balkenhol 2015). Alternatively, most modern estimators account for autocorrelation by fitting an underlying movement model to the data, making them more suitable to work with acoustic telemetry (Calabrese et al., 2016; Noonan et al., 2019). Of such estimators are the recently developed series of AKDEs (Fleming et al., 2018, 2015; Fleming and Calabrese, 2017) and state-space models (Alós et al., 2016; Pedersen and Weng, 2013). The former methods correct biases that are frequently encountered when working with autocorrelated movement data, like failing to consider autocorrelation, small effective sample sizes, and missing or irregularly sampled data, producing comparatively unbiased home range estimates relative to traditional methods (Noonan et al., 2019). Since restrictions to movement are not explicitly included in the estimation process, AKDE can still present drawbacks such as positive bias from spilling over boundaries, but corrections can be made to address this (Noonan et al., 2019; Silva et al., 2021). AKDEs have also been improved in user-friendliness, as they were compiled into one publication with guidelines and an R script to facilitate their use (Silva et al., 2021). Furthermore, in addition to the R package *ctmm* (Calabrese et al., 2016), a point-and-click graphical interface is available and can be installed using the R console or used directly through a website (Calabrese et al., 2021).

With the advancement of tracking technologies and improved computational capacities, it is becoming easier for researchers to collect movement information in larger quantities and greater detail. The combination of these conditions presents the chance to take fuller advantage of the data by performing more complex analyses. Hull-based estimators discard much of the information, so to this end they should be avoided, and newer, more refined space use estimators should be preferred and set as the standard in the field.

2.12.1 Active telemetry

Active acoustic telemetry, following the movements of tagged individuals from a moving vessel using a hydrophone, is a methodology that has been applied to track animals for a long time, e.g., (Carey et al., 1990). Despite the finer resolution of active tracking (Heupel et al., 2006), its use to inform the design of a passive acoustic array (Fetterplace et al., 2016), and recent technological advances like replacing humans with autonomous underwater vehicles to do the tracking (White et al., 2016), passive acoustic telemetry remains the preferred method today. In active tracking, data collection is usually done on one focal individual at a time and its duration directly depends on the researchers' capacities and weather conditions. Because of this, tracking periods usually span from a few hours to a few days (not sampled continuously).

Moreover, the presence of the monitoring vessel could disturb the tracked individuals and alter their behaviour (Heupel et al., 2006; Kessel et al., 2014a). Nevertheless, most of the methods described here are applicable to active telemetry datasets, including minimum convex polygons (Welsh and Bellwood, 2012), local convex hulls (Freedman et al., 2016), kernel utilization distributions (Fetterplace et al., 2016; Welsh and Bellwood, 2012), and the Brownian bridge movement model (Meese and Lowe, 2020; White et al., 2016).

2.12.2 Summary

Technological advances in acoustic telemetry and the increased complexity and refinement of analytical methods have provided unprecedented insight into movement in aquatic environments (Hussey et al., 2015). The capability of collecting animal movement data has also increased from tens of locations by direct observation or radio collars, to thousands of high-frequency fixes from long-term monitoring using acoustic arrays (Hussey et al., 2015; Kays et al., 2015). However, quantifying a complex and continuous phenomenon such as animal movement is a challenging task. Correct space use analysis requires careful selection of the estimation method, as alternatives have diversified over the years, and each has different properties and presents different advantages and drawbacks. This decision is influenced by factors like the type of data, study design, researcher experience, monetary restrictions and processing capacities, and the questions behind the research. The present work showcases some of the estimators used and the methodologies used to evaluate their performance and execute analyses.

Declarations

Ethical Approval and Consent to participate

Not applicable.

Consent for publication

Not applicable.

Availability of supporting data

Available upon request.

Competing interests

The authors declare that they have no competing interests.

Funding

SK was supported by the "la Caixa" Foundation (ID 100010434) grant LCF/BQ/DI20/11780001; MG was supported by the Portuguese national funding agency for science, research and technology (FCT) grant UI/BD/151309/2021; SK, MG, ACW and DA were supported by the INFORBIOMARES project (POSEUR-03-2215-FC-000047), and FCT projects UIDB/04326/2020, UIDP/04326/2020 and LA/P/0101/2020; DA was supported by the FCT transitional norm DL57/2016/CP1361/CT0036.

Authors' contributions

SK wrote the manuscript, SK and MG prepared the figures. All authors contributed in written and intellectual form to the development of the manuscript, reviewed, and approved the final version.

Acknowledgements

The authors have no acknowledgements to make.

2.13 References

Abecasis, D., Bentes, L., Lino, P.G., Santos, M.N., Erzini, K., 2013. Residency, movements and habitat use of adult white seabream (*Diplodus sargus*) between natural and artificial reefs. Estuarine, Coastal and Shelf Science 118, 80–85. https://doi.org/10.1016/j.ecss.2012.12.014

Afonso, P., Fontes, J., Holland, K.N., Santos, R.S., 2008. Social status determines behaviour and habitat usage in a temperate parrotfish: implications for marine reserve design. Marine Ecology Progress Series 359, 215–227. https://doi.org/10.3354/meps07272

Ainslie, M.A., McColm, J.G., 1998. A simplified formula for viscous and chemical absorption in sea water. The Journal of the Acoustical Society of America 103, 1671–1672. https://doi.org/10.1121/1.421258

Albertsen, C.M., Whoriskey, K., Yurkowski, D., Nielsen, A., Flemming, J.M., 2015. Fast fitting of non-Gaussian state-space models to animal movement data via Template Model Builder. Ecology 96, 2598–2604. https://doi.org/10.1890/14-2101.1

Alós, J., Palmer, M., Balle, S., Arlinghaus, R., 2016. Bayesian State-Space Modelling of Conventional Acoustic Tracking Provides Accurate Descriptors of Home Range Behavior in a Small-Bodied Coastal Fish Species. PLoS ONE 11, e0154089. https://doi.org/10.1371/journal.pone.0154089

Aspillaga, E., Arlinghaus, R., Martorell-Barceló, M., Follana-Berná, G., Lana, A., Campos-Candela, A., Alós, J., 2021. Performance of a novel system for high-resolution tracking of marine fish societies. Animal Biotelemetry 9, 1. https://doi.org/10.1186/s40317-020-00224-w

Aspillaga, E., Bartumeus, F., Starr, R.M., López-Sanz, À., Linares, C., Díaz, D., Garrabou, J., Zabala, M., Hereu, B., 2017. Thermal stratification drives movement of a coastal apex predator. Scientific Reports 7, 526. https://doi.org/10.1038/s41598-017-00576-z

Aspillaga, E., Safi, K., Hereu, B., Bartumeus, F., 2019. Modelling the three-dimensional space use of aquatic animals combining topography and Eulerian telemetry data. Methods in Ecology and Evolution 10, 1551–1557. https://doi.org/10.1111/2041-210X.13232

Baidai, Y., Dagorn, L., Amandè, M.J., Gaertner, D., Capello, M., 2020. Tuna aggregation dynamics at Drifting Fish Aggregating Devices: a view through the eyes of commercial echosounder buoys. ICES Journal of Marine Science 77, 2960–2970. https://doi.org/10.1093/icesjms/fsaa178

Baktoft, H., Gjelland, K.Ø., Økland, F., Rehage, J.S., Rodemann, J.R., Corujo, R.S., Viadero, N., Thygesen, U.H., 2019. Opening the black box of high resolution fish tracking using yaps (preprint). Animal Behavior and Cognition. https://doi.org/10.1101/2019.12.16.877688

Baktoft, H., Gjelland, K.Ø., Økland, F., Thygesen, U.H., 2017. Positioning of aquatic animals based on time-of-arrival and random walk models using YAPS (Yet Another Positioning Solver). Scientific Reports 7, 14294. https://doi.org/10.1038/s41598-017-14278-z

Barrat, A., Barthelemy, M., Pastor-Satorras, R., Vespignani, A., 2004. The architecture of complex weighted networks. Proceedings of the National Academy of Sciences 101, 3747–3752. https://doi.org/10.1073/pnas.0400087101

Bastille-Rousseau, G., Douglas-Hamilton, I., Blake, S., Northrup, J.M., Wittemyer, G., 2018. Applying network theory to animal movements to identify properties of landscape space use. Ecological Applications 28, 854–864. https://doi.org/10.1002/eap.1697

Benhamou, S., 2011. Dynamic Approach to Space and Habitat Use Based on Biased Random Bridges. PLoS ONE 6, e14592. https://doi.org/10.1371/journal.pone.0014592

Benhamou, S., Cornélis, D., 2010. Incorporating Movement Behavior and Barriers to Improve Kernel Home Range Space Use Estimates. Journal of Wildlife Management 74, 1353–1360. https://doi.org/10.2193/2009-441

Berger, K.M., Gese, E.M., 2007. Does interference competition with wolves limit the distribution and abundance of coyotes? Journal of Animal Ecology 76, 1075–1085. https://doi.org/10.1111/j.1365-2656.2007.01287.x

Biesinger, Z., Bolker, B.M., Marcinek, D., Grothues, T.M., Dobarro, J.A., Lindberg, W.J., 2013. Testing an autonomous acoustic telemetry positioning system for fine-scale space use in marine animals. Journal of Experimental Marine Biology and Ecology 448, 46–56. https://doi.org/10.1016/j.jembe.2013.06.007

Blackwell, P.G., 1997. Random diffusion models for animal movements. Ecological Modelling 100, 87–102.

Blonder, B., Wey, T.W., Dornhaus, A., James, R., Sih, A., 2012. Temporal dynamics and network analysis: Temporal dynamics and network analysis. Methods in Ecology and Evolution 3, 958–972. https://doi.org/10.1111/j.2041-210X.2012.00236.x

Bodin, Ö., Ramirez-Sanchez, S., Ernstson, H., Prell, C., 2011. Some basic structural characteristics of networks, in: Bodin, Ö., Prell, C. (Eds.), Social Networks and Natural Resource Management: Uncovering the Social Fabric of Environmental Governance. Cambridge University Press, Cambridge, pp. 29–43. https://doi.org/10.1017/CBO9780511894985

Bonnell, T.R., Vilette, C., 2021. Constructing and analysing time-aggregated networks: The role of bootstrapping, permutation and simulation. Methods in Ecology and Evolution 12, 114–126. https://doi.org/10.1111/2041-210X.13351

Börger, L., Franconi, N., De Michele, G., Gantz, A., Meschi, F., Manica, A., Lovari, S., Coulson, T., 2006. Effects of sampling regime on the mean and variance of home range size estimates. Journal of Animal Ecology 75, 1393–1405. https://doi.org/10.1111/j.1365-2656.2006.01164.x

Boyle, S.A., Lourenço, W.C., da Silva, L.R., Smith, A.T., 2009. Home Range Estimates Vary with Sample Size and Methods. Folia Primatol 80, 33–42. https://doi.org/10.1159/000201092

Bullard, F., 1999. Estimating the home range of an animal: a Brownian bridge approach. (Ph.D. Thesis). University of North Carolina, Chapel Hill, North Carolina, USA.

Burgman, M.A., Fox, J.C., 2003. Bias in species range estimates from minimum convex polygons: implications for conservation and options for improved planning. Animal Conservation 6, 19–28. https://doi.org/10.1017/S1367943003003044

Burt, W.H., 1943. Territoriality and Home Range Concepts as Applied to Mammals. Journal of Mammalogy 24, 346. https://doi.org/10.2307/1374834

Butts, C., 2013. sna: tools for social network analysis. R package ver. 2.3-1.

Byrne, M.E., Clint McCoy, J., Hinton, J.W., Chamberlain, M.J., Collier, B.A., 2014. Using dynamic Brownian bridge movement modelling to measure temporal patterns of habitat selection. Journal of Animal Ecology 83, 1234–1243. https://doi.org/10.1111/1365-2656.12205

Calabrese, J.M., Fleming, C.H., Gurarie, E., 2016. ctmm: an R package for analyzing animal relocation data as a continuous-time stochastic process. Methods in Ecology and Evolution 7, 1124–1132. https://doi.org/10.1111/2041-210X.12559

Calabrese, J.M., Fleming, C.H., Noonan, M.J., Dong, X., 2021. ctmmweb: A Graphical User Interface for Autocorrelation-Informed Home Range Estimation. Wildlife Society Bulletin 45, 162–169. https://doi.org/10.1002/wsb.1154

Calenge, C., 2006. The package "adehabitat" for the R software: A tool for the analysis of space and habitat use by animals. Ecological Modelling 197, 516–519. https://doi.org/10.1016/j.ecolmodel.2006.03.017

Campbell, H.A., Watts, M.E., Dwyer, R.G., Franklin, C.E., 2012. V-Track: software for analysing and visualising animal movement from acoustic telemetry detections. Marine and Freshwater Research 63, 815. https://doi.org/10.1071/MF12194

Capello, M., Robert, M., Soria, M., Potin, G., Itano, D., Holland, K., Deneubourg, J.-L., Dagorn, L., 2015. A Methodological Framework to Estimate the Site Fidelity of Tagged Animals Using Passive Acoustic Telemetry. PLoS ONE 10, e0134002. https://doi.org/10.1371/journal.pone.0134002

Carey, F.G., Scharold, J.V., Kalmijn, Ad.J., 1990. Movements of blue sharks (*Prionace glauca*) in depth and course. Marine Biology 106, 329–342. https://doi.org/10.1007/BF01344309

Carlisle, A.B., Tickler, D., Dale, J.J., Ferretti, F., Curnick, D.J., Chapple, T.K., Schallert, R.J., Castleton, M., Block, B.A., 2019. Estimating Space Use of Mobile Fishes in a Large Marine Protected Area With Methodological Considerations in Acoustic Array Design. Frontiers in Marine Science 6, 256. https://doi.org/10.3389/fmars.2019.00256

Chacón, J.E., Duong, T., 2018. Multivariate Kernel Smoothing and its Applications, 1st ed. Chapman and Hall/CRC. https://doi.org/10.1201/9780429485572

Chapman, D.D., Feldheim, K.A., Papastamatiou, Y.P., Hueter, R.E., 2015. There and Back Again: A Review of Residency and Return Migrations in Sharks, with Implications for Population Structure and Management. Annual Review of Marine Science 7, 547–570. https://doi.org/10.1146/annurev-marine-010814-015730

Charles, C., Blanchfield, P., Gillis, D., 2017. Site fidelity of escaped rainbow trout to an experimental freshwater aquaculture facility and habitat overlap with native fish fauna. Aquaculture Environment Interactions 9, 415–428. https://doi.org/10.3354/aei00243

Cochran, J.E.M., Braun, C.D., Cagua, E.F., Campbell, M.F., Hardenstine, R.S., Kattan, A., Priest, M.A., Sinclair-Taylor, T.H., Skomal, G.B., Sultan, S., Sun, L., Thorrold, S.R., Berumen, M.L., 2019. Multi-method assessment of whale shark (*Rhincodon typus*) residency, distribution, and dispersal behavior at an aggregation site in the Red Sea. PLoS ONE 14, e0222285. https://doi.org/10.1371/journal.pone.0222285

Cooke, S.J., Niezgoda, G.H., Hanson, K.C., Suski, C.D., Phelan, F.J.S., Tinline, R., Philipp, D.P., 2005. Use of CDMA Acoustic Telemetry to Document 3-D Positions of Fish: Relevance to the Design and Monitoring of Aquatic Protected Areas. Marine Technology Society Journal 39, 31–41. https://doi.org/10.4031/002533205787521659

Cooper, N.W., Sherry, T.W., Marra, P.P., 2014. Modeling three-dimensional space use and overlap in birds. The Auk 131, 681–693. https://doi.org/10.1642/AUK-14-17.1

Cooper, W.E., 1978. Home range criteria based on temporal stability of areal occupation. Journal of Theoretical Biology 73, 687–695. https://doi.org/10.1016/0022-5193(78)90130-3

Cote, D., Scruton, D.A., Niezgoda, G.H., McKinley, R.S., Rowsell, D.F., Lindstorm, R.T., Ollerhead, L.M.N., Whitt, C.J., 1998. A Coded Acoustic Telemetry System for High Precision Monitoring of Fish Location and Movement: Application to the Study of Nearshore Nursery Habitat of Juvenile Atlantic Cod (*Gadus morhua*). Marine Technology Society Journal 32, 54–62.

Croft, D.P., Madden, J.R., Franks, D.W., James, R., 2011. Hypothesis testing in animal social networks. Trends in Ecology & Evolution 26, 502–507. https://doi.org/10.1016/j.tree.2011.05.012

Csardi, G., Nepusz, T., 2006. The igraph software package for complex network research. Complex Systems 1695, 1–9.

Cushman, S.A., Chase, M., Griffin, C., 2005. Elephants in space and time. Oikos 109, 331–341. https://doi.org/10.1111/j.0030-1299.2005.13538.x

Dale, M.R.T., Fortin, M.-J., 2010. From Graphs to Spatial Graphs. Annual Review of Ecology, Evolution, and Systematics 41, 21–38. https://doi.org/10.1146/annurev-ecolsys-102209-144718

De Solla, S.R., Bonduriansky, R., Brooks, R.J., 1999. Eliminating autocorrelation reduces biological relevance of home range estimates. Journal of Animal Ecology 68, 221–234. https://doi.org/10.1046/j.1365-2656.1999.00279.x

Dougherty, E.R., Carlson, C.J., Blackburn, J.K., Getz, W.M., 2017. A cross-validation-based approach for delimiting reliable home range estimates. Movement Ecology 5, 19. https://doi.org/10.1186/s40462-017-0110-4

Downs, J.A., 2010. Time-Geographic Density Estimation for Moving Point Objects, in: Fabrikant, S.I., Reichenbacher, T., van Kreveld, M., Schlieder, C. (Eds.), Geographic Information Science. Springer Berlin Heidelberg, Berlin, Heidelberg, pp. 16–26.

Downs, J.A., Heller, J.H., Loraamm, R., Stein, D.O., McDaniel, C., Onorato, D., 2012. Accuracy of home range estimators for homogeneous and inhomogeneous point patterns. Ecological Modelling 225, 66–73. https://doi.org/10.1016/j.ecolmodel.2011.11.010

Downs, J.A., Horner, M.W., 2009. A Characteristic-Hull Based Method for Home Range Estimation: A Characteristic-Hull Based Method for Home Range Estimation. Transactions in GIS 13, 527–537. https://doi.org/10.1111/j.1467-9671.2009.01177.x

Downs, J.A., Horner, M.W., 2008. Effects of Point Pattern Shape on Home-Range Estimates. Journal of Wildlife Management 72, 1813–1818. https://doi.org/10.2193/2007-454

Downs, J.A., Horner, M.W., 2007. Characterising Linear Point Patterns, in: Proceedings of the GIScience Research UK Conference. Maynooth, Ireland.

Downs, J.A., Horner, M.W., Lamb, D., Loraamm, R.W., Anderson, J., Wood, B., 2018. Testing time-geographic density estimation for home range analysis using an agent-based model of animal movement. International Journal of Geographical Information Science 32, 1505–1522. https://doi.org/10.1080/13658816.2017.1421764

Downs, J.A., Horner, M.W., Tucker, A.D., 2011. Time-geographic density estimation for home range analysis. Annals of GIS 17, 163–171. https://doi.org/10.1080/19475683.2011.602023

Duckham, M., Kulik, L., Worboys, M., Galton, A., 2008. Efficient generation of simple polygons for characterizing the shape of a set of points in the plane. Pattern Recognition 41, 3224–3236. https://doi.org/10.1016/j.patcog.2008.03.023

Duong, T., 2007. ks : Kernel Density Estimation and Kernel Discriminant Analysis for Multivariate Data in R. Journal of Statistical Software 21. https://doi.org/10.18637/jss.v021.i07

Eddelbuettel, D., François, R., 2011. Rcpp: Seamless R and C++ integration. Journal of Statistical Software 40, 1–18.

Eidous, O.M., Marie, M.A.A.S., Ebrahem, M.H.B.A.-H., 2010. A Comparative Study for Bandwidth Selection in Kernel Density Estimation. Journal of Modern Applied Statistical Methods 9, 263–273. https://doi.org/10.22237/jmasm/1272687900

Epanechnikov, V.A., 1969. Nonparametric estimation of a multidimensional probability density. Theory of Probability and Its Applications 14, 153–158.

Espinoza, M., Farrugia, T.J., Webber, D.M., Smith, F., Lowe, C.G., 2011. Testing a new acoustic telemetry technique to quantify long-term, fine-scale movements of aquatic animals. Fisheries Research 108, 364–371. https://doi.org/10.1016/j.fishres.2011.01.011

Espinoza, M., Lédée, E.J.I., Simpfendorfer, C.A., Tobin, A.J., Heupel, M.R., 2015. Contrasting movements and connectivity of reef-associated sharks using acoustic telemetry: implications for management. Ecological Applications 25, 2101–2118. https://doi.org/10.1890/14-2293.1

Ewer, R.F., 1968. Ethology of Mammals. Springer New York, NY. https://doi.org/10.1007/978-1-4899-4656-0

Farine, D.R., 2018. When to choose dynamic vs. static social network analysis. Journal of Animal Ecology 87, 128–138. https://doi.org/10.1111/1365-2656.12764

Farine, D.R., Whitehead, H., 2015. Constructing, conducting and interpreting animal social network analysis. Journal of Animal Ecology 84, 1144–1163. https://doi.org/10.1111/1365-2656.12418

Fashing, P.J., Mulindahabi, F., Gakima, J.-B., Masozera, M., Mununura, I., Plumptre, A.J., Nguyen, N., 2007. Activity and Ranging Patterns of *Colobus angolensis ruwenzorii* in Nyungwe Forest, Rwanda: Possible Costs of Large Group Size. International Journal of Primatology 28, 529–550. https://doi.org/10.1007/s10764-006-9095-3

Fetterplace, L.C., Davis, A.R., Neilson, J.M., Taylor, M.D., Knott, N.A., 2016. Active acoustic tracking suggests that soft sediment fishes can show site attachment: a preliminary assessment of the movement patterns of the blue-spotted flathead (*Platycephalus caeruleopunctatus*). Animal Biotelemetry 4, 15. https://doi.org/10.1186/s40317-016-0107-6

Fieberg, J., Börger, L., 2012. Could you please phrase “home range” as a question? Journal of Mammalogy 93, 890–902. https://doi.org/10.1644/11-MAMM-S-172.1

Finn, J.T., Brownscombe, J.W., Haak, C.R., Cooke, S.J., Cormier, R., Gagne, T., Danylchuk, A.J., 2014. Applying network methods to acoustic telemetry data: Modeling the movements of tropical marine fishes. Ecological Modelling 293, 139–149. https://doi.org/10.1016/j.ecolmodel.2013.12.014

Flávio, H., Baktoft, H., 2021. actel: Standardised analysis of acoustic telemetry data from animals moving through receiver arrays. Methods in Ecology and Evolution 12, 196–203. https://doi.org/10.1111/2041-210X.13503

Fleming, C.H., Calabrese, J.M., 2017. A new kernel density estimator for accurate home-range and species-range area estimation. Methods in Ecology and Evolution 8, 571–579. https://doi.org/10.1111/2041-210X.12673

Fleming, C.H., Calabrese, J.M., Mueller, T., Olson, K.A., Leimgruber, P., Fagan, W.F., 2014a. From Fine-Scale Foraging to Home Ranges: A Semivariance Approach to Identifying Movement Modes across Spatiotemporal Scales. The American Naturalist 183, E154–E167. https://doi.org/10.1086/675504

Fleming, C.H., Calabrese, J.M., Mueller, T., Olson, K.A., Leimgruber, P., Fagan, W.F., 2014b. Non-Markovian maximum likelihood estimation of autocorrelated movement processes. Methods in Ecology and Evolution 5, 462–472. https://doi.org/10.1111/2041-210X.12176

Fleming, C.H., Fagan, W.F., Mueller, T., Olson, K.A., Leimgruber, P., Calabrese, J.M., 2016. Estimating where and how animals travel: An optimal framework for path reconstruction from autocorrelated tracking data. Ecology 97, 576–582. https://doi.org/10.1890/15-1607.1

Fleming, C.H., Fagan, W.F., Mueller, T., Olson, K.A., Leimgruber, P., Calabrese, J.M., 2015. Rigorous home range estimation with movement data: a new autocorrelated kernel density estimator. Ecology 96, 1182–1188. https://doi.org/10.1890/14-2010.1

Fleming, C.H., Sheldon, D., Fagan, W.F., Leimgruber, P., Mueller, T., Nandintsetseg, D., Noonan, M.J., Olson, K.A., Setyawan, E., Sianipar, A., Calabrese, J.M., 2018. Correcting for missing and irregular data in home-range estimation. Ecological Applications 28, 1003–1010. https://doi.org/10.1002/eap.1704

Forget, F., Cowley, P.D., Capello, M., Filmalter, J.D., Dagorn, L., 2020. Drifting along in the open-ocean: The associative behaviour of oceanic triggerfish and rainbow runner with floating objects. Marine Environmental Research 161, 104994. https://doi.org/10.1016/j.marenvres.2020.104994

Fortuna, M.A., Popa-Lisseanu, A.G., Ibáñez, C., Bascompte, J., 2009. The roosting spatial network of a bird-predator bat. Ecology 90, 934–944. https://doi.org/10.1890/08-0174.1

Freedman, R.M., Espasandin, C., Holcombe, E.F., Whitcraft, C.R., Allen, B.J., Witting, D., Lowe, C.G., 2016. Using Movements and Habitat Utilization as a Functional Metric of Restoration for Estuarine Juvenile Fish Habitat. Marine and Coastal Fisheries 8, 361–373. https://doi.org/10.1080/19425120.2016.1161681

Friedman, J.H., 1984. A variable span scatterplot smoother (Technical Report No. 5). Laboratory for Computational Statistics, Stanford University.

Galpern, P., Manseau, M., Fall, A., 2011. Patch-based graphs of landscape connectivity: A guide to construction, analysis and application for conservation. Biological Conservation 144, 44–55. https://doi.org/10.1016/j.biocon.2010.09.002

Getz, W.M., Fortmann-Roe, S., Cross, P.C., Lyons, A.J., Ryan, S.J., Wilmers, C.C., 2007. LoCoH: Nonparameteric Kernel Methods for Constructing Home Ranges and Utilization Distributions. PLoS ONE 2, e207. https://doi.org/10.1371/journal.pone.0000207

Getz, W.M., Wilmers, C., 2004. A local nearest-neighbor convex-hull construction of home ranges and utilization distributions. Ecography 27, 489–505. https://doi.org/10.1111/j.0906-7590.2004.03835.x

Girard, I., Ouellet, J.P., Courtois, R., Dussault, C., Breton, L., 2002. Effects of Sampling Effort Based on GPS Telemetry on Home-Range Size Estimations. The Journal of Wildlife Management 66, 1290–1300. https://doi.org/10.2307/3802962

Govinden, R., Capello, M., Forget, F., Filmalter, J.D., Dagorn, L., 2021. Behavior of skipjack (*Katsuwonus pelamis*), yellowfin (*Thunnus albacares*), and bigeye (*T. obsesus*) tunas associated with drifting fish aggregating devices (dFADs) in the Indian Ocean, assessed through acoustic telemetry. Fisheries Oceanography 30, 542–555. https://doi.org/10.1111/fog.12536

Govinden, R., Jauhary, R., Filmalter, J., Forget, F., Soria, M., Adam, S., Dagorn, L., 2013. Movement behaviour of skipjack (*Katsuwonus pelamis*) and yellowfin (*Thunnus albacares*) tuna at anchored fish aggregating devices (FADs) in the Maldives, investigated by acoustic telemetry. Aquatic Living Resources 26, 69–77. https://doi.org/10.1051/alr/2012022

Green, S., Matley, J., Smith, D., Castillo B, I., Akins, J., Nemeth, R., Pollock, C., Reale-Munroe, K., 2021. Broad-scale acoustic telemetry reveals long-distance movements and large home ranges for invasive lionfish on Atlantic coral reefs. Marine Ecology Progress Series 673, 117–134. https://doi.org/10.3354/meps13818

Grueter, C.C., Li, D., Ren, B., Wei, F., 2009. Choice of analytical method can have dramatic effects on primate home range estimates. Primates 50, 81–84. https://doi.org/10.1007/s10329-008-0113-2

Gurarie, E., Andrews, R.D., Laidre, K.L., 2009. A novel method for identifying behavioural changes in animal movement data. Ecology Letters 12, 395–408. https://doi.org/10.1111/j.1461-0248.2009.01293.x

Guyomard, D., Lee, K.A., Perry, C., Jaquemet, S., Cliff, G., 2020. SMART drumlines at Réunion Island do not attract bull sharks *Carcharhinus leucas* into nearshore waters: Evidence from acoustic monitoring. Fisheries Research 225, 105480. https://doi.org/10.1016/j.fishres.2019.105480

Guzzo, M.M., Van Leeuwen, T.E., Hollins, J., Koeck, B., Newton, M., Webber, D.M., Smith, F.I., Bailey, D.M., Killen, S.S., 2018. Field testing a novel high residence positioning system for monitoring the fine-scale movements of aquatic organisms. Methods in Ecology and Evolution 9, 1478–1488. https://doi.org/10.1111/2041-210X.12993

Hägerstrand, T., 1970. What about people in regional science? Papers of the Regional Science Association 24, 7–21.

Hanson, K.C., Cooke, S.J., Suski, C.D., Niezgoda, G., Phelan, F.J.S., Tinline, R., Philipp, D.P., 2007. Assessment of largemouth bass (*Micropterus salmoides*) behaviour and activity at multiple spatial and temporal scales utilizing a whole-lake telemetry array, in: Almeida, P.R., Quintella, B.R., Costa, M.J., Moore, A. (Eds.), Developments in Fish Telemetry: Proceedings of the Sixth Conference on Fish Telemetry Held in Europe. pp. 243–256.

Harrington, D.P., Fleming, T.R., 1982. A class of rank test procedures for censored survival data. Biometrika 69, 553–566. https://doi.org/10.1093/biomet/69.3.553

Hayne, D.W., 1949. Calculation of Size of Home Range. Journal of Mammalogy 30, 1–16. https://doi.org/10.2307/1375189

Hedger, R.D., Martin, F., Dodson, J.J., Hatin, D., Caron, F., Whoriskey, F.G., 2008. The optimized interpolation of fish positions and speeds in an array of fixed acoustic receivers. ICES Journal of Marine Science 65, 1248–1259. https://doi.org/10.1093/icesjms/fsn109

Hemson, G., Johnson, P., South, A., Kenward, R., Ripley, R., Macdonald, D., 2005. Are kernels the mustard? Data from global positioning system (GPS) collars suggests problems for kernel home-range analyses with least-squares cross-validation: Kernel home-range analyses and LSCV problems. Journal of Animal Ecology 74, 455–463. https://doi.org/10.1111/j.1365-2656.2005.00944.x

Heupel, M.R., Munroe, S.E.M., Lédée, E.J.I., Chin, A., Simpfendorfer, C.A., 2019. Interspecific interactions, movement patterns and habitat use in a diverse coastal shark assemblage. Marine Biology 166, 68. https://doi.org/10.1007/s00227-019-3511-7

Heupel, M.R., Semmens, J.M., Hobday, A.J., 2006. Automated acoustic tracking of aquatic animals: scales, design and deployment of listening station arrays. Marine and Freshwater Research 57, 1. https://doi.org/10.1071/MF05091

Heupel, M.R., Simpfendorfer, C.A., Fitzpatrick, R., 2010. Large–Scale Movement and Reef Fidelity of Grey Reef Sharks. PLoS ONE 5, e9650. https://doi.org/10.1371/journal.pone.0009650

Hijmans, R.J., van Etten, J., 2012. raster: Geographic analysis and modeling with raster data.

Horne, J.S., Garton, E.O., Krone, S.M., Lewis, J.S., 2007. Analyzing animal movements using Brownian Bridges. Ecology 88, 2354–2363. https://doi.org/10.1890/06-0957.1

Hussey, N.E., Kessel, S.T., Aarestrup, K., Cooke, S.J., Cowley, P.D., Fisk, A.T., Harcourt, R.G., Holland, K.N., Iverson, S.J., Kocik, J.F., Mills Flemming, J.E., Whoriskey, F.G., 2015. Aquatic animal telemetry: A panoramic window into the underwater world. Science 348, 1255642–1255642. https://doi.org/10.1126/science.1255642

IUCN, 2012. IUCN Red List categories and criteria, version 3.1. Second edition. IUCN, Gland, Switzerland and Cambridge, UK.

Jacoby, D.M.P., Brooks, E.J., Croft, D.P., Sims, D.W., 2012a. Developing a deeper understanding of animal movements and spatial dynamics through novel application of network analyses. Methods in Ecology and Evolution 3, 574–583. https://doi.org/10.1111/j.2041-210X.2012.00187.x

Jacoby, D.M.P., Croft, D.P., Sims, D.W., 2012b. Social behaviour in sharks and rays: analysis, patterns and implications for conservation: Shark social behaviour. Fish and Fisheries 13, 399–417. https://doi.org/10.1111/j.1467-2979.2011.00436.x

Jacoby, D.M.P., Freeman, R., 2016. Emerging Network-Based Tools in Movement Ecology. Trends in Ecology & Evolution 31, 301–314. https://doi.org/10.1016/j.tree.2016.01.011

Jennrich, R.I., Turner, F.B., 1969. Measurement of non-circular home range. Journal of Theoretical Biology 22, 227–237. https://doi.org/10.1016/0022-5193(69)90002-2

Johnson, D.S., London, J.M., Lea, M.-A., Durban, J.W., 2008. CONTINUOUS-TIME CORRELATED RANDOM WALK MODEL FOR ANIMAL TELEMETRY DATA. Ecology 89, 1208–1215. https://doi.org/10.1890/07-1032.1

Joo, R., Boone, M.E., Clay, T.A., Patrick, S.C., Clusella-Trullas, S., Basille, M., 2020. Navigating through the R packages for movement. Journal of Animal Ecology 89, 248–267. https://doi.org/10.1111/1365-2656.13116

Joppa, L.N., Butchart, S.H.M., Hoffmann, M., Bachman, S.P., Akçakaya, H.R., Moat, J.F., Böhm, M., Holland, R.A., Newton, A., Polidoro, B., Hughes, A., 2016. Impact of alternative metrics on estimates of extent of occurrence for extinction risk assessment: Extent of Occurrence and Extinction Risk. Conservation Biology 30, 362–370. https://doi.org/10.1111/cobi.12591

José-Domínguez, J.M., Savini, T., Asensio, N., 2015. Ranging and site fidelity in northern pigtailed macaques (*Macaca leonina*) over different temporal scales: Ranging and Site Fidelity in Northern Pigtailed Macaques. American Journal of Primatology 77, 841–853. https://doi.org/10.1002/ajp.22409

Kays, R., Crofoot, M.C., Jetz, W., Wikelski, M., 2015. Terrestrial animal tracking as an eye on life and planet. Science 348, aaa2478–aaa2478. https://doi.org/10.1126/science.aaa2478

Kessel, S.T., Chapman, D.D., Franks, B.R., Gedamke, T., Gruber, S.H., Newman, J., White, E., Perkins, R., 2014a. Predictable temperature-regulated residency, movement and migration in a large, highly mobile marine predator (*Negaprion brevirostris*). Marine Ecology Progress Series 514, 175–190. https://doi.org/10.3354/meps10966

Kessel, S.T., Cooke, S.J., Heupel, M.R., Hussey, N.E., Simpfendorfer, C.A., Vagle, S., Fisk, A.T., 2014b. A review of detection range testing in aquatic passive acoustic telemetry studies. Reviews in Fish Biology and Fisheries 24, 199–218. https://doi.org/10.1007/s11160-013-9328-4

Kie, J.G., 2013. A rule-based ad hoc method for selecting a bandwidth in kernel home-range analyses. Animal Biotelemetry 1, 13. https://doi.org/10.1186/2050-3385-1-13

Kie, J.G., Matthiopoulos, J., Fieberg, J., Powell, R.A., Cagnacci, F., Mitchell, M.S., Gaillard, J.-M., Moorcroft, P.R., 2010. The home-range concept: are traditional estimators still relevant with modern telemetry technology? Philosophical Transactions of the Royal Society B 365, 2221–2231. https://doi.org/10.1098/rstb.2010.0093

Klinard, N.V., Matley, J.K., 2020. Living until proven dead: addressing mortality in acoustic telemetry research. Reviews in Fish Biology and Fisheries. https://doi.org/10.1007/s11160-020-09613-z

Kranstauber, B., Kays, R., LaPoint, S.D., Wikelski, M., Safi, K., 2012. A dynamic Brownian bridge movement model to estimate utilization distributions for heterogeneous animal movement: The dynamic Brownian bridge movement model. Journal of Animal Ecology 81, 738–746. https://doi.org/10.1111/j.1365-2656.2012.01955.x

Laver, P.N., Kelly, M.J., 2008. A Critical Review of Home Range Studies. Journal of Wildlife Management 72, 290–298. https://doi.org/10.2193/2005-589

Lédée, E.J.I., Heupel, M.R., Tobin, A.J., Knip, D.M., Simpfendorfer, C.A., 2015. A comparison between traditional kernel-based methods and network analysis: an example from two nearshore shark species. Animal Behaviour 103, 17–28. https://doi.org/10.1016/j.anbehav.2015.01.039

Lee, K., Huveneers, C., Duong, T., Harcourt, R., 2017. The ocean has depth: two- versus three-dimensional space use estimators in a demersal reef fish. Marine Ecology Progress Series 572, 223–241. https://doi.org/10.3354/meps12097

Lichti, N.I., Swihart, R.K., 2011. Estimating utilization distributions with kernel versus local convex hull methods. The Journal of Wildlife Management 75, 413–422. https://doi.org/10.1002/jwmg.48

Lino, P., 2012. Potential of fisheries restocking off the Algarve coast using aquaculture produced marine fish (Ph.D. Thesis). Universidade do Algarve, Faro, Portugal.

Long, J.A., Nelson, T.A., 2012. Time geography and wildlife home range delineation: Time Geography Home Range. The Journal of Wildlife Management 76, 407–413. https://doi.org/10.1002/jwmg.259

Lusseau, D., Whitehead, H., Gero, S., 2008. Incorporating uncertainty into the study of animal social networks. Animal Behaviour 75, 1809–1815. https://doi.org/10.1016/j.anbehav.2007.10.029

Lyons, A.J., Turner, W.C., Getz, W.M., 2013. Home range plus: a space-time characterization of movement over real landscapes. Movement Ecology 1, 2. https://doi.org/10.1186/2051-3933-1-2

Manicacci, F.-M., Mourier, J., Babatounde, C., Garcia, J., Broutta, M., Gualtieri, J.-S., Aiello, A., 2022. A Wireless Autonomous Real-Time Underwater Acoustic Positioning System. Sensors 22, 8208. https://doi.org/10.3390/s22218208

March, D., Palmer, M., Alós, J., Grau, A., Cardona, F., 2010. Short-term residence, home range size and diel patterns of the painted comber *Serranus scriba* in a temperate marine reserve. Marine Ecology Progress Series 400, 195–206. https://doi.org/10.3354/meps08410

Meckley, T.D., Holbrook, C.M., Wagner, C., Binder, T.R., 2014. An approach for filtering hyperbolically positioned underwater acoustic telemetry data with position precision estimates. Animal Biotelemetry 2, 7. https://doi.org/10.1186/2050-3385-2-7

Meese, E.N., Lowe, C.G., 2020. Active acoustic telemetry tracking and tri-axial accelerometers reveal fine-scale movement strategies of a non-obligate ram ventilator. Movement Ecology 8, 8. https://doi.org/10.1186/s40462-020-0191-3

Melnychuk, M.C., 2012. Detection efficiency in telemetry studies: definitions and evaluation methods, in: Adams, N.S., Beeman, J.W., Eiler, J.H. (Eds.), Telemetry Techniques: A User Guide for Fisheries Research. American Fisheries Society, Bethesda, Maryland, pp. 339–357.

Miller, H., 2005. A measurement theory for time geography. Geographical Analysis 37, 17–45.

Misra, P., Enge, P., 2006. Global Positioning System: Signals, Measurements, and Performance. Ganga-Jamuna Press, Lincoln MA.

Mohr, C.O., 1947. Table of Equivalent Populations of North American Small Mammals. American Midland Naturalist 37, 223. https://doi.org/10.2307/2421652

Morales, J.M., Haydon, D.T., Frair, J., Holsinger, K.E., Fryxell, J.M., 2004. Extracting more out of relocation data: building movement models as mixtures of random walks. Ecology 85, 2436–2445. https://doi.org/10.1890/03-0269

Mourier, J., Brown, C., Planes, S., 2017. Learning and robustness to catch-and-release fishing in a shark social network. Biology Letters 13, 20160824. https://doi.org/10.1098/rsbl.2016.0824

Mourier, J., Lédée, E., Guttridge, T., Jacoby, D.M.P., 2018. Network Analysis and Theory in Shark Ecology - Methods and Applications, in: Carrier, J., Heithaus, M., Simpfendorfer, C. (Eds.), Shark Research: Emerging Technologies and Applications for the Field and Laboratory. CRC Press, Boca Raton, USA, pp. 337–356.

Mourier, J., Soria, M., Blaison, A., Simier, M., Certain, G., Demichelis, A., Hattab, T., 2021. Dynamic use of coastal areas by bull sharks and the conciliation of conservation and management of negative human–wildlife interactions. Aquatic Conservation: Marine and Freshwater Ecosystems 31, 2926–2937. https://doi.org/10.1002/aqc.3674

Muñoz, L., Aspillaga, E., Palmer, M., Saraiva, J.L., Arechavala-Lopez, P., 2020. Acoustic Telemetry: A Tool to Monitor Fish Swimming Behavior in Sea-Cage Aquaculture. Frontiers in Marine Science 7, 645. https://doi.org/10.3389/fmars.2020.00645

Nathan, R., Getz, W.M., Revilla, E., Holyoak, M., Kadmon, R., Saltz, D., Smouse, P.E., 2008. A movement ecology paradigm for unifying organismal movement research. Proceedings of the National Academy of Sciences 105, 19052–19059. https://doi.org/10.1073/pnas.0800375105

Nathan, R., Monk, C.T., Arlinghaus, R., Adam, T., Alós, J., Assaf, M., Baktoft, H., Beardsworth, C.E., Bertram, M.G., Bijleveld, A.I., Brodin, T., Brooks, J.L., Campos-Candela, A., Cooke, S.J., Gjelland, K.Ø., Gupte, P.R., Harel, R., Hellström, G., Jeltsch, F., Killen, S.S., Klefoth, T., Langrock, R., Lennox, R.J., Lourie, E., Madden, J.R., Orchan, Y., Pauwels, I.S., Říha, M., Roeleke, M., Schlägel, U.E., Shohami, D., Signer, J., Toledo, S., Vilk, O., Westrelin, S., Whiteside, M.A., Jarić, I., 2022. Big-data approaches lead to an increased understanding of the ecology of animal movement. Science 375, eabg1780. https://doi.org/10.1126/science.abg1780

Niella, Y., Flávio, H., Smoothey, A.F., Aarestrup, K., Taylor, M.D., Peddemors, V.M., Harcourt, R., 2020. Refined Shortest Paths (RSP): Incorporation of topography in space use estimation from node-based telemetry data. Methods in Ecology and Evolution 11, 1733–1742. https://doi.org/10.1111/2041-210X.13484

Niezgoda, G., Benfield, M., Sisak, M., Anson, P., 2002. Tracking acoustic transmitters by code division multiple access (CDMA)-based telemetry. Hydrobiologia 483, 275–286. https://doi.org/10.1023/A:1021368720967

Nilsen, E.B., Pedersen, S., Linnell, J.D.C., 2008. Can minimum convex polygon home ranges be used to draw biologically meaningful conclusions? Ecological Research 23, 635–639. https://doi.org/10.1007/s11284-007-0421-9

Noonan, M.J., Tucker, M.A., Fleming, C.H., Akre, T.S., Alberts, S.C., Ali, A.H., Altmann, J., Antunes, P.C., Belant, J.L., Beyer, D., Blaum, N., Böhning-Gaese, K., Cullen, L., Paula, R.C., Dekker, J., Drescher-Lehman, J., Farwig, N., Fichtel, C., Fischer, C., Ford, A.T., Goheen, J.R., Janssen, R., Jeltsch, F., Kauffman, M., Kappeler, P.M., Koch, F., LaPoint, S., Markham, A.C., Medici, E.P., Morato, R.G., Nathan, R., Oliveira-Santos, L.G.R., Olson, K.A., Patterson, B.D., Paviolo, A., Ramalho, E.E., Rösner, S., Schabo, D.G., Selva, N., Sergiel, A., Xavier da Silva, M., Spiegel, O., Thompson, P., Ullmann, W., Zięba, F., Zwijacz-Kozica, T., Fagan, W.F., Mueller, T., Calabrese, J.M., 2019. A comprehensive analysis of autocorrelation and bias in home range estimation. Ecological Monographs 89. https://doi.org/10.1002/ecm.1344

Ohta, I., Kakuma, S., 2005. Periodic behavior and residence time of yellowfin and bigeye tuna associated with fish aggregating devices around Okinawa Islands, as identified with automated listening stations. Marine Biology 146, 581–594. https://doi.org/10.1007/s00227-004-1456-x

Olsen, J., Downs, J.A., Tucker, T., Trost, S., 2011. Home-Range Size and Territorial Calling of Southern Boobooks (*Ninox novaeseelandiae*) in Adjacent Territories. Journal of Raptor Research 45, 136–142. https://doi.org/10.3356/JRR-10-92.1

Opsahl, T., 2009. Structure and evolution of weighted networks. University of London, London.

Orrell, D., Hussey, N., 2022. Using the VEMCO Positioning System (VPS) to explore fine-scale movements of aquatic species: applications, analytical approaches and future directions. Marine Ecology Progress Series 687, 195–216. https://doi.org/10.3354/meps14003

Papastamatiou, Y.P., Bodey, T.W., Caselle, J.E., Bradley, D., Freeman, R., Friedlander, A.M., Jacoby, D.M.P., 2020. Multiyear social stability and social information use in reef sharks with diel fission–fusion dynamics. Proceedings of the Royal Society B: Biological Sciences 287, 20201063. https://doi.org/10.1098/rspb.2020.1063

Pasquaretta, C., Dubois, T., Gomez-Moracho, T., Delepoulle, V.P., Le Loc'h, G., Heeb, P., Lihoreau, M., 2021. Analysis of temporal patterns in animal movement networks. Methods in Ecology and Evolution 12, 101–113. https://doi.org/10.1111/2041-210X.13364

Patterson, T., Thomas, L., Wilcox, C., Ovaskainen, O., Matthiopoulos, J., 2008. State–space models of individual animal movement. Trends in Ecology & Evolution 23, 87–94. https://doi.org/10.1016/j.tree.2007.10.009

Payne, N., Gillanders, B., Webber, D., Semmens, J., 2010. Interpreting diel activity patterns from acoustic telemetry: the need for controls. Marine Ecology Progress Series 419, 295–301. https://doi.org/10.3354/meps08864

Pedersen, M.W., Patterson, T.A., Thygesen, U.H., Madsen, H., 2011. Estimating animal behavior and residency from movement data. Oikos 120, 1281–1290. https://doi.org/10.1111/j.1600-0706.2011.19044.x

Pedersen, M. W., Weng, K.C., 2013. Estimating individual animal movement from observation networks. Methods in Ecology and Evolution 4, 920–929. https://doi.org/10.1111/2041-210X.12086

Pérez, G., Dagorn, L., Deneubourg, J.-L., Forget, F., Filmalter, J.D., Holland, K., Itano, D., Adam, S., Jauharee, R., Beeharry, S.P., Capello, M., 2020. Effects of habitat modifications on the movement behavior of animals: the case study of Fish Aggregating Devices (FADs) and tropical tunas. Movement Ecology 8, 47. https://doi.org/10.1186/s40462-020-00230-w

Peterson, A.T., 2017. Problems with reductive, polygon-based methods for estimating species' ranges: reply to Pimm et al. 2017: Estimating Species' Ranges. Conservation Biology 31, 948–951. https://doi.org/10.1111/cobi.12929

Peterson, A.T., Navarro-Sigüenza, A.G., Gordillo, A., 2016. Assumption-versus data-based approaches to summarizing species' ranges. Conservation Biology 32, 568–575. https://doi.org/10.1111/cobi.12801

Pimm, S.L., Harris, G., Jenkins, C.N., Ocampo-Peñuela, N., Li, B.V., 2017. Unfulfilled promise of data-driven approaches: response to Peterson et al.: Data-Driven Approaches. Conservation Biology 31, 944–947. https://doi.org/10.1111/cobi.12928

Piper, W.H., 2011. Making habitat selection more “familiar”: a review. Behavioral Ecology and Sociobiology 65, 1329–1351. https://doi.org/10.1007/s00265-011-1195-1

Piraino, M.N., Szedlmayer, S.T., 2014. Fine-Scale Movements and Home Ranges of Red Snapper around Artificial Reefs in the Northern Gulf of Mexico. Transactions of the American Fisheries Society 143, 988–998. https://doi.org/10.1080/00028487.2014.901249

Powell, R.A., 2000. Animal home ranges and territories and home range estimators, in: Boitani, L., Fuller, T.K. (Eds.), Research Technologies in Animal Ecology - Controversies and Consequences. Columbia Univeristy Press, New York, pp. 65–110.

Powell, R.A., Mitchell, M.S., 2012. What is a home range? Journal of Mammalogy 93, 948–958. https://doi.org/10.1644/11-MAMM-S-177.1

Quinton, B.J., 2016. The Effect of Home Range Estimation Techniques on Habitat Use Analysis (Master’s Thesis). University of South Florida, Tampa, Florida, USA.

R Core Team, 2020. R: A language and environment for statistical computing. R Foundation for Statistical Computing, Vienna, Austria.

Roy, R., Beguin, J., Argillier, C., Tissot, L., Smith, F., Smedbol, S., De-Oliveira, E., 2014. Testing the VEMCO Positioning System: spatial distribution of the probability of location and the positioning error in a reservoir. Animal Biotelemetry 2, 1. https://doi.org/10.1186/2050-3385-2-1

Ryan, S.J., Knechtel, C.U., Getz, W.M., 2006. Range and Habitat Selection of African Buffalo in South Africa. Journal of Wildlife Management 70, 764–776. https://doi.org/10.2193/0022-541X(2006)70[764:RAHSOA]2.0.CO;2

Sanderson, G.C., 1966. The Study of Mammal Movements: A Review. The Journal of Wildlife Management 30, 215–235. https://doi.org/10.2307/3797914

Scull, P., Palmer, M., Frey, F., Kraly, E., 2012. A comparison of two home range modeling methods using Ugandan mountain gorilla data. International Journal of Geographical Information Science 26, 2111–2121. https://doi.org/10.1080/13658816.2012.691507

Seaman, D.E., Powell, R.A., 1996. An Evaluation of the Accuracy of Kernel Density Estimators for Home Range Analysis. Ecology 77, 2075–2085. https://doi.org/10.2307/2265701

Shizuka, D., Barve, S., Johnson, A.E., Walters, E.L., 2022. Constructing social networks from automated telemetry data: A worked example using within- and across-group associations in cooperatively breeding birds. Methods in Ecology and Evolution 13, 133–143. https://doi.org/10.1111/2041-210X.13737

Signer, J., Balkenhol, N., 2015. Reproducible home ranges (rhr): A new, user-friendly R package for analyses of wildlife telemetry data: Reproducible Home-Range Analysis With R. Wildlife Society Bulletin 39, 358–363. https://doi.org/10.1002/wsb.539

Signer, J., Fieberg, J., Avgar, T., 2019. Animal movement tools (amt): R package for managing tracking data and conducting habitat selection analyses. Ecology and Evolution 9, 880–890. https://doi.org/10.1002/ece3.4823

Signer, J., Fieberg, J.R., 2021. A fresh look at an old concept: home-range estimation in a tidy world. PeerJ 9, e11031. https://doi.org/10.7717/peerj.11031

Silva, I., Crane, M., Marshall, B.M., Strine, C.T., 2020. Reptiles on the wrong track? Moving beyond traditional estimators with dynamic Brownian Bridge Movement Models. Movement Ecology 8, 43. https://doi.org/10.1186/s40462-020-00229-3

Silva, I., Crane, M., Suwanwaree, P., Strine, C., Goode, M., 2018. Using dynamic Brownian Bridge Movement Models to identify home range size and movement patterns in king cobras. PLoS ONE 13, e0203449. https://doi.org/10.1371/journal.pone.0203449

Silva, I., Fleming, C.H., Noonan, M.J., Alston, J., Folta, C., Fagan, W.F., Calabrese, J.M., 2021. Autocorrelation-informed home range estimation: a review and practical guide. Methods in Ecology and Evolution 2041–210X.13786. https://doi.org/10.1111/2041-210X.13786

Simpfendorfer, C.A., Heupel, M.R., Hueter, R.E., 2002. Estimation of short-term centers of activity from an array of omnidirectional hydrophones and its use in studying animal movements. Canadian Journal of Fisheries and Aquatic Sciences 59, 23–32. https://doi.org/10.1139/f01-191

Simpfendorfer, C.A., Huveneers, C., Steckenreuter, A., Tattersall, K., Hoenner, X., Harcourt, R., Heupel, M.R., 2015. Ghosts in the data: false detections in VEMCO pulse position modulation acoustic telemetry monitoring equipment. Animal Biotelemetry 3, 55. https://doi.org/10.1186/s40317-015-0094-z

Simpfendorfer, C.A., Olsen, E.M., Heupel, M.R., Moland, E., 2012. Three-dimensional kernel utilization distributions improve estimates of space use in aquatic animals. Canadian Journal of Fisheries and Aquatic Sciences 69, 565–572. https://doi.org/10.1139/f2011-179

Smith, F., 2013. Understanding HPE in the VEMCO Positioning System (VPS) - V 1.0.

Soria, M., Dagorn, L., Potin, G., Fréon, P., 2009. First field-based experiment supporting the meeting point hypothesis for schooling in pelagic fish. Animal Behaviour 78, 1441–1446. https://doi.org/10.1016/j.anbehav.2009.09.025

Soria, M., Heithaus, M., Blaison, A., Crochelet, E., Forget, F., Chabanet, P., 2019. Residency and spatial distribution of bull sharks *Carcharhinus leucas* in and around Reunion Island marine protected area. Marine Ecology Progress Series 630, 101–113. https://doi.org/10.3354/meps13139

Stehfest, K.M., Patterson, T.A., Barnett, A., Semmens, J.M., 2014. Markov models and network analysis reveal sex-specific differences in the space-use of a coastal apex predator. Oikos 124, 307–318. https://doi.org/10.1111/oik.01429

Swihart, R.K., Slade, N.A., 1985a. Influence of Sampling Interval on Estimates of Home-Range Size. The Journal of Wildlife Management 49, 1019–1025.

Swihart, R.K., Slade, N.A., 1985b. Testing For Independence of Observations in Animal Movements. Ecology 66, 1176–1184. https://doi.org/10.2307/1939170

Therneau, T., 2015. A Package for Survival Analysis in S. Version 2.38. https://CRAN.R-project.org/package=survival.

Tickler, D.M., Carlisle, A.B., Chapple, T.K., Curnick, D.J., Dale, J.J., Schallert, R.J., Block, B.A., 2019. Potential detection of illegal fishing by passive acoustic telemetry. Animal Biotelemetry 7, 1. https://doi.org/10.1186/s40317-019-0163-9

Tolotti, M.T., Forget, F., Capello, M., Filmalter, J.D., Hutchinson, M., Itano, D., Holland, K., Dagorn, L., 2020. Association dynamics of tuna and purse seine bycatch species with drifting

fish aggregating devices (FADs) in the tropical eastern Atlantic Ocean. Fisheries Research 226, 105521. https://doi.org/10.1016/j.fishres.2020.105521

Tracey, J.A., Sheppard, J., Zhu, J., Wei, F., Swaisgood, R.R., Fisher, R.N., 2014. Movement-Based Estimation and Visualization of Space Use in 3D for Wildlife Ecology and Conservation. PLoS ONE 9, e101205. https://doi.org/10.1371/journal.pone.0101205

Udyawer, V., Dwyer, R.G., Hoenner, X., Babcock, R.C., Brodie, S., Campbell, H.A., Harcourt, R.G., Huveneers, C., Jaine, F.R.A., Simpfendorfer, C.A., Taylor, M.D., Heupel, M.R., 2018. A standardised framework for analysing animal detections from automated tracking arrays. Animal Biotelemetry 6, 17. https://doi.org/10.1186/s40317-018-0162-2

Udyawer, V., Simpfendorfer, C.A., Heupel, M.R., 2015. Diel patterns in three-dimensional use of space by sea snakes. Animal Biotelemetry 3, 29. https://doi.org/10.1186/s40317-015-0063-6

Uhlenbeck, G.E., Ornstein, L.S., 1930. On the Theory of the Brownian Motion. Physical Review Journals 36, 823–841. https://doi.org/10.1103/PhysRev.36.823

Urban, D.L., Minor, E.S., Treml, E.A., Schick, R.S., 2009. Graph models of habitat mosaics. Ecology Letters 12, 260–273. https://doi.org/10.1111/j.1461- 0248.2008.01271.x

Van Winkle, W., 1975. Comparison of Several Probabilistic Home-Range Models. The Journal of Wildlife Management 39, 118. https://doi.org/10.2307/3800474

Véras, L.Q., Capello, M., Forget, F., Tolotti, M.T., Véras, D.P., Dagorn, L., Hazin, F.H., 2020. Aggregative capacity of experimental anchored Fish Aggregating Devices (aFADs) in Northeastern Brazil revealed through electronic tagging data. Ocean and Coastal Research 68, e20284. https://doi.org/10.1590/s2675-28242020068284

Vergeynst, J., Baktoft, H., Mouton, A., De Mulder, T., Nopens, I., Pauwels, I., 2020a. The influence of system settings on positioning accuracy in acoustic telemetry, using the YAPS algorithm. Animal Biotelemetry 8, 25. https://doi.org/10.1186/s40317-020-00211-1

Vergeynst, J., Vanwyck, T., Baeyens, R., De Mulder, T., Nopens, I., Mouton, A., Pauwels, I., 2020b. Acoustic positioning in a reflective environment: going beyond point-by-point algorithms. Animal Biotelemetry 8, 16. https://doi.org/10.1186/s40317-020-00203-1

Wand, M.P., Jones, M.C., 1995. Kernel smoothing, 1st ed. ed, Monographs on statistics and applied probability. Chapman & Hall, London; New York.

Weinz, A.A., Matley, J.K., Klinard, N.V., Fisk, A.T., Colborne, S.F., 2020. Identification of predation events in wild fish using novel acoustic transmitters. Animal Biotelemetry 8, 28. https://doi.org/10.1186/s40317-020-00215-x

Welsh, J.Q., Bellwood, D.R., 2012. Spatial ecology of the steephead parrotfish (*Chlorurus microrhinos*): an evaluation using acoustic telemetry. Coral Reefs 31, 55–65. https://doi.org/10.1007/s00338-011-0813-8

West, D.B., 2001. Introduction to graph theory. Prentice Hall, London.

White, C.F., Lin, Y., Clark, C.M., Lowe, C.G., 2016. Human vs robot: Comparing the viability and utility of autonomous underwater vehicles for the acoustic telemetry tracking of marine organisms. Journal of Experimental Marine Biology and Ecology 485, 112–118. https://doi.org/10.1016/j.jembe.2016.08.010

Winton, M.V., Kneebone, J., Zemeckis, D.R., Fay, G., 2018. A spatial point process model to estimate individual centres of activity from passive acoustic telemetry data. Methods in Ecology and Evolution 9, 2262–2272. https://doi.org/10.1111/2041-210X.13080

Worton, B.J., 1989. Kernel Methods for Estimating the Utilization Distribution in Home-Range Studies. Ecology 70, 164–168. https://doi.org/10.2307/1938423

Worton, B.J., 1987. A review of models of home range for animal movement. Ecological Modelling 38, 277–298. https://doi.org/10.1016/0304-3800(87)90101-3

Chapter 3

Small coastal marine protected areas offer recurring, seasonal protection to the common stingray (*Dasyatis pastinaca*)

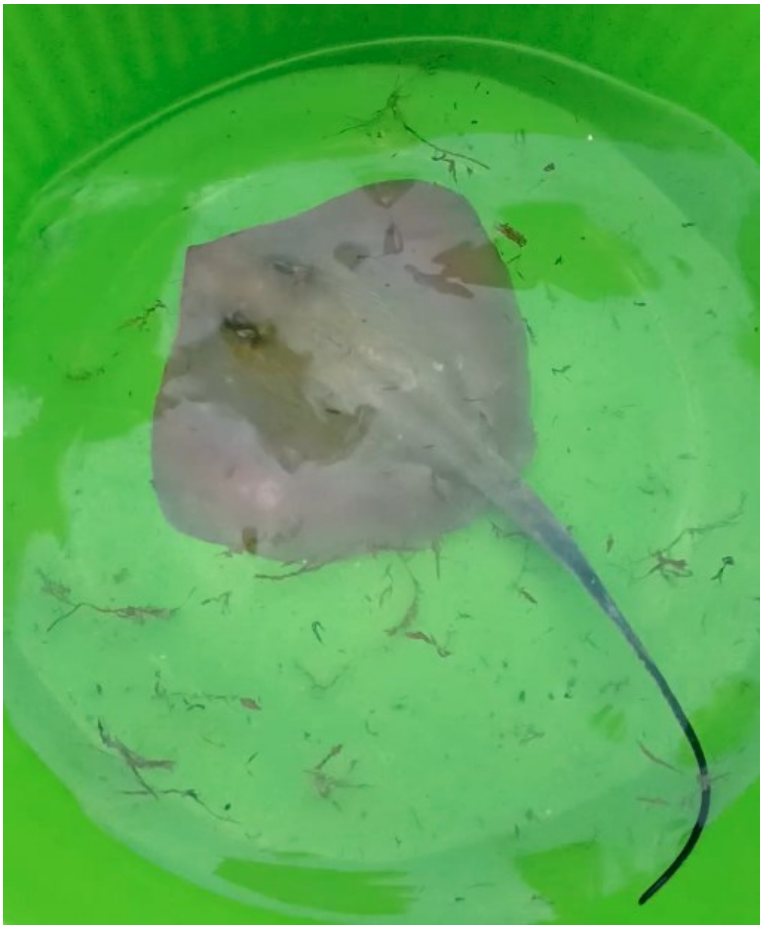

Dasyatis pastinaca ready for tagging

Chapter published as:

Kraft, S., Winkler, A. C., Abecasis, D. 2023. Small coastal marine protected areas offer recurring, seasonal protection to the common stingray (*Dasyatis pastinaca*). Ocean & Coastal Management, 246, 106891. https://doi.org/10.1016/j.ocecoaman.2023.106891

Abstract

Marine protected areas (MPAs) are a crucial tool in safeguarding marine biodiversity. However, elasmobranchs are often not the primary protection target of MPAs, and their contribution to protect these species remains to be better understood. In this study we examine the movement patterns of *Dasyatis pastinaca* in the Professor Luiz Saldanha marine park, a Portuguese temperate coastal MPA. Using acoustic telemetry, we tagged 31 common stingrays and analyzed their spatial and temporal distribution within the MPA and adjacent areas using a long-term data set. Our findings indicate that this species exhibits seasonal site fidelity, with greater presence during the colder months and reduced presence during warmer months. Space use areas did not exceed the size of the fully protected area, and nocturnal and crepuscular activity was significantly higher than during daytime. Additionally, we observed that most individuals seasonally migrated between this MPA and the nearby Sado estuary, likely to reproduce in the latter. These results demonstrate the site fidelity of common stingrays to an area within the marine park, however the protection provided is only seasonal. Seasonal protection of the movement corridor between the marine park and the estuary would improve the management of this species.

Keywords: Acoustic telemetry, conservation, Dasyatidae, residency, space use

3.1 Introduction

Elasmobranchs (sharks, skates and rays) are among the most susceptible groups to overfishing, due to the long-lived life strategies of most species. These are characterized by slow growth, late maturity and low fecundity (Musick, 1999), and given their inherent vulnerability to overfishing, it is regarded as the main reason for their population declines and the major threat these animals are facing (Dulvy et al., 2021). Among the strategies implemented to counter the consequences overfishing has on elasmobranchs and other marine species is the establishment of marine protected areas (MPAs) (Gell and Roberts, 2003). MPAs are "clearly defined geographical space, recognized, dedicated and managed, through legal or other effective means, to achieve the long-term conservation of nature with associated ecosystem services and cultural values" (Dudley, 2008). MPAs have positively impacted fisheries and several other areas, including human well-being, economics, knowledge development, and conservation and management actions of marine species and habitats (Ban et al., 2019; Lester et al., 2009).

However, their implementation can be complex, and their contribution to the protection of elasmobranchs is not as explored and well understood compared to other groups like bony fishes. Although evidence of swift MPA-induced improvements for elasmobranchs exists (Le Port et al., 2012; Speed et al., 2018), the magnitude of this effect is variable and often considered moderate, at least when isolated MPAs are implemented (Dwyer et al., 2020; MacKeracher et al., 2019). Protecting movement corridors and creating networks of connected MPAs have been mentioned as effective steps to improve the protection of elasmobranchs (Chapman et al., 2005; Lédée et al., 2015). Most MPAs might not properly encompass their movements, because many MPAs are not established considering elasmobranchs as one of their conservation targets and these are highly mobile species that often undergo long migrations (Dwyer et al., 2020; MacKeracher et al., 2019). Therefore, to evaluate and eventually improve the protection given by established MPAs to elasmobranchs, a better understanding of their movement patterns is needed (Davidson and Dulvy, 2017; MacKeracher et al., 2019).

Acoustic telemetry is a well-suited method to study the movements of marine animals in an area of interest, like an MPA, and evaluate its protection efficiency (Abecasis et al., 2014c). It allows to monitor the long-term movements of multiple individuals in a continuous and mostly automated way, and collect large amounts of data (Hussey et al., 2015). This way, acoustic telemetry can improve our understanding of animal movement patterns, which are important sources of information to evaluate how protection can change over time (Heupel and

Simpfendorfer, 2005) and evaluate and optimize protected areas (Chevis et al., 2017). Nonetheless, there is a general scarcity in studies on the spatial ecology of batoids (Myliobatiformes, Rajiformes, Rhinopristiformes and Torpediniformes) (Matley et al., 2021).

The Professor Luís Saldanha Marine Park (LSMP), part of the Arrábida Natural Park, is a 53 km^2 coastal MPA off the Setúbal peninsula designated in 1998 and completely established by 2009 (Portuguese legislation, Council of Ministers Resolution 141/2005). The geographic area where this MPA is established is important because of its high biodiversity (Cunha et al., 2014; Gonçalves et al., 2002; Henriques et al., 2009), its role as a transition area between colder water species of higher latitudes and warmer water species of lower latitudes (Henriques et al., 2007), and because of a nearby upwelling hotspot (Fiúza, 1983). After its establishment, the LSMP's spatial protection was explored for commercially important species of fish (Abecasis et al., 2015, 2014a) and cuttlefish (Abecasis et al., 2013) using acoustic telemetry. Additionally, some batoids have also been studied (Cabral, 2014; Sousa et al., 2019). However, because of the low number of individuals in these studies and their short duration, the benefits this marine park is providing to them remains to be further evaluated.

The common stingray (*Dasyatis pastinaca*) is a medium-sized batoid found in the northeastern Atlantic, from the British Isles to Mauritania, and the Mediterranean (Last et al., 2016). It occurs to depths of at least 160 metres (Ellis et al., 2004). In Portugal, common stingrays are landed along most of the country's coast, although generally not labeled at the species level (Alves et al., 2020). Landings average 0.15 tonnes per year, while an additional 2.66 tonnes are landed as *Dasyatis* spp. (Alves et al., 2020). Declines in abundance of this species have been reported in the Central Mediterranean (Colloca et al., 2020) and the Atlantic coast of France (Quero, 1998). Coastal and shallow-occurring elasmobranchs are more threatened due to greater exposure to human activities like fishing, coastal development, and habitat degradation (Dulvy et al., 2021). In turn, the family Dasyatidae is one of the most endangered elasmobranch families (Dulvy et al., 2021) and common stingrays are currently catalogued as vulnerable by the IUCN Red List in the species' global, European and Mediterranean assessments (IUCN, 2020).

In this study, we tracked common stingrays using acoustic telemetry to understand their presence and movement patterns in the LSMP and surrounding area. Then we aimed at relating this to the marine park's design and regulations to find possible improvements. Therefore, our objectives in this study were to 1) estimate residency and space use of common stingrays within the LSMP; 2) study their small- and large-scale movement patterns and the influence of environmental variables (i.e., diel phases, temperature); and 3) evaluate the marine park's

contribution to protecting this species under the current regulations and propose changes to improve them.

3.2 Materials and methods

3.2.1 Study area

The LSMP's 53 km^2 are divided into three protection levels: a total protection area -or marine reserve- of 4.3 km^2 to which access and any kind of fishing are prohibited; four partial protection areas totaling 21 km^2 where only octopus traps and jigs are allowed beyond 200 m from the coastline; and three complementary protection areas or buffer areas of a total 28 km^2 where only local licensed fishing boats under 7 m are allowed to operate. To the east is the Sado estuary (hereafter Sado) in which a natural reserve is in place, the Reserva Natural do Estuário do Sado. Additionally, the Tejo estuary (hereafter, Tejo) is found to the north, with its mouth at around 30 km in a straight line from the LSMP. Inside Tejo, another natural reserve is established, the Reserva Natural do Estuário do Tejo, which covers the innermost area of the estuary and the land surrounding it (Figure 3.1). The LSMP was implemented with the goal of protecting marine biodiversity and sustaining the livelihoods of the local fishers. The Tejo and Sado natural reserves are RAMSAR sites (wetland sites designated of international importance under the Ramsar Convention) due to their importance for many aquatic birds and as a nursery area for several fish and invertebrate species.

3.2.2 Study species

Common stingrays are viviparous, giving birth to litters of around 10 pups (Saadaoui et al., 2015). Pups are born after a gestation period estimated to last between four to six months (Ismen, 2003; Saadaoui et al., 2015), suggesting a yearly reproductive cycle (Saadaoui et al., 2015). Studies from various localities show that the reproductive season of common stingrays takes place during the warmer months of the year, in spring and summer (Chaikin et al., 2020; Ismen, 2003; Morey et al., 2006; Saadaoui et al., 2015). Estimates of maturity sizes have been obtained mostly from the central and eastern Mediterranean (Tunisia, north Aegean Sea, Turkey) and one study presented some data from Senegal. These estimations show regional variability; males mature at sizes between 22 and 33 cm in disc width and females between 24 and 42 cm disc width (Saadaoui et al., 2015). Common stingrays are mostly captured as bycatch, and depending on the location can be discarded (Tiralongo et al., 2018) or retained

(Yaglioglu et al., 2015). Because of their venomous tail stinger, it is not uncommon to kill them before removing them from fishing gear (Tiralongo et al., 2018).

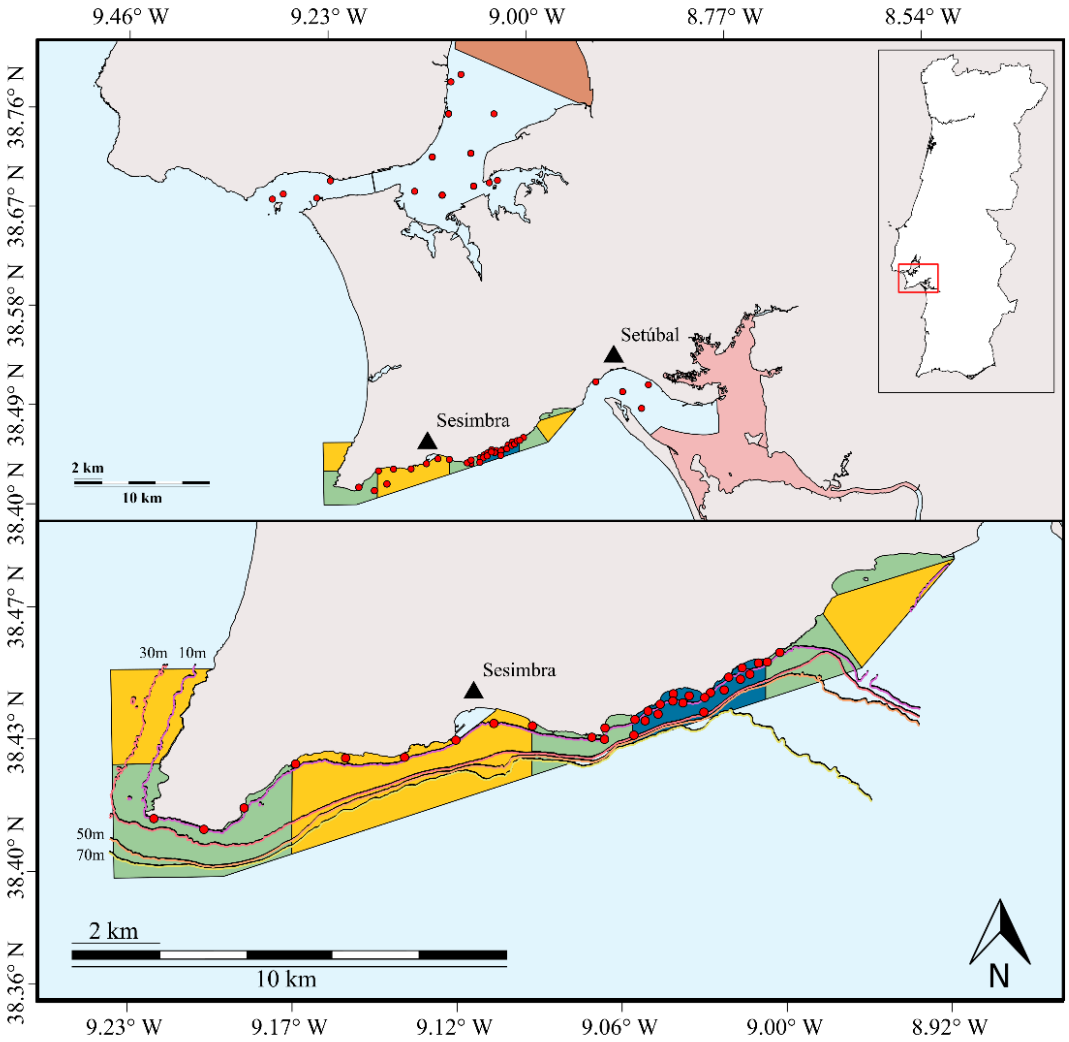

Figure 3.1: Top panel shows a general overview of the Setúbal peninsula with the Tejo estuary and its Natural Reserve (orange) to the north and the Sado estuary and its Natural reserve (red) to the East. Also to the south is the Professor Luis Saldanha Marine Park (bottom panel). The three different protection levels are shown: the total protection area (blue), complementary protection areas (green), and buffer areas (yellow). Only the aquatic portions of the Natural Reserves are shown. Acoustic receivers are indicated by red circles and isobaths are colour coded.

3.2.3 Tagging and tracking

We used monofilament trammel nets and longlines to capture stingrays inside the LSMP in April (n = 10) and October (n = 10) 2019 and in April (n = 10) and October (n = 1) 2021. The trammel nets were 500 m in length, 1.6 m in height, with inner panels of stretched mesh of 100 mm and outer panels of 600 mm. We deployed trammel nets in the morning (6-7 AM) and left them for 24 hours. We mounted one longline with 120 hooks (size 4/0), baited them

with chopped sardines and deployed it in the afternoon of October 15, 2021, for 12 hours. Thirty stingrays were captured with trammel nets and a single individual was captured with the longline.

We placed each captured specimen in an onboard tank with water and used a hydrophone to detect previously tagged individuals. We measured individuals (disc width, total length, and clasper length for males) and evaluated sex by looking for the presence of claspers. We made a small incision of approximately 2 cm with a scalpel in the peritoneal cavity to insert an acoustic transmitter and stitched it using absorbable suture. We selected the tag (Innovasea, either V9, V13, or V9P) based on individual size and transmitter availability. Tags had a frequency of 69 kHz and an emission interval of 60-120 s, with an average of 90 s. Additionally, we fitted either a disc or t-tag (www.floytag.com) with a unique identifier and contact information to the pectoral fin. Before release, we checked that the inserted tag was operational using the hydrophone.

We monitored the study area using an array of 33 Innovasea VR2W acoustic receivers (Figure 3.1). Not all receivers were active throughout the study period, and a few stations had receivers for shorter times than the study duration. We had four active receivers at different times in Sado and obtained additional detections from an array located in Tejo by accessing data available through the European Tracking Network (ETN). Previous evaluations of detection efficiency in the LSMP have shown no major variations due to environmental variables, diel patterns and/or background noises (Abecasis et al., 2014a; Sousa et al., 2019).

3.2.4 Data analysis

Before analyzing the data, we visually examined individual detection plots to determine fish fates following Villegas-Ríos et al., (2020). We classified individuals that were detected throughout the study period, i.e., until or near the battery expiration date/last data download, as “survived”, and individuals for which detections were not recorded for a long time before the aforementioned dates, and whose last detections were in a peripheral station of the acoustic array, as “dispersed”. We classified individuals that were last detected in Sado as "dispersed" and "fishing mortality" because the array design did not allow distinguishing these two classes. We excluded dead individuals from further analysis (Table 3.1).

We estimated two residency indices (Kraft et al., 2023) separately for the LSMP and Sado: I_R, obtained as total number of days detected by at least one receiver (D_d) divided by the duration of the monitoring period (D_t, time between release and last data download or tag expiration dates): $I_R = D_d/D_t$, and as a weighted residency index (Iw_R), obtained by multiplying

I_R by the days between first and last detection (D_i) divided by D_t: $I_{WR} = (D_d/D_t)$ x (D_i/D_t). We replaced D_t with tag lifetime in the equations if the latter was shorter than the total monitoring period (Abecasis et al., 2013).

We calculated centers of activity (COAs; Simpfendorfer et al., 2002) every 30 minutes to estimate space use in the LSMP using the dynamic Brownian bridge movement model (dBBMM) (Kranstauber et al., 2012). We selected this probability distribution-based occurrence estimator because the acoustic array only partially covered part of the stingrays' movements in the marine park and not their entire home range area. Occurrence estimators are a better fit in these situations because the former look into the space use during the monitoring period, while home range estimators assume the entire space use is surveyed (Fleming et al., 2015; Kraft et al., 2023).

We calculated minimum distance covered every 30 minutes as a proxy of activity in the LSMP, calculating a straight line between consecutive COAs (step length) using the R package *adehabitatLT* (Calenge, 2006). We estimated activity per diel phase by assigning them it into day, night, and twilight using the R package *suncalc* (Thieurmel and Elmarhraoui, 2019). "Day" included time between sunrise and sunset (appearance and disappearance of the sun over the horizon), "twilight" included dawn and dusk, and "night" was the period between morning twilight and evening twilight. We only retained step lengths between consecutive COAs (i.e., every 30 minutes) and discarded longer step lengths (i.e., calculated between COAs that were apart 60 min or more). This is because, the individual could have left the area and then returned during the time with no detections, covering a much greater distance than the straight line obtained for those 60 minutes. We evaluated differences in step length and depth across these three categories (day, night, and twilight) with a repeated measures ANOVA (RM-ANOVA) using the R package *stats* (R Core Team, 2020). The average number of detections per hour per individual was calculated to investigate diel variations in the presence of individuals in the array, removing simultaneous detections first.

We investigated depth by calculating average depth every 10 minutes using data from two individuals. To standardize values and remove the influence of tides on depth estimations in the LSMP, we obtained local daily high and low tides for the study period using the R package *PTtidaltools* (Martins, 2021) and subtracted tide height from the corresponding depth value. We conducted a t-test to compare depth differences among diel phases.

To evaluate the drivers of MPA use, we used a Generalized Additive Model via the R package *mgcv* (Wood, 2011) to study the relationship between the presence of stingrays in the LSMP (as daily presence/absence) and sea surface temperature (SST), day of the year (doy),

stingray size, sex, and individual. We used a cyclic cubic spline to model the effect of day of the year and temperature and treated individual-level effects as random. We obtained daily SST using the Copernicus Marine Service (https://marine.copernicus.eu) and evaluated the level of correlation between SST and day of the year. We used the function gam because it performs better with binary data than the gamm function (Wood, 2011). We obtained a correlation of 0.58, which can be considered a moderate degree of correlation. We decided to run the models without SST to favour a more conservative approach (Johnston et al., 2019). Furthermore, coastal SST estimates from satellite data can vary greatly from those obtained in situ (Smit et al., 2013) and SST estimates from large-scale satellite data can often have poor predictive performance (Santos et al., 2021). Finally, we tested different models combining the mentioned explanatory variables using the Akaike Information Criterion (AIC) in the R package *AICcmodavg* (Mazerolle, 2023). The full model (model 1) was:

Probability of presence ~ s(doy, bs = "cc") + size + sex + s(individual, bs = "re")

We tested variations to this model: model 2 did not consider size (doy+sex+individual), model 3 did not consider sex (doy+size+individual), and model 4 did not consider either (doy+individual).

3.3 Results

We captured and tagged 31 individuals (17 males, 14 females) between April 2019 and October 2021 (Table 3.1), thirty individuals using trammel nets and one using the longline (*Dasyatis pastinaca* [Dp] individual 31, released with the hook in). We tagged 14 individuals inside the total protection area and 17 in the partially protected areas adjacent to it. The sex ratio did not differ from an expected 1:1 ratio (two-tailed binomial test $p = 0.12$). Overall average disc width was 34 cm, 35 cm for males and 33 cm for females (Table 3.1). According to most estimations of size at maturity, all or most of the individuals qualify as mature (Saadaoui et al., 2015). Based on the criteria proposed by Villegas-Ríos et al., (2020) to identify post-release mortality, we identified at least five mortality events. The detection patterns of Dp 01, 10, 14 and 29 showed that they remained stationary shortly after release, suggesting they either dropped the tag or suffered from post-release mortality (Villegas-Ríos et al., 2020). Similarly, after Dp 02 moved to Sado it remained there even after the other tagged individuals returned to the LSMP and was only detected by a single receiver. For these reasons we also considered it as potentially deceased. Dp 22 and 28 were never detected, suggesting they left the study area immediately after tagging (Figure 3.2). We obtained an average of 611

monitoring days. Using the full dataset (LSMP, Sado, and Tejo), each stingray was detected on average on 143 days and had a detection interval of 379 days (Table 3.1). Dp 19 and 26 were not included in the calculations of occurrence area and step length because no detections.

Table 3.1: Biological data, tagging data, and residency and space use values of the 31 tagged common stingrays. Tag durations marked with an asterisk indicate those that completed their battery life during the study. Tag delay was 90 seconds. Individuals that were considered deceased or presented insufficient tracking data were not used in residency and space use estimations (Dp 02 in the LSMP was the only exception). D_d = number of days detected by at least one receiver, D_i = number of days between first and last detection or detection interval, and D_t = monitoring period defined as the number of days between release and last data download/tag expiration date. Fish fate categories based on Villegas-Ríos et al., (2020).

							LSMP				Sado				LSMP		
Fish ID	**Sex**	**Disc width (cm)**	**Release date**	**Tag type (Innovasea)**	**Tag duration (days)**	**D_t**	**D_d**	**D_i**	**I_R**	**I_{WR}**	**D_d**	**D_i**	**I_R**	**I_{WR}**	**Core area (50%, km2)**	**Occurrence area (95%, km2)**	**Fish fate**
Dp 01	F	39.5	02/04/2019	V9	651*	652	173	535	-	-	-	-	-	-	-	-	Deceased
Dp 02	M	29.6	03/04/2019	V9	651*	652	3	3	-	-	96	282	-	-	0.80	3.33	Deceased
Dp 03	F	30.8	03/04/2019	V9	651*	652	21	343	0.03	0.02	7	239	0.01	0.00	0.45	3.54	Fishing mortality/dispersed
Dp 04	F	30.4	03/04/2019	V9	651*	652	2	2	0.00	0.00	1	1	0.00	0.00	-	-	Fishing mortality/dispersed
Dp 05	M	35.7	03/04/2019	V13	1317	1130	331	1063	0.29	0.28	102	969	0.09	0.08	0.23	1.41	Survived
Dp 06	M	35.5	03/04/2019	V13	1317	1130	155	366	0.14	0.04	9	207	0.01	0.00	0.22	1.02	Fishing mortality/dispersed
Dp 07	M	31.1	03/04/2019	V9	651*	652	191	368	0.29	0.17	17	346	0.03	0.01	0.30	1.88	Fishing mortality/dispersed
Dp 08	F	30.2	03/04/2019	V9	651*	652	106	329	0.16	0.08	5	131	0.01	0.00	0.35	2.10	Fishing mortality/dispersed
Dp 09	M	28.5	03/04/2019	V9	651*	652	2	2	0.00	0.00	-	-	-	-	-	-	Dispersed
Dp 10	F	35.5	03/04/2019	V13	1317	1130	975	1127	-	-	-	-	-	-	-	-	Deceased
Dp 11	F	36.5	20/10/2019	V13	1317	930	113	738	0.12	0.10	53	760	0.06	0.05	0.61	2.78	Fishing mortality/dispersed
Dp 12	M	36.0	20/10/2019	V9	651*	652	76	126	0.12	0.02	24	300	0.04	0.02	0.36	2.31	Fishing mortality/dispersed
Dp 13	M	39.0	20/10/2019	V9	651*	652	128	454	0.20	0.14	76	576	0.12	0.10	0.15	1.13	Fishing mortality/dispersed
Dp 14	M	34.5	20/10/2019	V9	651*	652	491	496	-	-	-	-	-	-	-	-	Deceased
Dp 15	M	39.0	20/10/2019	V9	651*	652	195	474	0.30	0.22	70	657	0.11	0.11	0.52	2.93	Survived
Dp 16	M	37.5	20/10/2019	V9	651*	652	271	505	0.42	0.32	40	655	0.06	0.06	0.37	1.88	Survived
Dp 17	F	39.5	20/10/2019	V9	651*	652	135	487	0.21	0.15	13	377	0.02	0.01	0.36	2.30	Dispersed
Dp 18	M	41.0	20/10/2019	V13	1317	930	136	166	0.15	0.03	13	26	0.01	0.00	0.19	0.99	Dispersed
Dp 19	F	38.5	22/10/2019	V9	651*	652	1	1	0.00	0.00	2	2	0.00	0.00	-	-	Fishing mortality/dispersed
Dp 20	M	42.0	22/10/2019	V9P	404*	405	179	410	0.44	0.45	96	367	0.24	0.21	0.39	1.63	Survived
Dp 21	M	38.0	06/04/2021	V9	651	396	163	375	0.41	0.39	7	376	0.02	0.02	0.16	1.38	Survived
Dp 22	F	25.0	07/04/2021	V9	651	395	-	-	-	-	-	-	-	-	-	-	Not detected
Dp 23	F	26.0	07/04/2021	V9	651	395	117	342	0.30	0.26	7	340	0.02	0.02	0.33	1.77	Survived
Dp 24	M	33.0	07/04/2021	V9	651	395	154	354	0.39	0.35	2	154	0.01	0.00	0.16	1.17	Survived
Dp 25	F	34.0	07/04/2021	V9	651	395	4	5	0.01	0.00	-	-	-	-	-	-	Dispersed
Dp 26	F	30.0	07/04/2021	V9	651	395	1	1	0.00	0.00	1	1	0.00	0.00	-	-	Fishing mortality/dispersed
Dp 27	M	31.0	07/04/2021	V9	651	395	137	338	0.35	0.30	36	337	0.09	0.08	0.26	2.04	Survived
Dp 28	F	39.0	09/04/2021	V9P	404	393	-	-	-	-	-	-	-	-	-	-	Not detected
Dp 29	M	25.0	09/04/2021	V9	651	393	287	391	-	-	-	-	-	-	-	-	Deceased
Dp 30	F	26.0	09/04/2021	V9	651	393	121	338	0.31	0.26	6	337	0.02	0.01	0.39	1.84	Survived
Dp 31	M	37.0	15/10/2021	V9P	404	204	120	151	0.59	0.44	5	151	0	0.02	0.20	1.37	Survived
Male avg.		34.9			758	636	160	368	0.29	0.22	38	394	0.06	0.05	0.27	1.63	
Female avg.		32.9			712	577	62	259	0.11	0.09	11	243	0.02	0.01	0.42	2.39	
Total avg.		34.0			738	611	119	322	0.22	0.17	27	332	0.04	0.04	0.32	1.87	

3.3.1 Detection patterns and residency

The detection patterns noted among the 25 individuals (Figure 3.2) can be sorted into two broad categories. The dominant pattern among individuals in this study was a consistent seasonal movement between the LSMP and Sado, while a few permanently dispersed from the LSMP at some point during the study, some after tagging (e.g., Dp 04, 09, 25, 26) and some after some months (Dp 18).

Individuals were mostly detected in the fully protected area (FPA) and its adjacent partially protected areas (PPAs), and only Dp 11, 18 and 27 were detected in the buffer area off the port of Sesimbra. Dp 18 was also the only stingray detected in the westernmost PPA at the tip of the peninsula on its way to Tejo, where it was detected over 60 km from its tagging point in two separate detection intervals. These intervals were at approximately the same time the other stingrays were detected in Sado: from April 28th to October 12th, 2020, and April 21st to October 17th, 2021 (Figure 3.2). There was a three-month detection gap in the Tejo array during the six months between these two detection periods, from December 23rd, 2020, and March 23rd, 2121. Dp 18 was not detected in the LSMP again after moving to Tejo.

The overall residency in the LSMP was low (I_R = 0.21), ranging between 0.00 and 0.59 (Table 3.1). Residency was lower for females (I_R = 0.11) than males (I_R = 0.27). Monthly residences were highest between October/November until March/April of each year, reaching values of I_R = 1 or very close to 1 several times (Figure 3.2, supplementary material 3.1). During these periods the median detection frequency per individual was 154 s (range = 104-2801 s) after removing possible simultaneous detections (all detections under the delay interval of the tags). Only two of the 25 individuals had averages higher than 8 minutes (Dp 26 with 23.6 min and Dp 30 with 46.7 min). In contrast, from March/April to October/November stingrays became virtually absent from the LSMP, as only a few were detected for short periods. A residency value of 0 was obtained between June-September 2019, May-August 2020, and May-October 2021. During these low residency periods in the LSMP, 23 of the 25 valid individuals (92%) travelled to Sado at least once, some in two and even three consecutive years (Figure 3.2).

Of the individuals detected in Sado, 14 were male and 9 were female. Males were detected in Sado on more days than females (average 42.4 vs. 10.5 days per individual) which resulted in a higher residency index (average I_{Rmales} = 0.07, range 0.01-0.24 vs. $I_{Rfemales}$ = 0.02, range 0.00-0.06). Brief ventures returning to the area where they departed from were seen a

few times (i.e., a brief period back in Sado after moving to the LSMP and vice versa, e.g., Dp 03, 05, 08, 11, 13, 15 – Figure 3.2).

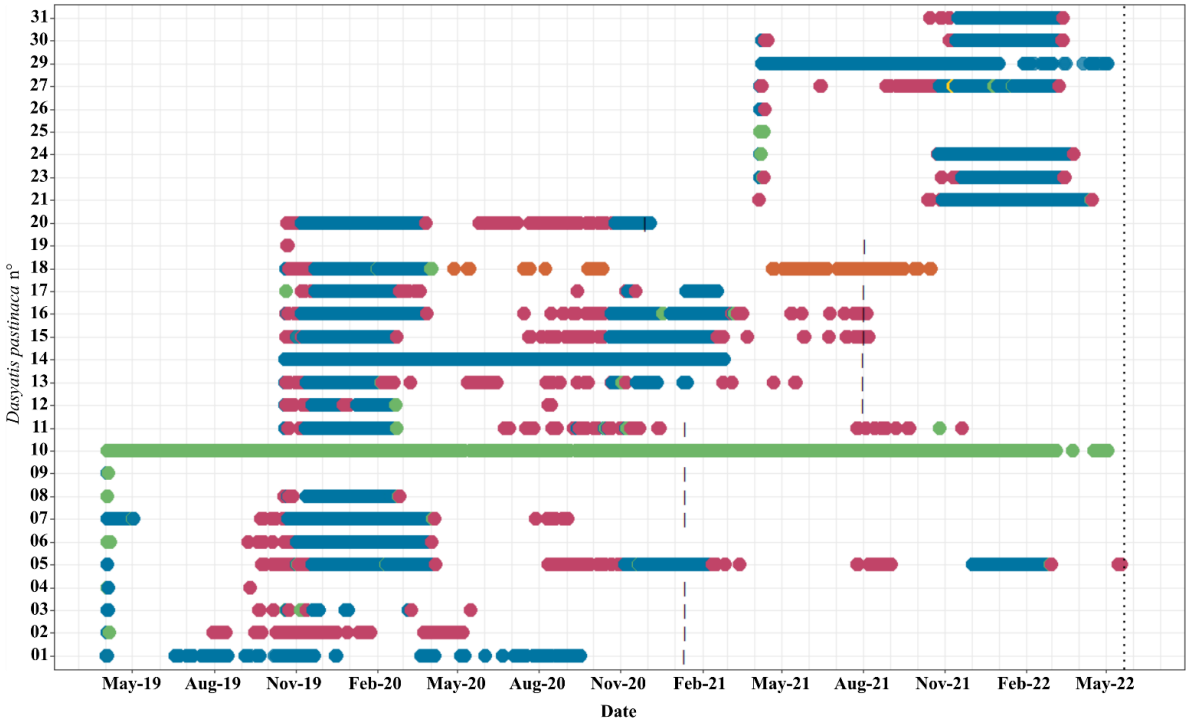

Figure 3.2: Abacus plot of the common stingrays tagged and monitored in this study, between April 2019 and May 2022. Detections are colour-coded as fully protected area (blue), partially protected area (green), buffer area (yellow), Sado (red) and Tejo (orange). All first detections were on the release date. Tag expiration dates are indicated by a vertical line and the dotted line indicates date of last data download.

3.3.2 Space use

We calculated activity space for 19 individuals (13 males and 6 females, Table 3.1) and excluded Dp 04, 09, 19, 25, and 26 because of an insufficient number of COAs. We also excluded the space use estimate of Dp 02 because of the low number of days (D_d = 3). The average 50% or core area size was 0.32 km^2 (range 0.15-0.80 km^2) and 95% or occurrence area was 1.87 km^2 (range 0.99-3.54 km^2). The locations of the space use estimations were mostly in the fully protected area, and all were of smaller size. Space use estimates were larger for females and showed significant statistical difference (Mann-Whitney U Test for 50% area estimates: U-value = 15, p = 0.04, and for 95% area estimates: U-value = 15, p = 0.04). Individual plots are available in supplementary material 3.2.

3.3.3 Activity

We obtained a total of 114729 step lengths of 30 minutes for 20 individuals and removed 3198 steps with intervals between 60 minutes and 351 days. In addition to the individuals already removed considered dead (Dp 01, 10, 14, 19, 26 and 29), we removed three Dp 04 and Dp 09 were detected only one day during daytime (8 and 15 steps respectively), and Dp 25 yielded insufficient step lengths (n = 7, all equal to zero), suggesting it remained static before leaving the array. Average step length was similar across individuals, except for Dp 02 which also had the lowest number of steps (n = 47) (Figure 3.3, supplementary material 3.3). Between males and females, there was neither a statistically significative difference in the average number of steps (two-tailed t-test, t = 1.79, p = 0.09) nor in the average step length (two-tailed t-test, t = -0.07, p = 0.95). Average distance was larger during twilight (64.09 m), followed by night (57.97 m) and lowest during the day (48.22 m), and was statistically significant among diel phases and individuals (RM-ANOVA: F=11.29, p = 0.0003 and F= 10.35, p = 0.0003, respectively). During daytime a greater proportion of values of 0 or close to 0 were obtained compared to the night and crepuscular hours.

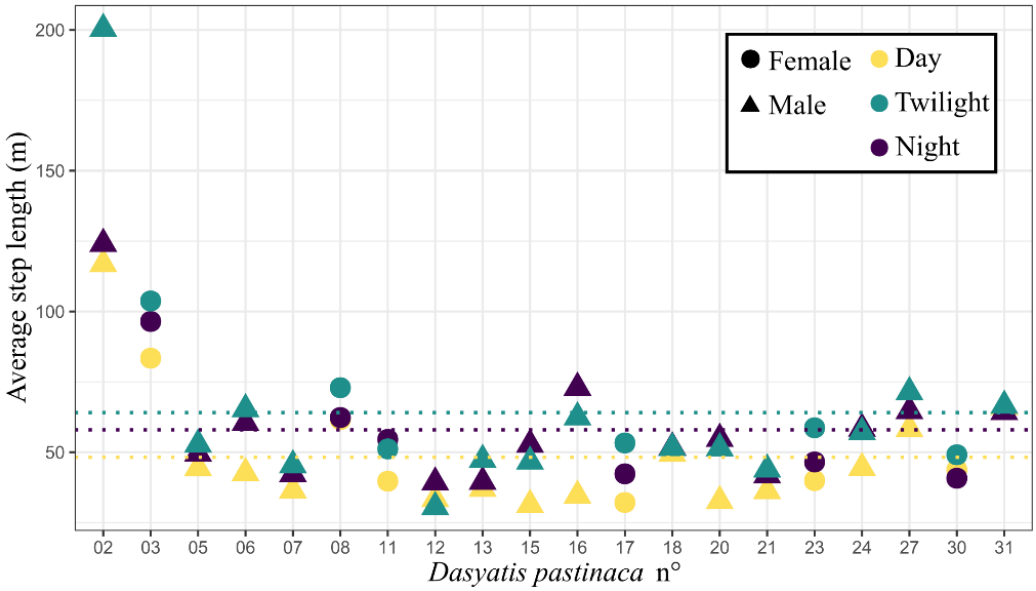

Figure 3.3: Average step length per diel phase per individual common stingray: day (yellow), twilight (green), and night (purple). Females are shown with a circle and males with a triangle. Horizontal dotted lines indicate overall average. Detailed data on step length are available in supplementary material 3.3.

The average number of detections per hour per individual was similar throughout the day (Figure 3.4), also including hours with 0 detections. All individuals but Dp 02 shared this pattern of steady detection frequency. During the two days it was detected in the MPA, it

showed a higher average number of detections during earlier hours of the day, which lowered with the progress of the day. We also detected this individual for only three days in the MPA. Hourly averages ranged from 25.3 to 27.4 detections per hour, and average number of detections per hour per individual averaged between 17.5 (Dp 15) and 30.2 (Dp 05).

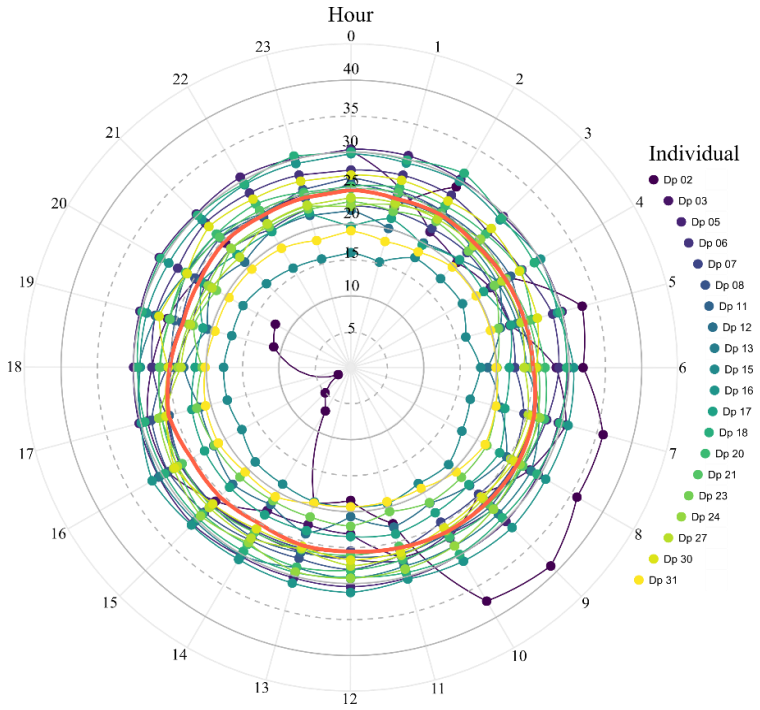

Figure 3.4: Average number of detections per hour per individual common stingray over a 24-hour period. Red line shows the hourly average.

3.3.4 Depth

Two V9P tags produced enough information for analysis. We obtained a total of 21974 average depth values every 10 minutes for Dp 20 (male, 42.0 cm DW): 9284 for daytime, 9886 for night-time and 2804 values for twilight. The total for Dp 31 (male, 37.0 cm DW) was 14206: 6071 for daytime, 6268 for night-time and 1867 values for twilight. Following the correction for tidal height, average depth for Dp 20 was greatest during the night (16.1m ±2.6m, range 5.4-26.9m), followed by twilight (15.6m ±2.6m, range 8.4-25.9m) and shallowest during the day (15.4m ±2.8m, 3.5-23.3m). For Dp 31 the results were inverted, on average occurring deeper during the day (12.4m ±2.5, range 4.6-24.6m), followed by twilight (11.1m ±3.1m, range 2.5-29.2m) and shallowest at night (10.6m ±3.3m, range 1.0-27.3m). The statistical significance of depth across diel phases was not evaluated due to the low number of individuals.

3.3.5 Environmental drivers of MPA use

Of the four models tested, the AIC selected the full model (model 1, AIC = 5769.36), however, the model without size scored only slightly higher (model 2, AIC = 5769.39). The models that scored the highest were the model without sex (model 3, AIC = 5863.77) and the model that only considered individual effect in addition to the day of the year (model 4, AIC = 5863.81). Because of the small difference between models 1 and 2, we selected the latter (day of the year, sex and individual effect as variables) because it was simpler and gave similar results. For model 2 we obtained statistically significant relationships with the probability of presence for day of the year and individual effect (both $p < 0.001$), while sex was non-significant ($p = 0.08$) (Table 3.2).

Throughout the year, the highest probability of presence was in autumn and winter months, i.e., the days at the start and end of the year. Contrastingly, probability of presence fell to near zero or zero between these days, declining rapidly before the 100th day of the year and increased again, also rapidly, after the 300th day of the year (Figure 3.5), roughly coinciding with the transition from winter to spring and from summer to autumn, respectively.

Table 3.2: Summary of the model output investigating the probability of presence of common stingrays in the LSMP, showing the included variables.

Parametric coefficients				
	Estimate	Std. Error	z value	Pr(>|z|)
(Intercept)	-5.1468	0.7576	-6.794	0.4789
sex (male)	1.2844	0.7259	1.769	0.0768
Approximate significance of smooth terms:				
	edf	Ref.df	Chi.sq	p-value
s(doy)	6.418	8	51635	< 0.001
s(individual)	16.794	17	1114	< 0.001

R-sq.(adj) = 0.582, deviance explained = 55.6%, -REML = 2977.6,
scale est. = 1, n = 11922

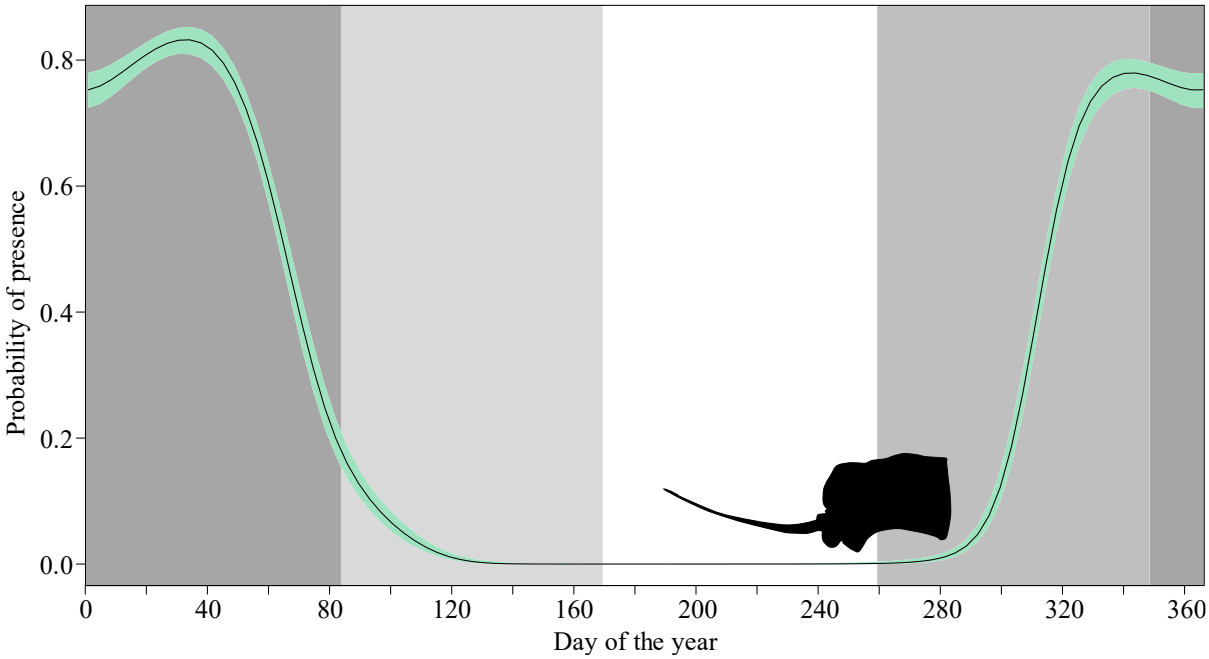

Figure 3.5: Predicted probability of presence of common stingrays (n=19) in the LSMP as a function of the day of the year. The area in green represents the 95% confidence interval. Grey shading represents seasons of the year (from left to right: winter, spring, summer, autumn, winter).

3.4 Discussion

In this study, we obtained long-term movement data of common stingrays and investigated diel and seasonal movements. Diel activity was higher during nocturnal and crepuscular hours compared to daytime hours. At a larger scale, most individuals showed a markedly seasonal presence in the marine park and appeared to be permanent/year-round residents of the southern coast of the Setúbal peninsula, moving seasonally between the LSMP and Sado. A few individuals dispersed after tagging, possibly to other areas (e.g., Dp 18 to Tejo). We were able to obtain these results because different sites were monitored during the study (LSMP, Sado, and Tejo), allowing us to identify other areas that were visited and the time of the year in which they were visited. This is, to our knowledge, the first acoustic telemetry study on common stingrays in the world, through which we were able to enhance the understanding of their spatial ecology in this area, which will help in assessing and improving their protection.

3.4.1 Residency in the LSMP and seasonal pattern

During their presence in the LSMP, they moved mostly inside the FPA. The reasonably stable average number of detections per hour and among individuals suggests they do not engage in significant daily on/offshore movements, and likely stay close to the array throughout the entire day. If individuals were to make considerable movements towards deeper waters (and thus away from the acoustic array), as seen in other batoids (Humphries et al., 2017), we would expect greater intervals between detections. The depth data indicates something similar, as we only found small differences between diel phases. Despite the statistical significance, these depth differences might not be ecologically significative. Although based on only two individuals, these results suggest that they might stay at similar depths throughout the day. Contrastingly, activity levels did vary throughout the day, in a pattern that is common among elasmobranchs (Hammerschlag et al., 2016). Greater nocturnal and crepuscular activity compared to daytime is usually associated with foraging (Hammerschlag et al., 2016), while the shorter average step length during daytime suggests that stingrays are less active and/or spend more time resting during these hours. Other species in the family Dasyatidae show similar patterns (Cartamil et al., 2003; Ward et al., 2019). It must be noted that net displacements of zero meters could be obtained if during successive COAs a stingray moved within the detection range of the same receiver. This underestimates activity because, despite there being movement, net displacement is zero because only one pair of coordinates is included in the estimation of COAs. Nonetheless, increases in the distances covered were large enough to overcome this and note diel differences in activity.

Considering the design of the acoustic array, which was denser in the fully protected area, additional support for their preference can be found in previous work. During a biannual experimental fishing study conducted in the LSMP, sampling in autumn and spring from 2007-2015 and 2018-2019, no stingrays were captured in the buffer area (Martínez-Ramírez et al., 2021). One possibility is that this preference relates to the influence of bottom type on the distribution of batoids (Santos et al., 2021; Serra-Pereira et al., 2014). In the LSMP, most protection levels represent similar substrata (Henriques et al., 2015), however, the part closest to Sado is dominated by coarse sand, while in the part where the array is found (fully protected area and part of the adjacent partially protected areas) other bottom types first appear (fine, medium, and mixed sand, muddy to sandy mud) which these individuals seem to be favouring. In addition to closeness to Sado, this preference might be influenced by predator and/or prey

distributions (although large predators like sharks are not common in this area) and protection from currents to minimize energy expenditure (Campbell et al., 2012).

The seasonal residency pattern displayed by most stingrays and supported by the abacus plot and the GAMM results can be defined as site fidelity or autumn and winter residency (Chapman et al., 2015) strongly influenced by the day of the year. This pattern did not appear to be influenced by the sex of individuals; however, this could also be a result of low sample size in the GAMM. We obtained sex-related differences in residency, as males had an average residency over twice as high. The latter result could be influenced by the low number of individuals considered in the analysis. However, the GAMM results did show inter-individual differences in presence, suggesting this is an important factor in shaping their residency patterns. This study adds to the similar seasonal patterns that have been reported for this species in other areas (Chaikin et al., 2020; Yaglioglu et al., 2015).

Seasonal movements occur for various reasons, like in response to fluctuations in prey availability, predator avoidance, shifts in environmental conditions, and onset of the reproductive season (Jaine et al., 2014; Papastamatiou and Lowe, 2012). Regarding the latter, reproductive migrations are undertaken by mature individuals, and estimates of maturity size of common stingrays have been obtained elsewhere and show high regional variability (Saadaoui et al., 2015). Disc width at 50% maturity ranged from 22 to 33 cm for males and 24 to 42 cm for females (including transformed total length values in studies providing the equations to convert them). Using the lowest maturity sizes results in all individuals being classified as mature, while using the greatest size estimates yields most males and none of the females as mature. Considering this, we assume an intermediate scenario where most individuals of both sexes are mature. Joint migration of mature and large sub-adults have been reported, for example, in smalltooth sawfish *Pristis pectinata* (Graham et al., 2021). The same area could be used for different purposes, like reproduction for mature individuals and seasonal feeding grounds/refuges for immature individuals and subadults.

Further evidence to link the seasonal migration and Sado to the reproduction of common stingrays can be drawn from the timing of their movement and duration of their absence from the LSMP, as these coincide with the time and span of their reproductive season as shown by studies in other areas. For example, high abundances of stingrays have been reported in the Balearic Islands in June, likely for reproduction (Morey et al., 2006); pregnant females with fully developed offspring appear in the Gulf of Gabès in June, neonates during the end of June and beginning of July (Saadaoui et al., 2015); and pregnant females have been seen in Iskenderun Bay between May and early September and parturition events beginning in

July (Ismen, 2003). Similarly, in the coast of the Levant stingrays aggregate and display courtship behaviour in March and more females in advanced gravid states are seen in June (Chaikin et al., 2020). The gestation period is estimated to last from four to six months (Ismen, 2003; Saadaoui et al., 2015), which suggest a yearly reproductive cycle (Saadaoui et al., 2015). Finally, estuaries provide shelter and thermoregulatory advantages for the reproduction of several elasmobranchs (Schlaff et al., 2014). The higher temperatures of estuaries are thought to provide stingrays with energetic advantages that shorten the gestation period (Jirik and Lowe, 2012). Considering this evidence, this seasonal pattern could be interpreted as parturition site fidelity to Sado (Chapman et al., 2015).

3.4.2 Conservation and management

Interpreting protection as being proportional to time spent inside a protected area, the overall (year-round) protection received by common stingrays in the LSMP is low, as indicated by the low global residency index (I_R = 0.21). However, residency also fluctuated greatly throughout the year as an outcome of their migration, which highlights the relevance of understanding long-term movements to optimize the efficiency of conservation and management efforts.

Stingrays mainly occupied the FPA and adjacent PPAs, where elasmobranchs in general are under full protection because the activities permitted in them do not target these species. In the part of the LSMP where they were mostly detected the protected areas cover a continuous 11.09 km^2, over three times the largest 95% space use area we obtained However, the marine park is much narrower in an offshore direction, between approximately 450 metres to a maximum of under 2 km along this segment. Therefore, compared to movements along the coast, offshore movements could expose them more to edge effect (Ohayon et al., 2021) and fishing the line (Kellner et al., 2007).

When migrating to Sado, stingrays seasonally expanded their space use beyond the LSMP's boundaries, which increases risk exposure (Villegas-Ríos et al., 2021). A natural reserve is already in place in Sado, however, the receivers at its entrance also were the ones to detect nine out of 23 individuals (39%) for the last time. This could be attributed to tag malfunction or loss, dispersal (e.g., Dp 18), but also to fishing mortality. However, with our study design we were not able to discern whether or not they were captured and if this occurred inside or outside of the reserve. The area between the LSMP and Sado is not protected and, at least until the LSMP's establishment, near-shore illegal drift nets were placed east of the marine park during spring and summer (Horta e Costa et al., 2013c). Considering this, a permanent or seasonal

protected corridor linking the LSMP and the Reserva Natural do Estuário do Sado could improve the contribution of both areas to the protection of common stingrays. For example, restrictions on fishing gear (e.g. banning the use of trammel nets and longlines) would reduce exposure to fishing pressure and improve the overall performance of the marine park (Chapman et al., 2005) and could even enhance the LSMP's early signs of reserve effect. Preliminary evidence of increases in size, biomass and abundance was found for four batoid species (Martínez-Ramírez et al., 2021; Sousa et al., 2018). Although some of the cited results must be interpreted with caution (Martínez-Ramírez et al., 2021), such findings are usually regarded as one of the initial signs of reserve effect (Di Franco et al., 2009). An increase in total length was also detected for common stingrays, although this data was not analyzed in depth due to sampling issues (Martínez-Ramírez et al., unpublished data). Future evaluations of the LSMP will be well complemented by the results on the movement patterns of common stingrays presented here, to adapt the currently implemented protection measures.

3.4.3 Shortcomings, future directions

Possible sources of bias in our study design could be found in the array's greater coverage of the FPA compared to the PPAs and BAs, and the tendency of some animals to remain around their tagging location (Espinoza et al., 2015). However, these results can also be the outcome of true area preferences for a few reasons. First, while stingrays were in the LSMP, the detection frequency median was 154 seconds, suggesting a steady presence in this area. Secondly, during the nearly three years of the study only three individuals were briefly detected by the receivers in the buffer area, suggesting little use of this area. These could be transit areas in some cases, like for Dp 18. Lastly, during a previous experimental fishing study that took place twice a year over a total of 11 non-consecutive years no stingrays were captured in the buffer area (Martínez-Ramírez et al., 2021), hence the difficulty of tagging individuals in those areas.

Calculating step lengths using COAs served as proxy of the activity, however, this approach is too coarse to robustly infer their activity patterns. Future efforts using better suited devices like acceleration tags could produce data of greater detail and provide better estimations (Pereñíguez et al., 2022).

Other future efforts should focus on exploring sex-related differences. Although these results were not all robust, the much higher residency of males suggests there might be differences in protection, which should be clarified in the future to detect possible inequalities in protection.

Finally, the dispersal of individuals and the detection of one in Tejo using data obtained from the ETN exemplify the need and benefits of collaborations to expand detection capabilities in future studies. Establishing collaborations with researchers that operate acoustic arrays in other areas can fulfil this requirement, improving subsequent studies and eventually the data that is used in conservation and management decisions (Abecasis et al., 2018; Ellis et al., 2019).

Contributions

DA and SK conceptualized and designed the study. SK, ACW and DA captured and tagged the individuals of this study and acquired the data. SK, ACW and DA maintained the receiver network. SK conducted the analyses, prepared the figures for publication, and drafted the article. SK, ACW and DA interpreted the data. SK, ACW and DA revised it critically for important intellectual content. All authors have approved the final article.

Permits

Capture, handling, and tagging were done under the 'catch and release' practices of the Portuguese Institute for Nature Conservation and Forests (permit n°11478683) and the Veterinary General Directorate (permit n° 2018-08-29 015730).

Funding

SK was supported by the "la Caixa" Foundation grant LCF/BQ/DI20/11780001. This study received funding from the INFORBIOMARES project (POSEUR-03-2215-FC-000047), and FCT projects UIDB/04326/2020, UIDP/04326/2020 and LA/P/0101/2020. DA acknowledges FCT support through the transitional norm DL57/2016/CP1361/CT0036.

Acknowledgements

We would like to thank Juliano Macedo (operation of vessel and trammel nets), Joffrey Baeyaert (tagging, deploying, and maintaining receivers), Lucas Martínez-Ramírez and C. Robert Priester (tagging and receiver maintenance), and "Flipper Divers" dive centre (receiver maintenance), Miguel Gandra and Eliza Fragkopoulou (data analysis). Data was sourced from the European Tracking Network data portal (http://www.lifewatch.be/etn/), developed by the Flanders Marine Institute as part of the Flemish contribution to LifeWatch.

Declaration of competing interest

The authors declare no conflicts of interest.

Declaration of Generative AI and AI-assisted technologies in the writing process

No Generative AI and AI-assisted technologies were used to write this manuscript.

3.5 References

Abecasis, D., Afonso, P., Erzini, K., 2014a. Combining multispecies home range and distribution models aids assessment of MPA effectiveness. Marine Ecology Progress Series 513, 155–169. https://doi.org/10.3354/meps10987

Abecasis, D., Afonso, P., Erzini, K., 2014b. Can small MPAs protect local populations of a coastal flatfish, *Solea senegalensis*? Fisheries Management and Ecology 21, 175–185. https://doi.org/10.1111/fme.12061

Abecasis, D., Afonso, P., O'Dor, R.K., Erzini, K., 2013. Small MPAs do not protect cuttlefish (*Sepia officinalis*). Fisheries Research 147, 196–201. https://doi.org/10.1016/j.fishres.2013.05.004

Abecasis, D., Horta e Costa, B., Afonso, P., Gonçalves, E.J., Erzini, K., 2015. Early reserve effects linked to small home ranges of a commercial fish, *Diplodus sargus*, Sparidae. Marine Ecology Progress Series 518, 255–266. https://doi.org/10.3354/meps11054

Abecasis, D., Steckenreuter, A., Reubens, J., Aarestrup, K., Alós, J., Badalamenti, F., Bajona, L., Boylan, P., Deneudt, K., Greenberg, L., Brevé, N., Hernández, F., Humphries, N., Meyer, C., Sims, D., Thorstad, E.B., Walker, A.M., Whoriskey, F., Afonso, P., 2018. A review of acoustic telemetry in Europe and the need for a regional aquatic telemetry network. Animal Biotelemetry 6, 12. https://doi.org/10.1186/s40317-018-0156-0

Alves, L.M.F., Correia, J.P.S., Lemos, M.F.L., Novais, S.C., Cabral, H., 2020. Assessment of trends in the Portuguese elasmobranch commercial landings over three decades (1986–2017). Fisheries Research 230, 105648. https://doi.org/10.1016/j.fishres.2020.105648

Ban, N.C., Gurney, G.G., Marshall, N.A., Whitney, C.K., Mills, M., Gelcich, S., Bennett, N.J., Meehan, M.C., Butler, C., Ban, S., Tran, T.C., Cox, M.E., Breslow, S.J., 2019. Well-being outcomes of marine protected areas. Nature Sustainability 2, 524–532. https://doi.org/10.1038/s41893-019-0306-2

Cabral, S., 2014. *Raja* spp. spatial dynamics in the Arrábida Marine Park (M. Sc. Thesis). Universidade do Algarve.

Calenge, C., 2006. The package "adehabitat" for the R software: A tool for the analysis of space and habitat use by animals. Ecological Modelling 197, 516–519. https://doi.org/10.1016/j.ecolmodel.2006.03.017

Campbell, H.A., Hewitt, M., Watts, M.E., Peverell, S., Franklin, C.E., 2012. Short- and long-term movement patterns in the freshwater whipray (*Himantura dalyensis*) determined by the signal processing of passive acoustic telemetry data. Marine and Freshwater Research 63, 341–350. https://doi.org/10.1071/MF11229

Cartamil, D.P., Vaudo, J.J., Lowe, C.G., Wetherbee, B.M., Holland, K.N., 2003. Diel movement patterns of the Hawaiian stingray, *Dasyatis lata*: implications for ecological interactions between sympatric elasmobranch species. Marine Biology 142, 841–847. https://doi.org/10.1007/s00227-003-1014-y

Chaikin, S., Belmaker, J., Barash, A., 2020. Coastal breeding aggregations of threatened stingrays and guitarfish in the Levant. Aquatic Conservation: Marine and Freshwater Ecosystems 30, 1160–1171. https://doi.org/10.1002/aqc.3305

Chapman, D.D., Feldheim, K.A., Papastamatiou, Y.P., Hueter, R.E., 2015. There and Back Again: A Review of Residency and Return Migrations in Sharks, with Implications for

Population Structure and Management. Annual Review of Marine Science 7, 547–570. https://doi.org/10.1146/annurev-marine-010814-015730

Chapman, D.D., Pikitch, E.K., Babcock, E., Shivji, M.S., 2005. Marine Reserve Design and Evaluation Using Automated Acoustic Telemetry: A Case-study Involving Coral Reef-associated Sharks in the Mesoamerican Caribbean. Marine Technology Society Journal 39, 42–55. https://doi.org/10.4031/002533205787521640

Chevis, M.G., Godley, B.J., Lewis, J.P., Jackson Lewis, J., Scales, K.I., Graham, R.T., 2017. Movement patterns of juvenile hawksbill turtles *Eretmochelys imbricata* at a Caribbean coral atoll: long-term tracking using passive acoustic telemetry. Endangered Species Research 32, 309–319. https://doi.org/10.3354/esr00812

Colloca, F., Carrozzi, V., Simonetti, A., Di Lorenzo, M., 2020. Using Local Ecological Knowledge of Fishers to Reconstruct Abundance Trends of Elasmobranch Populations in the Strait of Sicily. Frontiers in Marine Science 7, 508. https://doi.org/10.3389/fmars.2020.00508

Cunha, A.H., Erzini, K., Serrão, E.A., Gonçalves, E., Borges, R., Henriques, M., Henriques, V., Guerra, M., Duarte, C., Marbá, N., Fonseca, M., 2014. Biomares, a LIFE project to restore and manage the biodiversity of Prof. Luiz Saldanha Marine Park. Journal of Coastal Conservation 18, 643–655. https://doi.org/10.1007/s11852-014-0336-x

Davidson, L.N.K., Dulvy, N.K., 2017. Global marine protected areas to prevent extinctions. Nature Ecology & Evolution 1, 0040. https://doi.org/10.1038/s41559-016-0040

Di Franco, A., Bussotti, S., Navone, A., Panzalis, P., Guidetti, P., 2009. Evaluating effects of total and partial restrictions to fishing on Mediterranean rocky-reef fish assemblages. Marine Ecology Progress Series 387, 275–285. https://doi.org/10.3354/meps08051

Dudley, N. (Ed.), 2008. Guidelines for Applying Protected Area Management Categories. IUCN, Gland, Switzerland.

Dulvy, N.K., Pacoureau, N., Rigby, C.L., Pollom, R.A., Jabado, R.W., Ebert, D.A., Finucci, B., Pollock, C.M., Cheok, J., Derrick, D.H., Herman, K.B., Sherman, C.S., VanderWright, W.J., Lawson, J.M., Walls, R.H.L., Carlson, J.K., Charvet, P., Bineesh, K.K., Fernando, D., Ralph, G.M., Matsushiba, J.H., Hilton-Taylor, C., Fordham, S.V., Simpfendorfer, C.A., 2021. Overfishing drives over one-third of all sharks and rays toward a global extinction crisis. Current Biology 31, 4773-4787.e8. https://doi.org/10.1016/j.cub.2021.08.062

Dwyer, R.G., Krueck, N.C., Udyawer, V., Heupel, M.R., Chapman, D., Pratt, H.L., Garla, R., Simpfendorfer, C.A., 2020. Individual and Population Benefits of Marine Reserves for Reef Sharks. Current Biology 30, 480-489.e5. https://doi.org/10.1016/j.cub.2019.12.005

Ellis, J.R., Cruz-Martínez, A., Rackham, B.D., Rogers, S.I., 2004. The Distribution of Chondrichthyan Fishes Around the British Isles and Implications for Conservation. Journal of Northwest Atlantic Fishery Science 35, 195–213. https://doi.org/10.2960/J.v35.m485

Ellis, R.D., Flaherty-Walia, K.E., Collins, A.B., Bickford, J.W., Boucek, R., Walters Burnsed, S.L., Lowerre-Barbieri, S.K., 2019. Acoustic telemetry array evolution: From species- and project-specific designs to large-scale, multispecies, cooperative networks. Fisheries Research 209, 186–195. https://doi.org/10.1016/j.fishres.2018.09.015

Espinoza, M., Heupel, M. R., Tobin, A.J., Simpfendorfer, C.A., 2015. Movement patterns of silvertip sharks (*Carcharhinus albimarginatus*) on coral reefs. Coral Reefs 34, 807–821. https://doi.org/10.1007/s00338-015-1312-0

Fiúza, A.F.G., 1983. Upwelling Patterns off Portugal, in: Suess, E., Thiede, J. (Eds.), Coastal Upwelling Its Sediment Record. Springer US, Boston, MA, pp. 85–98. https://doi.org/10.1007/978-1-4615-6651-9_5

Fleming, C.H., Fagan, W.F., Mueller, T., Olson, K.A., Leimgruber, P., Calabrese, J.M., 2015. Rigorous home range estimation with movement data: a new autocorrelated kernel density estimator. Ecology 96, 1182–1188. https://doi.org/10.1890/14-2010.1

Gell, F.R., Roberts, C.M., 2003. Benefits beyond boundaries: the fishery effects of marine reserves. Trends in Ecology & Evolution 18, 448–455. https://doi.org/10.1016/S0169-5347(03)00189-7

Gonçalves, E.J., Henriques, R., Almada, V.C., 2002. Use of a temperate reef-fish community to identify priorities in the establishment of a Marine Protected Area, in: Beumer, J.P., Grant, A., Smith, D.C. (Eds.), Aquatic Protected Areas: What Works Best And How Do We Know? Proceedings of the World Congress on Aquatic Protected Areas. Cairns, Australia, pp. 261–272.

Graham, J., Kroetz, A., Poulakis, G., Scharer, R., Carlson, J., Lowerre-Barbieri, S., Morley, D., Reyier, E., Grubbs, R., 2021. Large-scale space use of large juvenile and adult smalltooth sawfish *Pristis pectinata*: implications for management. Endangered Species Research 44, 45–59. https://doi.org/10.3354/esr01088

Hammerschlag, N., Skubel, R.A., Calich, H., Nelson, E.R., Shiffman, D.S., Wester, J., Macdonald, C.C., Cain, S., Jennings, L., Enchelmaier, A., Gallagher, A.J., 2016. Nocturnal and crepuscular behavior in elasmobranchs: a review of movement, habitat use, foraging, and reproduction in the dark. Bulletin of Marine Science 93, 355–374. https://doi.org/10.5343/bms.2016.1046

Henriques, M., Gonçalves, E., Almada, V., 2007. Rapid shifts in a marine fish assemblage follow fluctuations in winter sea conditions. Marine Ecology Progress Series 340, 259–270. https://doi.org/10.3354/meps340259

Henriques, V., Guerra, M., Gaudêncio, M.J., Fonseca, P., Campos, A., Mendes, B., 2009. Biomares. Restoration and management of biodiversity in the Marine Park site Arrábida-Espichel (PTCON0010). Action A4. Marine habitat characterization. Progress report 2009. Relatório IPIMAR.

Henriques, V., Guerra, M.T., Mendes, B., Gaudêncio, M.J., Fonseca, P., 2015. Benthic habitat mapping in a Portuguese Marine Protected Area using EUNIS: An integrated approach. Journal of Sea Research 100, 77–90. https://doi.org/10.1016/j.seares.2014.10.007

Heupel, M.R., Simpfendorfer, C.A., 2005. Using Acoustic Monitoring to Evaluate MPAs for Shark Nursery Areas: The Importance of Long-term Data. Marine Technology Society Journal 39, 10–18. https://doi.org/10.4031/002533205787521749

Horta e Costa, B., Gonçalves, L., Gonçalves, E.J., 2013. Vessels' site fidelity and spatio-temporal distribution of artisanal fisheries before the implementation of a temperate multiple-use marine protected area. Fisheries Research 148, 27–37. https://doi.org/10.1016/j.fishres.2013.08.001

Humphries, N., Simpson, S., Sims, D., 2017. Diel vertical migration and central place foraging in benthic predators. Marine Ecology Progress Series 582, 163–180. https://doi.org/10.3354/meps12324

Hussey, N.E., Kessel, S.T., Aarestrup, K., Cooke, S.J., Cowley, P.D., Fisk, A.T., Harcourt, R.G., Holland, K.N., Iverson, S.J., Kocik, J.F., Mills Flemming, J.E., Whoriskey, F.G., 2015. Aquatic animal telemetry: A panoramic window into the underwater world. Science 348, 1255642–1255642. https://doi.org/10.1126/science.1255642

Ismen, A., 2003. Age, growth, reproduction and food of common stingray (*Dasyatis pastinaca* L., 1758) in İskenderun Bay, the eastern Mediterranean. Fisheries Research 60, 169–176. https://doi.org/10.1016/S0165-7836(02)00058-9

IUCN, 2020. *Dasyatis pastinaca*: Jabado, R.W., Chartrain, E., De Bruyne, G., Derrick, D., Dia, M., Diop, M., Doherty, P., Leurs, G.H.L., Metcalfe, K., Pacoureau, N., Pires, J.D., Ratão, S., Seidu, I., Serena, F., Soares, A.-L., Tamo, A., VanderWright, W.J. & Williams, A.B.: The IUCN Red List of Threatened Species 2021: e.T161453A124488102. https://doi.org/10.2305/IUCN.UK.2021-2.RLTS.T161453A124488102.en

Jaine, F., Rohner, C., Weeks, S., Couturier, L., Bennett, M., Townsend, K., Richardson, A., 2014. Movements and habitat use of reef manta rays off eastern Australia: offshore excursions, deep diving and eddy affinity revealed by satellite telemetry. Marine Ecology Progress Series 510, 73–86. https://doi.org/10.3354/meps10910

Jirik, K.E., Lowe, C.G., 2012. An elasmobranch maternity ward: female round stingrays *Urobatis halleri* use warm, restored estuarine habitat during gestation. Journal of Fish Biology 80, 1227–1245. https://doi.org/10.1111/j.1095-8649.2011.03208.x

Johnston, J.D., Dunn, C.J., Vernon, M.J., 2019. Tree traits influence response to fire severity in the western Oregon Cascades, USA. Forest Ecology and Management 433, 690–698. https://doi.org/10.1016/j.foreco.2018.11.047

Kellner, J.B., Tetreault, I., Gaines, S.D., Nisbet, R.M., 2007. Fishing the line near marine reserves in single and multispecies fisheries. Ecological Applications 17, 1039–1054. https://doi.org/10.1890/05-1845

Kraft, S., Gandra, M., Lennox, R.J., Mourier, J., Winkler, A.C., Abecasis, D., 2023. Residency and space use estimation methods based on passive acoustic telemetry data. Movement Ecology 11, 12. https://doi.org/10.1186/s40462-022-00364-z

Kranstauber, B., Kays, R., LaPoint, S.D., Wikelski, M., Safi, K., 2012. A dynamic Brownian bridge movement model to estimate utilization distributions for heterogeneous animal movement: The dynamic Brownian bridge movement model. Journal of Animal Ecology 81, 738–746. https://doi.org/10.1111/j.1365-2656.2012.01955.x

Last, P.R., Manjaji-Matsumoto, B.M., Naylor, G. J. P., White, W. T., 2016. Stingrays, family Dasyatidae, in: Last, P.R., White, William Toby, de Carvalho, M.R., Séret, B., Stehmann, M., Naylor, Gavin J. P., Marshall, L. (Eds.), Rays of the World. CSIRO Publishing, Clayton South VIC, pp. 522–618.

Le Port, A., Lavery, S., Montgomery, J.C., 2012. Conservation of coastal stingrays: seasonal abundance and population structure of the short-tailed stingray *Dasyatis brevicaudata* at a Marine Protected Area. ICES Journal of Marine Science 69, 1427–1435. https://doi.org/10.1093/icesjms/fss120

Lédée, E.J.I., Heupel, M.R., Tobin, A.J., Knip, D.M., Simpfendorfer, C.A., 2015. A comparison between traditional kernel-based methods and network analysis: an example from two nearshore shark species. Animal Behaviour 103, 17–28. https://doi.org/10.1016/j.anbehav.2015.01.039

Lester, S., Halpern, B., Grorud-Colvert, K., Lubchenco, J., Ruttenberg, B., Gaines, S., Airamé, S., Warner, R., 2009. Biological effects within no-take marine reserves: a global synthesis. Marine Ecology Progress Series 384, 33–46. https://doi.org/10.3354/meps08029

MacKeracher, T., Diedrich, A., Simpfendorfer, C.A., 2019. Sharks, rays and marine protected areas: A critical evaluation of current perspectives. Fish and Fisheries 20, 255–267. https://doi.org/10.1111/faf.12337

Martínez-Ramírez, L., Priester, C.R., Sousa, I., Erzini, K., Abecasis, D., 2021. Reserve effect of a small North-East Atlantic marine protected area (Arrábida, Portugal) on soft-sediment fish species. Aquatic Conservation: Marine and Freshwater Ecosystems 31, 1584–1595. https://doi.org/10.1002/aqc.3577

Martins, M., 2021. PTtidaltools - R package to retrieve and manipulate data from the Portuguese National Hydrographic Institute. https://doi.org/10.5281/ZENODO.4562490

Matley, J.K., Klinard, N.V., Barbosa Martins, A.P., Aarestrup, K., Aspillaga, E., Cooke, S.J., Cowley, P.D., Heupel, M.R., Lowe, C.G., Lowerre-Barbieri, S.K., Mitamura, H., Moore, J.-S., Simpfendorfer, C.A., Stokesbury, M.J.W., Taylor, M.D., Thorstad, E.B., Vandergoot, C.S., Fisk, A.T., 2021. Global trends in aquatic animal tracking with acoustic telemetry. Trends in Ecology & Evolution S0169534721002470. https://doi.org/10.1016/j.tree.2021.09.001

Mazerolle, M.J., 2023. AICcmodavg: Model selection and multimodel inference based on (Q)AIC(c). R package version 2.3.2.

Morey, G., Moranta, J., Riera, F., Grau, A.M., Morales-Nin, B., 2006. Elasmobranchs in trammel net fishery associated to marine reserves in the Balearic Islands (NW Mediterranean). Cybium 30, 125–132. https://doi.org/10.26028/cybium/2006-304supp-017

Musick, J.A., 1999. Life in the Slow Lane: Ecology and Conservation of Long-Lived Marine Animals, in: Musick, J.A. (Ed.), Ecology and Conservation of Long-Lived Marine Animals. American Fisheries Society. https://doi.org/10.47886/9781888569155

Ohayon, S., Granot, I., Belmaker, J., 2021. A meta-analysis reveals edge effects within marine protected areas. Nature Ecology & Evolution 5, 1301–1308. https://doi.org/10.1038/s41559-021-01502-3

Papastamatiou, Y.P., Lowe, C.G., 2012. An analytical and hypothesis-driven approach to elasmobranch movement studies. Journal of Fish Biology 80, 1342–1360. https://doi.org/10.1111/j.1095-8649.2012.03232.x

Pereñíguez, J.M., Venerus, L.A., Gutiérrez-Cánovas, C., Abecasis, D., Ciancio, J.E., Jiménez-Montalbán, P., García-Charton, J.A., 2022. Acoustic telemetry and accelerometers: a field comparison of different proxies for activity in the marine environment. ICES Journal of Marine Science 79, 2600–2613. https://doi.org/10.1093/icesjms/fsac190

Quero, J.C., 1998. Changes in the Euro-Atlantic fish species composition resulting from fishing and ocean warming. Italian Journal of Zoology 65, 493–499. https://doi.org/10.1080/11250009809386873

R Core Team, 2020. R: A language and environment for statistical computing.

Saadaoui, A., Saïdi, B., Enajjar, S., Bradai, M.N., 2015. Reproductive biology of the common stingray *Dasyatis pastinaca* (Linnaeus, 1758) off the Gulf of Gabès (Central Mediterranean Sea). Cahiers de Biologie Marine 56, 389–396.

Santos, R., Medeiros-Leal, W., Novoa-Pabon, A., Crespo, O., Pinho, M., 2021. Biological Knowledge of Thornback Ray (*Raja clavata*) from the Azores: Improving Scientific Information for the Effectiveness of Species-Specific Management Measures. Biology 10, 676. https://doi.org/10.3390/biology10070676

Schlaff, A.M., Heupel, M.R., Simpfendorfer, C.A., 2014. Influence of environmental factors on shark and ray movement, behaviour and habitat use: a review. Reviews in Fish Biology and Fisheries 24, 1089–1103. https://doi.org/10.1007/s11160-014-9364-8

Serra-Pereira, B., Erzini, K., Maia, C., Figueiredo, I., 2014. Identification of Potential Essential Fish Habitats for Skates Based on Fishers' Knowledge. Environmental Management 53, 985–998. https://doi.org/10.1007/s00267-014-0257-3

Simpfendorfer, C.A., Heupel, M.R., Hueter, R.E., 2002. Estimation of short-term centers of activity from an array of omnidirectional hydrophones and its use in studying animal movements. Canadian Journal of Fisheries and Aquatic Sciences 59, 23–32. https://doi.org/10.1139/f01-191

Smit, A.J., Roberts, M., Anderson, R.J., Dufois, F., Dudley, S.F.J., Bornman, T.G., Olbers, J., Bolton, J.J., 2013. A Coastal Seawater Temperature Dataset for Biogeographical Studies: Large Biases between In Situ and Remotely-Sensed Data Sets around the Coast of South Africa. PLoS ONE 8, e81944. https://doi.org/10.1371/journal.pone.0081944

Sousa, I., Baeyaert, J., Gonçalves, J.M.S., Erzini, K., 2019. Preliminary insights into the spatial ecology and movement patterns of a regionally critically endangered skate (*Rostroraja alba*) associated with a marine protected area. Marine and Freshwater Behaviour and Physiology 52, 283–299. https://doi.org/10.1080/10236244.2019.1705805

Sousa, I., Gonçalves, J.M.S., Claudet, J., Coelho, R., Gonçalves, E.J., Erzini, K., 2018. Soft-bottom fishes and spatial protection: findings from a temperate marine protected area. PeerJ 6, e4653. https://doi.org/10.7717/peerj.4653

Speed, C.W., Cappo, M., Meekan, M.G., 2018. Evidence for rapid recovery of shark populations within a coral reef marine protected area. Biological Conservation 220, 308–319. https://doi.org/10.1016/j.biocon.2018.01.010

Thieurmel, B., Elmarhraoui, A., 2019. R Package "suncalc": compute sun position, sunlight phases, moon position and lunar phase.

Tiralongo, F., Messina, G., Lombardo, B.M., 2018. Discards of elasmobranchs in a trammel net fishery targeting cuttlefish, *Sepia officinalis* Linnaeus, 1758, along the coast of Sicily (central Mediterranean Sea). Regional Studies in Marine Science 20, 60–63. https://doi.org/10.1016/j.rsma.2018.04.002

Villegas-Ríos, D., Claudet, J., Freitas, C., Moland, E., Thorbjørnsen, S.H., Alonso-Fernández, A., Olsen, E.M., 2021. Time at risk: Individual spatial behaviour drives effectiveness of marine protected areas and fitness. Biological Conservation 263, 109333. https://doi.org/10.1016/j.biocon.2021.109333

Villegas-Ríos, D., Freitas, C., Moland, E., Thorbjørnsen, S.H., Olsen, E.M., 2020. Inferring individual fate from aquatic acoustic telemetry data. Methods in Ecology and Evolution 11, 1186–1198. https://doi.org/10.1111/2041-210X.13446

Ward, C.R.E., Bouyoucos, I.A., Brooks, E.J., O'Shea, O.R., 2019. Novel attachment methods for assessing activity patterns using triaxial accelerometers on stingrays in the Bahamas. Marine Biology 166, 53. https://doi.org/10.1007/s00227-019-3499-z

Wood, S.N., 2011. Fast stable restricted maximum likelihood and marginal likelihood estimation of semiparametric generalized linear models. Journal of the Royal Statistical Society (B) 73, 3–36. https://doi.org/10.1111/j.1467-9868.2010.00749.x

Yaglioglu, D., Deniz, T., Gürleck, M., Ergüden, D., Turan, C., 2015. Elasmobranches bycatch in a bottom trawl fishery in the Iskenderun Bay, Northeastern Mediterranean. Cahiers de Biologie Marine 56, 237–243.

3.6 Supplementary material

Supplementary material 3.1: Monthly residency indices per common stingray individual in the LSMP and Sado over the study period. Cells with no values indicate either that the animal was not tagged yet or that the tag had expired. Values calculated for each area are not comparable between them because of the differences in receiver coverage. Vertical dotted lines indicate change of year. Continues on next page.

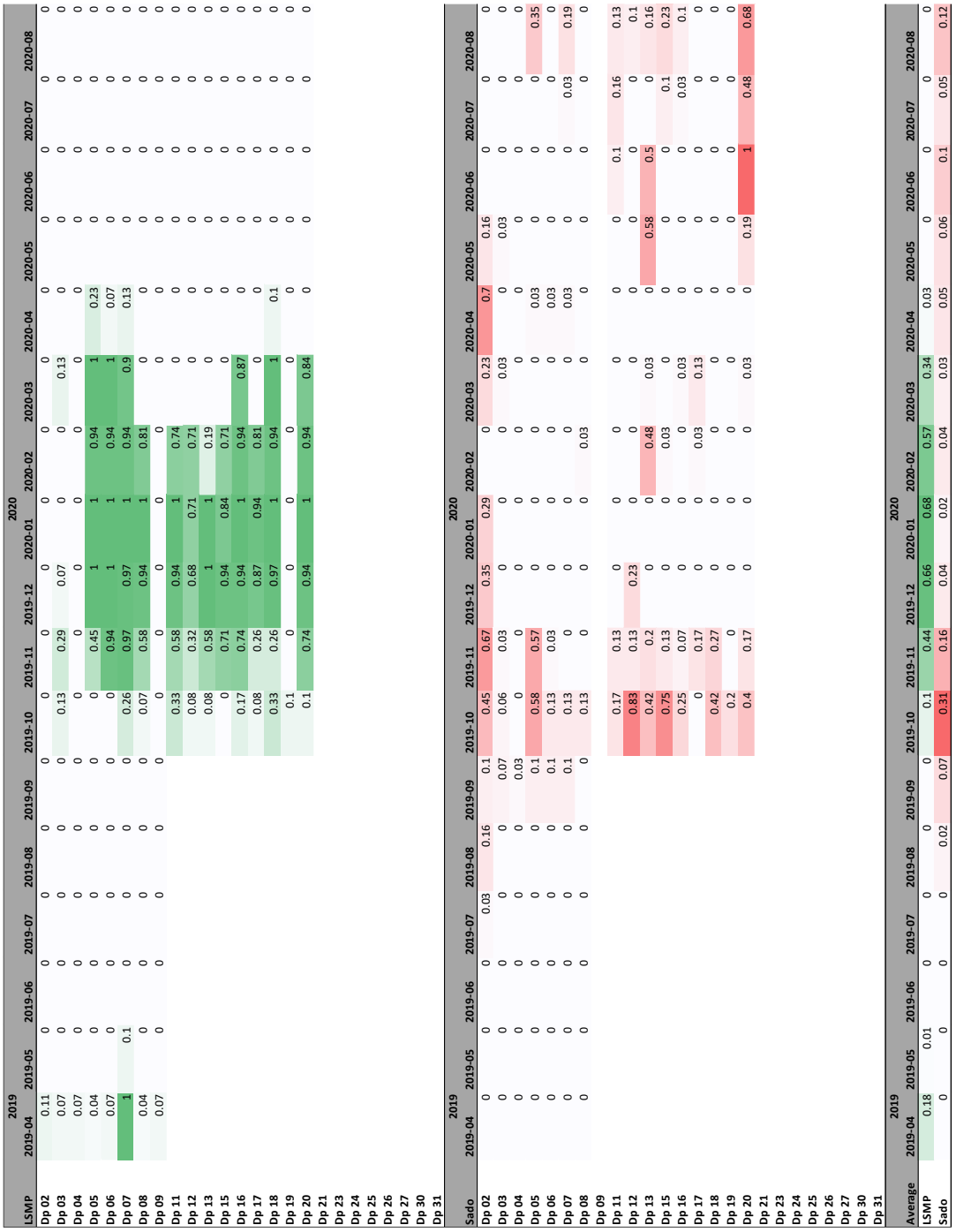

	2019										2020									
LSMP	2019-04	2019-05	2019-06	2019-07	2019-08	2019-09	2019-10	2019-11	2019-12	2020-01	2020-02	2020-03	2020-04	2020-05	2020-06	2020-07	2020-08			
Dp 02		0.11	0	0	0	0	0	0	0	0	0	0	0	0	0	0	0			
Dp 03		0.07	0	0	0	0	0	0.13	0.29	0.07	0	0	0.13	0	0	0	0			
Dp 04		0.07	0	0	0	0	0	0	0	0	0	0	0	0	0	0	0			
Dp 05		0.04	0	0	0	0	0	0	0.45	1	1	0.94	1	0.23	0	0	0			
Dp 06		0.07	0	0	0	0	0	0	0.94	1	1	0.94	1	0.07	0	0	0			
Dp 07	1		0.1	0	0	0	0	0.26	0.97	0.97	1	0.94	0.9	0.13	0	0	0			
Dp 08		0.04	0	0	0	0	0	0.07	0.58	0.94	1	0.81	0	0	0	0	0			
Dp 09		0.07	0	0	0	0	0	0	0	0	0	0	0	0	0	0	0			
Dp 11							0.33	0.58	0.94	1	0.74	0	0	0	0	0	0			
Dp 12							0.08	0.32	0.68	0.71	0.71	0	0	0	0	0	0			
Dp 13							0.08	0.58	1	1	1	0.19	0	0	0	0	0			
Dp 15							0	0.71	0.94	0.84	0.71	0	0	0	0	0	0			
Dp 16							0.17	0.74	0.94	1	0.94	0.87	0	0	0	0	0			
Dp 17							0.08	0.26	0.87	0.94	0.81	0	0	0	0	0	0			
Dp 18							0.33	0.26	0.97	1	0.94	1	0.1	0	0	0	0			
Dp 19							0.1	0	0	0	0	0	0	0	0	0	0			
Dp 20							0.1	0.74	0.94	1	0.94	0.84	0	0	0	0	0			
Dp 21																				
Dp 23																				
Dp 24																				
Dp 25																				
Dp 26																				
Dp 27																				
Dp 30																				
Dp 31																				

	2019										2020									
Sado	2019-04	2019-05	2019-06	2019-07	2019-08	2019-09	2019-10	2019-11	2019-12	2020-01	2020-02	2020-03	2020-04	2020-05	2020-06	2020-07	2020-08			
Dp 02		0	0	0	0.03	0.16	0.1	0.45	0.67	0.35	0.29	0	0.23	0.7	0.16	0	0			
Dp 03		0	0	0	0	0	0.07	0.06	0.03	0	0	0	0.03	0	0.03	0	0			
Dp 04		0	0	0	0	0	0.03	0	0	0	0	0	0	0	0	0	0			
Dp 05		0	0	0	0	0	0.1	0.58	0.57	0	0	0	0.03	0	0	0	0.35			
Dp 06		0	0	0	0	0	0.1	0.13	0.03	0	0	0	0.03	0	0	0	0			
Dp 07		0	0	0	0	0	0.1	0.13	0	0	0	0	0.03	0	0	0.03	0.19			
Dp 08		0	0	0	0	0	0	0.13	0	0	0	0.03	0	0	0	0	0			
Dp 09																				
Dp 11							0.17	0.13	0	0	0	0	0	0	0	0.1	0.16	0.13		
Dp 12							0.83	0.13	0.23	0	0	0	0	0	0	0	0	0.1		
Dp 13							0.42	0.2	0	0	0.48	0.03	0	0.58	0.5	0	0	0.16		
Dp 15							0.75	0.13	0	0	0.03	0	0	0	0	0.1	0.23			
Dp 16							0.25	0.07	0	0	0	0.03	0	0	0	0.03	0.1			
Dp 17							0	0.17	0	0	0.03	0.13	0	0	0	0	0			
Dp 18							0.42	0.27	0	0	0	0	0	0	0	0	0			
Dp 19							0.2	0	0	0	0	0	0	0	0	0	0			
Dp 20							0.4	0.17	0	0	0	0.03	0	0.19	1	0.48	0.68			
Dp 21																				
Dp 23																				
Dp 24																				
Dp 25																				
Dp 26																				
Dp 27																				
Dp 30																				
Dp 31																				

	2019										2020									
Average	2019-04	2019-05	2019-06	2019-07	2019-08	2019-09	2019-10	2019-11	2019-12	2020-01	2020-02	2020-03	2020-04	2020-05	2020-06	2020-07	2020-08			
LSMP	0.18	0.01	0	0	0	0	0.1	0.44	0.66	0.68	0.57	0.34	0.03	0	0	0	0			
Sado	0	0	0	0	0.02	0.07	0.31	0.16	0.04	0.02	0.04	0.03	0.05	0.06	0.1	0.05	0.12			

	2021																2022				
LSMP	2020-09	2020-10	2020-11	2020-12	2021-01	2021-02	2021-03	2021-04	2021-05	2021-06	2021-07	2021-08	2021-09	2021-10	2021-11	2021-12	2022-01	2022-02	2022-03	2022-04	2022-05
Dp 02	0	0	0	0	0																
Dp 03	0	0	0	0	0																
Dp 04	0	0	0	0	0																
Dp 05	0	0	0.81	1	1	0.36	0	0	0	0	0	0	0	0	0	0.97	1	0.9	0	0	0
Dp 06	0	0	0	0	0	0	0	0	0	0	0	0	0	0	0	0	0	0	0	0	0
Dp 07	0	0	0	0	0																
Dp 08	0	0	0	0	0																
Dp 09	0	0	0	0	0																
Dp 11	0.07	0.1	0.07	0	0	0	0	0	0	0	0	0	0	0.03	0	0	0	0	0	0	0
Dp 12	0	0	0	0	0	0	0	0	0	0	0	0									
Dp 13	0	0.29	0.48	0.39	0.16	0	0	0	0	0	0										
Dp 15	0	0.36	0.71	0.81	0.74	0.48	0	0	0	0	0										
Dp 16	0	0.32	0.94	0.77	1	0.87	0.29	0	0	0	0										
Dp 17	0	0	0.32	0	0.55	0.58	0	0	0	0	0										
Dp 18	0	0	0	0	0	0	0	0	0	0	0	0	0	0	0	0	0	0	0	0	0
Dp 19	0	0	0	0	0	0	0	0	0	0	0										
Dp 20	0	0.19	0.97																		
Dp 21								0.04	0	0	0	0	0	0.07	0.97	1	1	0.9	0.81	0.48	0
Dp 23								0.17	0	0	0	0	0	0	0.32	0.97	1	0.9	0.45	0	0
Dp 24								0.08	0	0	0	0	0	0.23	0.97	0.97	1	0.9	0.84	0	0
Dp 25								0.17	0	0	0	0	0	0	0	0	0	0	0	0	0
Dp 26								0.04	0	0	0	0	0	0	0	0	0	0	0	0	0
Dp 27								0.04	0	0	0	0	0	0.19	0.97	1	1	0.9	0.32	0	0
Dp 30								0.09	0	0	0	0	0	0	0.55	1	1	0.9	0.39	0	0
Dp 31														0.06	0.48	1	1	0.9	0.45	0	0

	2021																2022				
Sado	2020-09	2020-10	2020-11	2020-12	2021-01	2021-02	2021-03	2021-04	2021-05	2021-06	2021-07	2021-08	2021-09	2021-10	2021-11	2021-12	2022-01	2022-02	2022-03	2022-04	2022-05
Dp 02	0	0	0	0	0																
Dp 03	0	0	0	0	0																
Dp 04	0	0	0	0	0																
Dp 05	0.5	0.26	0	0	0	0.14	0.03	0	0	0	0.1	0.52	0.03	0	0	0	0	0	0.03	0	0.1
Dp 06	0	0	0	0	0	0	0	0	0	0	0	0	0	0	0	0	0	0	0	0	0
Dp 07	0.07	0	0	0	0																
Dp 08	0	0	0	0	0																
Dp 09																					
Dp 11	0.2	0.23	0.3	0.06	0	0	0	0	0	0	0.06	0.16	0.1	0	0.03	0	0	0	0	0	0
Dp 12	0	0	0	0	0	0	0	0	0	0	0	0									
Dp 13	0.13	0.03	0.03	0	0	0.04	0.03	0.03	0.1	0	0	0									
Dp 15	0.63	0.19	0	0	0	0.18	0.03	0	0.06	0.03	0.19	0.19									
Dp 16	0.2	0.13	0	0	0	0	0.16	0	0.1	0.03	0.23	0.13									
Dp 17	0.03	0	0.07	0	0	0	0	0	0	0	0	0									
Dp 18	0	0	0	0	0	0	0	0	0	0	0	0	0	0	0	0	0	0	0	0	0
Dp 19	0	0	0	0	0	0	0	0	0	0	0	0									
Dp 20	0.3	0.16	0	0	0	0	0	0	0	0	0	0	0	0	0	0	0	0	0	0	0
Dp 21								0.04	0	0	0	0	0	0.16	0	0	0	0	0	0.03	0
Dp 23								0.04	0	0	0	0	0	0.03	0.1	0	0	0	0.06	0	0
Dp 24								0	0	0	0	0	0	0.03	0	0	0	0	0.03	0	0
Dp 25								0.04	0	0	0	0	0	0	0	0	0	0	0	0	0
Dp 26								0.08	0	0	0	0	0	0	0	0	0	0	0	0	0
Dp 27								0.08	0	0.07	0	0.1	0.5	0.42	0	0	0	0	0.03	0	0
Dp 30								0	0	0	0	0	0	0	0.07	0	0	0	0.06	0	0
Dp 31														0.18	0.03	0	0	0	0.03	0	0

	2021																2022				
Average	2020-09	2020-10	2020-11	2020-12	2021-01	2021-02	2021-03	2021-04	2021-05	2021-06	2021-07	2021-08	2021-09	2021-10	2021-11	2021-12	2022-01	2022-02	2022-03	2022-04	2022-05
LSMP	0	0.07	0.25	0.19	0.22	0.23	0.03	0.04	0	0	0	0	0	0.05	0.36	0.58	0.58	0.53	0.27	0.04	0
Sado	0.13	0.06	0.03	0	0	0.03	0.02	0.02	0.01	0.01	0.03	0.06	0.05	0.06	0.02	0	0	0	0.02	0	0.01

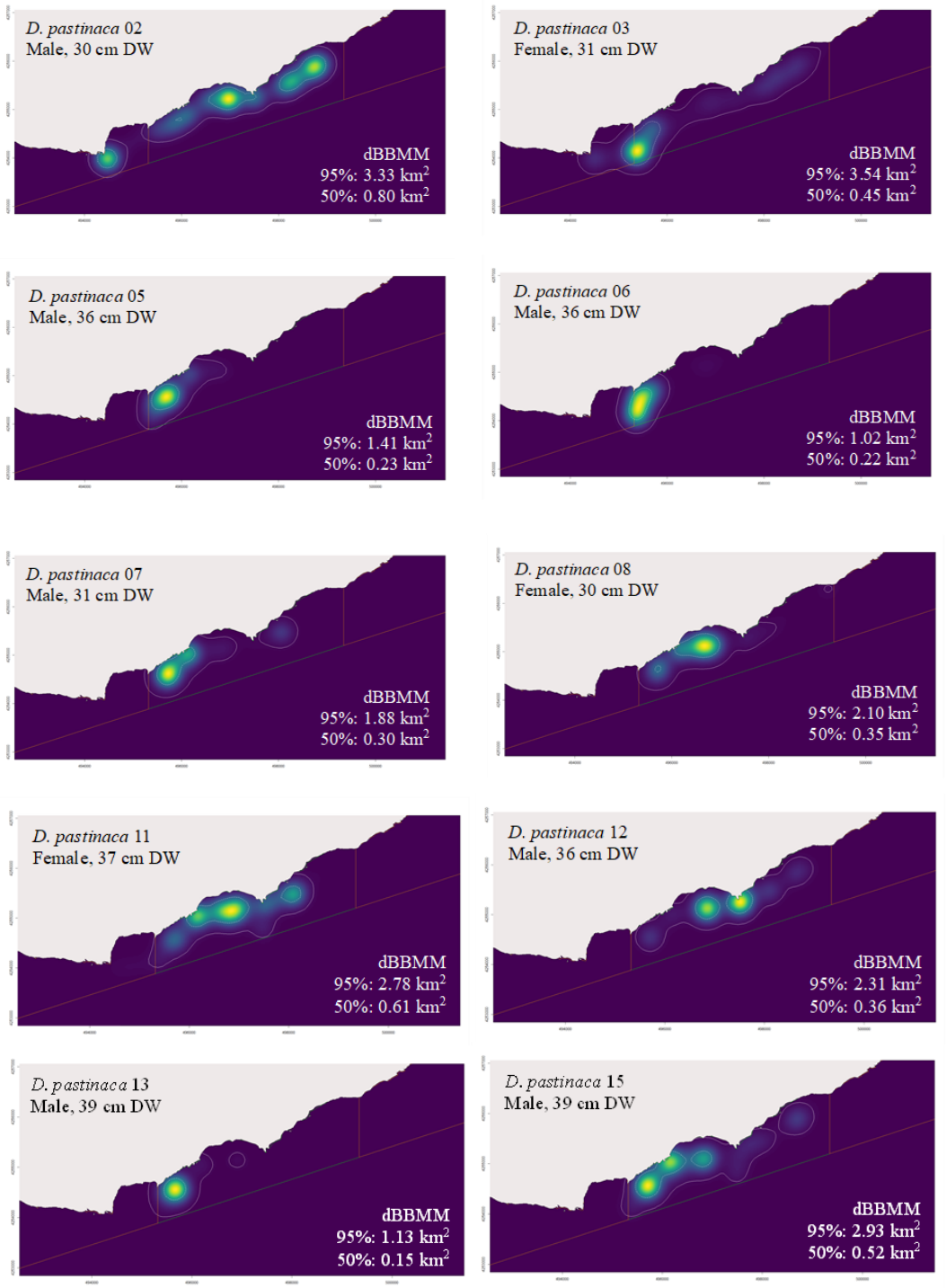

Supplementary material 3.2: Occurrence range of individual common stingrays (n = 21) at the 95% (solid line) and 50% (dotted line) isopleths. The brighter the colour, the higher the concentration of COAs. The border of the fully protected area is indicated by a green line, and the border of the partially protected areas by orange lines. Some common stingrays were not included because they did not provide sufficient COAs to estimate the dBBMM occurrence area (continued in the next page).

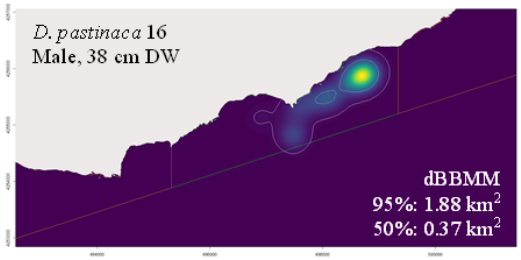
D. pastinaca 16
Male, 38 cm DW
dBBMM
95%: 1.88 km²
50%: 0.37 km²

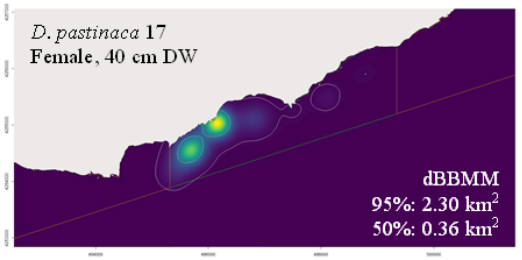
D. pastinaca 17
Female, 40 cm DW
dBBMM
95%: 2.30 km²
50%: 0.36 km²

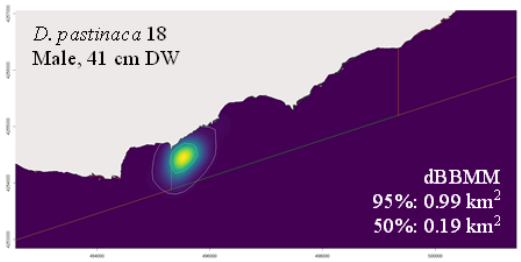
D. pastinaca 18
Male, 41 cm DW
dBBMM
95%: 0.99 km²
50%: 0.19 km²

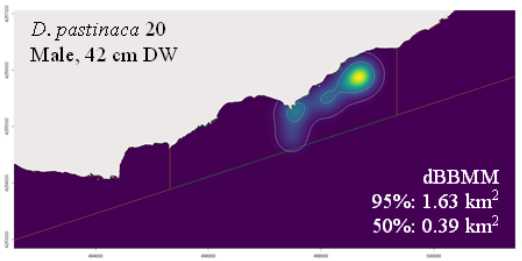
D. pastinaca 20
Male, 42 cm DW
dBBMM
95%: 1.63 km²
50%: 0.39 km²

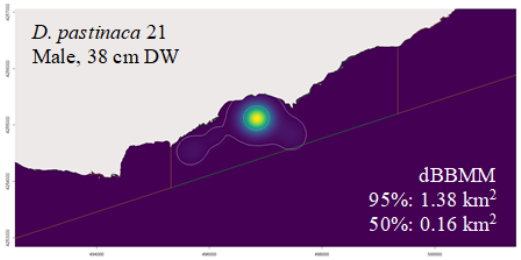
D. pastinaca 21
Male, 38 cm DW
dBBMM
95%: 1.38 km²
50%: 0.16 km²

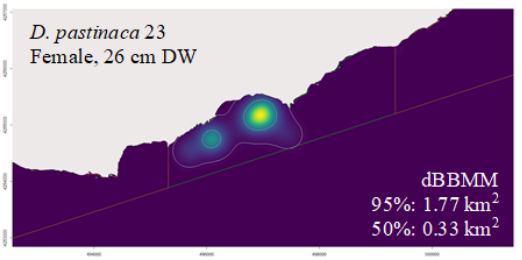
D. pastinaca 23
Female, 26 cm DW
dBBMM
95%: 1.77 km²
50%: 0.33 km²

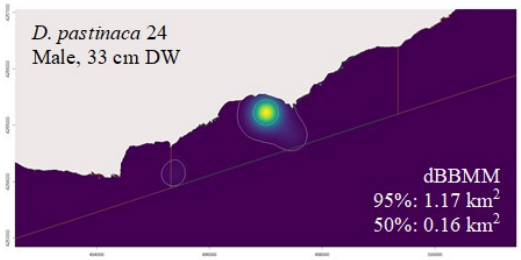
D. pastinaca 24
Male, 33 cm DW
dBBMM
95%: 1.17 km²
50%: 0.16 km²

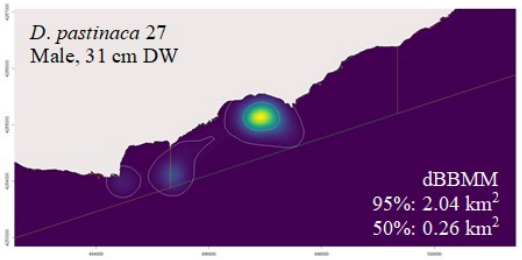
D. pastinaca 27
Male, 31 cm DW
dBBMM
95%: 2.04 km²
50%: 0.26 km²

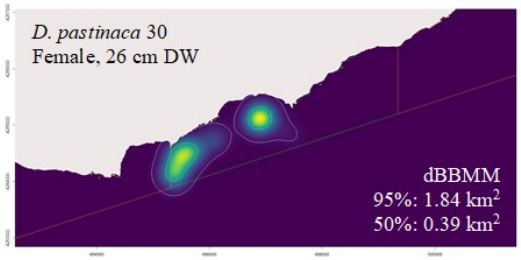
D. pastinaca 30
Female, 26 cm DW
dBBMM
95%: 1.84 km²
50%: 0.39 km²

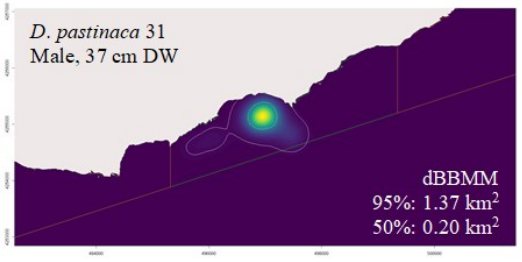
D. pastinaca 31
Male, 37 cm DW
dBBMM
95%: 1.37 km²
50%: 0.20 km²

Supplementary material 3.3: Average step length and number of step lengths per diel phase per common stingray individual. Averages calculated by averaging individuals and averaging all step lengths per diel phase.

	Average step length				Step length count			
Dasyatis pastinaca	**Day**	**Twilight**	**Night**	**Total**	**Day**	**Twilight**	**Night**	**Total**
02	116.88	200.42	124.05	130.18	28	6	8	42
03	83.42	103.73	96.46	91.97	241	77	258	576
04	156.85	-	-	156.85	8	-	-	8
05	44.37	52.77	49.56	47.74	6292	1845	6540	14677
06	42.62	65.32	60.43	53.48	2889	877	3025	6791
07	36.45	45.39	42.23	39.92	3436	938	2941	7315
08	61.59	72.93	62.33	63.34	1787	518	1830	4135
09	175.06	-	-	175.06	15	-	-	15
11	39.72	51.19	54.56	47.62	1847	526	1829	4202
12	33.38	30.55	39.30	35.76	758	220	835	1813
13	37.05	47.31	39.52	39.48	2309	706	2493	5508
15	31.32	46.70	52.73	42.73	1705	512	1741	3958
16	34.57	62.41	72.95	55.32	4701	1400	4973	11074
17	32.16	53.29	42.33	38.84	1683	430	1446	3559
18	49.51	51.53	51.76	50.74	2679	775	2653	6107
20	32.67	51.45	54.79	45.08	3145	948	3398	7491
21	36.22	43.90	41.81	39.67	3092	924	3173	7189
23	39.92	58.68	46.55	45.25	1852	544	1980	4376
24	44.39	57.18	58.39	52.11	2883	833	2876	6592
25	0.00	0.00	0.00	0.00	3	2	2	7
27	58.27	71.38	64.64	62.76	2587	761	2684	6032
30	43.76	49.11	40.78	43.08	2146	648	2339	5133
31	66.11	66.55	64.31	65.36	2103	627	2211	4941
Total (individuals)	48.22	64.09	57.97	54.52	2408	706	2462	5576
Total (step lenghts)	42.58	55.40	53.73					

Chapter 4

Horizontal and vertical movements of the critically endangered *Rostroraja alba* in a coastal marine protected area

Rostroraja alba released after tagging

Chapter published as:

Kraft, S., Winkler, A.C., Abecasis, D. Horizontal and vertical movements of the critically endangered *Rostroraja alba* in a coastal marine protected area. Aquatic Conservation: Marine and Freshwater Ecosystems 34, e4204. https://doi.org/10.1002/aqc.4204

Abstract

Elasmobranchs are slow growing marine predators whose populations have declined mostly due to their susceptibility to fishing, especially affecting species of large size. To address the effects of overfishing and promote the recovery of marine species and habitats, marine protected areas (MPAs) are a commonly implemented management strategy. A critical aspect for their success is using information on species' movement patterns; however, this is frequently not assessed for elasmobranchs. In this study, acoustic telemetry was used to monitor 30 *Rostroraja alba*, a large skate currently classified as Critically Endangered. Their long-term movements were assessed in the context of a coastal MPA, the Professor Luís Saldanha Marine Park (LSMP), to evaluate the contribution of coastal MPAs to the conservation of this species. Immature individuals were more frequently captured than adults, which postulates this area as a potential nursery. Average residency was moderate and relatively consistent throughout the year, as was area use. No marked size or sex-based differences in movement were noted. Individuals were more active and occurred in shallower waters at night and twilight, and occasional quick vertical movements into the water column, isolated or in sequence, were also noted. In general, the LSMP seems to offer stable protection to immature *R. alba*, with no strong seasonal variation. These results provide relevant input for adaptive management measures of this and other similar MPAs and highlight the contribution of these conservation efforts to the protection of nursery areas.

Keywords: Conservation, management, nursery area, passive acoustic telemetry, Rajidae, White skate

4.1 Introduction

The subclass Elasmobranchii (sharks, rays and skates) is an important group of marine predators, several of which exhibit slow growth, late maturity and low fecundity (Musick, 1999). These traits render them highly sensitive to anthropogenic threats, especially overfishing, reflected in their declining populations worldwide during the last decades (Dulvy et al., 2021). Among skates, body size is considered a useful predictor of vulnerability (Dulvy and Reynolds, 2002), and large-bodied batoids (skates and rays) are considered to be of the most at-risk fish groups because of their delayed sexual maturity and low population growth rates (Dulvy et al., 2021, 2000). Examples of large skates that have been severely affected by overfishing are *Dipturus batis*, which disappeared from the Irish Sea and is believed to be the first documentation of a fish being brought to near extinction by commercial fishing (Brander, 1981), *D. laevis* (Casey and Myers, 1998) and *D. oxyrinchus* (Rogers and Ellis, 2000).

Rostroraja alba is another large skate species, reaching maximum total lengths (TL) of 240 cm for females and 198 cm for males (Ebert et al., 2008). Individuals of this species also mature late and at large sizes, at around 24 years and 129.4/95.8 cm TL/disc width (DW) for females and 20 years and 119.3/94.2 cm TL/DW for males (Kadri et al., 2014). As many large and slow growing species, *R. alba* also has a very protracted lifespan, estimated at around 77 years for females and 51 years for males (Kadri et al., 2014). This species is distributed on continental shelves and slopes from the United Kingdom and Ireland to Mozambique, including the Mediterranean (Last et al., 2016; Quigley, 1984), and can be found at 10 to 750 meters in depth (Last et al., 2016).

As other large skates with slow life histories facing overfishing, *Rostroraja alba* disappeared from the Irish Sea and Bristol Channel (Dulvy et al., 2000) and its populations have declined around the United Kingdom and Ireland (Rogers and Ellis, 2000), the Mediterranean (Colloca et al., 2020), and South Africa (Best et al., 2013). As a result of overexploitation, *Rostroraja alba* is currently catalogued as Endangered globally (IUCN, 2024) and Critically Endangered in the northeastern Atlantic (IUCN, 2015). Because of its imperiled status, and to improve sustainable fishing practices, since 2009 no total allowable catch of *R. alba* has been authorized to protect it in waters under the jurisdiction of the European Union (CEC, 2009). This resulted in a prohibition to fish, retain, or land *R. alba*, and the encouragement to develop techniques and equipment that allowed the quick and safe release of captured individuals (CEC, 2009).

One of the ways to counter the effects of overfishing is by establishing marine protected areas (MPAs), which provide protection to marine species and habitats by regulating or banning fishing within a defined geographic area (Bohnsack, 1998). Elasmobranchs, including batoids, have shown positive results under such area-based conservation measures, especially when protection is provided over long timescales (i.e., monthly and seasonal) and when key areas for their reproduction and growth are protected (Karlovic et al., 2021; Lavender et al., 2021; Le Port et al., 2012). However, most MPAs are not designed for elasmobranchs, so protection is usually moderate or insufficient because their movements are nor properly encompassed (Dwyer et al., 2020; MacKeracher et al., 2019). In this context, information on the long-term movements of species is required to evaluate and improve the protection provided by an MPA (Knip et al., 2012).

A widely applied method to gather this information is passive acoustic telemetry, which allows to simultaneously track numerous individuals for an extended period and obtain results on aspects like their residency and area use inside a MPA (Knip et al., 2012). However, besides preliminary studies on *R. alba* (Sousa et al., 2019), this fundamental information is largely absent for this species. Therefore, advancing our knowledge on the spatial ecology of *R. alba* and estimating the protection coastal MPAs can provide constitute important steps towards better management and conservation efforts of this and other ecologically similar species (Sousa et al., 2018).

To tackle this, individuals of *R. alba* were acoustically tagged in the Professor Luís Saldanha Marine Park (LSMP), a coastal MPA off the Setúbal peninsula in Portugal, and their long-term movements were studied. This data was collected using an acoustic telemetry array already in place in the LSMP. The interannual movements (of up to three years) of *R. alba* were tracked with the objective of: 1) estimating total and weekly area use and residency in the LSMP; 2) studying their diel patterns of movement; and 3) contextualizing these findings in terms of a coastal MPA's contribution to the protection of a large skate species.

4.2 Materials and Methods

4.2.1 Study area

The LSMP covers 53 km^2 over 38 km of coastline and is organised into three different protection levels: a total protection area or marine reserve of 4.3 km^2, four partial protection areas that cover a total of 21 km^2, and three complementary protection areas or buffer areas of a combined 28 km^2 (Figure 4.1). All anthropogenic activities including any kind of fishing are

prohibited in the total protection area. In the partial protection areas small scale fishing operations are allowed, mainly comprising octopus traps and manual cuttlefish jigging beyond 200 m from the coastline, while in the buffer areas only local licensed small scale fishing boats under 7 m can operate. The LSMP is part of the Arrábida natural park, managed by the Portuguese Institute for Nature Conservation and Forests (ICNF) and is part of the European network of nature protection areas Natura 2000 since 2006. Further marine protected areas can be found to the east of the LSMP in the Sado River estuary, the natural reserve Reserva Natural do Estuário do Sado. Additionally, the Tejo River estuary located to the north contains the Reserva Natural do Estuário do Tejo, which covers the innermost area of the estuary and the land surrounding it (Figure 4.1).

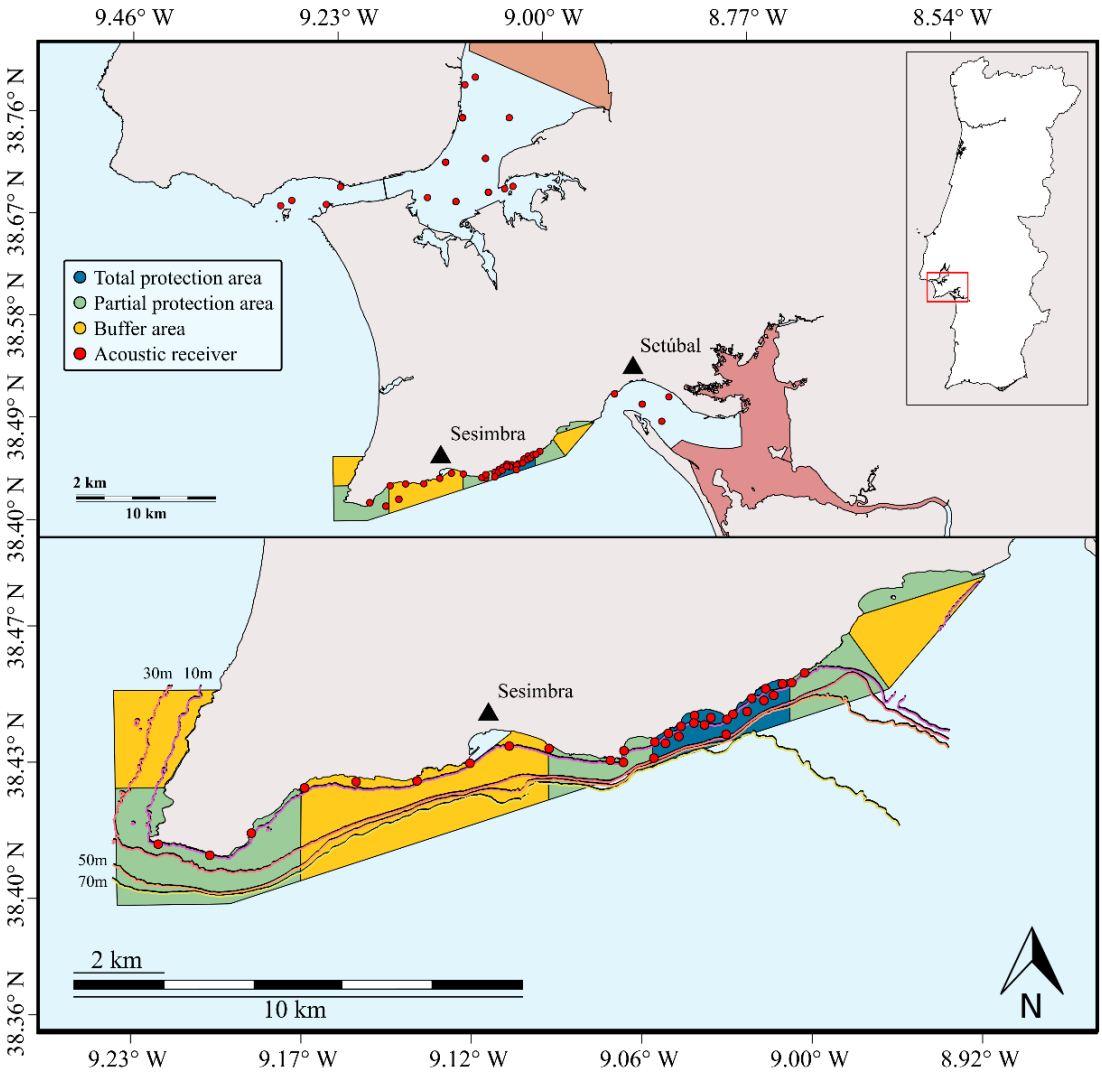

Figure 4.1: Top panel: general overview of the Professor Luis Saldanha Marine Park and the Setúbal peninsula, with the Tejo estuary and its Natural Reserve (orange) to the north and the Sado estuary and its Natural reserve (red) to the East. Bottom panel: Professor Luis Saldanha Marine Park and the three different protection levels. Only the aquatic portions of the Natural Reserves are shown. Isobaths are colour coded.

4.2.2 Tagging and tracking

Individuals were captured in April, May, and October 2019, 2021, and 2022 using trammel nets (2019 and 2021) and longlines (2021 and 2022) in the total protection area and adjacent partially protected areas. Monofilament trammel nets were 500 m in length and 1.6 m in height, with 100-mm inner panels of stretched mesh and outer panels of 600 mm. Longlines were mounted with 100 to 150 hooks and baited with chopped sardines. Both kinds of gear were deployed in the morning (soak time of 24h), at depths of 5-40 m in the total protection area and two adjacent partial protection areas. Upon capture, each skate was placed in a container with seawater, with water being changed after each skate. A hydrophone was then used to detect previously tagged individuals and hooks were removed from individuals captured with a longline. Total length, disc width and clasper length of males were recorded. To insert the acoustic tag, a 2-cm incision was made in the peritoneal cavity, which was then closed using absorbable suture. Innovasea V9 (n=12), V9P with pressure sensor (n=7, depth limit of ~76 meters), and V13 (n=11) acoustic tags were used based on skate size and tag availability. Expected battery lifetimes for these tags were 651, 404, and 1317 days, respectively. Tag frequency was 69 kHz, and the emission interval was 60-120 s with an average of 90 s.

We monitored the LSMP and Sado study areas with an array of Innovasea VR2W acoustic receivers (Figure 4.1). This acoustic array was initially deployed with less receivers in the fully protected area and adjacent partially protected areas to monitor commercially important species in the area of most protection and in several habitat types (Abecasis et al., 2014b). Over time, receivers were added to expand the array to the buffer area and Sado estuary, while some receivers were also lost, e.g., through weather and illegal fishing, removal of the supporting structures such as buoys by third parties. Most receivers were active throughout the present study period. Additional detections were obtained from an array located in Tejo by accessing data available through the European Tracking Network (ETN). A Peterson disc with a unique ID and contact information was also attached to the pectoral fin of each individual. Capture, handling, and tagging were done under the 'catch and release' practices permits of the Portuguese Institute for Nature Conservation and Forests (permits n°145/2019/CAPT; 13/2020/CAPT; 70/2021/CAPT; 38/2022/CAPT) and the Veterinary General Directorate (permit n° 2018-08-29 015730). Tagging procedures were also approved by the Animal Welfare Committee of the Centro de Ciências do Mar (CCMAR - ORBEA).

4.2.3 Data analysis

The first 24 hours of data per individual were eliminated before analysis, except for estimation of residency, to avoid possible behavioural anomalies produced by the tagging process. Previous evaluations in the LSMP showed no major variations in detection efficiency from environmental variables, diel patterns, and/or background noises so it was assumed to be constant across the receiver array (Abecasis et al., 2014a). Detection patterns were visually inspected, and the fate of skates was assessed following Villegas-Ríos et al. (2020) to identify events like emigration from the study site, post-release mortality, tag loss, and fishing mortality. Detections were classified into diel phases using the R package *suncalc* (Thieurmel and Elmarhraoui, 2019), considering "daytime" as the time between sunrise and sunset (appearance and disappearance of the sun over the horizon), "twilight" as morning and evening twilight, and "night" as the period between evening twilight and morning twilight.

Residency (I_R) was obtained as the total number of days detected by at least one receiver (D_d) divided by the duration of the monitoring period (D_t, time between release and last data download or tag expiration dates). D_t was replaced with tag lifetime if the latter was shorter than the total monitoring period.

Presence in the LSMP throughout the year was evaluated using a Generalized Additive Mixed Model (GAMM) in the R package *mgcv* (Wood, 2011). To properly investigate the long-term detection patterns, only individuals with detection intervals of at least a year (n=15, D_i=359-1306 days) were included to reduce the possible biases introduced by transient or fished individuals. For example, transient individuals can increase the probability of presence before leaving, while an unaccounted transient or fished individual will lower the estimated probability of presence. The detections were converted to daily presence or absence per individual, and day of the year, individual size, and sex were included as covariates. Day of the year was modelled using a cyclic cubic spline and individual was treated as random effect. REML was used as smoothing parameter estimation method, and a binominal distribution was fitted as the distribution function because the response variable is binary (1: presence, 0: absence). Four combinations of the response variable and covariates were tested using the Akaike Information Criterion (AIC) in the R package *AICcmodavg* (Mazerolle, 2023) to select the most appropriate model. The first model included day of the year and individual, while the three others additionally included either size or sex or both covariates.

To investigate space use, 30-minute centers of activity (COAs) were estimated (Simpfendorfer et al., 2002). Then, total and weekly area use at the 50% and 95% level were

estimated per individual using the probability distribution-based occurrence estimator dynamic Brownian bridge movement model (dBBMM) (Kranstauber et al., 2012) using the R package *move* (Kranstauber et al., 2021). This model was chosen over other "classic" home range estimators because it accounts for the natural autocorrelation of movement data and because the acoustic array did not cover the entire home range of the tracked individuals (Fleming et al., 2015). The dBBMM reconstructs movement paths by connecting pairs of consecutive COAs to create segments, around which an associated probability of occurrence is calculated based on the distance and time difference between points. This yields the utilisation distribution (UD). Segments longer than 24 hours were removed before estimating UDs to avoid unrealistic large uncertainty areas. Location error was set to 200 meters based on conservative estimates in the study area and window size (w = 31) and margin size (m = 11) were set to default values. Weekly area use were calculated to evaluate activity space changes over time implementing a GAMM in the R package *mgcv* (Wood, 2011). Week of the year was modelled using a cyclic cubic spline and individual was set as random effect. For each contour level, these two variables were tested in combination with sex and size, including both, one, or none. The models were tested using AIC to select the most appropriate combination of variables. REML was used as smoothing parameter estimation method, and a log-linked Gamma distribution was fitted as the distribution function because the response variable is positive, continuous, and right skewed. The influence of diel phase on occurrence areas was explored using a linear mixed-effects model as implemented in the R package *lme4* (Bates et al., 2015).

Before analysing depth, tidal effect was incorporated by obtaining local daily tide values using the R package *PTtidaltools* (Martins, 2021). Tidal height was subtracted from the raw depth values, so the corrected depth values are compared to the local lowest historical tide. To investigate daily changes in depth, differences among diel phases were calculated using a linear mixed-effects model with individual and day of the year as random effects with the R package *lme4* (Bates et al., 2015) with individual as random effect. This approach was selected because of the uneven sampling size of the depth data. To avoid pseudo-replication, a mean depth value per diel phase per day was calculated before running the model. To study vertical movements, 10-minute COAs were calculated to average tag depth and position. Seafloor depth at each COA was obtained by plotting each point over a bathymetry raster of the study site obtained from the European Marine Observation and Data Network (EMODnet, https://emodnet.ec.europa.eu/geoviewer/). Tag and seafloor depth were then compared including a line that represents an animal that is constantly at seafloor depth (i.e., each COA has the same depth for the tag and for the seafloor).

To estimate activity, minimum distance covered per time unit (hereon, step length) was used as a proxy. Using the R package *adehabitatLT* (Calenge, 2006), trajectories were obtained by calculating the distance between successive 30-minute COAs. Step lengths of longer duration (i.e., 60 minutes or more) were discarded to avoid including movements outside of the marine park, as a missing COA indicates absence from the array or missed detections. Differences in activity across diel phases were evaluated using a linear mixed-effects model as implemented in the R package *lme4* (Bates et al., 2015). Step length was set as the response variable, diel phase, sex, and size were set as fixed effects and individual as random effect.

4.3 Results

Thirty *Rostroraja alba* with average 60 cm DW (range 29–98 cm) and 84 cm TL (range 39-137 cm) were tagged (Table 4.1). Males and females had similar average DW (59 vs. 61 cm) and even sex ratio (1:1). All but two individuals were immature based on published size at maturity estimates, 129.4/95.8 cm TL/DW for females and 119.3/94.2 cm TL/DW for males (Kadri et al., 2014). Monitoring time per skate averaged 651 days (range 379-1306 days) and detection interval averaged 350 days (range 1-1306 days). Eighteen tags (60%) completed their battery life during the study.

4.3.1 Detections and residency

Rostroraja alba displayed several detection patterns (Figure 4.2). Most individuals were assumed to have left the study area before the end of transmitter battery life either shortly after tagging (e.g., Ra 09 or 26) or after months of being detected (e.g., Ra 11 or 13). Ten individuals, including the only one released with the hook still in (Ra 28), were classified as “survived”, 20 as “dispersed”, and none as “dead” or “fished”. Individuals that “survived” were either detected throughout the study until the end of battery life or data collection (e.g., Ra 04 or 30) or were absent at the end of battery life or study but for a shorter time than previous detection gaps (e.g., Ra 02 or 21). They could be considered as temporarily away instead of dispersed. Two of the three skates that were detected in the buffer area were last seen there (Ra 03, 05, and 22). Only Ra 04 was detected at the westernmost receiver off the tip of the peninsula. No individuals were detected in the Sado and Tejo estuaries, nor in any operational European Tracking Network receivers scattered along the European coastlines.

Table 4.1: Summary data of the tagged *Rostroraja alba* individuals; residency indices (D_d = days detected, D_i = detection interval, D_t = monitoring time, I_R = residency index); dynamic Brownian bridge movement model (dBBMM) areas at the 50% and 95%; and individual fish fate following Villegas-Ríos et al., (2020). Total lengths of Ra 01 to 11 were calculated multiplying disc width *1.5 (Last et al., 2016).

Fish ID	Sex	Disc width (cm)	Total length (cm)	Maturity	Tagging date	Tag	Expiration date/ last data download	D_d	D_i	D_t	I_R	dBBMM (km^2)		Fish fate
												95%	50%	
Ra 01	M	44	66	Immature	30/03/2019	V9	09/01/2021	282	642	651	0.43	3.74	0.74	Survived
Ra 02	F	64	96	Immature	20/10/2019	V13	18/05/2023	1060	1306	1306	0.81	3.17	0.64	Survived
Ra 03	F	87	131	Immature	20/10/2019	V9	01/08/2021	86	283	651	0.13	5.83	0.94	Dispersed
Ra 04	M	42	62	Immature	20/10/2019	V13	18/05/2023	853	1273	1306	0.65	2.78	0.55	Survived
Ra 05	M	68	102	Immature	20/10/2019	V13	18/05/2023	315	1210	1306	0.24	2.93	0.51	Survived
Ra 06	F	54	81	Immature	22/10/2019	V9	03/08/2021	366	395	651	0.56	3.06	0.35	Dispersed
Ra 07	M	66	99	Immature	22/10/2019	V9	03/08/2021	26	80	651	0.04	1.12	0.17	Dispersed
Ra 08	F	42	63	Immature	22/10/2019	V9	03/08/2021	47	75	651	0.07	2.00	0.35	Dispersed
Ra 09	M	52	78	Immature	22/10/2019	V9	03/08/2021	15	21	651	0.02	1.13	0.28	Dispersed
Ra 10	F	49	74	Immature	22/10/2019	V9	03/08/2021	23	26	651	0.04	1.10	0.25	Dispersed
Ra 11	M	30	45	Immature	22/10/2019	V9	03/08/2021	359	379	651	0.55	2.18	0.31	Dispersed
Ra 12	M	65	86	Immature	06/04/2021	V13	18/05/2023	1	1	772	0.00	-	-	Dispersed
Ra 13	F	62	82	Immature	06/04/2021	V13	18/05/2023	238	506	772	0.31	3.22	0.47	Dispersed
Ra 14	F	45	61	Immature	06/04/2021	V9	17/01/2023	2	2	651	0.00	0.52	0.11	Dispersed
Ra 15	M	42	55	Immature	06/04/2021	V9	17/01/2023	1	1	651	0.00	-	-	Dispersed
Ra 16	F	74	102	Immature	07/04/2021	V13	18/05/2023	91	359	771	0.12	3.73	0.54	Dispersed
Ra 17	F	29	39	Immature	07/04/2021	V9	18/01/2023	449	634	651	0.69	1.60	0.34	Survived
Ra 18	F	55	72	Immature	09/04/2021	V9P	18/05/2022	40	75	404	0.10	3.90	0.41	Dispersed
Ra 19	M	56	74	Immature	09/04/2021	V13	18/05/2023	238	238	769	0.31	1.15	0.19	Dispersed
Ra 20	M	59	76	Immature	09/04/2021	V13	18/05/2023	189	445	769	0.25	2.59	0.37	Dispersed
Ra 21	F	43	56	Immature	09/04/2021	V9	20/01/2023	324	575	651	0.50	3.83	0.72	Survived
Ra 22	F	42	57	Immature	18/05/2021	V9P	26/06/2022	103	113	404	0.25	1.09	0.20	Dispersed
Ra 23	M	78	111	Immature	20/05/2021	V9P	28/06/2022	57	57	404	0.14	2.16	0.36	Dispersed
Ra 24	M	66	86	Immature	13/10/2021	V9P	21/11/2022	269	289	404	0.67	2.02	0.42	Dispersed
Ra 25	F	87	108	Immature	14/10/2021	V9P	22/11/2022	1	1	404	0.00	-	-	Dispersed
Ra 26	M	51	71	Immature	15/10/2021	V9P	23/11/2022	1	1	404	0.00	-	-	Dispersed
Ra 27	M	73	99	Immature	03/05/2022	V9P	17/05/2023	311	380	380	0.82	3.27	0.65	Survived
Ra 28	M	96	124	Mature	03/05/2022	V13	17/05/2023	380	380	380	1.00	2.35	0.43	Survived
Ra 29	F	82	114	Immature	03/05/2022	V13	17/05/2023	269	380	380	0.71	3.65	0.63	Survived
Ra 30	F	98	137	Mature	03/05/2022	V13	16/05/2023	367	379	379	0.97	3.64	0.67	Survived
Total avg.	30	60	84					225	350	651	0.35	2.61	0.45	
Males avg.	15	59	82					220	360	677	0.34	2.28	0.41	
Females avg.	15	61	85					231	341	625	0.35	2.88	0.47	

Overall residency was moderate (I_R = 0.35) and ranged between 0.00 and 1.00 (Table 4.1). Individual residency did not correlate with monitoring time (Pearson's correlation test $r(28) = 0.00$, p = 1), skate size (Pearson's correlation test $r(28) = 0.23$, p = 0.24), nor did it vary between males and females (two-tailed t-test, p = 0.94). For the GAMM, all covariate combinations scored similarly (AIC range: 11993.70-11994.17), so the simplest model with day of the year and individual effects was favoured. Additionally, in the full model neither size (p = 0.20) nor sex (p = 0.51) had an effect on occurrence. The probability of presence of *R. alba* varied throughout the year, as there was an effect of day of the year (GAMM: edf=5.416, Chi.sq=187.8, p = 3.79e-06) and was also subject to individual variability (GAMM: edf=12.859, Chi.sq=1850.7, p <2e-16). The deviance explained by the model was 18.9%. Throughout the year, probability of presence remained relatively stable, ranging between 0.53-0.65 (possible range of values: 0.0-1.0) and showed no marked seasonal trend (Figure 4.3).

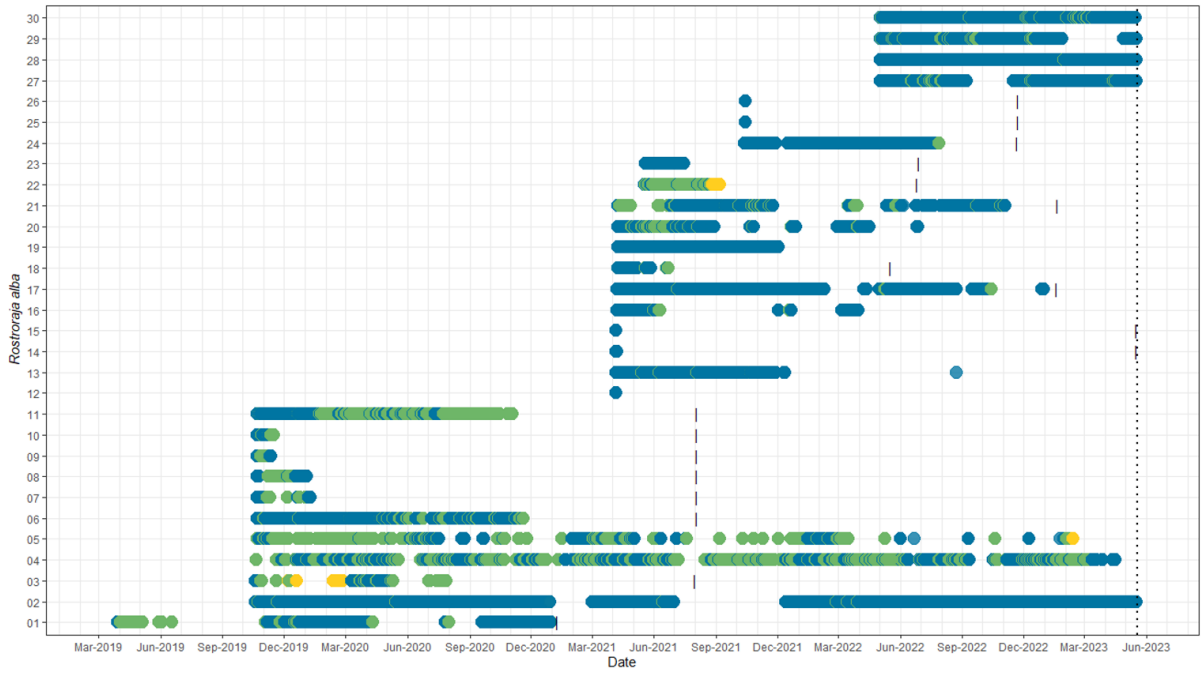

Figure 4.2: Abacus plot of the detections of *Rostroraja alba* during the study. The protection areas in which the detection occurred are colour-coded: total protection area (blue), complementary protection area (green), and buffer area (yellow). Vertical solid dashes indicate expected battery expiration date, and the dotted vertical line marks the end of the study period.

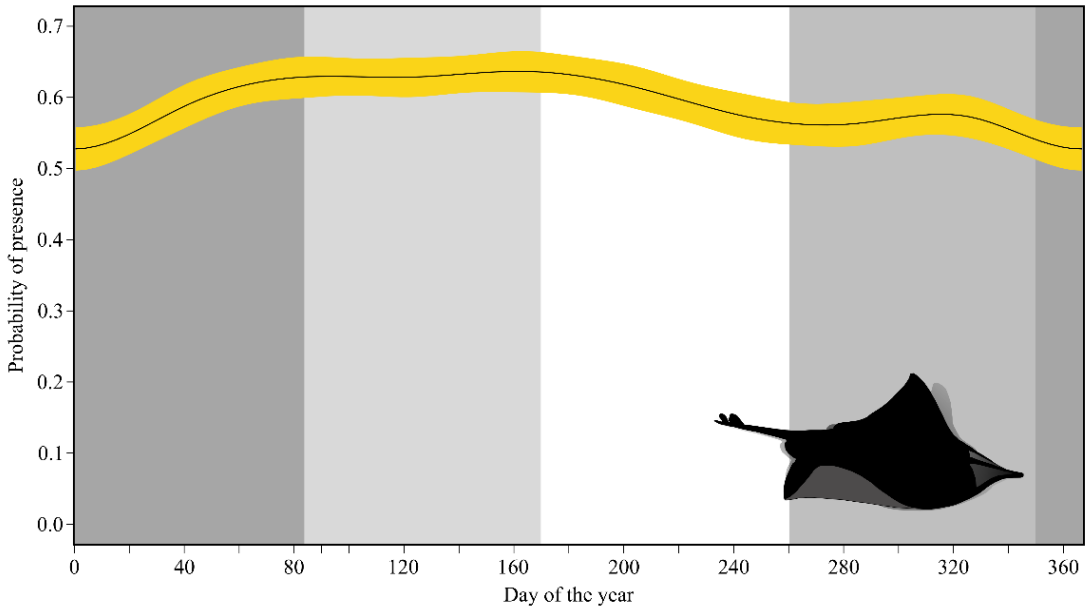

Figure 4.3: Predicted probability of presence of *Rostroraja alba* in the LSMP as a function of the day of the year, using only the individuals with detection intervals greater than one year (n = 15). The yellow area represents the 95% confidence interval. Grey shading represents seasons of the year (from left to right: winter, spring, summer, autumn, winter).

4.3.2 Area use

Area use was estimated for 26 individuals (supplementary material 4.1), while 4 had insufficient data. All areas used by *R. alba* except that of Ra 03 were smaller than the total protection area (4.3 km^2), but several were neither centred in nor completely encompassed by it. Ra 03 was the only to extend to a buffer area (95% contour). The total 50% estimations averaged 0.45 km^2 (range 0.11-0.94 km^2) and the 95% estimations averaged 2.61 km^2 (range 0.52-5.83 km^2) (Table 4.1). Area use was positively correlated with individual size (Pearson's correlation test: $r(23) = 0.42$ for 50%, $p = 0.04$ and $r(23) = 0.43$, $p = 0.04$ for 95%). Area use did not differ between sexes (two-tailed t-test, $p = 0.48$ at 50% and $p = 0.22$ at 95%). Average 50% and 95% area use were larger at night (0.46 km^2, range = 0.15-0.85 km^2, and 2.57 km^2, range = 0.89-4.50 km^2) and twilight (0.39 km^2, range = 0.11-0.72 km^2, and 2.25 km^2, range = 0.52-3.90 km^2) than during daytime (0.38 km^2, range = 0.12-0.68 km^2, and 2.22 km^2, range = 0.53-3.78 km^2). The linear mixed-effects model showed that 95% occurrence areas were smaller during daytime than during night (t-value = 4.736, p = 1.97e-05) but not twilight (t-value = 0.474, p = 0.64). The same pattern was obtained for the 50% occurrence areas: daytime vs. night (t-value = 4.916, p = 1.07e-05) and daytime vs. twilight (t-value = 0.709, p = 0.482). Relative to daytime, this represented an increase of 3.1% (50% areas) and 1.6% (95% areas) during twilight, and an increase of 21.3% (50% areas) and 15.8% (95% areas) during the night. For the 95% contour level, the model included individual and size, while for the 50% contour level the best fit model only included individual. There was no effect of week of the year on either the 95% utilization distribution (GAMM: edf = 1.08, F = 0.367, p = 0.131) or the 50% area use (GAMM: edf = 0.04861, F = 0.006, p = 0.356). Individual effect was significant for both with p <2e-16 (GAMM results for 95%: edf = 16.94, F = 3.289; for 50%: edf = 18.98231, F = 4.856; supplementary material 4.2.

4.3.3 Depth

Five V9P tags (2 females, 3 males) yielded 40-311 days of detections and detection intervals between 57-380 days. Two additional individuals were detected only on their release day and were not included in analyses. Four individuals were detected below 50 meters depth, with three reaching depths close to the tag's limit of ~76 m (Supplementary material 4.3a). As for general daily patterns, all individuals had a deeper median depth during daytime than during twilight and night (Table 4.2). Hourly depth profiles also show they generally occurred deeper

during daytime (supplementary material 4.3b). Ra 18 and Ra 22 displayed a greater depth amplitude compared to the other three, which had more compressed depth profiles.

Table 4.2: Median depth and range per diel phase per *Rostroraja alba* individual with a V9P Innovasea tag.

	Day			Twilight			Night			Total		
R. alba	Min	Max	Median	Min	Max	Median	Min	Max	Median	Min	Max	Median
18	0.37	29.70	18.20	0.00	32.10	13.40	0.00	54.50	9.29	0.00	54.50	16.60
22	8.82	25.10	15.00	7.36	23.80	12.70	5.23	20.50	10.40	5.23	25.10	14.10
23	7.84	71.40	16.20	6.64	69.60	14.40	5.90	31.50	13.50	5.90	71.40	15.30
24	2.83	33.30	11.90	1.29	33.90	10.60	0.18	63.80	10.70	0.18	63.80	11.10
27	3.85	75.30	14.40	3.28	75.30	12.90	1.24	41.30	12.30	1.24	75.30	13.20

There were depth differences among diel phases, as the model indicated depth was shallower at night (fixed effect = 3.18, standard error (SE) = 0.21, t-value = -14.94) and twilight (fixed effect = -2.06, SE = 0.22, t-value = -9.54) compared to daytime (intercept estimate = 15.48, standard error (SE) = 0.84, t-value = 18.39). A post-hoc test showed that there are statistical differences among all diel phases ($p<0.0001$ for all).

To interpret the tag vs seafloor data, two factors need to be considered. First, receivers can detect a tag at distances of hundreds of meters so COAs and seafloor depths are also subject to this error margin. Secondly, the time window of 10 minutes permitted to obtain fine resolution depth data yet in turn lowered the precision in the calculation of COA positions. As in most instances not enough time passed for the tag to be detected by more than one receiver, most COAs were assigned the position of the receiver that detected them. This resulted, for example, in instances of sudden changes in seafloor depth without a similar change in tag depth (supplementary material 4.4a) as the COA's coordinates moved from one receiver to the next. However, tag and seafloor depth values also frequently changed in the same direction, generally agreeing with the movement of an animal on a slope (supplementary material 4.4b, c) and the described pattern, such individuals often remained at a more stable depth in the day than during twilight and night (supplementary material 4.4 a-d).

The distribution of tag and seafloor depths shows the data deviates from the tag-at-seafloor line (Figure 4.4, dashed diagonal line). Considering seafloor depth increases in an offshore direction, tags seen deeper than their respective seafloor value (i.e., below the diagonal) occur from the COA being situated farther offshore (and therefore deeper) than the receiver(s) used to calculate this COA, which was more frequently seen at shallower depths.

This in turn is a likely result of the skate being at seafloor level but was detected by a more inshore (and therefore shallower) receiver. This pattern inverted at greater depths (tags generally shallower than the seafloor, and therefore above the diagonal), indicating that tags were more frequently detected closer to shore than the receiver(s) that detected them (supplementary material 4.4 a-d). This means that the skate was likely found at seafloor level but was detected by a receiver at shallower depth. Additionally, skates were also detected in the water column, particularly when tags were close to the surface (Figure 4.5). The linear regressions for each diel phase also indicate greater depth during daytime, which was maintained throughout the depth range and increased with greater seafloor depth.

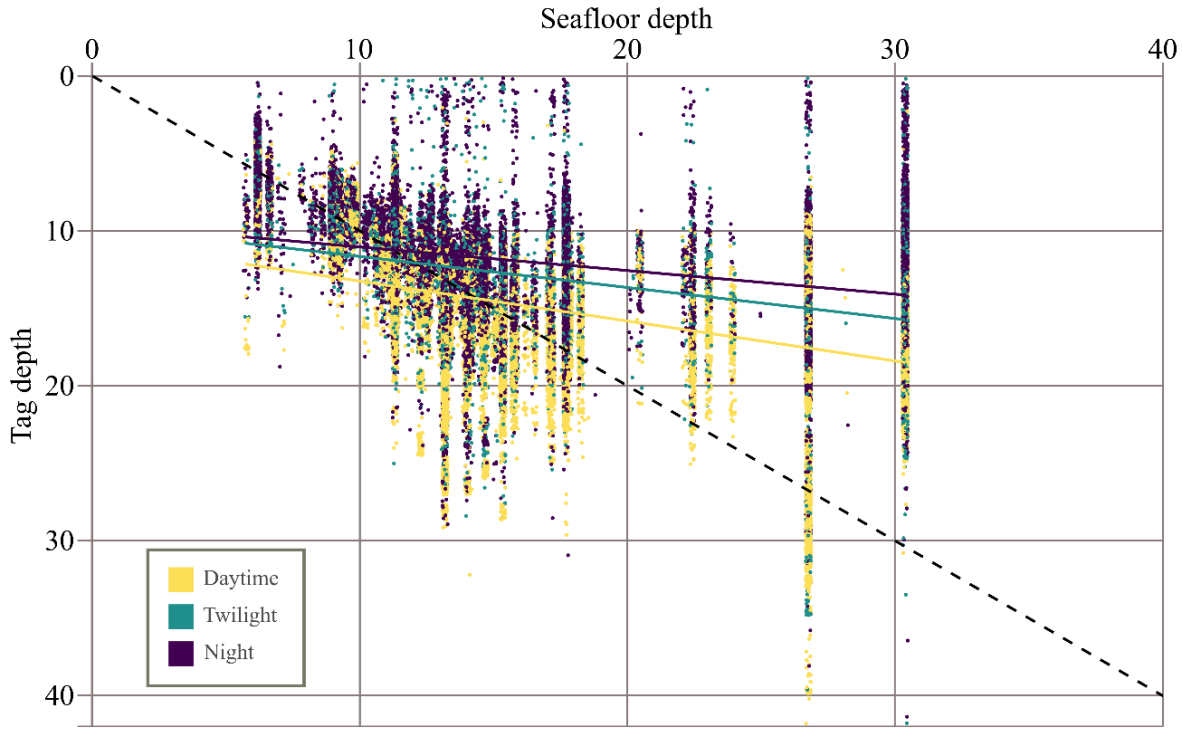

Figure 4.4: Scatterplot and regression lines showing the relationship between tag depth of individual *Rostroraja alba* and seafloor depth, calculated using 10-minute COAs and colour-coded by diel phase. The dotted line indicates a 1:1 relationship. Tag depth is shown up to 40 m for clarity.

Instances of vertical and horizontal movements in the water column were also identified, although the latter were rarer. During twilight and night, single or consecutive vertical movements of up to over 15 m were performed (supplementary material 4.4). In these short forays into the water column, the individual ascended and dived back down one or multiple times. Most depth changes appeared to follow the seafloor, following the seafloor slope while ascending (supplementary material 4.4c) and descending (Figure 4.5, bottom

panel). Vertical movements were generally of short duration and occurred as isolated events or in a repeated manner, long horizontal displacements of up to several hours near the surface were also noted (Figure 4.5). This figure shows a long-distance movement close to the surface at night and into the morning twilight, over seafloor depths between 17-30 m. The seemingly great distance covered in some instances on the segment between COAs 26 and 38 is likely influenced by the short time window (10 min) used to estimate these COAs. However, the existence of movement can be inferred from the tag's alternating detections between receivers, presented as a back-and-forth movement.

4.3.4 Activity

The 25 individuals yielded 211,075 step length values, ranging between 80-32,750 steps per individual (supplementary material 4.6). Average step length was greater during twilight (87.8 m) and the night (82.4 m) and almost half during daytime (45.9 m). This difference was reflected in the results of the linear mixed-effects model, which found that both night (estimate = 36.537, $p < 0.001$) and twilight (estimate = 41.931, $p < 0.001$) were associated with greater step length than during daytime. No significant effects were found for sex or *R. alba* size.

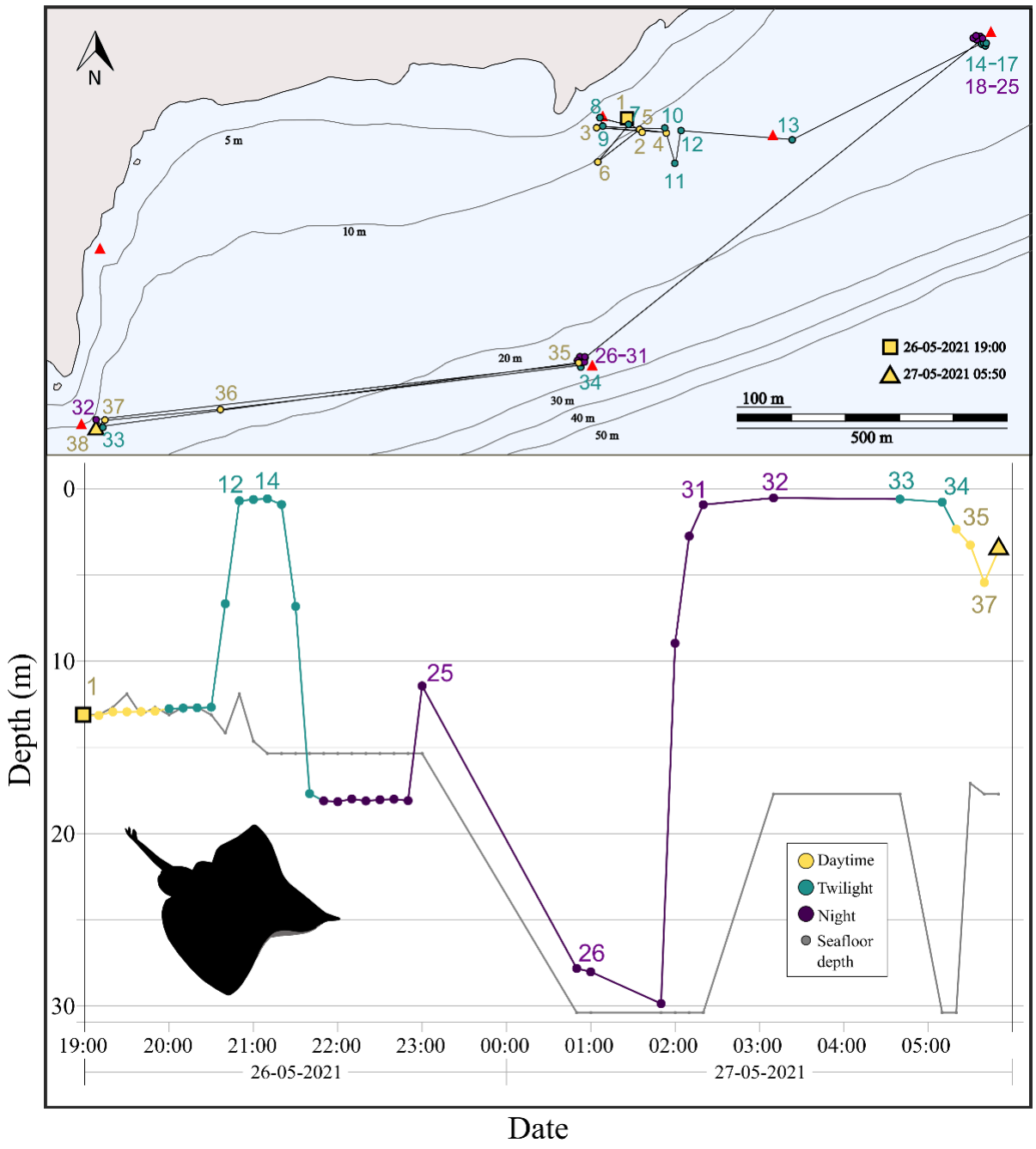

Figure 4.5: Description of the horizontal (top panel) and vertical movements (bottom panel) of *Rostroraja alba* 18 between 19:00h of May 26th and 06:00h of May 27th, 2021, using 10-minute COAs. The start of the trajectory is shown with a yellow square and the end with a yellow triangle. Numbers in the bottom panel indicate the start and end of the longer displacements seen in the top panel. Approximate seafloor depth at the time and position of COAs indicated by a grey line, and the time of COAs is colour coded to indicate daylight (yellow), twilight (green), and night (purple). Receivers are indicated by red triangles, some of which were slightly moved to avoid their concealment by the COAs positioned over them.

4.4 Discussion

Due to their low reproductive rates, many elasmobranch species are currently imperiled by overfishing (Dulvy et al., 2021). Management strategies such as marine protected areas are commonly used to provide refugia; however, this often occurs without proper data on elasmobranch spatial ecology, which despite being fundamental for the functioning of MPAs is unavailable for many species (Dwyer et al., 2020; MacKeracher et al., 2019). In this study, the movements of 30 Critically Endangered *Rostroraja alba* were studied in a coastal MPA, the majority of which were immature individuals. Residency and areas of use were relatively steady throughout the year. Activity and areas of use were also greatest at night and twilight, times at which *R. alba* also occurred shallower and occasionally moved into the water column. These results and their implications for this area and the conservation of batoids in coastal areas are discussed in this section.

Not much is known about the population structure of *R. alba*, but smaller specimens appear to occur inshore more frequently than adults which are thought to move into deeper waters seasonally (Quigley, 1984). Based on the sizes of the individuals captured in the present study and two additional studies (Martínez-Ramírez et al., 2021; Sousa et al., 2019), this coastline appears to be dominated by immature *R. alba*. The average total length of these 184 individuals was 62 cm and only 4 skates were larger than the published sizes at maturity sizes (Kadri et al., 2014), indicating a dominance of juvenile/sub-adult *R. alba* in this area. This may also explain the absence of clear size and sex-based differences in the studied movement metrics, as the ontogenetic changes and sex-based differences triggered at maturity have yet to become apparent (Moura et al., 2008; Simpson et al., 2021). This dominance of immature individuals and stable presence throughout the year suggests this site might be an important nursery area for *R. alba* (Heupel et al., 2007; Martins et al., 2018). With the exception of deep-water species (Hoff, 2016), and some large skate species such as *Dipturus intermedius*, where the larger size classes tend to occur in shallower coastal waters (Thorburn et al., 2021), many skates and other elasmobranchs use shallow coastal areas for this purpose (Ellis et al., 2004; Yokota and Lessa, 2006).

High biological productivity (Sigman and Hain, 2012) and the abundance of structurally complex environments like mangroves, seagrass prairies, macroalgae forests, and rock formations are fundamental factors that promote many marine animals at vulnerable early life stages to seek shelter in coastal areas (Lefcheck et al., 2019). Shallow coastal areas are also generally advantageous to immature skates for these reasons, allowing them to reduce their

predation risk and optimizing their growth until maturity (Heupel et al., 2007; Martins et al., 2018). The LSMP's coastline presents many of these beneficial characteristics, offering protected areas and soft bottom habitats with abundant prey (Abecasis et al., 2014a), highlighting the role this and other coastal MPAs can have in protecting key environments for the development of elasmobranchs. After maturity, the requirements of an individual can change and prompt it to expand their area use or relocate to other areas that better suit these new necessities (Dale et al., 2011). Ontogenetic changes before reaching maturity in *R. alba* have been mentioned as a plausible hypothesis to explain differences in the movement of one male tagged in the LSMP before (Sousa et al., 2019). This could therefore explain the low occurrence of adults in the LSMP, which might be more common in deeper areas, as seen in other coastal skates (Ellis et al., 2012).

In addition to protecting areas that are vital to the life cycle of numerous marine species like nurseries, coastal areas also provide fundamental ecosystemic services to humans. Coastal resources are easily accessible and generally abundant, which has prompted a large proportion of the human population to settle in sites by shorelines (Small and Nicholls, 2003). This led to the development of infrastructure and human activities, which also brought a wide range of consequences such as habitat degradation and loss, pollution, species invasion, and removal of individuals by fishing (Halpern et al., 2008). Because of their highly productive environments and proximity to ports, coastal areas can be highly active in coastal fishing operations, which is an important component of fishing in many countries (Lloret et al., 2018). In some countries like Portugal, most skate catches are made in small-scale fishery operations by the coastal polyvalent fleet (Figueiredo et al., 2020). In turn, high fishing pressures in coastal environments have greatly impacted coastal fish species (Brown et al., 2018), which emphasizes the importance of identifying and protecting coastal areas, playing fundamental roles in the life cycle of marine species.

This dual condition of nursery areas, as sites of high importance to the life cycle of species but also of high vulnerability and exposure to anthropogenic risks, emphasizes the role of coastal MPAs in the conservation of the species that use coastal areas as nurseries and the habitats found in them. Adult survival has been proposed as the greatest contributor to the population growth of large and long-lived elasmobranchs because they spend a larger proportion of their life as mature individuals and contribute greatly to the recovery of populations (Frisk et al., 2002; Kinney and Simpfendorfer, 2009). However, the protection of adult elasmobranchs can at times be difficulted by their higher vagility (Cerutti-Pereyra et al., 2014; Kinney and Simpfendorfer, 2009). The capability of moving long distances has also been

shown for undulatory batoids such as *R. alba*, as demonstrated by an individual tagged in the LSMP that travelled 43 km (Sousa et al., 2019). Other examples include adult *Dipturus intermedius* that can travel at least 120 km (Thorburn et al., 2021) and *Dasyatis chrysonota*, which can regularly move up to 200 km (Elston et al., 2023). Although the protection of adults remains as an important contributor to the conservation of elasmobranchs (Kinney and Simpfendorfer, 2009), an advantage of conservation efforts that focus on the less mobile life stages of a species is that efforts can be optimized as immature individuals may be more likely to remain in more restricted areas (Cerutti-Pereyra et al., 2014; Kinney and Simpfendorfer, 2009). In addition to juvenile nurseries, other strategies like the protection of egg case nurseries can also be fundamental for the conservation of egg-laying skates (Dodd et al., 2022; Spies et al., 2021). Juvenile nursery areas are considered essential habitats for batoids (Martins et al., 2018), which highlights the importance of identifying and protecting them to improve conservation planning around elasmobranchs (Heupel and Simpfendorfer, 2005), particularly in the case of a Critically Endangered species like *R. alba*. Indeed, protecting juvenile nurseries in coastal areas to avoid overfishing has been particularly important in the conservation of some threatened elasmobranchs, with sawfishes (Pristidae) as probably the most emblematic example (Huston et al., 2017; Morgan et al., 2017).

In order to identify the expanse of an area used by individuals and how they utilise this area, animal movement studies, such as this study, can highlight the role of coastal MPAs in protecting elasmobranchs (Knip et al., 2012). Movement information can be important to infer how individuals are exposed to anthropogenic risk and how this risk exposure may change over time with ontogeny, therefore, providing the necessary evidence for adaptive regulations if required. For example, the delimitation of a *Pristis pectinata* nursery was expanded after finding diel differences in the movement of juveniles, which moved away from the coast during the night (Huston et al., 2017). Similarly, *R. alba* displayed greater activity and area use primarily during the night and twilight, which likely relates to foraging behaviour as observed in other elasmobranchs (Hammerschlag et al., 2016; Humphries et al., 2017). The vertical movements observed during the same diel periods is likely related to similar drivers (Wearmouth and Sims, 2009). However, the latter were more scarcely observed, which is common for elasmobranchs in general (Hammerschlag et al., 2016). *Rostroraja alba* also occurred deeper during daytime and shallower in twilight and the night, resembling the diel vertical migration or nocturnal ascent behaviour described in several elasmobranchs (Humphries et al., 2017; Wearmouth and Sims, 2009). Changes in seasonal resource

distribution and availability have been suggested as drivers of changes in depth use of other large skates like *Dipturus intermedius* (Thorburn et al., 2021).

Unfortunately, greater activity, area use, and more frequent vertical movements, may also suggest an increase in the probability of encounter with passive fishing gear like trammel nets, gill nets, and longlines (Hammerschlag et al., 2016; Uusiheikkila et al., 2008). Greater activity, area use, and depth changes can also be indicative of how probable it is for an individual to cross the borders of an MPA and increase their susceptibility of capture (Villegas-Ríos et al., 2021). On the other hand, the occupation of deeper waters by *R. alba* during daytime likely implies they are at a greater distance from shore, and, considering the narrow shape of the LMSP, close to or even beyond the MPA's border. Taken collectively, these results on the movements of *R. alba* illustrate how their exposure to threats such as edge effect (Ohayon et al., 2021), "fishing the line" (Kellner et al., 2007), and illegal fishing (Martínez-Ramírez et al., 2021) can vary over time. Illegal fishing, despite being difficult to assess, remains an important issue to consider in the operation of this marine park (Martínez-Ramírez et al., 2021).

The distribution of suitable habitats can also underlie the movement and distribution of individuals in nurseries (Nagelkerken et al., 2015). This may be a relevant factor to consider, as it can originate changes in the horizontal and vertical distribution of individuals, as a natural outcome of ontogeny or as a way to reduce resource competition among conspecifics (Thorburn et al., 2021). Investigating the use of relevant habitats across large spatial scales can be achieved by using acoustic telemetry as shown by a study on *Pristis pectinata* that found several potential areas of importance along the coast of Florida (Graham et al., 2021). In the case of *R. alba*, the presence of individuals that left the array permanently (e.g., Ra 06 and 11) or for several months (e.g., Ra 02) suggest that some individuals make significant use of sites outside of the array. Such short and long term residences were noted in a previous study on three individuals of this species (Sousa et al., 2019) and on *Dasyatis pastinaca* (Kraft et al., 2023). This indicates that other areas along the coast, adjacent or more distant, may be relevant to the growth of *R. alba*. Long-term tagging of more individuals and an expanded array, perhaps combined investigating depth using data storage tags, may provide information on these questions.

Finally, to frame the importance of the LSMP using the "Important Shark and Ray Area" (ISRA) designation criteria (Hyde et al., 2022), two criteria can be applied: criterion A of vulnerability, as *R. alba* is a species of high conservation concern; and criterion C, particularly sub-criterion C1 of life history-reproductive areas, because of the importance of this area to immature *R. alba*.

4.5 References

Abecasis, D., Afonso, P., Erzini, K., 2014a. Can small MPAs protect local populations of a coastal flatfish, *Solea senegalensis*? Fisheries Management and Ecology 21, 175–185. https://doi.org/10.1111/fme.12061

Abecasis, D., Afonso, P., Erzini, K., 2014b. Combining multispecies home range and distribution models aids assessment of MPA effectiveness. Marine Ecology Progress Series 513, 155–169. https://doi.org/10.3354/meps10987

Bates, D., Mächler, M., Bolker, B., Walker, S., 2015. Fitting Linear Mixed-Effects Models Using lme4. Journal of Statistical Software 67. https://doi.org/10.18637/jss.v067.i01

Best, L.N., Attwood, C.G., da Silva, C., Lamberth, S.J., 2013. Chondrichthyan occurrence and abundance trends in False Bay, South Africa, spanning a century of catch and survey records. African Zoology 48, 201–227. https://doi.org/10.1080/15627020.2013.11407587

Bohnsack, J.A., 1998. Application of marine reserves to reef fisheries management. Austral Ecology 23, 298–304. https://doi.org/10.1111/j.1442-9993.1998.tb00734.x

Brander, K., 1981. Disappearance of common skate *Raia batis* from Irish Sea. Nature 290, 48–49. https://doi.org/10.1038/290048a0

Brown, E.J., Vasconcelos, R.P., Wennhage, H., Bergström, U., Støttrup, J.G., Van De Wolfshaar, K., Millisenda, G., Colloca, F., Le Pape, O., 2018. Conflicts in the coastal zone: human impacts on commercially important fish species utilizing coastal habitat. ICES Journal of Marine Science 75, 1203–1213. https://doi.org/10.1093/icesjms/fsx237

Calenge, C., 2006. The package "adehabitat" for the R software: A tool for the analysis of space and habitat use by animals. Ecological Modelling 197, 516–519. https://doi.org/10.1016/j.ecolmodel.2006.03.017

Casey, J.M., Myers, R.A., 1998. Near extinction of a large, widely distributed fish. Science (New York, N.Y.) 281, 690–692. https://doi.org/10.1126/science.281.5377.690

CEC, 2009. Council Regulation (EC) No 43/2009 of 16 January 2009 fixing for 2009 the fishing opportunities and associated conditions for certain fish stocks and groups of fish stocks, applicable in Community waters and, for Community vessels, in waters where catch limitations are required. Official Journal of the European Communities L22, 1–125. https://eur-lex.europa.eu/eli/reg/2009/43/oj

Cerutti-Pereyra, F., Thums, M., Austin, C.M., Bradshaw, C.J.A., Stevens, J.D., Babcock, R.C., Pillans, R.D., Meekan, M.G., 2014. Restricted movements of juvenile rays in the lagoon of Ningaloo Reef, Western Australia – evidence for the existence of a nursery. Environmental Biology of Fishes 97, 371–383. https://doi.org/10.1007/s10641-013-0158-y

Colloca, F., Carrozzi, V., Simonetti, A., Di Lorenzo, M., 2020. Using Local Ecological Knowledge of Fishers to Reconstruct Abundance Trends of Elasmobranch Populations in the Strait of Sicily. Frontiers in Marine Science 7, 508. https://doi.org/10.3389/fmars.2020.00508

Dale, J., Wallsgrove, N., Popp, B., Holland, K., 2011. Nursery habitat use and foraging ecology of the brown stingray Dasyatis lata determined from stomach contents, bulk and amino acid stable isotopes. Marine Ecology Progress Series 433, 221–236. https://doi.org/10.3354/meps09171

Dodd, J., Baxter, J.M., Donnan, D.W., James, B.D., Lavender, E., McSorley, C.A., Mogg, A.O.M., Thorburn, J.A., 2022. First report of an egg nursery for the Critically Endangered flapper skate *Dipturus intermedius* (Rajiformes: Rajidae). Aquatic Conservation: Aquatic Conservation: Marine and Freshwater Ecosystems aqc.3857. https://doi.org/10.1002/aqc.3857

Dulvy, N.K., Metcalfe, J.D., Glanville, J., Pawson, M.G., Reynolds, J., 2000. Fishery stability, local extinctions, and shifts in community structure in skates. Conservation Biology 14, 283–293. https://doi.org/10.1046/j.1523-1739.2000.98540.x

Dulvy, N.K., Pacoureau, N., Rigby, C.L., Pollom, R.A., Jabado, R.W., Ebert, D.A., Finucci, B., Pollock, C.M., Cheok, J., Derrick, D.H., Herman, K.B., Sherman, C.S., VanderWright, W.J., Lawson, J.M., Walls, R.H.L., Carlson, J.K., Charvet, P., Bineesh, K.K., Fernando, D., Ralph, G.M., Matsushiba, J.H., Hilton-Taylor, C., Fordham, S.V., Simpfendorfer, C.A., 2021. Overfishing drives over one-third of all sharks and rays toward a global extinction crisis. Current Biology 31, 4773-4787.e8. https://doi.org/10.1016/j.cub.2021.08.062

Dulvy, N.K., Reynolds, J.D., 2002. Predicting Extinction Vulnerability in Skates. Conservation Biology 16, 440–450. https://doi.org/10.1046/j.1523-1739.2002.00416.x

Dwyer, R.G., Krueck, N.C., Udyawer, V., Heupel, M.R., Chapman, D., Pratt, H.L., Garla, R., Simpfendorfer, C.A., 2020. Individual and Population Benefits of Marine Reserves for Reef Sharks. Current Biology 30, 480-489.e5. https://doi.org/10.1016/j.cub.2019.12.005

Ebert, D.A., Compagno, L.J.V., Cowley, P.D., 2008. Aspects of the reproductive biology of skates (Chondrichthyes: Rajiformes: Rajoidei) from southern Africa. ICES Journal of Marine Science 65, 81–102. https://doi.org/10.1093/icesjms/fsm169

Ellis, J.R., Cruz-Martínez, A., Rackham, B.D., Rogers, S.I., 2004. The Distribution of Chondrichthyan Fishes Around the British Isles and Implications for Conservation. Journal of Northwest Atlantic Fishery Science 35, 195–213. https://doi.org/10.2960/J.v35.m485

Ellis, J.R., McCully, S.R., Brown, M.J., 2012. An overview of the biology and status of undulate ray *Raja undulata* in the north-east Atlantic Ocean. Journal of Fish Biology 80, 1057–1074. https://doi.org/10.1111/j.1095-8649.2011.03211.x

Elston, C., Cowley, P.D., Murray, T.S., Parkinson, M.C., 2023. Novel insights into coastal site affinity and habitat connectivity of a benthic stingray with implications for management. Biodiversity and Conservation https://doi.org/10.1007/s10531-022-02494-7

Figueiredo, I., Maia, C., Lagarto, N., Serra-Pereira, B., 2020. Bycatch estimation of Rajiformes in multispecies and multigear fisheries. Fisheries Research 232, 105727. https://doi.org/10.1016/j.fishres.2020.105727

Fleming, C.H., Fagan, W.F., Mueller, T., Olson, K.A., Leimgruber, P., Calabrese, J.M., 2015. Rigorous home range estimation with movement data: a new autocorrelated kernel density estimator. Ecology 96, 1182–1188. https://doi.org/10.1890/14-2010.1

Frisk, M., Miller, T.J., Fogarty, M.J., 2002. The population dynamics of little skate Leucoraja erinacea, winter skate Leucoraja ocellata, and barndoor skate *Dipturus laevis*: predicting exploitation limits using matrix analyses. ICES Journal of Marine Science 59, 576–586. https://doi.org/10.1006/jmsc.2002.1177

Graham, J., Kroetz, A., Poulakis, G., Scharer, R., Carlson, J., Lowerre-Barbieri, S., Morley, D., Reyier, E., Grubbs, R., 2021. Large-scale space use of large juvenile and adult smalltooth

sawfish *Pristis pectinata*: implications for management. Endangered Species Research 44, 45–59. https://doi.org/10.3354/esr01088

Halpern, B.S., Walbridge, S., Selkoe, K.A., Kappel, C.V., Micheli, F., D'Agrosa, C., Bruno, J.F., Casey, K.S., Ebert, C., Fox, H.E., Fujita, R., Heinemann, D., Lenihan, H.S., Madin, E.M.P., Perry, M.T., Selig, E.R., Spalding, M., Steneck, R., Watson, R., 2008. A Global Map of Human Impact on Marine Ecosystems. Science 319, 948–952. https://doi.org/10.1126/science.1149345

Hammerschlag, N., Skubel, R.A., Calich, H., Nelson, E.R., Shiffman, D.S., Wester, J., Macdonald, C.C., Cain, S., Jennings, L., Enchelmaier, A., Gallagher, A.J., 2016. Nocturnal and crepuscular behavior in elasmobranchs: a review of movement, habitat use, foraging, and reproduction in the dark. Bulletin of Marine Science 93, 355–374. https://doi.org/10.5343/bms.2016.1046

Heupel, M., Carlson, J., Simpfendorfer, C., 2007. Shark nursery areas: concepts, definition, characterization and assumptions. Marine Ecology Progress Series 337, 287–297. https://doi.org/10.3354/meps337287

Heupel, M.R., Simpfendorfer, C.A., 2005. Using Acoustic Monitoring to Evaluate MPAs for Shark Nursery Areas: The Importance of Long-term Data. Marine Technology Society Journal 39, 10–18. https://doi.org/10.4031/002533205787521749

Hoff, G.R., 2016. Identification of multiple nursery habitats of skates in the eastern Bering Sea: nursery habitat of oviparous elasmobranchs. Journal of Fish Biology 88, 1746–1757. https://doi.org/10.1111/jfb.12939

Humphries, N., Simpson, S., Sims, D., 2017. Diel vertical migration and central place foraging in benthic predators. Marine Ecology Progress Series 582, 163–180. https://doi.org/10.3354/meps12324

Huston, C., Stevens, P., Blaxton, R., Tolley, S., Scharer, R., Tornwall, B., Poulakis, G., 2017. Diel movements of juvenile smalltooth sawfish: implications for defining the size of a nursery hotspot. Endangered Species Research 34, 311–322. https://doi.org/10.3354/esr00851

Hyde, C.A., Notarbartolo di Sciara, G., Sorrentino, L., Boyd, C., Finucci, B., Fowler, S.L., Kyne, P.M., Leurs, G., Simpfendorfer, C.A., Tetley, M.J., Womersley, F., Jabado, R.W., 2022. Putting sharks on the map: A global standard for improving shark area-based conservation. Frontiers in Marine Science 9, 968853. https://doi.org/10.3389/fmars.2022.968853

IUCN, 2015. Ellis, J., Morey, G & Walls, R. 2015. *Rostroraja alba*. The IUCN Red List of Threatened Species 2015: e.T61408A48954174.

IUCN, 2024. *Rostroraja alba*: Serena, F., Charles, R., Ellis, J.R., Johnston, G. & Pacoureau, N. 2024. The IUCN Red List of Threatened Species 2024: e.T61408A183781512.

Kadri, H., Marouani, S., Bradai, M.N., Bouaïn, A., Morize, E., 2014. Age, Growth, Mortality, Longevity and Reproductive Biology of the White Skate, *Rostroraja alba* (Chondrichthyes: Rajidae) of the Gulf of Gabès (Southern Tunisia, Central Mediterranean). Turkish Journal of Fisheries and Aquatic Sciences 14. https://doi.org/10.4194/1303-2712-v14_1_21

Karlovic, T.C., Gomes, R.R., Paiva, P.C., Babcock, E.A., Dias, J.F., 2021. Functionality and Effectiveness of Marine Protected Areas in Southeastern Brazilian Waters for Demersal Elasmobranchs. Frontiers in Marine Science 8, 694846. https://doi.org/10.3389/fmars.2021.694846

Kellner, J.B., Tetreault, I., Gaines, S.D., Nisbet, R.M., 2007. Fishing the line near marine reserves in single and multispecies fisheries. Ecological Applications 17, 1039–1054. https://doi.org/10.1890/05-1845

Kinney, M.J., Simpfendorfer, C.A., 2009. Reassessing the value of nursery areas to shark conservation and management. Conservation Letters 2, 53–60. https://doi.org/10.1111/j.1755-263X.2008.00046.x

Knip, D.M., Heupel, M.R., Simpfendorfer, C.A., 2012. Evaluating marine protected areas for the conservation of tropical coastal sharks. Biological Conservation 148, 200–209. https://doi.org/10.1016/j.biocon.2012.01.008

Kraft, S., Winkler, A.C., Abecasis, D., 2023. Small coastal marine protected areas offer recurring, seasonal protection to the common stingray (*Dasyatis pastinaca*). Ocean & Coastal Management 246, 106891. https://doi.org/10.1016/j.ocecoaman.2023.106891

Kranstauber, B., Kays, R., LaPoint, S.D., Wikelski, M., Safi, K., 2012. A dynamic Brownian bridge movement model to estimate utilization distributions for heterogeneous animal movement: The dynamic Brownian bridge movement model. Journal of Animal Ecology 81, 738–746. https://doi.org/10.1111/j.1365-2656.2012.01955.x

Kranstauber, B., Smolla, M., Scharf, A.K., 2021. move: Visualizing and analyzing animal track data. Rpackage version 4.0.6. http://cran.r-project.org/package=move.

Last, P. R., Séret, B., Stehmann, M.F.W., Weigmann, S., 2016. Skates, family Rajidae, in: Last, Peter Robert, White, W.T., de Carvalho, M.R., Séret, Bernard, Stehmann, M., Naylor, G.J.P., Marshall, L. (Eds.), Rays of the World. CSIRO Publishing, Clayton South VIC, pp. 204–363.

Lavender, E., Aleynik, D., Dodd, J., Illian, J., James, M., Wright, P.J., Smout, S., Thorburn, J., 2021. Movement patterns of a Critically Endangered elasmobranch (*Dipturus intermedius*) in a Marine Protected Area. Aquatic Conservation: Marine and Freshwater Ecosystems aqc.3753. https://doi.org/10.1002/aqc.3753

Le Port, A., Lavery, S., Montgomery, J.C., 2012. Conservation of coastal stingrays: seasonal abundance and population structure of the short-tailed stingray *Dasyatis brevicaudata* at a Marine Protected Area. ICES Journal of Marine Science 69, 1427–1435. https://doi.org/10.1093/icesjms/fss120

Lefcheck, J.S., Hughes, B.B., Johnson, A.J., Pfirrmann, B.W., Rasher, D.B., Smyth, A.R., Williams, B.L., Beck, M.W., Orth, R.J., 2019. Are coastal habitats important nurseries? A meta-analysis. CONSERVATION LETTERS 12, e12645. https://doi.org/10.1111/conl.12645

Lloret, J., Cowx, I.G., Cabral, H., Castro, M., Font, T., Gonçalves, J.M.S., Gordoa, A., Hoefnagel, E., Matić-Skoko, S., Mikkelsen, E., Morales-Nin, B., Moutopoulos, D.K., Muñoz, M., Dos Santos, M.N., Pintassilgo, P., Pita, C., Stergiou, K.I., Ünal, V., Veiga, P., Erzini, K., 2018. Small-scale coastal fisheries in European Seas are not what they were: Ecological, social and economic changes. Marine Policy 98, 176–186. https://doi.org/10.1016/j.marpol.2016.11.007

MacKeracher, T., Diedrich, A., Simpfendorfer, C.A., 2019. Sharks, rays and marine protected areas: A critical evaluation of current perspectives. Fish and Fisheries 20, 255–267. https://doi.org/10.1111/faf.12337

Martínez-Ramírez, L., Priester, C.R., Sousa, I., Erzini, K., Abecasis, D., 2021. Reserve effect of a small North-East Atlantic marine protected area (Arrábida, Portugal) on soft-sediment fish

species. Aquatic Conservation: Marine and Freshwater Ecosystems 31, 1584–1595. https://doi.org/10.1002/aqc.3577

Martins, A., Heupel, M., Chin, A., Simpfendorfer, C., 2018. Batoid nurseries: definition, use and importance. Marine Ecology Progress Series 595, 253–267. https://doi.org/10.3354/meps12545

Martins, M., 2021. PTtidaltools - R package to retrieve and manipulate data from the Portuguese National Hydrographic Institute. https://doi.org/10.5281/ZENODO.4562490

Mazerolle, M.J., 2023. AICcmodavg: Model selection and multimodel inference based on (Q)AIC(c). R package version 2.3.2.

Morgan, D., Ebner, B., Allen, M., Gleiss, A., Beatty, S., Whitty, J., 2017. Habitat use and site fidelity of neonate and juvenile green sawfish *Pristis zijsron* in a nursery area in Western Australia. Endangered Species Research 34, 235–249. https://doi.org/10.3354/esr00847

Moura, T., Figueiredo, I., Farias, I., Serra-Pereira, B., Neves, A., Borges, M.D.F., Serrano Gordo, L., 2008. Ontogenetic dietary shift and feeding strategy of *Raja undulata* Lacepède, 1802 (Chondrichthyes: Rajidae) on the Portuguese continental shelf. Scientia Marina 72, 311–318. https://doi.org/10.3989/scimar.2008.72n2311

Musick, J.A., 1999. Life in the Slow Lane: Ecology and Conservation of Long-Lived Marine Animals, in: Musick, J.A. (Ed.), Ecology and Conservation of Long-Lived Marine Animals. American Fisheries Society. https://doi.org/10.47886/9781888569155

Nagelkerken, I., Sheaves, M., Baker, R., Connolly, R.M., 2015. The seascape nursery: a novel spatial approach to identify and manage nurseries for coastal marine fauna. Fish and Fisheries 16, 362–371. https://doi.org/10.1111/faf.12057

Ohayon, S., Granot, I., Belmaker, J., 2021. A meta-analysis reveals edge effects within marine protected areas. Nature Ecology & Evolution 5, 1301–1308. https://doi.org/10.1038/s41559-021-01502-3

Quigley, D.T.G., 1984. White skate *Raja alba* Lacepede 1803 (*R. marginata* Lacep.) in Irish waters: a further record and review of Irish records. The Irish Naturalists' Journal 21, 217–220.

Rogers, S.I., Ellis, J.R., 2000. Changes in the demersal fish assemblages of British coastal waters during the 20th century. ICES Journal of Marine Science 57, 866–881. https://doi.org/10.1006/jmsc.2000.0574

Sigman, D.M., Hain, M.P., 2012. The biological productivity of the ocean. Nature Education Knowledge 3, 1–16.

Simpfendorfer, C.A., Heupel, M.R., Hueter, R.E., 2002. Estimation of short-term centers of activity from an array of omnidirectional hydrophones and its use in studying animal movements. Canadian Journal of Fisheries and Aquatic Sciences 59, 23–32. https://doi.org/10.1139/f01-191

Simpson, S., Humphries, N., Sims, D., 2021. Habitat selection, fine-scale spatial partitioning and sexual segregation in Rajidae, determined using passive acoustic telemetry. Marine Ecology Progress Series 666, 115–134. https://doi.org/10.3354/meps13701

Small, C., Nicholls, R.J., 2003. A Global Analysis of Human Settlement in Coastal Zones. Journal of Coastal Research 19, 584–599. https://www.jstor.org/stable/4299200

Sousa, I., Baeyaert, J., Gonçalves, J.M.S., Erzini, K., 2019. Preliminary insights into the spatial ecology and movement patterns of a regionally critically endangered skate (*Rostroraja alba*) associated with a marine protected area. Marine and Freshwater Behaviour and Physiology 52, 283–299. https://doi.org/10.1080/10236244.2019.1705805

Sousa, I., Gonçalves, J.M.S., Claudet, J., Coelho, R., Gonçalves, E.J., Erzini, K., 2018. Soft-bottom fishes and spatial protection: findings from a temperate marine protected area. PeerJ 6, e4653. https://doi.org/10.7717/peerj.4653

Spies, I., Orr, J., Stevenson, D., Goddard, P., Hoff, G., Guthridge, J., Hollowed, M., Rooper, C., 2021. Skate egg nursery areas support genetic diversity of Alaska and Aleutian skates in the Bering Sea. Marine Ecology Progress Series 669, 121–138. https://doi.org/10.3354/meps13736

Thieurmel, B., Elmarhraoui, A., 2019. R Package "suncalc": compute sun position, sunlight phases, moon position and lunar phase.

Thorburn, J., Wright, P.J., Lavender, E., Dodd, J., Neat, F., Martin, J.G.A., Lynam, C., James, M., 2021. Seasonal and Ontogenetic Variation in Depth Use by a Critically Endangered Benthic Elasmobranch and Its Implications for Spatial Management. Frontiers in Marine Science 8, 656368. https://doi.org/10.3389/fmars.2021.656368

Uusiheikkila, S., Wolter, C., Klefoth, T., Arlinghaus, R., 2008. A behavioral perspective on fishing-induced evolution. Trends in Ecology & Evolution 23, 419–421. https://doi.org/10.1016/j.tree.2008.04.006

Villegas-Ríos, D., Claudet, J., Freitas, C., Moland, E., Thorbjørnsen, S.H., Alonso-Fernández, A., Olsen, E.M., 2021. Time at risk: Individual spatial behaviour drives effectiveness of marine protected areas and fitness. Biological Conservation 263, 109333. https://doi.org/10.1016/j.biocon.2021.109333

Villegas-Ríos, D., Freitas, C., Moland, E., Thorbjørnsen, S.H., Olsen, E.M., 2020. Inferring individual fate from aquatic acoustic telemetry data. Methods in Ecology and Evolution 11, 1186–1198. https://doi.org/10.1111/2041-210X.13446

Wearmouth, V.J., Sims, D.W., 2009. Movement and behaviour patterns of the critically endangered common skate *Dipturus batis* revealed by electronic tagging. Journal of Experimental Marine Biology and Ecology 380, 77–87. https://doi.org/10.1016/j.jembe.2009.07.035

Wood, S.N., 2011. Fast stable restricted maximum likelihood and marginal likelihood estimation of semiparametric generalized linear models. Journal of the Royal Statistical Society (B) 73, 3–36. https://doi.org/10.1111/j.1467-9868.2010.00749.x

Yokota, L., Lessa, R.P., 2006. A nursery Area for Sharks and Rays in Northeastern Brazil. Environmental Biology of Fishes 75, 349–360. https://doi.org/10.1007/s10641-006-0038-9

Contributions

DA and SK conceptualized and designed the study. SK, ACW and DA captured and tagged the individuals of this study and acquired the data. SK, ACW and DA maintained the receiver network. SK conducted the analyses, prepared the figures for publication, and drafted the article. SK, ACW and DA interpreted the data. SK, ACW and DA revised it critically for important intellectual content. All authors have approved of the final article.

Conflict of Interest

The authors declare no conflicts of interest.

Funding

SK was supported by the "la Caixa" Foundation (ID 100010434) grant LCF/BQ/DI20/11780001. This study received funding from the INFORBIOMARES project (POSEUR-03-2215-FC-000047), and FCT projects UIDB/04326/2020, UIDP/04326/2020 and LA/P/0101/2020. DA acknowledges FCT support through the transitional norm DL57/2016/CP1361/CT0036.

Acknowledgements

We thank Juliano Macedo (operation of vessel and trammel nets), Joffrey Baeyaert (tagging, deploying, and maintaining receivers), Lucas Martínez-Ramírez and C. Robert Priester (receiver maintenance), "Flipper Divers" dive centre (receiver maintenance), and Miguel Gandra (data analysis).

Data sharing

The data used in this work is deposited in the European Tracking Network data portal (http://www.lifewatch.be/etn/), developed by the Flanders Marine Institute as part of the Flemish contribution to LifeWatch. The data that support the findings of this study are available on request from the corresponding author. The data are not publicly available due to privacy or ethical restrictions.

4.6 Supplementary material

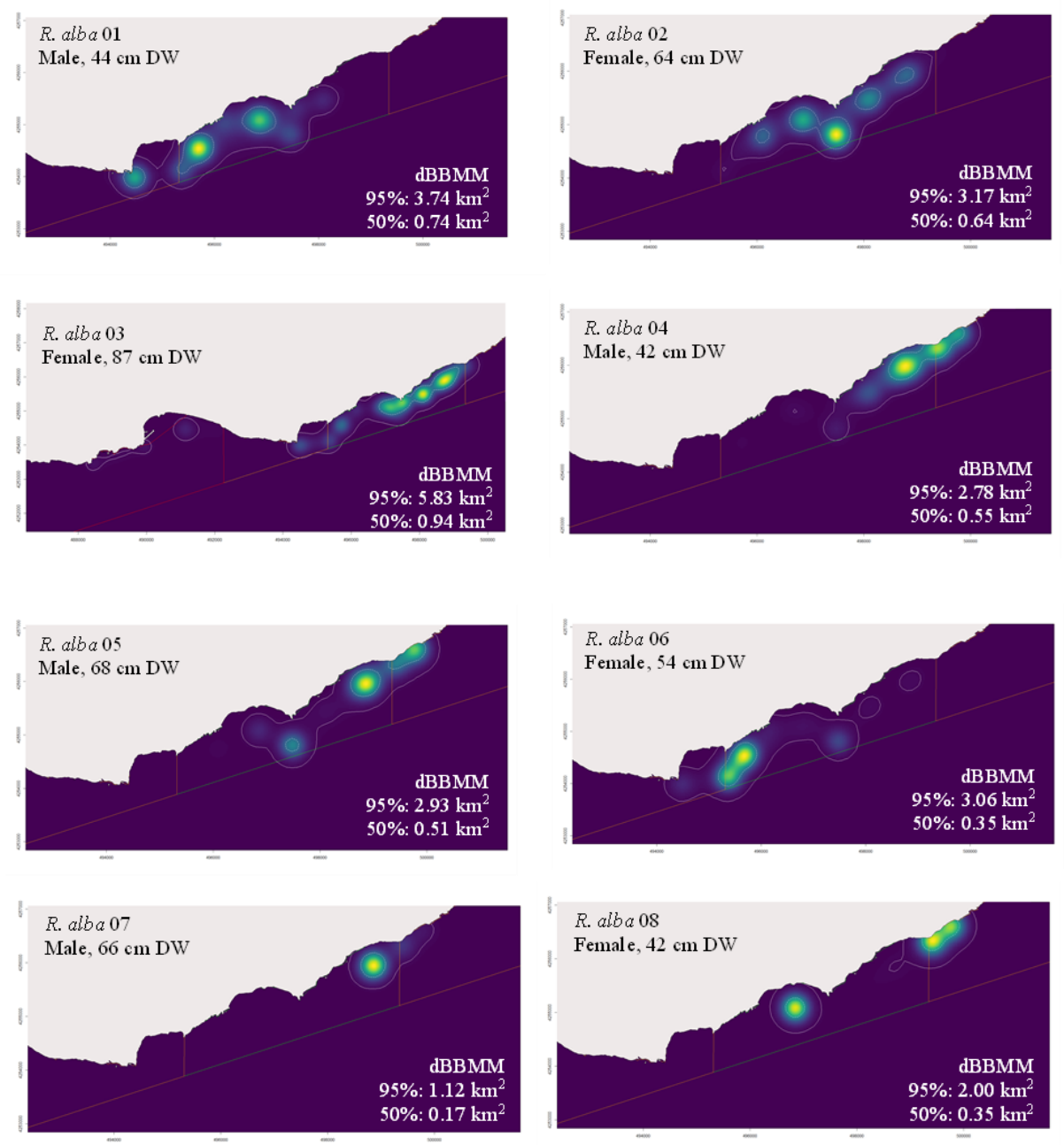

Supplementary material 4.1: Occurrence range of individual *Rostroraja alba* (n = 26) at the 95% (solid line) and 50% (dotted line) isopleths. The brighter the colour, the higher the concentration of COAs. The border of the fully protected area is indicated by a green line, and the border of the partially protected areas by orange lines. Some *R. alba* were not included because they did not provide sufficient COAs to estimate the dBBMM occurrence area (continued in the next two pages).

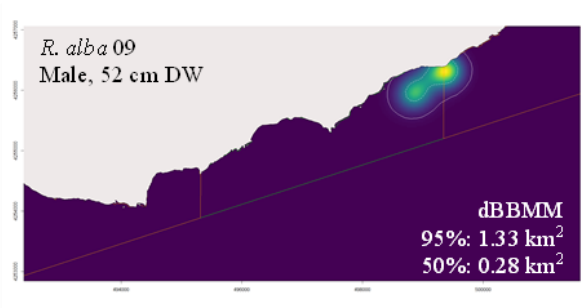
R. alba 09
Male, 52 cm DW
dBBMM
95%: 1.33 km²
50%: 0.28 km²

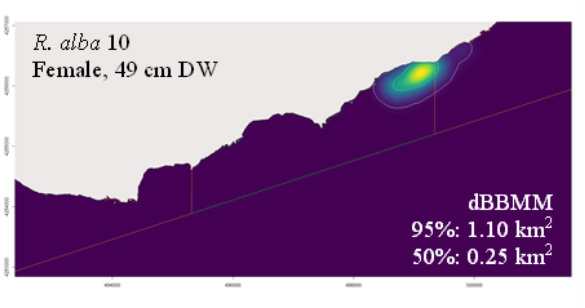
R. alba 10
Female, 49 cm DW
dBBMM
95%: 1.10 km²
50%: 0.25 km²

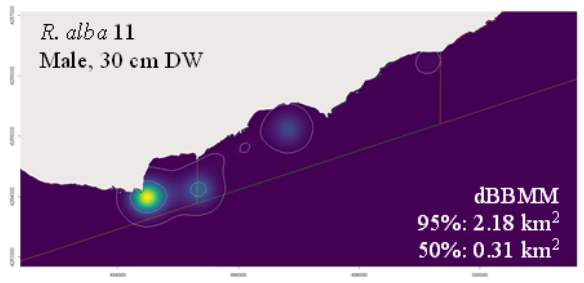
R. alba 11
Male, 30 cm DW
dBBMM
95%: 2.18 km²
50%: 0.31 km²

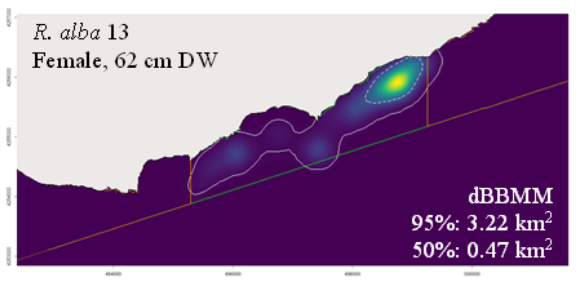
R. alba 13
Female, 62 cm DW
dBBMM
95%: 3.22 km²
50%: 0.47 km²

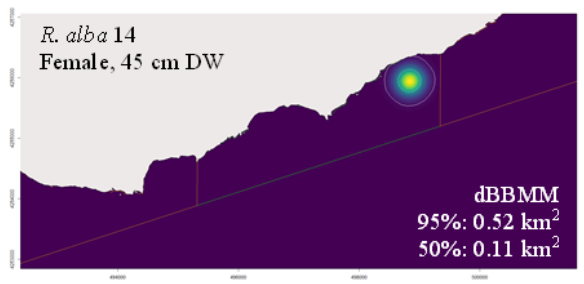
R. alba 14
Female, 45 cm DW
dBBMM
95%: 0.52 km²
50%: 0.11 km²

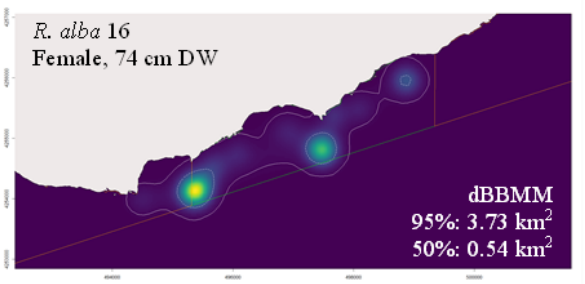
R. alba 16
Female, 74 cm DW
dBBMM
95%: 3.73 km²
50%: 0.54 km²

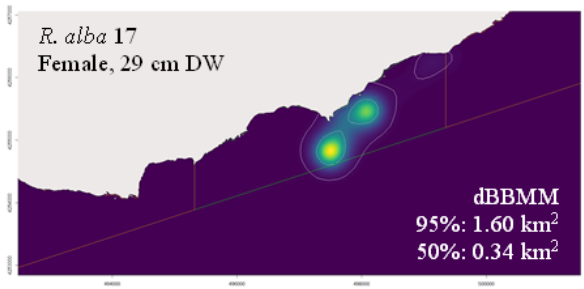
R. alba 17
Female, 29 cm DW
dBBMM
95%: 1.60 km²
50%: 0.34 km²

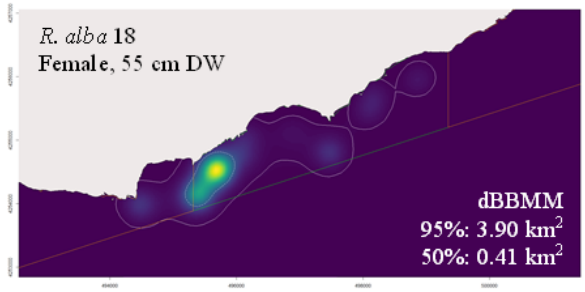
R. alba 18
Female, 55 cm DW
dBBMM
95%: 3.90 km²
50%: 0.41 km²

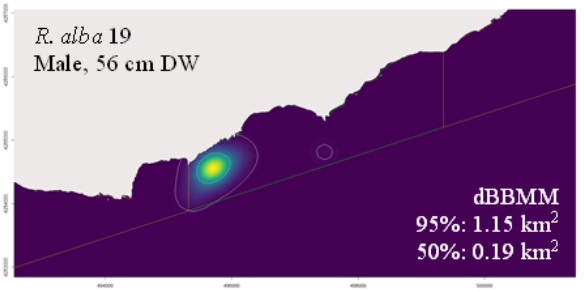
R. alba 19
Male, 56 cm DW
dBBMM
95%: 1.15 km²
50%: 0.19 km²

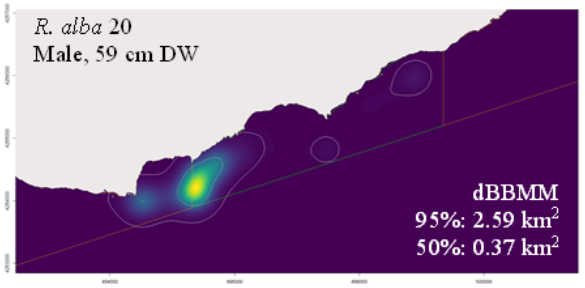
R. alba 20
Male, 59 cm DW
dBBMM
95%: 2.59 km²
50%: 0.37 km²

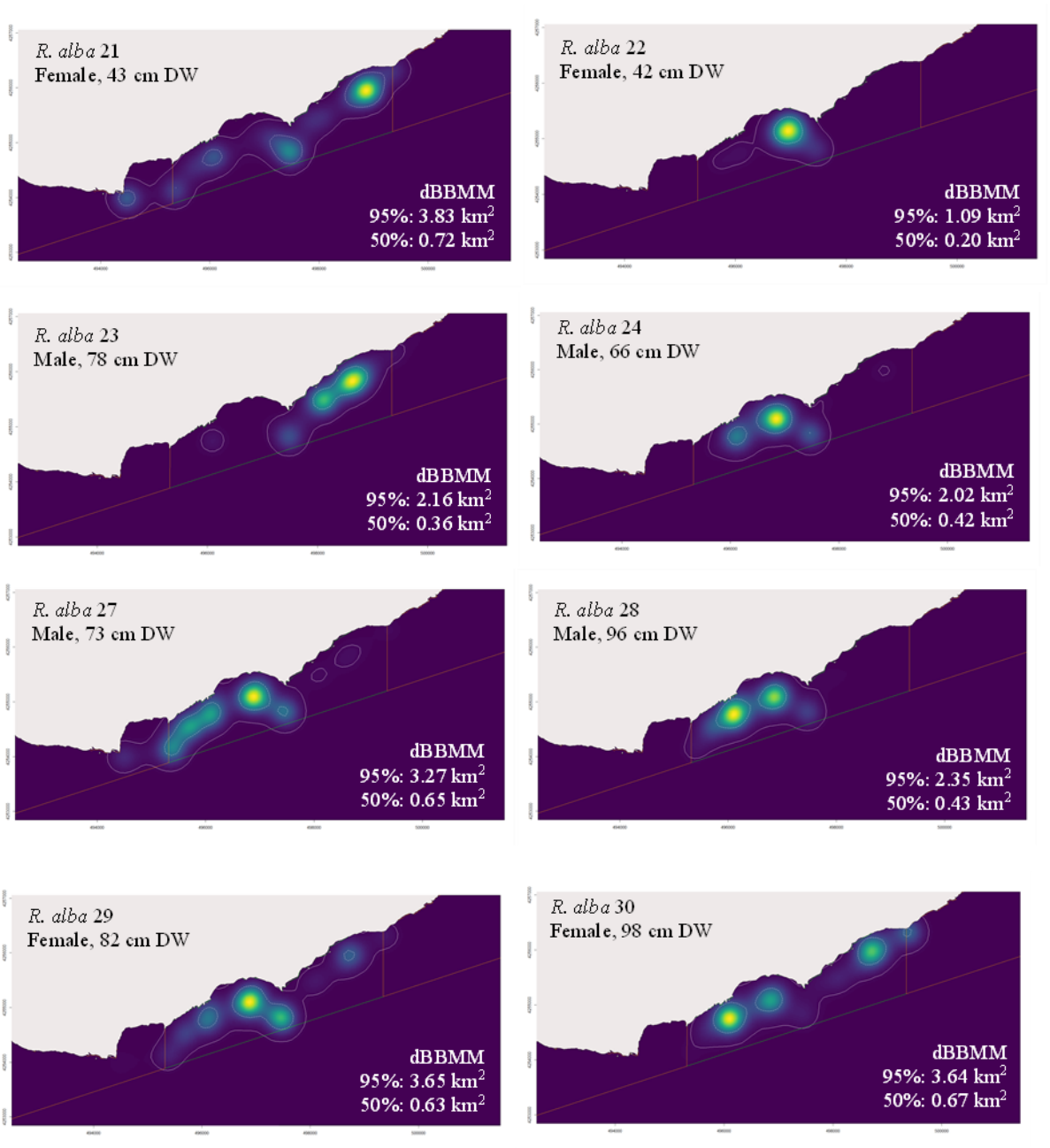
R. alba 21
Female, 43 cm DW
dBBMM
95%: 3.83 km²
50%: 0.72 km²
R. alba 22
Female, 42 cm DW
dBBMM
95%: 1.09 km²
50%: 0.20 km²
R. alba 23
Male, 78 cm DW
dBBMM
95%: 2.16 km²
50%: 0.36 km²
R. alba 24
Male, 66 cm DW
dBBMM
95%: 2.02 km²
50%: 0.42 km²
R. alba 27
Male, 73 cm DW
dBBMM
95%: 3.27 km²
50%: 0.65 km²
R. alba 28
Male, 96 cm DW
dBBMM
95%: 2.35 km²
50%: 0.43 km²
R. alba 29
Female, 82 cm DW
dBBMM
95%: 3.65 km²
50%: 0.63 km²
R. alba 30
Female, 98 cm DW
dBBMM
95%: 3.64 km²
50%: 0.67 km²

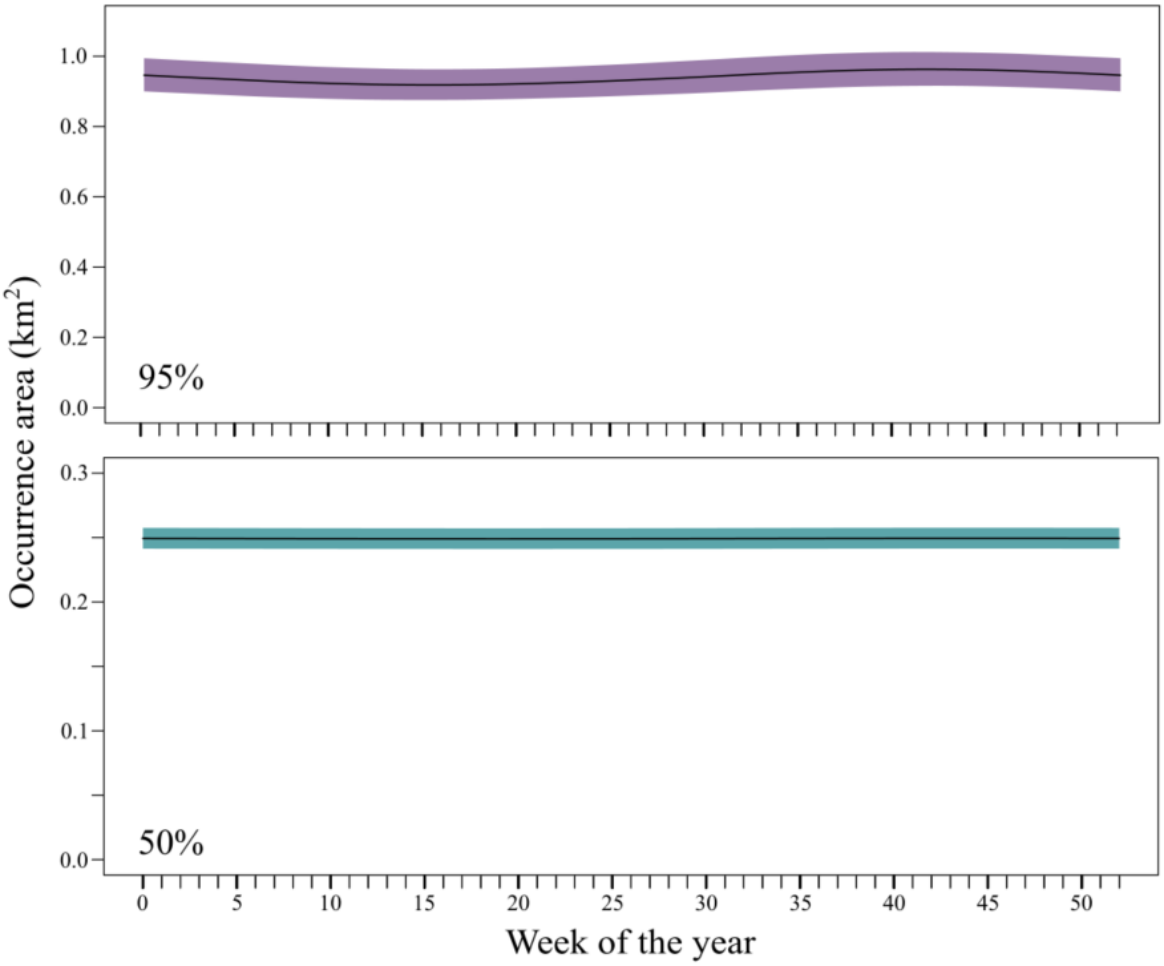

Supplementary material 4.2: General Additive Model of the 50% and 95% weekly occurrence areas of *Rostroraja alba* as a function of week of the year (fixed effect) and individual (random effect).

Supplementary material 4.3: Median depth and range per diel phase per *Rostroraja alba* individual with a V9P Innovasea tag.

	Day			Twilight			Night			Total		
R. alba	Min	Max	Median	Min	Max	Median	Min	Max	Median	Min	Max	Median
18	0.37	29.70	18.20	0.00	32.10	13.40	0.00	54.50	9.29	0.00	54.50	16.60
22	8.82	25.10	15.00	7.36	23.80	12.70	5.23	20.50	10.40	5.23	25.10	14.10
23	7.84	71.40	16.20	6.64	69.60	14.40	5.90	31.50	13.50	5.90	71.40	15.30
24	2.83	33.30	11.90	1.29	33.90	10.60	0.18	63.80	10.70	0.18	63.80	11.10
27	3.85	75.30	14.40	3.28	75.30	12.90	1.24	41.30	12.30	1.24	75.30	13.20

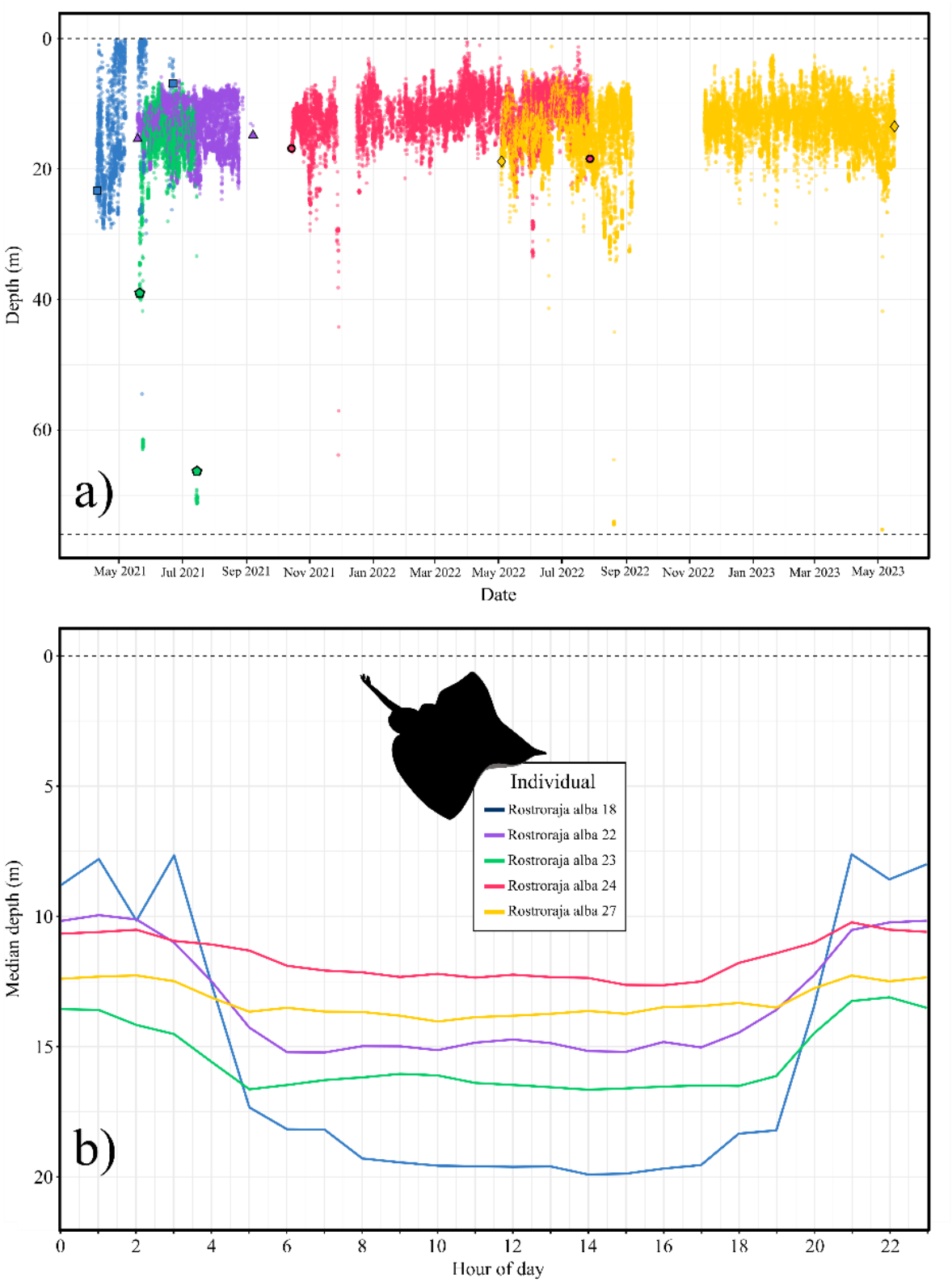

Supplementary material 4.4: Summaries of the depth data: a) depth values per individual recorded over the study period. First and last detections per individual are highlighted as unique symbols per individual with black borders; b) average depth per individual per hour of the day. Horizontal dashed lines indicate historical tide minimum (0 m depth after correction) and maximum depth of the tag's sensor (76 m). Individual *Rostroraja alba* are colour coded.

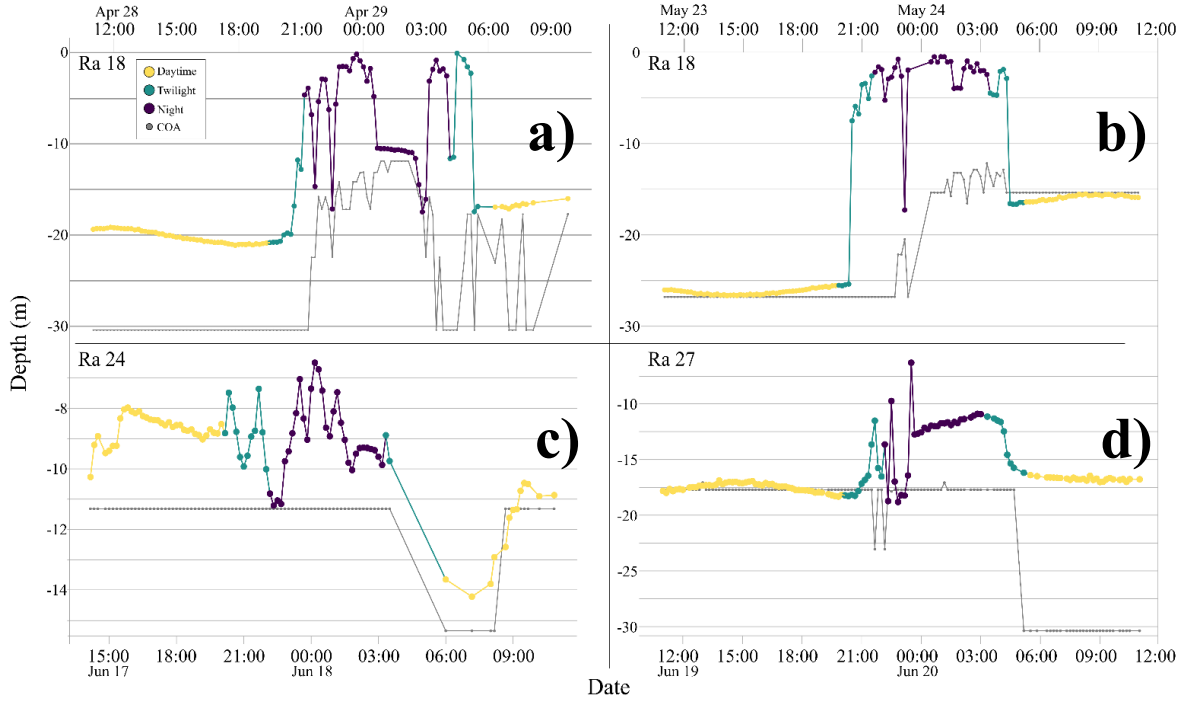

Supplementary material 4.5: Examples of vertical movements inferred from the depth data of three *Rostroraja alba* individuals, showing consecutive vertical movements, swimming near the surface, and depth changes following the seafloor. Depth values are colour-coded by diel phase and seafloor depth at each COA is shown in grey.

Supplementary material 4.6: Summary of the step length results per individual and diel phase, showing values and count.

R. alba	Sex	Disc width	Step length				Step count		
			Day	Night	Twilight	Total	Day	Night	Twilight
R. alba 01	M	44	9.31	65.86	61.75	45.08	1,868	2,638	720
R. alba 02	F	64	41.99	81.80	94.49	64.79	15,446	12,738	4,566
R. alba 03	F	87	55.42	68.27	76.18	63.57	802	739	243
R. alba 04	M	42	38.69	71.73	103.36	60.60	11,110	9,521	3,215
R. alba 05	M	68	39.97	64.26	99.06	55.92	2,877	1,922	692
R. alba 06	F	54	40.38	61.75	66.69	52.10	7,016	5,613	1,930
R. alba 07	M	66	17.33	25.32	25.08	21.77	266	261	76
R. alba 08	F	42	110.27	104.99	44.69	101.03	35	146	16
R. alba 09	M	52	49.64	86.51	56.54	70.49	25	43	12
R. alba 10	F	49	53.85	59.26	74.29	59.50	278	422	113
R. alba 11	M	30	43.62	51.51	55.95	48.14	7,358	5,296	1,973
R. alba 12	M	65	-	-	-	-	-	-	-
R. alba 13	F	62	56.09	84.26	97.19	72.41	3,904	2,935	1,169
R. alba 14	F	45	-	-	-	-	-	-	-
R. alba 15	M	42	-	-	-	-	-	-	-
R. alba 16	F	74	26.81	54.07	74.49	42.67	1,580	974	439
R. alba 17	F	29	66.75	109.24	116.48	90.35	6,890	5,506	2,243
R. alba 18	F	55	32.72	109.50	113.59	65.52	640	297	165
R. alba 19	M	56	60.32	58.12	71.63	61.19	5,843	3,530	1,524
R. alba 20	M	59	55.64	96.54	104.98	74.80	4,030	2,098	1,047
R. alba 21	F	43	49.37	74.27	77.30	62.43	4,979	3,696	1,432
R. alba 22	F	42	75.30	69.84	113.85	80.21	2,411	912	633
R. alba 23	M	78	42.61	120.58	125.23	73.47	1,487	549	387
R. alba 24	M	66	24.75	76.83	64.68	53.17	2,754	2,869	901
R. alba 25	F	87	-	-	-	-	-	-	-
R. alba 26	M	51	-	-	-	-	-	-	-
R. alba 27	M	73	42.76	107.83	113.46	75.57	6,059	4,181	1,687
R. alba 28	M	96	32.99	140.19	132.16	91.15	5,303	4,862	1,705
R. alba 29	F	82	34.62	91.70	98.93	65.96	4,466	3,644	1,401
R. alba 30	F	98	46.19	126.75	133.83	95.04	4,048	4,357	1,537

Chapter 5
Seasonal movement dynamics of the commercially important thornback ray (*Raja clavata*) in a coastal marine protected area

Raja clavata on board for tagging
© Kim Birnie-Gauvin

Chapter published as:

Kraft, S., Winkler, A.C., Abecasis, D. Seasonal movement dynamics of the commercially important thornback ray (*Raja clavata*) in a coastal marine protected area. Ocean & Coastal Management 254, 107210. https://doi.org/10.1016/j.ocecoaman.2024.107210

Abstract

Elasmobranchs are a group of slow growing species whose various populations are in decline mostly due to their susceptibility to overfishing. A common approach to protect marine species is to establish marine protected areas (MPAs). Data on the spatial ecology of species is key information for MPA implementation and management. However, this information is usually lacking, particularly for elasmobranchs. In this study, thornback rays were tagged with acoustic transmitters to track their movement patterns in a marine protected area in Portugal. Individuals were detected for up to 1,323 days, and transient and resident behaviours were observed. Residents exhibited a seasonal pattern of presence, peaking during late winter and spring. Weekly occurrence range size reached its maximum from mid-summer to mid-autumn. Diel changes in movement, mainly as increases in activity, were detected during night and twilight. These findings highlight the seasonal and daily dynamics of thornback rays and how these can influence their protection in an MPA. The area where the LSMP is established appears to be dominated by males, indicating that most of the protection provided to this species is towards this sex. These results provide valuable insights for the conservation and adaptive management of this commercially relevant species.

Keywords: Acoustic telemetry, conservation, Rajidae, sexual segregation, skates

5.1. Introduction

Global fishing activity has grown prominently over the last decades, driven by an increasing demand for food security and economic stability (FAO, 2020). To meet this rising need, this industry has expanded in reach, catches have increased in volume, and more people have been employed, in turn increasing pressure on marine ecosystems (FAO, 2020). Elasmobranchs (sharks, skates, and rays) are largely caught as bycatch in a range of fisheries globally, and their captures reflect the same pattern of increased exploitation (Dulvy et al., 2021). Moreover, the increase in fishing pressure has generated declines in many elasmobranch populations (McCauley et al., 2015). Most elasmobranchs are ill-equipped to withstand this pressure because of their k-selected life history strategies (Hoenig and Gruber, 1990; Musick, 1999), exhibiting high longevity, slow growth rates, late maturity, and low fecundity. As a result, over a third of these species are currently threatened with extinction due to overfishing (Dulvy et al., 2021). This is despite various conventional management approaches that have applied to reduce their decline (Davidson et al., 2016). To this end, additional approaches such as marine spatial planning have been used to help.

Marine protected areas (MPAs) are a common method used to address the effects of overfishing by providing spatial protection to species and habitats (Gell and Roberts, 2003). Marine protected areas are defined as "clearly defined geographical space, recognized, dedicated and managed, through legal or other effective means, to achieve the long-term conservation of nature with associated ecosystem services and cultural values" (Dudley, 2008) and can be multidimensional in their influence, benefiting areas like fisheries, human well-being, economics, knowledge development, and conservation and management (Ban et al., 2019; Lester et al., 2009). Elasmobranchs can respond positively to MPAs (Le Port et al., 2012; Speed et al., 2018), yet the effect is generally variable and often moderate (Dwyer et al., 2020; MacKeracher et al., 2019). This occurs because many MPAs are not specifically designed with elasmobranchs as their target and thus often fail to properly encompass their movements (Dwyer et al., 2020; MacKeracher et al., 2019).

Understanding species movement patterns is directly linked to protection success (Kramer and Chapman, 1999) and therefore a key factor to assess in the context of MPAs (MacKeracher et al., 2019). A well-suited method for this task is passive acoustic telemetry. Compared to traditional tagging methods like tag-recapture, using acoustic telemetry the long-term movements of multiple tagged individuals can be monitored, and detailed, more accurate data can be collected in a mostly automated way (Hussey et al., 2015). Indeed, acoustic

telemetry has improved knowledge on space use patterns, for example by providing more precise home range estimates and detecting previously unnoticed seasonal migrations and ontogenetic changes in movement (Siskey et al., 2019). This method is also very cost-effective after the establishment of the acoustic array, presenting a low maintenance compared to the amount of data it can provide (Heupel et al., 2006). This methodology has been used extensively to study the movements of elasmobranchs in the context of MPAs (Elston et al., 2023; Espinoza et al., 2015; Knip et al., 2012; Lavender et al., 2021).

The thornback ray (*Raja clavata*) is a batoid species that reaches a maximum total length (TL) of 130 cm (Last et al., 2016) and inhabits shelves and slopes at depths between 5–1,020 meters, from Iceland along the coast of Europe to South Africa and Madagascar, including the Mediterranean (Last et al., 2016). This species is among the most fished elasmobranchs (Carbonara et al., 2020; Figueiredo et al., 2020; Walker and Hislop, 1998); however, their catch data is likely underestimated because of a lack of historical species-specific identification in mixed-species stocks, mislabeling, unreported extraction, and discard at sea (Alves et al., 2020; Dulvy et al., 2000; Figueiredo et al., 2020). Mortality rates in the fisheries where they are captured as bycatch can be as high or higher than the targeted species (Piet et al., 2009). For example, in the North Sea, up to 71% of the standing biomass of thornback rays was estimated to be captured each year as by-catch by the bottom trawl and otter trawl fisheries (Piet et al., 2009). As a result, their populations have declined in areas such as the North Sea (Walker and Hislop, 1998), the Irish and Celtic seas (Dulvy et al., 2000) and the Adriatic Sea (Krstulović Šifner et al., 2009), and are currently classified as Near Threatened by the IUCN Red List (IUCN, 2024). In turn, efforts to restore their stocks have been carried out in recent years, resulting in increases in biomass in areas such as the North Sea and English Channel (ICES, 2024), while signs of recovery have also been noted in the western Mediterranean (Marongiu et al., 2017; Ramírez-Amaro et al., 2020).

This species is particularly important to artisanal or small-scale fisheries of some countries, like Portugal (Figueiredo et al., 2020). Mean annual landings are estimated at around 270 tons, and an additional 1,123 tons are landed as *Raja* spp. (Alves et al., 2020), but similar issues to those found elsewhere, such as multi-species fisheries, unreported catches, undocumented trips, misidentifications, make the estimation of landings of this species and other Rajiformes in Portugal a difficult task (Figueiredo et al., 2020). Nonetheless, management efforts have made it mandatory to land this species separately (i.e., as *Raja clavata*) since 2009 (EC, 2009) and a seasonal ban of their targeted capture was established during the months of May and June as well as a minimum landing size of 52 cm (Serra-Pereira

et al., 2018). These actions have resulted in a stable proportion of thornback rays in the landings of some fisheries during the last decade, such as bottom trawler landings (ICES, 2022).

The Professor Luiz Saldanha Marine Park (LSMP) is a coastal MPA found off the Setúbal peninsula, Portugal. In 2010, an acoustic telemetry array was deployed in the LSMP to study the spatial ecology and effects of the MPA implementation in protecting commercially important species of bony fishes and cuttlefish (Abecasis et al., 2014b), and four batoids (Cabral, 2014; Kraft et al., 2023b; Sousa et al., 2019). However, the study on thornback rays was based on three individuals and under two months of monitoring, thus a longer study with more individuals is warranted to answer these questions more robustly (Cabral, 2014). In this study, we acoustically tagged thornback rays and collected long-term movement data to study their movement patterns in the LSMP and to assess the contribution of coastal MPAs to the protection of this species. To obtain a better understanding of their spatial ecology, we estimated residency, occurrence areas, activity, and depth use. This information is relevant to the adaptive management of the LSMP and similar MPAs in other areas of the distribution of the thornback ray.

5.2. Materials and Methods

5.2.1 Study area

After its designation in 1998, the LSMP's initial zoning actions took place in 2005 and became fully implemented with all protection levels established by 2009 (Portuguese legislation, Council of Ministers Resolution 141/2005). Its 53 km^2 are divided into three protection levels, a total protection area of 4.3 km^2 to which access and any kind of fishing are prohibited except when authorized for research and educational purposes; four partial protection areas of a total 21 km^2 where only octopus traps and jigging are allowed beyond 200 m from the coastline; and three complementary protection areas or buffer areas of a total 28 km^2 where only local licensed fishing boats under 7 m are allowed to operate (Figure 5.1). The LSMP covers 38 km of the south-western shore of the Setúbal peninsula. To the east is the Sado estuary in which a natural reserve is in place, the Reserva Natural do Estuário do Sado. Further north is the Tejo estuary, inside which the Reserva Natural do Estuário do Tejo is placed. The latter two natural reserves are RAMSAR sites (wetland sites designated of international importance under the Ramsar Convention) due to their importance for many aquatic birds and as a nursery area for several fish and invertebrate species.

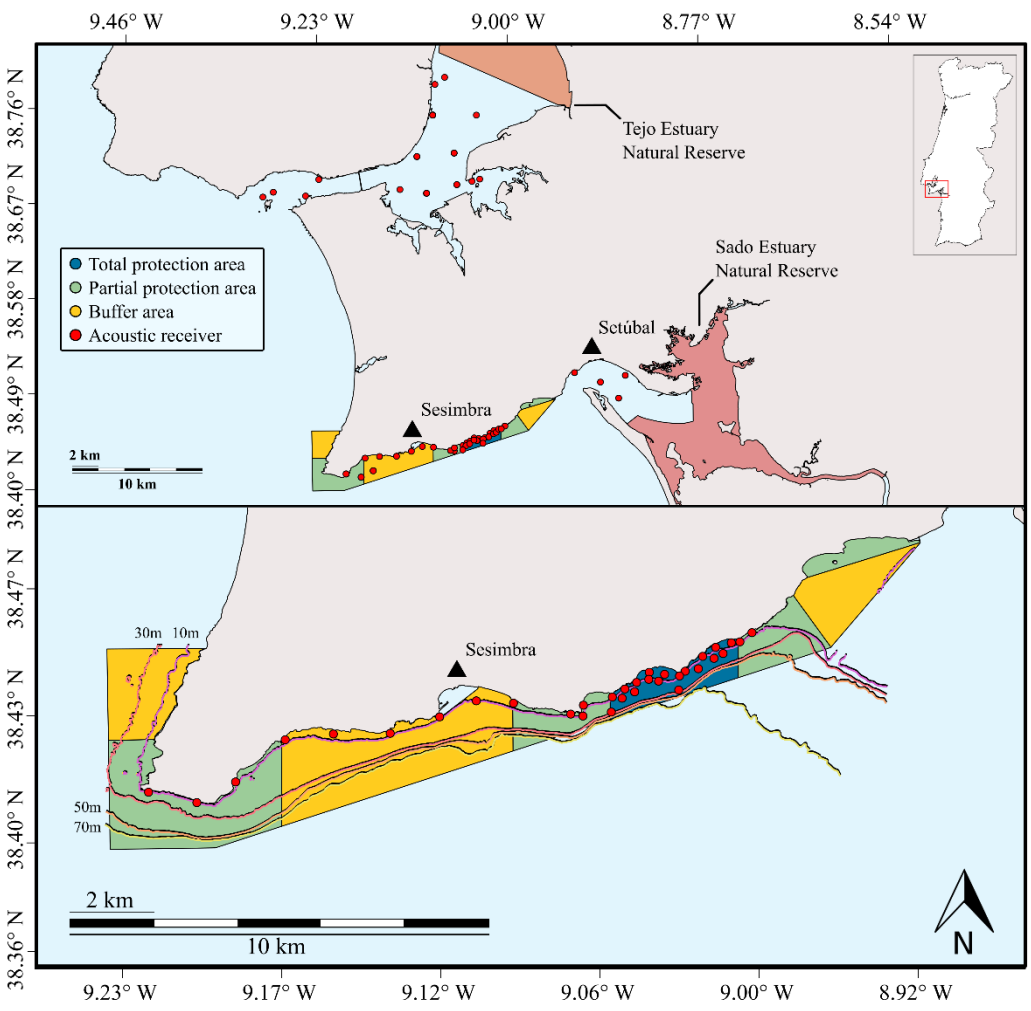

Figure 5.1: Map of the study area. Top panel: general overview of the Professor Luiz Saldanha Marine Park and the Setúbal peninsula, with the Tejo estuary and its natural reserve (orange) to the north and the Sado estuary and its natural reserve (red) to the East. Bottom panel: Professor Luiz Saldanha Marine Park and its three different protection levels. Only the aquatic portions of the Natural Reserves are shown. Isobaths are colour coded.

5.2.2 Data collection and tracking

Thornback rays were captured using trammel nets (2019 and 2021) and longlines (2021 and 2022). The monofilament trammel nets were 500 m in length and 1.6 m in height, with 100 mm inner panels of stretched mesh and outer panels of 600 mm. The longlines had between 100 and 150 hooks that were baited with 2-5 cm chunks of frozen European pilchard (*Sardina pilchardus*). The fishing gears were deployed at depths between 5-40 m, mostly inside the fully protected area, and also in the partial protection area. Deployments and retrievals were always done in the morning at approximately the same time resulting in a soaking time of around 24h.

Captured individuals were brought on board and placed into a container filled with seawater that was changed after every individual. First, hooks were removed from the individuals caught by longline if possible and a hydrophone was used to detect previously tagged individuals. A measuring tape was used to obtain total length (TL), disc width (DW), and clasper length for males. Sizes were compared to regional lengths at first maturity (TL_{50}=67.6 cm for males and 78.4 cm for females, Serra-Pereira et al., 2011) to determine if the individuals were over the total length size at 50% maturity. These individuals were classified as "mature" for reference purposes, as reproductive organs were not directly inspected. To implant the acoustic transmitters a 2 cm incision was made in the peritoneal cavity using a scalpel and then closed it using absorbable suture. Three types of Innovasea 69 kHz acoustic tags were used: V9, V13, and V9P (with pressure sensor). Respective expected battery lifetimes were 651, 1,317 and 404 days according to the manufacturer. The appropriate tag size was selected based on previously deployed tag types, tag type availability, and animal size, as to not exceed the 2% tag-to-body weight rule of thumb (Winter, 1996). Additionally, each individual was fitted with a Petersen disc tag (www.floytags.com) with a unique ID number and contact information. Capture, handling, and tagging were done under permits of the Portuguese Institute for Nature Conservation and Forests (permits n°145/2019/CAPT; 13/2020/CAPT; 70/2021/CAPT; 38/2022/CAPT) and the Veterinary General Directorate (permit n° 2018-08-29 015730). Tagging procedures were also approved by the Animal Welfare Committee of the Centro de Ciências do Mar (CCMAR - ORBEA).

Individuals were tracked using an array of 37 Innovasea VR2W acoustic receivers. The array was at its densest in the total protection area (19 receivers, Figure 5.1). Most receivers were active throughout the study period, but some were only present for a shorter period of at least 6 months (3 receivers in the buffer area, 1 in the partial protection area and 2 in the Sado estuary), either because they were lost to rough weather conditions, removed by fishing gear, or the structure they were attached to (e.g., a buoy) was removed from the water. Receivers were serviced once or twice a year.

5.2.3 Data analysis

The first 24 hours of data of each individual were deleted to eliminate possible behavioural anomalies that may have been produced by the tagging process (except for residency estimation to account for their presence on the day of capture). Detection efficacy was assumed to be constant based on previous evaluations that showed no major influence from environmental variables, diel patterns, and/or background noises (Abecasis et al., 2014a;

Sousa et al., 2019). Detections were classified into diel phases using the R package *suncalc* (Thieurmel and Elmarhraoui, 2019), setting "daytime" as the time between sunrise and sunset (appearance and disappearance of the sun over the horizon), "twilight" as morning and evening twilight, and "night" as the period between evening twilight and morning twilight.

5.2.3.1 Detection patterns and residency

Detection patterns were visually inspected and the fate of individuals was assessed following Villegas-Ríos et al., (2020) to identify events like emigration from the study site, post-release mortality or tag loss, and fishing mortality. We estimated two residency indices (Kraft et al., 2023a): I_R, obtained as total number of days detected by at least one receiver (D_d) divided by the duration of the monitoring period (D_t, time between release and last data download or tag expiration dates): $I_R = D_d/D_t$, and as a weighted residency index (Iw_R), obtained by multiplying I_R by the days between first and last detection (D_i) divided by D_t: $I_{WR} = (D_d/D_t) \times (D_i/D_t)$. We replaced D_t with tag lifetime in the equations if the latter was shorter than the total monitoring period (Abecasis et al., 2013). I_{WR} is sometimes preferred over I_R because it can reflect residence more accurately due to the higher robustness to periods without detections (Lino, 2012). The presence of thornback rays in the LSMP throughout the year was evaluated using a Generalized Additive Mixed Model (GAMM) in the R package *mgcv* (Wood, 2011). For this, the detections were transformed to daily presence (1) or absence (0) per individual. Four models were tested using day of the year (in all models) and individual size as covariates, and individual as random effect: the first model only with day of the year, the second model with day of the year and size, the third model with day of the year and individual effect, and the fourth full model with all factors (supplementary material 5.1). Sex was not included because of the uneven sex ratio. Day of the year was modelled using a cyclic cubic spline. The best model was selected using the Akaike Information Criterion (AIC) in the R package *AICcmodavg* (Mazerolle, 2023). The lowest scoring model was selected, and if two or more models had similar scores (AIC < 2), the simplest one was preferred. To properly investigate the long-term detection patterns in such a time frame, only individuals with detection intervals (i.e., number of days between first and last detection) of at least a year (n=23, D_i=350-1323 days) were used in the presence/absence GAMM to reduce the possible biases introduced by transient or fished individuals. For example, transient individuals will increase the probability of presence before leaving, and conversely, an unaccounted transient individual that leaves or an individual that is fished will artificially lower the estimated probability of presence.

5.2.3.2 Occurrence areas

Centers of activity (COAs) were estimated as a weighted mean position every 30 minutes (Simpfendorfer et al., 2002) before calculating space use areas. The dynamic Brownian bridge movement model (dBBMM) (Kranstauber et al., 2012) was implemented in the R package *move* (Kranstauber et al., 2021). This is a probability distribution-based occurrence estimator that estimates the area used during the study period by reconstructing its movement path and calculating an associated uncertainty around it. Consecutive location points are connected to create segments and the probability of occurrence is estimated around each one based on the distance and time difference between the pair of points, obtaining the utilisation distribution (UD). This model was chosen over other classic home range estimators because it accounts for the natural autocorrelation of movement data and because the acoustic array did not cover the entire home range of the tracked individuals (Fleming et al., 2015). A location error of 200 meters was used, while window size (w = 31) and margin size (m = 11) were set to default values. Segments longer than 24 hours were removed before estimating UDs to avoid unrealistic large uncertainty areas.

Weekly and total occurrence areas at the 50% (core) and 95% level were estimated. Weekly occurrence areas were used to evaluate changes over the year, implementing a GAMM in the R package *mgcv* (Wood, 2011). Week of the year was modelled using a cyclic cubic spline and individual was set as random effect. Four models were tested for each contour level (supplementary material 5.1): the first one only with week of the year as covariate; the second model with week of the year and size; the third model with week of the year and individual effect; and the fourth model with all variables (week of the year, size, and individual effect). All models used REML as the smoothing parameter estimation method, and a log-linked Gamma distribution was fitted as the distribution function because the response variable was positive, continuous, and right skewed. The best fitting model was chosen based on the lowest AIC value. If two or more models had similar scores (AIC <2), the simplest one was preferred.

5.2.3.3 Depth

Local daily tide values were obtained using the R package *PTtidaltools* (Martins, 2021) to remove the effect of tides on the pressure readings by subtracting tide height from the raw depth values. The final depth values correspond to depth compared to the local lowest historical tide, which were used to calculate average depth every 10 minutes. Depth was evaluated in two

forms: 1) throughout the year (per day of the year) and 2) throughout the day (per diel phase). Importantly, these depth assessments are constrained to the detection range of the array and may not reflect the true depth range occupied by the thornback rays in this area.

1) The variation of depth (response variable) throughout the year was evaluated using a GAMM as implemented in the R package *mgcv* (Wood, 2011). Four models were tested with day of the year (in all models) and individual size as covariates, while individual was set as random effect. The first model only contained day of the year, the second model had day of the year and size, the third model had day of the year and individual effect, and the fourth model had all factors. Sex was left out because all individuals with depth data were males. Day of the year was modelled using a cyclic cubic spline, and a log-linked Gamma as the distribution function because the response variable was positive, continuous, and right skewed. After setting up the models, the best one was selected using the AIC by selecting the lowest scoring model. If two or more models had similar scores (AIC <2), the simplest one was preferred. For this analysis, R was not able to set up the models because the dataset was too large, so it was reduced to one daily median depth value per individual.

2) Depth changes throughout the day were evaluated using linear mixed-effects models in the R package *nlme* (Pinheiro and Bates, 2023). Diel phases (daytime, night, twilight) were assigned using the R package *suncalc* (Thieurmel and Elmarhraoui, 2019). Diel phase was preferred over hour of the day for this analysis because with changing sunlight hours throughout a year, certain hours of the day can correspond to different diel phases, adding noise to the results; the models included depth as an autocorrelated variable, and individual and day of the year as random effects.

5.2.3.4 Activity

Mean activity was estimated as minimum distance covered per time unit (hereon, step length) between successive COAs in a straight line using the R package *adehabitatLT* (Calenge, 2006). Estimations were done as a global mean and per diel phase. Step lengths of 30 minutes were retained and discarded those of longer duration (i.e., 60 minutes or more) as these had detection gaps (no detections for 30 minutes or more) and were therefore more likely to also include movements outside of the marine park.

5.3. Results

5.3.1 Tagging and detection data

Thirty-five thornback rays were tagged with a sex ratio skewed towards males (29 vs. 6, two-tailed binomial test, $p < 0.0001$). For individuals Rc 01 to 11 only DW was measured, so their total length (TL) was estimated based on the size conversion factors of (Serra-Pereira et al., (2010). Average DW was 49.2 cm and ranged between 33.5-61.0 cm, and average TL was 72.8 cm and ranged between 45-93 cm (Table 5.1). Male DW averaged 49.4 cm (range 33.5-58.0 cm) and TL averaged 73.5 cm (range 47.2-93.0 cm), while the DW of females averaged 48.0 cm (range 38.0-61.0 cm) and TL averaged 69.0 cm (range 45-93 cm). Comparing our sizes to regional lengths at first maturity (TL_{50}=67.6 cm for males and 78.4 cm for females, Serra-Pereira et al., 2011), three of six females (50%) and 21 of 29 males (72%) were over the TL size at 50% maturity (Table 5.1). These individuals were classified as "mature" for reference purposes, as there was no direct visual inspection of the reproductive organs. Individuals Rc 22 and 23 were classified as deceased based on their detection patterns and subsequently removed from further analysis; of the 33 remaining individuals, 14 dispersed and 19 were detected throughout the study period. Of the eight individuals that were released with the hook still in, five survived, two dispersed, and one died (Rc 23). Per individual we obtained an average of 785 ± 375 days of monitoring and a detection interval of 477 ± 408 days (Table 5.1).

5.3.2 Detection patterns and residency

Different residency patterns were noted among individuals (Figure 5.2). Some individuals were steadily detected (e.g., Rc 07, Rc 13), while others had similar detection intervals but presented large detection gaps in-between (e.g., Rc 02, Rc 33). Some individuals were infrequently detected over long periods (e.g., Rc 03, Rc 32), while others permanently left the array shortly after tagging (e.g., Rc 08, Rc 09, Rc 19).

Average residency was I_R = 0.38 (range I_R = 0.00-0.99) and markedly contrasted between sexes, with a much higher average for males than females (I_R = 0.46 vs. 0.05) (Table 5.1). Two general detection patterns were seen among females. Three were detected sporadically over long detection intervals (Rc 11, 12 and 14, respective D_i =674, 242, 507) and had residency indexes between I_R=0.07-0.14, while the other three (Rc 17, 19 and 26) were detected only in their tagging day and had a residency of I_R=0.00. The female with the highest residency (Rc 11) was detected in 188 different days over a monitoring period of 1,317 days.

Average residency between tagging years (2019 and 2021) did not vary significantly ($I_{R\ 2019}$=0.44, $I_{R\ 2021}$=0.33: ANOVA, F= 0.29, p 0.75). Disc width was not correlated with residency (r (31) =0.0302, p =0.87).

Five males were detected in the buffer area in front of the port of Sesimbra. Four were detected in this area between days of the year 200 and 300 (mid-July to late October). These detections occurred in consecutive years in the cases of Rc 02 and Rc 18. The start of the detection window of Rc 28 overlapped with the window of the other individuals but extended to December and the first days of January. One mature female (Rc 11) was seasonally detected in Sado in two consecutive years, between late October and late November in 2019 and mid-August to early October in 2020 (Figure 5.2). No individuals were detected in the Tejo estuary.

Table 5.1: Summary data of the tagged thornback rays (asterisks indicate individuals with V9P pressure tags), including biological data on sex (M = males, F = females) and maturity based on length (in cm); residency indices (D_d = days detected, D_i = detection interval, D_t = monitoring time (all in number of days), I_R = residency index, I_{WR} = weighted residency index); dynamic Brownian bridge movement model (dBBMM) occurrence areas at the 50% and 95% (in km^2); and individual fish fate following Villegas-Ríos et al., (2020). Asterisks in total length indicate measurements obtained using disc width and the size conversion factors of Serra-Pereira et al. (2010). Asterisks in tag duration indicate tags that completed their expected lifetime during the study.

R. clavata n°	Sex	Maturity	Disc width (cm)	Total length (cm)	Tagging date	Tag duration	Exp. date/ last data download	D_d	D_i	D_t	I_R	dBBMM (km^2) 95%	dBBMM (km^2) 50%	Fish fate
01	M	Mature	52.00	77.27*	30/03/2019	1317*	06/11/2022	183	215	1317	0.14	1.93	0.32	Dispersed
02	M	Immature	46.00	65.81*	30/03/2019	1317*	06/11/2022	937	1323	1317	0.71	2.14	0.24	Survived
03	M	Immature	33.50	47.18*	02/04/2019	651*	12/01/2021	9	429	651	0.01	-	-	Survived
04	M	Immature	46.80	67.95*	03/04/2019	1317*	10/11/2022	1177	1225	1317	0.89	1.39	0.19	Survived
05	M	Immature	46.50	66.52*	03/04/2019	1317*	10/11/2022	471	1263	1317	0.36	1.48	0.16	Survived
06	M	Mature	48.00	68.67*	20/10/2019	1317	18/05/2023	986	1306	1306	0.75	0.96	0.21	Survived
07	M	Immature	45.00	64.38*	21/10/2019	1317	18/05/2023	1159	1306	1305	0.89	1.94	0.38	Survived
08	M	Mature	58.00	86.18*	21/10/2019	1317	18/05/2023	1	1	1305	0.00	-	-	Dispersed
09	M	Mature	56.00	83.21*	21/10/2019	1317	18/05/2023	2	4	1305	0.00	0.59	0.13	Dispersed
10	M	Immature	47.00	67.24*	22/10/2019	651*	03/08/2021	636	657	651	0.98	2.14	0.26	Survived
11	F	Mature	61.00	85.08*	22/10/2019	1317	18/05/2023	188	674	1304	0.14	1.54	0.24	Dispersed
12	F	Immature	38.00	56.00	06/04/2021	651*	17/01/2023	48	242	651	0.07	2.93	0.50	Dispersed
13	M	Mature	47.00	73.00	06/04/2021	1317	18/05/2023	762	773	773	0.99	1.19	0.20	Survived
14	F	Mature	54.00	81.00	06/04/2021	1317	18/05/2023	63	507	773	0.08	1.08	0.18	Dispersed
15	M	Mature	51.00	77.00	06/04/2021	1317	18/05/2023	228	773	773	0.29	4.29	0.42	Survived
16	M	Mature	51.00	78.00	06/04/2021	1317	18/05/2023	36	50	773	0.05	1.17	0.23	Dispersed
17	F	Immature	38.00	54.00	06/04/2021	651*	17/01/2023	1	1	651	0.00	-	-	Dispersed
18	M	Mature	50.00	75.00	07/04/2021	1317	18/05/2023	81	490	772	0.10	4.07	0.72	Dispersed
19	F	Immature	37.00	45.00	09/04/2021	651*	20/01/2023	1	1	651	0.00	-	-	Dispersed
20	M	Immature	42.00	57.00	20/05/2021	1317	18/05/2023	350	350	729	0.48	1.46	0.28	Dispersed (hook in)
21	M	Mature	58.00	83.00	20/05/2021	1317	18/05/2023	622	728	729	0.85	2.80	0.38	Survived
22	M	Mature	52.00	80.00	20/05/2021	404*	28/06/2022	-	-	-	-	-	-	Deceased
23	M	Mature	57.00	71.00	20/05/2021	651*	02/03/2023	-	-	-	-	-	-	Deceased (hook in)
24*	M	Mature	53.00	69.00	13/10/2021	404*	21/11/2022	401	409	404	0.99	2.27	0.22	Survived
25*	M	Immature	44.00	64.00	14/10/2021	404*	22/11/2022	158	322	404	0.39	1.91	0.21	Survived (hook in)
26	F	Mature	60.00	93.00	15/10/2021	1317	24/05/2025	1	1	1317	0.00	-	-	Dispersed (hook in)
27*	M	Mature	49.00	71.00	03/05/2022	404	18/05/2023	228	373	381	0.60	3.79	0.65	Survived
28*	M	Mature	54.00	86.00	03/05/2022	404	18/05/2023	318	379	381	0.83	4.22	0.59	Survived
29	M	Mature	48.00	82.00	04/05/2022	651	18/05/2023	103	378	380	0.27	2.94	0.32	Survived (hook in)
30*	M	Mature	50.00	80.00	04/05/2022	404	18/05/2023	164	369	380	0.43	1.61	0.32	Survived
31*	M	Mature	47.00	80.00	04/05/2022	404	18/05/2023	206	372	380	0.54	3.07	0.42	Survived (hook in)
32	M	Mature	54.00	78.00	04/05/2022	651	18/05/2023	79	331	380	0.21	2.91	0.53	Survived (hook in)
33	M	Mature	53.00	78.00	04/05/2022	651	18/05/2023	86	313	380	0.23	3.31	0.65	Survived (hook in)
34	M	Mature	48.00	80.00	04/05/2022	651	18/05/2023	128	148	380	0.34	2.33	0.33	Dispersed
35	M	Mature	46.00	77.00	04/05/2022	651	18/05/2023	8	16	380	0.02	1.69	0.32	Dispersed
Total	35	24 mat, 11 imm.	49.26	72.79		933		298	477	785	0.38	2.18	0.33	
Males	29	21 mat, 8 imm.	49.41	73.57		913		353	530	762	0.46	2.30	0.35	
Females	6	3 mat, 3 imm.	48.00	69.01		984		50	238	891	0.05	1.85	0.31	

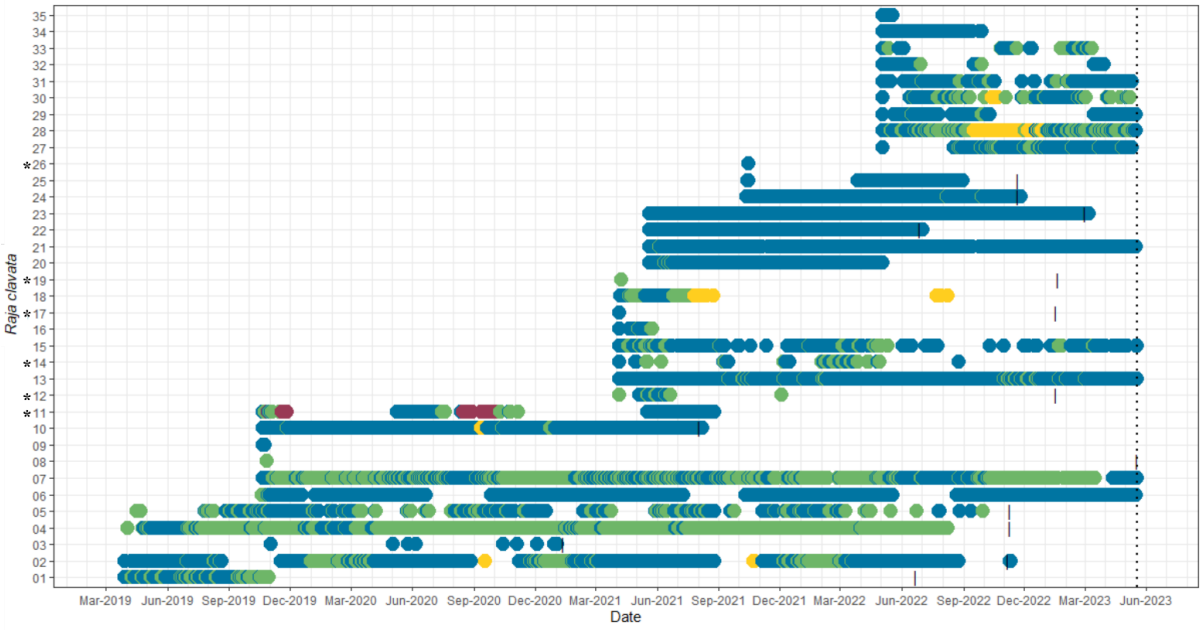

Figure 5.2. Abacus plot of thornback ray detections, colour-coded by area: total protection area (blue), complementary protection area (green), buffer area (yellow) and Sado estuary (red). Vertical solid dashes indicate expected battery expiration dates, and the dotted vertical line marks the end of the study period. Asterisks by individual names indicate females.

The best GAMM model for describing the presence of thornback rays in the LSMP included the effects of day of the year and individual factors (AIC 14769.61). The probability of presence of thornback rays varied throughout the year, as there was a significant effect of day of the year (GAMM: edf=7.26, Chi.sq= 30794), and as well as of individual variability (GAMM: edf=21.89, Chi.sq=4470), both with p <2e-16. The deviance explained by the model was 38%. Probability of presence varied between approximately 0.29-0.71. Its highest value was observed during late winter and throughout spring, after which it decreased during summer to its lowest at the beginning of autumn. Then it started increasing again throughout autumn and winter, with a period of stability at around 0.5 from late autumn to early winter (Figure 5.3).

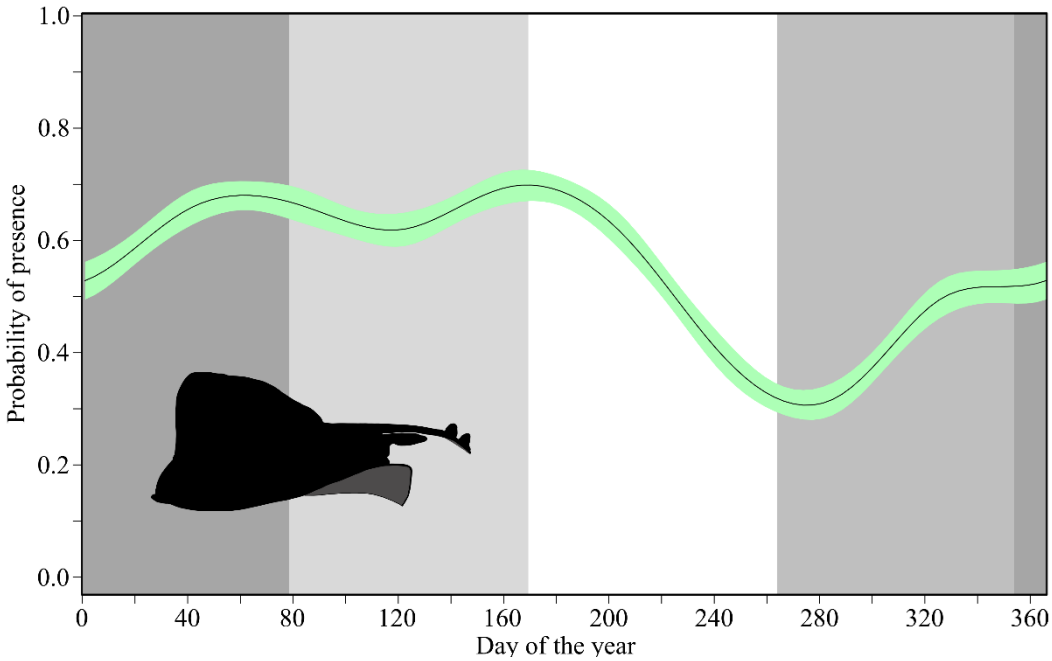

Figure 5.3: Predicted probability of presence of thornback rays in the LSMP throughout the year. Included were individuals with around a year or more of data (n=23). The area in green represents the 95% confidence interval. Grey shading represents seasons of the year (from left to right: winter, spring, summer, autumn, winter).

5.3.3 Occurrence area

Total and weekly occurrence areas were calculated for 28 of the 33 available individuals (supplementary material 5.2). Five individuals were excluded due to insufficient detections (Rc 03, 08, 17, 19 and 26, and Rc 03 for the calculation of occurrence area per diel phase). The total occurrence areas averaged 0.33 km^2 (range 0.00-0.72 km^2) at the 50% level and 2.18 km^2 (range 0.00-4.29 km^2) at the 95% level. The contours of all areas were located inside the partial and full protection areas, except for an isolated segment of the 95% contour of Rc 18, which fell in the buffer area. Rc 28 was also frequently detected in the buffer area, but none of its occurrence areas included this protection level (Figure 5.2). Per diel phase, the respective average 50% and 95% total occurrence areas were 0.30 and 1.82 km^2 for daytime, 0.43 and 2.00 km^2 for night-time and 0.28 and 1.68 km^2 for twilight.

Total occurrence area did not significantly correlate with disc width at the 50% ($r(27) = 0.22$, $p = 0.26$) or 95% levels ($r(27)= 0.24$, $p = 0.23$). To evaluate sex-based differences, a two-tailed Welch's t-test of uneven variances was used because of the uneven sex ratio (n = 26 vs. 3). No statistically significant differences were obtained for either 50% (Welch's t-test; $t = 0.26$, $p = 0.81$) or 95% area estimations (Welch's t-test; $t = 0.61$, $p = 0.60$).

The weekly occurrence area GAMM that best fit the data did not include size and included individual as random effect (AIC = -1895.06 for 50% and AIC = 3810.53 for the 95% level, supplementary material 5.1). In this model, week of the year significantly influenced the occurrence areas (50%: GAMM: edf = 3.49, F = 3.574, p = 1.41e-05 and 95%: GAMM: edf = 4.544, F = 3.891, p = 6.76e-07). Individual effect was also significant for both contour levels with p <2e-16 (GAMM results for 50%: edf = 22.20, F = 12.392; for 95%: edf = 20.172, F = 7.172). The deviance explained was 20.5% for the 50% weekly occurrence area and 14.8% for the 50% areas. Weekly occurrence area decreased from the beginning of the year to its lowest in spring, between mid-April and May. After this point, areas increased and reached their highest point in late summer and early autumn, to then start decreasing again towards the end of the year (Figure 5.4).

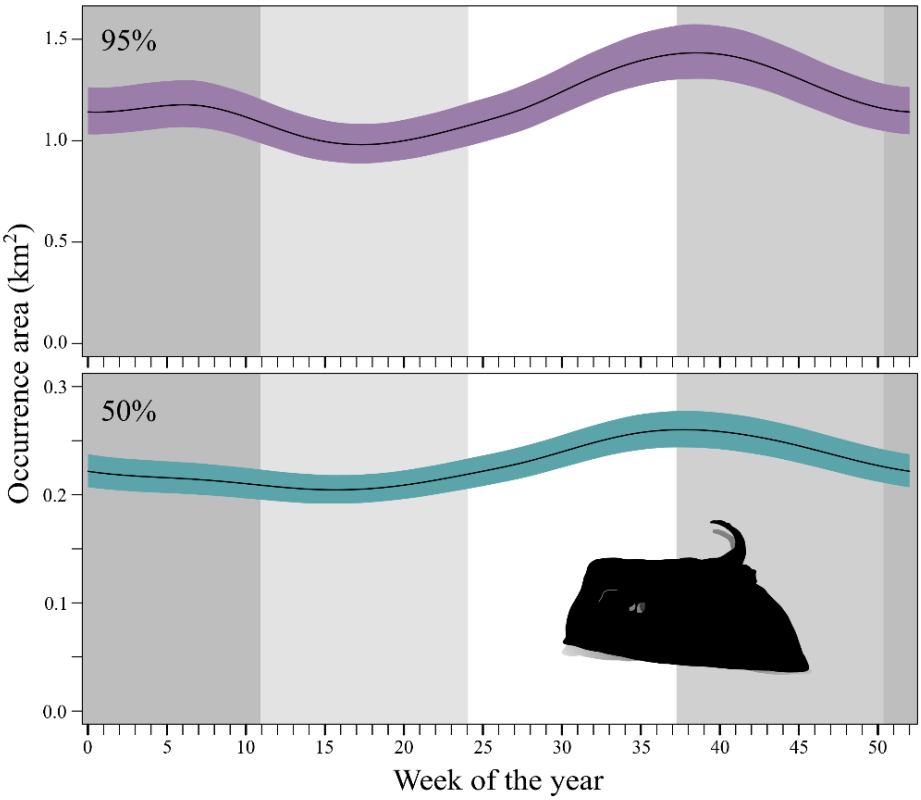

Figure 5.4: Occurrence area of thornback rays in the LSMP throughout the year. Predicted probability of the change in weekly occurrence area at the 50% (green) and 95% level (purple). Coloured area indicates the confidence intervals, and the shaded background indicates the seasons of the year (in order from left to right: winter, spring, summer, autumn, winter).

5.3.4 Depth

Six of the seven V9P tags yielded between 158-401 days of depth data. Depths ranged between 0.5-74.9 m, close to the tag's sensor limit of ~76 m. Of all depth readings, only 129 were shallower than 5 m; these were obtained from five of the six individuals: Ra 24 (8.5% of readings), Ra 25 (1.6%), Ra 27 (3.2%), Ra 28 (28.8%) and 6 of Ra 31 (60.8%). All individuals but Rc 25 were detected deeper than 60 m (max. depth of Rc 25 = 38 m).

Per diel phase, all individuals were deeper during daytime than twilight and the night. All individuals except Rc 25 were found at their shallowest at night (Table 5.2). The linear mixed-effects model indicated a significant effect of diel phase on depth. With daytime as reference level (estimate =19.26), the coefficients for twilight and night were respectively -1.00 and -0.94, predicting that they occur shallower in these diel phases. Post-hoc tests showed statistically significant differences between daylight and both twilight (difference = 1.00, p <.0001) and night (difference = 0.94, p <.0001), and not between night and twilight (difference = -0.6, p = 0.21).

Table 5.2: Minimum, maximum, and median depth of individual thornback rays per diel phase and overall.

Raja	Daytime			Twilight			Night			Total		
clavata	Min	Max	Median	Min	Max	Median	Min	Max	Median	Min	Max	Median
24	8.6	73.8	15.1	3.7	69.7	14.8	2.3	73.9	13.8	2.3	73.9	14.6
25	11.2	37.7	16.8	7.0	29.8	16.4	4.7	29.2	16.4	4.7	37.7	16.6
27	7.2	74.9	20.3	4.7	74.8	17.4	4.3	73.2	15.2	4.3	74.9	17.1
28	9.5	45.4	24.3	2.3	52.6	17.9	0.5	61.7	15.7	0.5	61.7	20.0
30	6.3	56.3	19.4	7.7	56.7	17.7	5.3	69.2	16.9	5.3	69.2	18.1
31	4.6	74.4	15.1	4.5	34.2	13.7	1.1	53.9	13.3	1.1	74.4	14.0

The best scoring GAMM included day of the year and individual as random effect (AIC = -12279.71, supplementary material 5.1). Day of the year had a significant effect on depth (GAMM edf: 6.295, F = 52.48, p <2e-16) and so did individual effect (GAMM edf: 4.891, F = 46.10, p <2e-16). Deviance explained was 38%. The GAMM predicted an increase in depth from day of the year 1 until around day 250 (early September), the deepest point in the year. Depth did not decrease uniformly: it declined steadily until day 120 (end of April-beginning of May) and then slightly increased until around day 180 (end of June), to then abruptly decrease until about day 250. Depth then increased rapidly until the end of the year. The shallowest depths were attained from late December to early February (Figure 5.5).

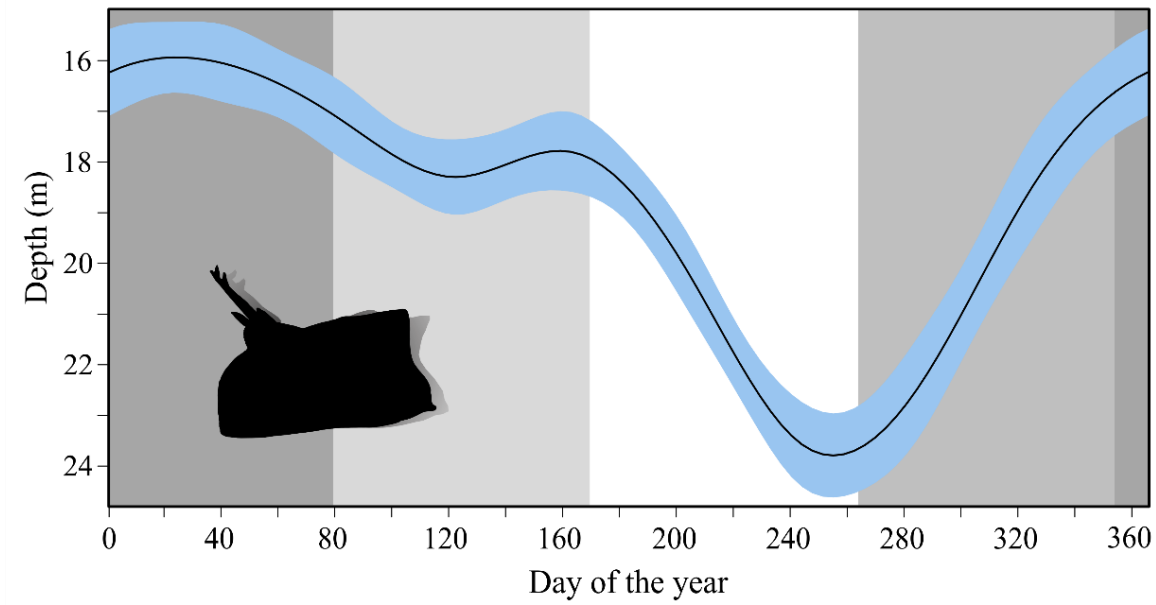

Figure 5.5: Depth variation of thornback rays in the LSMP throughout the year. Result of the General Additive Model assessing how depth varies throughout the year. Confidence interval shown in blue. Grey shading represents seasons of the year (from left to right: winter, spring, summer, autumn, winter).

5.3.5 Activity

Two individuals were removed for having an insufficient number of steps (Rc 03, 5 steps, and Rc 09, 28 steps). Overall, Rc32 presented the highest step length average (120.9 m), and Rc06 the lowest (28.9 m) (Figure 5.6). Per diel phase, the depth of all individuals combined was on average highest during twilight (79.3 m) followed closely by night (78.0 m) and lastly by daytime (62.0 m). Conversely, most individuals recorded their highest average during the night (n=15), followed by twilight (n=8), and day (n=3), while most recorded their lowest averages during the day (n=22), followed by night (n=3) and twilight (n=2).

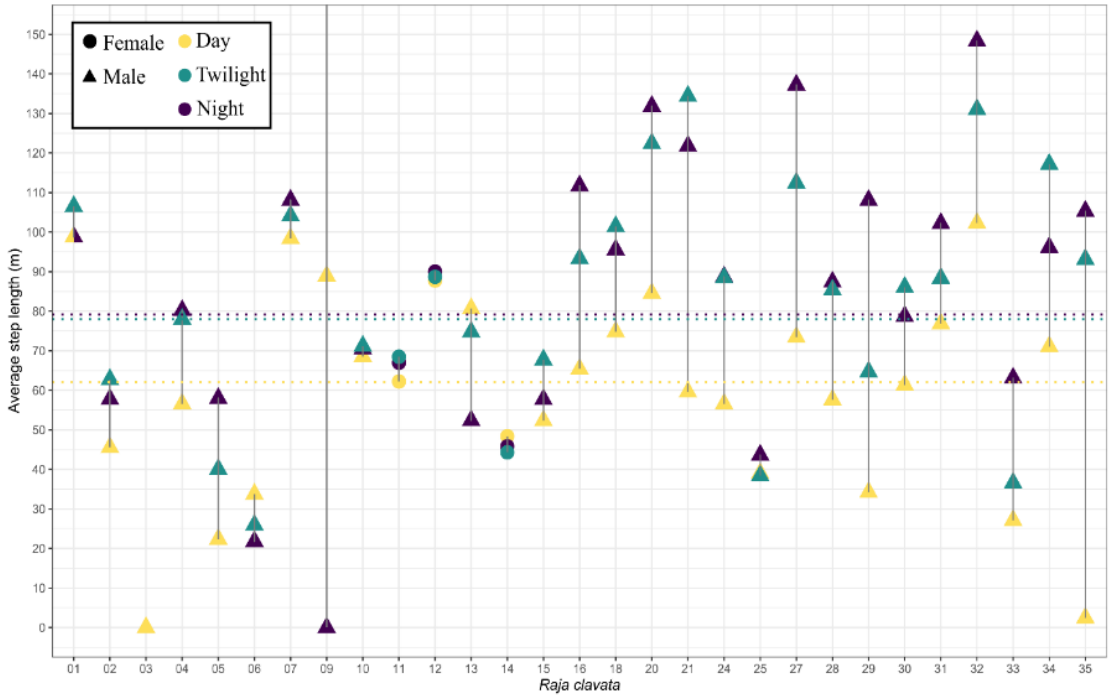

Figure 5.6: Average step length per thornback ray per diel phase. Averages represent the distance covered per 30 min per diel phase per individual. Dotted lines indicate the average distance per diel phase: day (62.0 m), night (78.0 m), and twilight (79.3 m). The average step length value for twilight of Rc 09 is not shown (431.7 m) to display the other values and their differences more appropriately.

5.4. Discussion

Understanding the effects of overexploitation on fish populations is a necessary step to address its ecological, economic, and social consequences (FAO, 2020). Thirty-five thornback rays were tracked to improve the understanding of their movement patterns and obtained results on their long-term residency, diel changes in occurrence area and activity, and (although limited) depth use. To our knowledge, this is the first long-term study to track this species in southern Europe, as most are from the English Channel. This provides movement data for a region with different environmental conditions, hydrology, and fishing pressure, which is valuable to inform local management decisions in the LSMP and other similar coastal MPAs.

5.4.1 Space use

5.4.1.1 Seasonal space use

In general, the thornback rays were mostly detected in the full and partial protection areas. Few individuals (n=6, 18% of tagged individuals) were detected in either the buffer areas or the Sado estuary, which could be partially attributed to the lower receiver coverage. The detections obtained from the five individuals in the buffer area indicate that there might be recurrence in these movements, as two individuals were detected in the buffer area at similar times of the year (i.e., after the 200th day of the year) in two consecutive years. The detection of three additional individuals in the buffer area occurred at a similar time of the year. The female that was detected in Sado also presented a similar pattern over two consecutive years. However, to more robustly assess this, receiver coverage would need to be increased in the buffer areas and Sado.

Although the results of the resident individuals indicate that the presence of thornback rays in the LSMP is related to the seasons of the year, they were still in the LSMP throughout the year and presence never decreased to 0, for example as noted for *Dasyatis pastinaca* (Chapter 3, Kraft et al., 2023b). This, and the general variability observed in detection patterns (i.e., transient and resident individuals), is a characteristic of populations that present partial migration, which has been reported in elasmobranchs as well but has been seldomly investigated (Chapman et al., 2012, 2015).

This seasonal pattern resembles findings from other areas of the North Atlantic, although the function is unclear. For example, thornback rays in the Bay of Douarnenez (France) move into shallower waters in early spring to mate (Rousset, 1990). A similar increase in presence in shallow waters was seen between March and August in the Thames estuary (United Kingdom), to then return to deeper waters during autumn and winter (Hunter et al., 2006), although in the western English Channel they appear to remain inshore year-round (Humphries et al., 2016). A seasonal presence was also described off the northwest Iberian Peninsula in Spain, with a high point in summer (Papadopoulo et al., 2023).

5.4.1.2 Diel space use

Before discussing results, an important difference between the present study and other studies that have investigated depth distribution in this species, e.g., (Humphries et al., 2016; Hunter et al., 2006), needs to be highlighted. In the present study, the estimation of depth was limited to the detection range of the array and the tag's depth (pressure) sensor limit of ~76 m. Other studies have used data storage tags (DSTs) (Humphries et al., 2016; Hunter et al., 2006), which are not constrained to an acoustic array and provide a more fitting alternative to study the depth preferences of these species. Consequently, our approach restricted our survey to the shallow end of the depth distribution of *R. clavata*, which can reach up to 1,000 m in many areas (Last et al., 2016). Therefore, although thornback rays can restrict their occurrence to shallow waters (e.g., Humphries et al., 2016), the underestimation of depth preferences cannot be ruled out in this study, limiting our interpretations to their movements within the array.

The diel changes in activity and depth displayed by the thornback rays are shared with several elasmobranchs (Hammerschlag et al., 2016). Diel vertical migrations or nocturnal ascent has been described for thornback rays and other skates in the genus *Raja* (Humphries et al., 2017; Poos et al., 2023; Speed et al., 2010; Wearmouth and Sims, 2009). This can function as a strategy to forage, as well as a predator avoidance strategy seen in central place foragers like many batoids, with which shallow productive feeding grounds are traded for deeper and safer areas (Humphries et al., 2017).

However, the diel changes in activity and in occurrence area in our study did not completely correlate; despite the increase in activity during all dark periods, occurrence area was greater in daytime than twilight. Although many elasmobranchs become more mobile during the night and twilight, reflected as increased activity and area of use (Hammerschlag et al., 2016; Humphries et al., 2017), the consistency of this as a general pattern in elasmobranchs is still to be demonstrated (Hammerschlag et al., 2016). A possible explanation for this result could be the coverage of the acoustic array. If it is not accurately covering the occurrence area of these individuals , the estimation of how changes across diel phases could be affected (i.e., the array is capable of assessing changes in activity, but not area use).

5.4.1.3 Sexual segregation

Combining the 195 males and 123 females captured in this and in a previous study in this area (Martínez-Ramírez et al., 2021) results in a male-biased sex ratio of 1.6:1. Although the combined estimate is more balanced than our study (29:6 or 4.8:1), it still deviates from an expected 1:1 ratio (binominal test, $p = 0.006$). The sampling in these studies was conducted in different seasons (mainly spring and autumn), which lowers the likelihood of a seasonal bias. Additionally, our results showed that females were not only less abundant but also spent over nine times less time within the protected area than males ($I_R = 0.05$ vs. 0.46).

These factors suggest there may be sexual segregation of individuals, with the frequency of females increasing with depth. Depth-related sexual segregation has been recorded for thornback rays before. For example, between Ericeira (West coast of Portugal, app. 100 km north of the LSMP) and Nazaré (app. 39° 36' N, 9° 04' W), females were more abundant closer to shore and males became more dominant deeper than 100 m (Serra-Pereira et al., 2014). Females also had an overall higher presence in the Azores (1:1.61) (Santos et al., 2021). In other areas, females have reported to be more abundant in the northwest Iberian Peninsula (Papadopoulo et al., 2023), in the Thames, England (Hunter et al., 2005), the Western English Channel (Simpson et al., 2021), and other areas of Ireland and the British Isles as well (Day, 1880). In other areas like the Bay of Douarnenez, France (Rousset, 1990) and the Gulf of Gabès, central Mediterranean (Kadri et al., 2014), males were more common and females increased in abundance in deeper waters.

This kind of population distribution in skates can arise from several factors, for example from physiological differences between sexes that result in distinct diet and habitat requirements, or from females seeking to avoid male harassment (Simpson et al., 2021). In connection with the previous comments on the depth limitations in this study, this could be further investigated by tagging females with data logging tags like pop-up satellite archival tags (PSATs) or DSTs to evaluate their depth preferences.

5.4.2 Conservation and management

A better understanding of the movement patterns of a species can directly benefit spatial protection efforts like MPAs by using this data to inform management and conservation decisions (Knip et al., 2012). Information on the spatial ecology of a species is important for this process, as it provides an idea of how the spatial characteristics of an MPA (e.g., size and

position) influence protection and mitigate risk exposure (Abecasis et al., 2014b; Papadopoulo et al., 2023; Villegas-Ríos et al., 2021).

The LSMP's reserve effect on soft bottom fish species was assessed by two studies using fishing surveys (Martínez-Ramírez et al., 2021; Sousa et al., 2018). While both found a statistically significant increase in thornback ray biomass over time, only one detected a significant increase in abundance, size, and a positive reserve effect (Sousa et al., 2018). Although reserve effect might be a long process for species of slow life history traits and large sizes like most elasmobranchs (Martínez-Ramírez et al., 2021; Sousa et al., 2018), spatial closures have been regarded as an effective management strategy for thornback rays, especially during their reproductive season (Hunter et al., 2006; Wiegand et al., 2011). Other protection measures have also been instituted. A seasonal closure is established during May and June, contributing to the protection of this species by prohibiting the capture of skates in mainland Portugal (Portaria no 315/2011 and Portaria no 47/2016). A minimum landing size of 52 cm in total length was also introduced (Serra-Pereira et al., 2018).

Considering the higher number of thornback ray males and their higher residency, males may be better protected than females in the LSMP. This is important to consider for the management of the marine park, as differences in protection from sexual segregation can result in uneven protection (Mucientes et al., 2009). The protection of large females is prioritized in the management of many elasmobranch fisheries because of their reproductive potential and the dependence populations have on them to recover (Dell'Apa et al., 2014; Wearmouth and Sims, 2008). It is important to acknowledge these intra-specific differences to obtain a more realistic estimation of the protection MPAs provide.

The LSMP's full protection area and the two adjacent partial protection areas provide a combined 11.09 km^2 of continuous protection to thornback rays and other elasmobranchs, as these species are not affected by the fishing activities allowed in these protection levels. This combined surface is almost 3 times the largest total 95% occurrence area estimate, and almost 6 times the total average. However, the LSMP can be as narrow as 450 m in this protected segment, which increases their chances of reaching or crossing the border. Because risk increases with greater proximity to the border when inside the protected area, the position of the occurrence areas of thornback rays in relation to the MPA's border is relevant as well (Villegas-Ríos et al., 2021).

In this sense, offshore movements could pose as a greater risk source compared to movements along the coast, exposing them to factors like edge effect (Ohayon et al., 2021) and fishing the line (Kellner et al., 2007). Similarly, the observed diel changes in movement, of

greater activity during night and twilight, could also indicate an increase in the chances of nearing or crossing an MPA's border and of encountering passive fishing gear, that are usually set for 24 h (Hammerschlag et al., 2016; Uusiheikkila et al., 2008).

Risk exposure can also change inside the marine park if it has different protection levels (Abecasis et al., 2014b). Ventures of thornback rays into the buffer area also expose them to fishing, as fishing activities are permitted in this protection level. The restricted time period in which individuals were detected there may suggest that this source of risk is seasonal, although this remains to be better assessed. The effectiveness of measures like temporal gear restrictions, despite increasing MPA's efficacy (Simpson et al., 2020), also remain to be evaluated. This is required to properly estimate the number of individuals that move into this area and gauge the effect such restrictions could have on other goals of the LSMP, which could be addressed in future studies.

Throughout the year, thornback rays seemed to be best protected during late winter and spring, as the simultaneous higher presence, smaller occurrence areas, and shallow depth suggest a restriction of their movements to around the coastal area of the LSMP. After spring, and especially after mid-summer, occurrence areas expanded and the presence of thornback rays decreased in the MPA, suggesting they gradually start making use of larger areas as summer progresses, which likely drives them out of the protected area. An example of this is the detection of a mature female in the Sado estuary in two consecutive years. To investigate the longer-distance movements, use of nearby areas, and true depth preferences of this species (i.e., not constrained to the detection range of the array and the acoustic tag's depth limit), additional tagging technologies such as PSATs and DSTs could be employed. This could contribute to the evaluation of the impact and placement of additional or expanded MPAs to support the protection of this species.

Contributions

DA and SK conceptualized and designed the study. SK, ACW and DA captured and tagged the individuals of this study and acquired the data. SK, ACW and DA maintained the receiver network. SK conducted the analyses, prepared the figures for publication, and drafted the article. SK, ACW and DA interpreted the data. SK, ACW and DA revised it critically for important intellectual content. All authors approved the final article.

Funding

This study received Portuguese national funds from the Foundation for Science and Technology (FCT) through projects UIDB/04326/2020 (DOI:10.54499/UIDB/04326/2020), UIDP/04326/2020 (DOI:10.54499/UIDP/04326/2020) and LA/P/0101/2020 (DOI:10.54499/LA/P/0101/2020) and from the INFORBIOMARES project (POSEUR-03-2215-FC-000047). SK acknowledges support by "la Caixa" Foundation (ID 100010434), grant LCF/BQ/DI20/11780001, and DA acknowledges support by the FCT transitional norm DL57/2016/CP1361/CT0036.

Acknowledgements

We thank Juliano Macedo (operation of vessel for samplings using trammel nets), Joffrey Baeyaert (tagging, deploying, and maintaining receivers), Lucas Martínez-Ramírez and C. Robert Priester (tagging and receiver maintenance), and "Flipper Divers" dive centre (receiver maintenance), and Miguel Gandra. Data was sourced from the European Tracking Network data portal (http://www.lifewatch.be/etn/), developed by the Flanders Marine Institute as part of the Flemish contribution to LifeWatch.

Declaration of competing interest

The authors declare no conflicts of interest.

Declaration of Generative AI and AI-assisted technologies in the writing process

No Generative AI and AI-assisted technologies were used to write this manuscript.

5.5 References

Abecasis, D., Afonso, P., Erzini, K., 2014a. Can small MPAs protect local populations of a coastal flatfish, *Solea senegalensis*? Fisheries Management and Ecology 21, 175–185. https://doi.org/10.1111/fme.12061

Abecasis, D., Afonso, P., Erzini, K., 2014b. Combining multispecies home range and distribution models aids assessment of MPA effectiveness. Marine Ecology Progress Series 513, 155–169. https://doi.org/10.3354/meps10987

Abecasis, D., Bentes, L., Lino, P.G., Santos, M.N., Erzini, K., 2013. Residency, movements and habitat use of adult white seabream (*Diplodus sargus*) between natural and artificial reefs. Estuarine, Coastal and Shelf Science 118, 80–85. https://doi.org/10.1016/j.ecss.2012.12.014

Alves, L.M.F., Correia, J.P.S., Lemos, M.F.L., Novais, S.C., Cabral, H., 2020. Assessment of trends in the Portuguese elasmobranch commercial landings over three decades (1986–2017). Fisheries Research 230, 105648. https://doi.org/10.1016/j.fishres.2020.105648

Ban, N.C., Gurney, G.G., Marshall, N.A., Whitney, C.K., Mills, M., Gelcich, S., Bennett, N.J., Meehan, M.C., Butler, C., Ban, S., Tran, T.C., Cox, M.E., Breslow, S.J., 2019. Well-being outcomes of marine protected areas. Nature Sustainability 2, 524–532. https://doi.org/10.1038/s41893-019-0306-2

Cabral, S., 2014. *Raja* spp. spatial dynamics in the Arrábida Marine Park (M. Sc. Thesis). Universidade do Algarve.

Calenge, C., 2006. The package "adehabitat" for the R software: A tool for the analysis of space and habitat use by animals. Ecological Modelling 197, 516–519. https://doi.org/10.1016/j.ecolmodel.2006.03.017

Carbonara, P., Bellodi, A., Palmisano, M., Mulas, A., Porcu, C., Zupa, W., Donnaloia, M., Carlucci, R., Sion, L., Follesa, M.C., 2020. Growth and Age Validation of the Thornback Ray (*Raja clavata* Linnaeus, 1758) in the South Adriatic Sea (Central Mediterranean). Frontiers in Marine Science 7, 586094. https://doi.org/10.3389/fmars.2020.586094

Chapman, B.B., Skov, C., Hulthén, K., Brodersen, J., Nilsson, P.A., Hansson, L. -A., Brönmark, C., 2012. Partial migration in fishes: definitions, methodologies and taxonomic distribution. Journal of Fish Biology 81, 479–499. https://doi.org/10.1111/j.1095-8649.2012.03349.x

Chapman, D.D., Feldheim, K.A., Papastamatiou, Y.P., Hueter, R.E., 2015. There and Back Again: A Review of Residency and Return Migrations in Sharks, with Implications for Population Structure and Management. Annual Review of Marine Science 7, 547–570. https://doi.org/10.1146/annurev-marine-010814-015730

Davidson, L.N.K., Krawchuk, M.A., Dulvy, N.K., 2016. Why have global shark and ray landings declined: improved management or overfishing? Fish and Fisheries 17, 438–458. https://doi.org/10.1111/faf.12119

Day, Francis, 1880. The fishes of Great Britain and Ireland. London, Williams and Norgate, 1880-1884.

Dell'Apa, A., Cudney-Burch, J., Kimmel, D.G., Rulifson, R.A., 2014. Sexual Segregation of Spiny Dogfish in Fishery-Dependent Surveys in Cape Cod, Massachusetts: Potential Management Benefits. Transactions of the American Fisheries Society 143, 833–844. https://doi.org/10.1080/00028487.2013.869257

Dudley, N. (Ed.), 2008. Guidelines for Applying Protected Area Management Categories. IUCN, Gland, Switzerland.

Dulvy, N.K., Metcalfe, J.D., Glanville, J., Pawson, M.G., Reynolds, J., 2000. Fishery stability, local extinctions, and shifts in community structure in skates. Conservation Biology 14, 283–293. https://doi.org/10.1046/j.1523-1739.2000.98540.x

Dulvy, N.K., Pacoureau, N., Rigby, C.L., Pollom, R.A., Jabado, R.W., Ebert, D.A., Finucci, B., Pollock, C.M., Cheok, J., Derrick, D.H., Herman, K.B., Sherman, C.S., VanderWright, W.J., Lawson, J.M., Walls, R.H.L., Carlson, J.K., Charvet, P., Bineesh, K.K., Fernando, D., Ralph, G.M., Matsushiba, J.H., Hilton-Taylor, C., Fordham, S.V., Simpfendorfer, C.A., 2021. Overfishing drives over one-third of all sharks and rays toward a global extinction crisis. Current Biology 31, 4773-4787.e8. https://doi.org/10.1016/j.cub.2021.08.062

Dwyer, R.G., Krueck, N.C., Udyawer, V., Heupel, M.R., Chapman, D., Pratt, H.L., Garla, R., Simpfendorfer, C.A., 2020. Individual and Population Benefits of Marine Reserves for Reef Sharks. Current Biology 30, 480-489.e5. https://doi.org/10.1016/j.cub.2019.12.005

EC, 2009. Council Regulation (EC) No 43/2009 of 16 January 2009 fixing for 2009 the fishing opportunities and associated conditions for certain fish stocks and groups of fish stocks, applicable in Community waters and, for Community vessels, in waters where catch limitations are required.

Elston, C., Cowley, P.D., Murray, T.S., Parkinson, M.C., 2023. Novel insights into coastal site affinity and habitat connectivity of a benthic stingray with implications for management. Biodiversity and Conservation https://doi.org/10.1007/s10531-022-02494-7

Espinoza, M., Lédée, E.J.I., Simpfendorfer, C.A., Tobin, A.J., Heupel, M.R., 2015. Contrasting movements and connectivity of reef-associated sharks using acoustic telemetry: implications for management. Ecological Applications 25, 2101–2118. https://doi.org/10.1890/14-2293.1

FAO, 2020. The State of World Fisheries and Aquaculture 2020: sustainability in action, The State of World Fisheries and Aquaculture (SOFIA). FAO, Rome, Italy.

Figueiredo, I., Maia, C., Lagarto, N., Serra-Pereira, B., 2020. Bycatch estimation of Rajiformes in multispecies and multigear fisheries. Fisheries Research 232, 105727. https://doi.org/10.1016/j.fishres.2020.105727

Fleming, C.H., Fagan, W.F., Mueller, T., Olson, K.A., Leimgruber, P., Calabrese, J.M., 2015. Rigorous home range estimation with movement data: a new autocorrelated kernel density estimator. Ecology 96, 1182–1188. https://doi.org/10.1890/14-2010.1

Gell, F.R., Roberts, C.M., 2003. Benefits beyond boundaries: the fishery effects of marine reserves. Trends in Ecology & Evolution 18, 448–455. https://doi.org/10.1016/S0169-5347(03)00189-7

Hammerschlag, N., Skubel, R.A., Calich, H., Nelson, E.R., Shiffman, D.S., Wester, J., Macdonald, C.C., Cain, S., Jennings, L., Enchelmaier, A., Gallagher, A.J., 2016. Nocturnal and crepuscular behavior in elasmobranchs: a review of movement, habitat use, foraging, and reproduction in the dark. Bulletin of Marine Science 93, 355–374. https://doi.org/10.5343/bms.2016.1046

Heupel, M.R., Semmens, J.M., Hobday, A.J., 2006. Automated acoustic tracking of aquatic animals: scales, design and deployment of listening station arrays. Marine and Freshwater Research 57, 1. https://doi.org/10.1071/MF05091

Hoenig, J.M., Gruber, S.H., 1990. Life history patterns in the elasmobranchs: implications for fisheries management, in: Elasmobranchs as Living Resources: Advances in the Biology, Ecology, Systematics, and the Status of the Fisheries., NOAA Technical Report NMFS 90. U.S. Department of Commerce, Washington, D.C., pp. 1–16.

Humphries, N., Simpson, S., Sims, D., 2017. Diel vertical migration and central place foraging in benthic predators. Marine Ecology Progress Series 582, 163–180. https://doi.org/10.3354/meps12324

Humphries, N., Simpson, S., Wearmouth, V., Sims, D., 2016. Two's company, three's a crowd: fine-scale habitat partitioning by depth among sympatric species of marine mesopredator. Marine Ecology Progress Series 561, 173–187. https://doi.org/10.3354/meps11937

Hunter, E., Berry, F., Buckley, A.A., Stewart, C., Metcalfe, J.D., 2006. Seasonal migration of thornback rays and implications for closure management: Ray migration and closure management. Journal of Applied Ecology 43, 710–720. https://doi.org/10.1111/j.1365-2664.2006.01194.x

Hunter, E., Buckley, A.A., Stewart, C., Metcalfe, J.D., 2005. Migratory behaviour of the thornback ray, *Raja clavata*, in the southern North Sea. Journal of the Marine Biological Association of the United Kingdom 85, 1095–1105. https://doi.org/10.1017/S0025315405012142

Hussey, N.E., Kessel, S.T., Aarestrup, K., Cooke, S.J., Cowley, P.D., Fisk, A.T., Harcourt, R.G., Holland, K.N., Iverson, S.J., Kocik, J.F., Mills Flemming, J.E., Whoriskey, F.G., 2015. Aquatic animal telemetry: A panoramic window into the underwater world. Science 348, 1255642–1255642. https://doi.org/10.1126/science.1255642

ICES, 2024. Thornback ray (*Raja clavata*) in Subarea 4 and in divisions 3.a and 7.d (North Sea, Skagerrak, Kattegat, and eastern English Channel). https://doi.org/10.17895/ICES.ADVICE.21856875

ICES, 2022. Thornback ray (*Raja clavata*) in Division 9.a (Atlantic Iberian waters). https://doi.org/10.17895/ICES.ADVICE.19754434.V1

IUCN, 2024. *Raja clavata*: Finucci, B., McCully-Phillips, S.R., Ellis, J.R., Giovos, I., Serena, F., Soldo, A., Pacoureau, N. & Charles, R. 2024. The IUCN Red List of Threatened Species 2024: e.T39399A183779744. International Union for Conservation of Nature. https://doi.org/10.2305/IUCN.UK.2016-3.RLTS.T39399A103110667.en

Kadri, H., Marouani, S., Saïdi, B., Bradai, M.N., Bouaïn, A., Morize, E., 2014. Age, growth, sexual maturity and reproduction of the thornback ray, *Raja clavata* (L.), of the Gulf of Gabès (south-central Mediterranean Sea). Marine Biology Research 10, 416–425. https://doi.org/10.1080/17451000.2013.797584

Kellner, J.B., Tetreault, I., Gaines, S.D., Nisbet, R.M., 2007. Fishing the line near marine reserves in single and multispecies fisheries. Ecological Applications 17, 1039–1054. https://doi.org/10.1890/05-1845

Knip, D.M., Heupel, M.R., Simpfendorfer, C.A., 2012. Evaluating marine protected areas for the conservation of tropical coastal sharks. Biological Conservation 148, 200–209. https://doi.org/10.1016/j.biocon.2012.01.008

Kraft, S., Gandra, M., Lennox, R.J., Mourier, J., Winkler, A.C., Abecasis, D., 2023a. Residency and space use estimation methods based on passive acoustic telemetry data. Movement Ecology 11, 12. https://doi.org/10.1186/s40462-022-00364-z

Kraft, S., Winkler, A.C., Abecasis, D., 2023b. Small coastal marine protected areas offer recurring, seasonal protection to the common stingray (*Dasyatis pastinaca*). Ocean & Coastal Management 246, 106891. https://doi.org/10.1016/j.ocecoaman.2023.106891

Kramer, D.L., Chapman, M.R., 1999. Implications of fish home range size and relocation for marine reserve function. Environmental Biology of Fishes 55, 65–79. https://doi.org/10.1023/A:1007481206399

Kranstauber, B., Kays, R., LaPoint, S.D., Wikelski, M., Safi, K., 2012. A dynamic Brownian bridge movement model to estimate utilization distributions for heterogeneous animal movement: The dynamic Brownian bridge movement model. Journal of Animal Ecology 81, 738–746. https://doi.org/10.1111/j.1365-2656.2012.01955.x

Kranstauber, B., Smolla, M., Scharf, A.K., 2021. move: Visualizing and analyzing animal track data. Rpackage version 4.0.6. http://cran.r-project.org/package=move.

Krstulović Šifner, S., Vrgoč, N., Dadić, V., Isajlović, I., Peharda, M., Piccinetti, C., 2009. Long-term changes in distribution and demographic composition of thornback ray, *Raja clavata*, in the northern and central Adriatic Sea. Journal of Applied Ichthyology 25, 40–46. https://doi.org/10.1111/j.1439-0426.2008.01204.x

Last, P.R., Séret, B., Stehmann, M.F.W., Weigmann, S., 2016. Skates, family Rajidae, in: Last, Peter Robert, White, W.T., de Carvalho, M.R., Séret, Bernard, Stehmann, M., Naylor, G.J.P., Marshall, L. (Eds.), Rays of the World. CSIRO Publishing, Clayton South VIC, pp. 204–363.

Lavender, E., Aleynik, D., Dodd, J., Illian, J., James, M., Wright, P.J., Smout, S., Thorburn, J., 2021. Movement patterns of a Critically Endangered elasmobranch (*Dipturus intermedius*) in a Marine Protected Area. Aquatic Conservation: Marine and Freshwater Ecosystems aqc.3753. https://doi.org/10.1002/aqc.3753

Le Port, A., Lavery, S., Montgomery, J.C., 2012. Conservation of coastal stingrays: seasonal abundance and population structure of the short-tailed stingray *Dasyatis brevicaudata* at a Marine Protected Area. ICES Journal of Marine Science 69, 1427–1435. https://doi.org/10.1093/icesjms/fss120

Lester, S., Halpern, B., Grorud-Colvert, K., Lubchenco, J., Ruttenberg, B., Gaines, S., Airamé, S., Warner, R., 2009. Biological effects within no-take marine reserves: a global synthesis. Marine Ecology Progress Series 384, 33–46. https://doi.org/10.3354/meps08029

Lino, P., 2012. Potential of fisheries restocking off the Algarve coast using aquaculture produced marine fish (Ph.D. Thesis). Universidade do Algarve, Faro, Portugal.

MacKeracher, T., Diedrich, A., Simpfendorfer, C.A., 2019. Sharks, rays and marine protected areas: A critical evaluation of current perspectives. Fish and Fisheries 20, 255–267. https://doi.org/10.1111/faf.12337

Marongiu, M.F., Porcu, C., Bellodi, A., Cannas, R., Cau, A., Cuccu, D., Mulas, A., Follesa, M.C., 2017. Temporal dynamics of demersal chondrichthyan species in the central western Mediterranean Sea: The case study in Sardinia Island. Fisheries Research 193, 81–94. https://doi.org/10.1016/j.fishres.2017.04.001

Martínez-Ramírez, L., Priester, C.R., Sousa, I., Erzini, K., Abecasis, D., 2021. Reserve effect of a small North-East Atlantic marine protected area (Arrábida, Portugal) on soft-sediment fish species. Aquatic Conservation: Marine and Freshwater Ecosystems 31, 1584–1595. https://doi.org/10.1002/aqc.3577

Martins, A., Heupel, M., Chin, A., Simpfendorfer, C., 2018. Batoid nurseries: definition, use and importance. Marine Ecology Progress Series 595, 253–267. https://doi.org/10.3354/meps12545

Martins, M., 2021. PTtidaltools - R package to retrieve and manipulate data from the Portuguese National Hydrographic Institute. https://doi.org/10.5281/ZENODO.4562490

Mazerolle, M.J., 2023. AICcmodavg: Model selection and multimodel inference based on (Q)AIC(c). R package version 2.3.2.

McCauley, D.J., Pinsky, M.L., Palumbi, S.R., Estes, J.A., Joyce, F.H., Warner, R.R., 2015. Marine defaunation: Animal loss in the global ocean. Science 347, 1255641. https://doi.org/10.1126/science.1255641

Mucientes, G.R., Queiroz, N., Sousa, L.L., Tarroso, P., Sims, D.W., 2009. Sexual segregation of pelagic sharks and the potential threat from fisheries. Biology Letters 5, 156–159. https://doi.org/10.1098/rsbl.2008.0761

Musick, J.A., 1999. Life in the Slow Lane: Ecology and Conservation of Long-Lived Marine Animals, in: Musick, J.A. (Ed.), Ecology and Conservation of Long-Lived Marine Animals. American Fisheries Society. https://doi.org/10.47886/9781888569155

Ohayon, S., Granot, I., Belmaker, J., 2021. A meta-analysis reveals edge effects within marine protected areas. Nature Ecology & Evolution 5, 1301–1308. https://doi.org/10.1038/s41559-021-01502-3

Papadopoulo, K., Villegas-Ríos, D., Mucientes, G., Hillinger, A., Alonso-Fernández, A., 2023. Drivers of the spatial behaviour of the threatened thornback skate (*Raja clavata*). Aquatic Living Resources 36, 21. https://doi.org/10.1051/alr/2023017

Piet, G.J., Van Hal, R., Greenstreet, S.P.R., 2009. Modelling the direct impact of bottom trawling on the North Sea fish community to derive estimates of fishing mortality for non-target fish species. ICES Journal of Marine Science 66, 1985–1998. https://doi.org/10.1093/icesjms/fsp162

Pinheiro, J., Bates, D., 2023. nlme: Linear and Nonlinear Mixed Effects Models. R package version 3.1-164. https://CRAN.R-project.org/package=nlme

Poos, J.J., Staeudle, T., Greenway, E., Batsleer, J., 2023. Spatial distribution, migration, and population structure of North Sea rays. Wageningen University & Research, Wageningen. https://doi.org/10.18174/632935

Ramírez-Amaro, S., Ordines, F., Esteban, A., García, C., Guijarro, B., Salmerón, F., Terrasa, B., Massutí, E., 2020. The diversity of recent trends for chondrichthyans in the Mediterranean reflects fishing exploitation and a potential evolutionary pressure towards early maturation. Scientific Reports 10, 547. https://doi.org/10.1038/s41598-019-56818-9

Rousset, J., 1990. Population structure of thornback rays *Raja clavata* and their movements in the Bay of Douarnenez. Journal of the Marine Biological Association of the United Kingdom 70, 261–268. https://doi.org/10.1017/S0025315400035384

Santos, R., Medeiros-Leal, W., Novoa-Pabon, A., Crespo, O., Pinho, M., 2021. Biological Knowledge of Thornback Ray (*Raja clavata*) from the Azores: Improving Scientific Information for the Effectiveness of Species-Specific Management Measures. Biology 10, 676. https://doi.org/10.3390/biology10070676

Serra-Pereira, B., Erzini, K., Maia, C., Figueiredo, I., 2014. Identification of Potential Essential Fish Habitats for Skates Based on Fishers' Knowledge. Environmental Management 53, 985–998. https://doi.org/10.1007/s00267-014-0257-3

Serra-Pereira, B., Farias, I., Moura, T., Gordo, L.S., Santos, M., Figueiredo, I., 2010. Morphometric ratios of six commercially landed species of skate from the Portuguese continental shelf, and their utility for identification. ICES Journal of Marine Science 67, 1596–1603. https://doi.org/10.1093/icesjms/fsq056

Serra-Pereira, B., Figueiredo, I., Gordo, L.S., 2011. Maturation, fecundity, and spawning strategy of the thornback ray, *Raja clavata*: do reproductive characteristics vary regionally? Marine Biology 158, 2187–2197. https://doi.org/10.1007/s00227-011-1723-6

Serra-Pereira, B., Maia, C., Lagarto, N., Figueiredo, I., 2018. A investigação realizada no IPMA de suporte ao aconselhamento científico para a gestão de espécies de raias (No. 21).

Simpfendorfer, C.A., Heupel, M.R., Hueter, R.E., 2002. Estimation of short-term centers of activity from an array of omnidirectional hydrophones and its use in studying animal movements. Canadian Journal of Fisheries and Aquatic Sciences 59, 23–32. https://doi.org/10.1139/f01-191

Simpson, S., Humphries, N., Sims, D., 2021. Habitat selection, fine-scale spatial partitioning and sexual segregation in Rajidae, determined using passive acoustic telemetry. Marine Ecology Progress Series 666, 115–134. https://doi.org/10.3354/meps13701

Simpson, S.J., Humphries, N.E., Sims, D.W., 2020. The spatial ecology of Rajidae from mark-recapture tagging and its implications for assessing fishery interactions and efficacy of Marine Protected Areas. Fisheries Research 228, 105569. https://doi.org/10.1016/j.fishres.2020.105569

Siskey, M.R., Shipley, O.N., Frisk, M.G., 2019. Skating on thin ice: Identifying the need for species-specific data and defined migration ecology of Rajidae spp. Fish and Fisheries 20, 286–302. https://doi.org/10.1111/faf.12340

Sousa, I., Baeyaert, J., Gonçalves, J.M.S., Erzini, K., 2019. Preliminary insights into the spatial ecology and movement patterns of a regionally critically endangered skate (*Rostroraja alba*) associated with a marine protected area. Marine and Freshwater Behaviour and Physiology 52, 283–299. https://doi.org/10.1080/10236244.2019.1705805

Sousa, I., Gonçalves, J.M.S., Claudet, J., Coelho, R., Gonçalves, E.J., Erzini, K., 2018. Soft-bottom fishes and spatial protection: findings from a temperate marine protected area. PeerJ 6, e4653. https://doi.org/10.7717/peerj.4653

Speed, C., Field, I., Meekan, M., Bradshaw, C., 2010. Complexities of coastal shark movements and their implications for management. Marine Ecology Progress Series 408, 275–293. https://doi.org/10.3354/meps08581

Speed, C.W., Cappo, M., Meekan, M.G., 2018. Evidence for rapid recovery of shark populations within a coral reef marine protected area. Biological Conservation 220, 308–319. https://doi.org/10.1016/j.biocon.2018.01.010

Thieurmel, B., Elmarhraoui, A., 2019. R Package “suncalc”: compute sun position, sunlight phases, moon position and lunar phase.

Uusiheikkila, S., Wolter, C., Klefoth, T., Arlinghaus, R., 2008. A behavioral perspective on fishing-induced evolution. Trends in Ecology & Evolution 23, 419–421. https://doi.org/10.1016/j.tree.2008.04.006

Villegas-Ríos, D., Claudet, J., Freitas, C., Moland, E., Thorbjørnsen, S.H., Alonso-Fernández, A., Olsen, E.M., 2021. Time at risk: Individual spatial behaviour drives effectiveness of marine protected areas and fitness. Biological Conservation 263, 109333. https://doi.org/10.1016/j.biocon.2021.109333

Villegas-Ríos, D., Freitas, C., Moland, E., Thorbjørnsen, S.H., Olsen, E.M., 2020. Inferring individual fate from aquatic acoustic telemetry data. Methods in Ecology and Evolution 11, 1186–1198. https://doi.org/10.1111/2041-210X.13446

Walker, P., Hislop, J.R.G., 1998. Sensitive skates or resilient rays? Spatial and temporal shifts in ray species composition in the central and north-western North Sea between 1930 and the present day. ICES Journal of Marine Science 55, 392–402. https://doi.org/10.1006/jmsc.1997.0325

Wearmouth, V.J., Sims, D.W., 2009. Movement and behaviour patterns of the critically endangered common skate *Dipturus batis* revealed by electronic tagging. Journal of Experimental Marine Biology and Ecology 380, 77–87. https://doi.org/10.1016/j.jembe.2009.07.035

Wearmouth, V.J., Sims, D.W., 2008. Chapter 2 Sexual Segregation in Marine Fish, Reptiles, Birds and Mammals, in: Advances in Marine Biology. Elsevier, pp. 107–170. https://doi.org/10.1016/S0065-2881(08)00002-3

Wiegand, J., Hunter, E., Dulvy, N.K., 2011. Are spatial closures better than size limits for halting the decline of the North Sea thornback ray, *Raja clavata*? Marine and Freshwater Research 62, 722. https://doi.org/10.1071/MF10141

Winter, J.D., 1996. Advances in underwater biotelemetry, in: Fisheries Techniques, 2nd Edition. American Fisheries Society, Bethesda, Maryland, pp. 555–590.

Wood, S.N., 2011. Fast stable restricted maximum likelihood and marginal likelihood estimation of semiparametric generalized linear models. Journal of the Royal Statistical Society (B) 73, 3–36. https://doi.org/10.1111/j.1467-9868.2010.00749.x

5.6 Supplementary material

Supplementary material 5.1: Table of GAMMs tested for presence/absence, occurrence area and depth of thornback rays.

Presence/absence GAMMs

Tested models:

	Day of year	Size	Individual	AIC
GAMM1	x			23308.68
GAMM2	x	x		22891.79
GAMM3	x		x	14769.61
GAMM4	x	x	x	14769.63

GAMM1

Parametric coefficients:

	Estimate	Std. Error	z value	Pr(>|z|)
(Intercept)	0.1710	0.0155	11.04	<2e-16 ***

Approximate significance of smooth terms:

	edf	Ref.df	Chi.sq	p-value
s(doy)	7.071	8	410.8	<2e-16 ***

R-sq.(adj) = 0.0243 Deviance explained = 1.8%

GAMM2

Parametric coefficients:

	Estimate	Std. Error	z value	Pr(>|z|)
(Intercept)	2.9490959	0.1399408	21.07	<2e-16 ***
size	-0.0056765	0.0002838	-20.00	<2e-16 ***

Approximate significance of smooth terms:

	edf	Ref.df	Chi.sq	p-value
s(doy)	7.106	8	435.2	<2e-16 ***

R-sq.(adj) = 0.0516 Deviance explained = 3.56%

GAMM3

Parametric coefficients:

	Estimate	Std. Error	z value	Pr(>|z|)
(Intercept)	0.1759	0.4531	0.388	0.698

Approximate significance of smooth terms:

	edf	Ref.df	Chi.sq	p-value
s(doy)	7.26	8	30794	<2e-16 ***
s(individual)	21.89	22	4470	<2e-16 ***

R-sq.(adj) = 0.442 Deviance explained = 38%

GAMM4

Parametric coefficients:

	Estimate	Std. Error	z value	Pr(>|z|)
(Intercept)	1.385026	4.144253	0.334	0.738
size	-0.002465	0.008396	-0.294	0.769

Approximate significance of smooth terms:

	edf	Ref.df	Chi.sq	p-value
s(doy)	7.26	8	27768	<2e-16 ***
s(individual)	20.91	21	3939	<2e-16 ***

R-sq.(adj) = 0.442 Deviance explained = 38%

Occurrence range GAMMs

50% occurrence range

Tested models:

	Week	Size	Individual	AIC
GAMM1	x			-1625.0
GAMM2	x	x		-1664.6
GAMM3	x		x	-1895.1
GAMM4	x	x	x	-1894.5

GAMM1

Parametric coefficients:

	Estimate	Std. Error	t value	Pr(>|t|)
(Intercept)	-1.54081	0.01696	-90.87	<2e-16 ***

Approximate significance of smooth terms:

	edf	Ref.df	F	p-value
s(week)	2.662	14	1.13	0.000247 ***

R-sq.(adj) = 0.0104 Deviance explained = 1.22%

GAMM2

Parametric coefficients:

	Estimate	Std. Error	t value	Pr(>|t|)
(Intercept)	-2.7395122	0.1756974	-15.592	< 2e-16 ***
size	0.0024632	0.0003542	6.954	5.35e-12 ***

Approximate significance of smooth terms:

	edf	Ref.df	F	p-value
s(week)	2.907	14	1.344	7.13e-05 ***

R-sq.(adj) = 0.0376 Deviance explained = 4.02%

GAMM3

Parametric coefficients:

	Estimate	Std. Error	t value	Pr(>|t|)
(Intercept)	-1.49098	0.05807	-25.67	<2e-16 ***

Approximate significance of smooth terms:

	edf	Ref.df	F	p-value
s(week)	3.49	14	3.574	1.41e-05 ***
s(individual)	22.20	27	12.392	< 2e-16 ***

R-sq.(adj) = 0.191 Deviance explained = 20.5%

GAMM4

Parametric coefficients:

	Estimate	Std. Error	t value	Pr(>|t|)
(Intercept)	-1.6942276	0.6105386	-2.775	0.00559 **
size	0.0004113	0.0012323	0.334 0	.73859

Approximate significance of smooth terms:

	edf	Ref.df	F	p-value
s(week)	3.488	14	3.59	1.53e-05 ***
s(individual)	21.437	26 1	1.00	< 2e-16 ***

R-sq.(adj) = 0.191 Deviance explained = 20.5%

95% occurrence range

Tested models:

	Week	Size	Individual	AIC
GAMM1	x			3974.8
GAMM2	x	x		3956.8
GAMM3	x		x	3810.53
GAMM4	x	x	x	3811.34

GAMM1

Parametric coefficients:

	Estimate	Std. Error	t value	Pr(>|t|)
(Intercept)	0.10429	0.02227	4.682	3.11e-06 ***

Approximate significance of smooth terms:

	edf	Ref.df	F	p-value
s(week)	3.698	14	1.646	2.28e-05 ***

R-sq.(adj) = 0.0153 Deviance explained = 1.78%

GAMM2

Parametric coefficients:

	Estimate	Std. Error	t value	Pr(>|t|)
(Intercept)	-0.9929459	0.2335380	-4.252	2.26e-05 ***
size	0.0022549	0.0004717	4.781	1.92e-06 ***

Approximate significance of smooth terms:

	edf	Ref.df	F	p-value
s(week)	3.738	14	1.86	5.42e-06 ***

R-sq.(adj) = 0.0281 Deviance explained = 3.12%

GAMM3

Parametric coefficients:

	Estimate	Std. Error	t value	Pr(>|t|)
(Intercept)	0.14796	0.06289	2.353	0.0188 *

Approximate significance of smooth terms:

	edf	Ref.df	F	p-value
s(week)	4.544	14	3.891	6.76e-07 ***
s(individual)	20.172	27	7.172	< 2e-16 ***

R-sq.(adj) = 0.134 Deviance explained = 14.8%

GAMM4

Parametric coefficients:

	Estimate	Std. Error	t value	Pr(>|t|)
(Intercept)	-0.0579322	0.6709571	-0.086	0.931
size	0.0004164	0.0013544	0.307	0.759

Approximate significance of smooth terms:

	edf	Ref.df	F	p-value
s(week)	4.536	14	3.899	7.47e-07 ***
s(individual)	19.495	26	6.590	< 2e-16 ***

R-sq.(adj) = 0.134 Deviance explained = 14.8%

Depth GAMMs

Tested models:

	Day of year	Size	Individual	AIC
GAMM1	x			-12369.69
GAMM2	x	x		-12371.47
GAMM3	x		x	-12279.71
GAMM4	x	x	x	-12282.06

GAMM1

Parametric coefficients:

	Estimate	Std. Error	t value	Pr(>|t|)
(Intercept)	18.4758	0.1594	115.9	<2e-16 ***

Approximate significance of smooth terms:

	edf	Ref.df	F	p-value
s(doy)	6.064	8	24.29	<2e-16 ***

GAMM2

Parametric coefficients:

	Estimate	Std. Error	t value	Pr(>|t|)
(Intercept)	12.841315	2.459873	5.220	1.88e-07 ***
size	0.011192	0.004876	2.295	0.0218 *

Approximate significance of smooth terms:

	edf	Ref.df	F	p-value
s(doy)	6.104	8	24.54	<2e-16 ***

GAMM3

Parametric coefficients:

	Estimate	Std. Error	t value	Pr(>|t|)
(Intercept)	18.671	1.012	18.45	<2e-16 ***

Approximate significance of smooth terms:

	edf	Ref.df	F	p-value
s(doy)	6.295	8	52.48	<2e-16 ***
s(individual)	4.891	5	46.10	<2e-16 ***

GAMM4

Parametric coefficients:

	Estimate	Std. Error	t value	Pr(>|t|)
(Intercept)	8.64916	15.74887	0.549	0.583
size	0.02024	0.03173	0.638	0.524

Approximate significance of smooth terms:

	edf	Ref.df	F	p-value
s(doy)	6.295	8	54.01	<2e-16 ***
s(individual)	3.924	5	44.88	<2e-16 ***

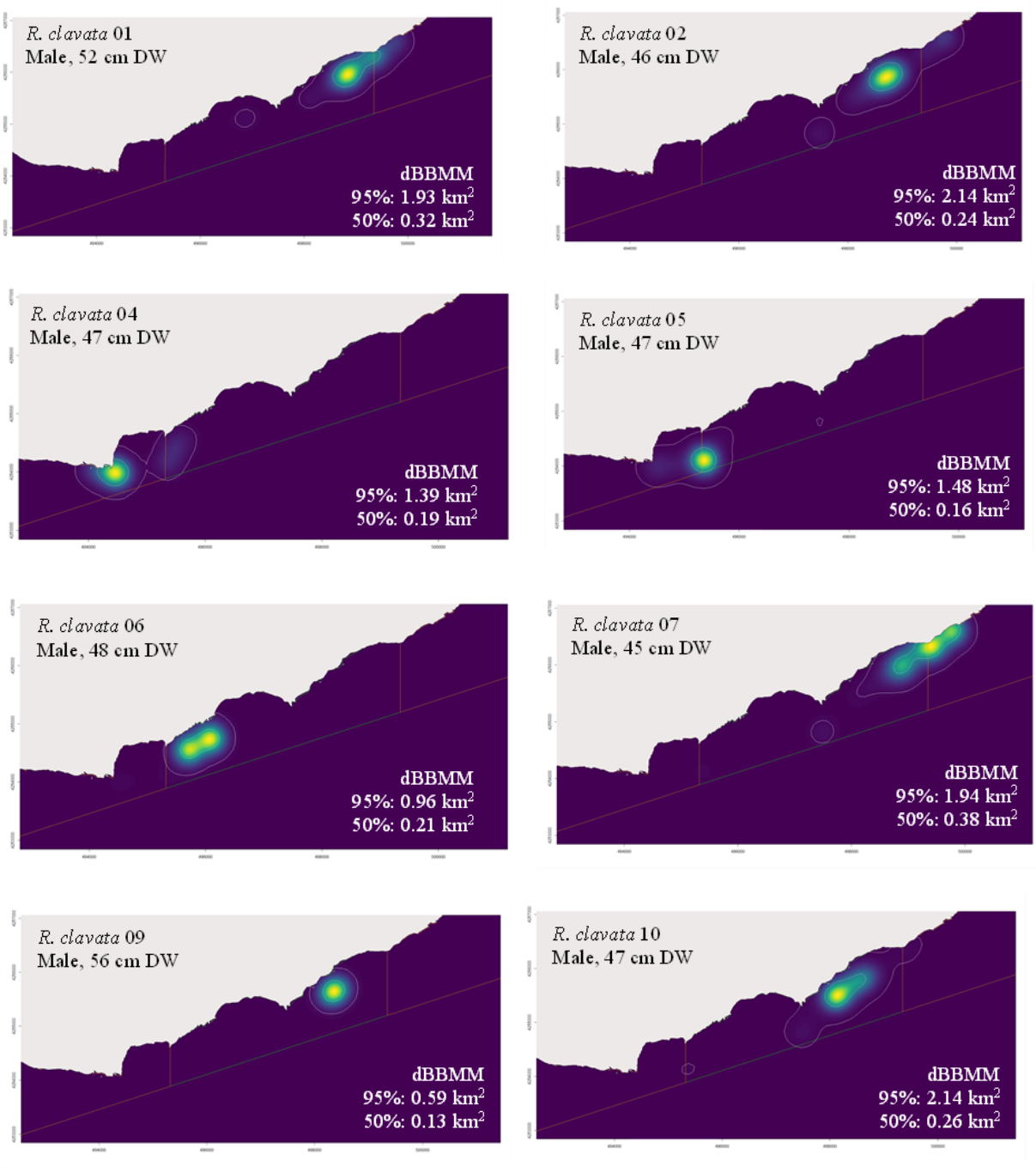

Supplementary material 5.2: Occurrence range of individual thornback rays (n = 28) at the 95% (solid line) and 50% (dotted line) isopleths. The brighter the colour, the higher the concentration of COAs. The border of the fully protected area is indicated by a green line, and the border of the partially protected areas by orange lines. Some thornback rays were not included because they did not provide sufficient COAs to estimate the dBBMM occurrence area (continued in the next two pages).

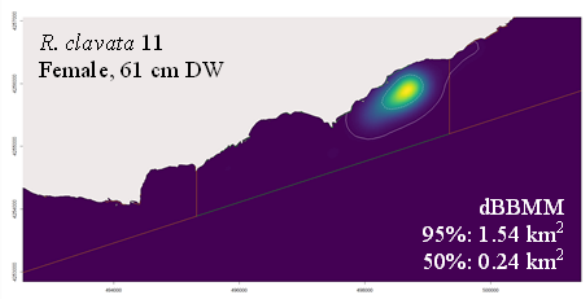
R. clavata 11
Female, 61 cm DW
dBBMM
95%: 1.54 km²
50%: 0.24 km²

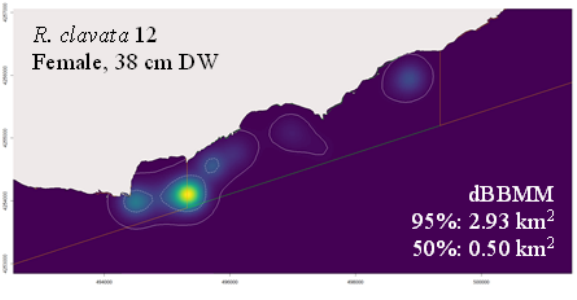
R. clavata 12
Female, 38 cm DW
dBBMM
95%: 2.93 km²
50%: 0.50 km²

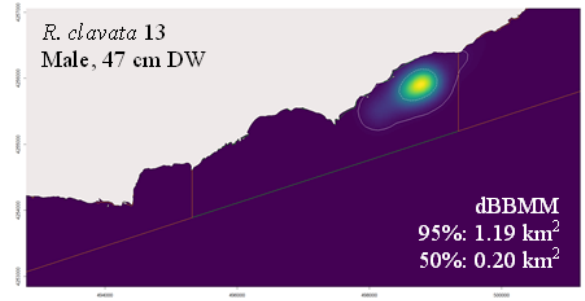
R. clavata 13
Male, 47 cm DW
dBBMM
95%: 1.19 km²
50%: 0.20 km²

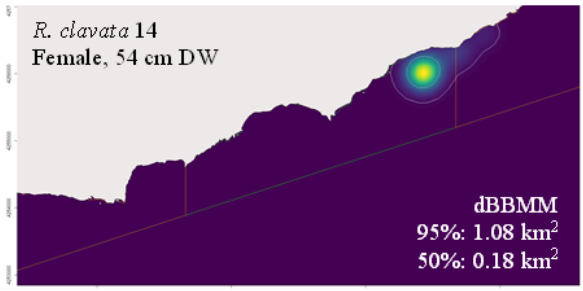
R. clavata 14
Female, 54 cm DW
dBBMM
95%: 1.08 km²
50%: 0.18 km²

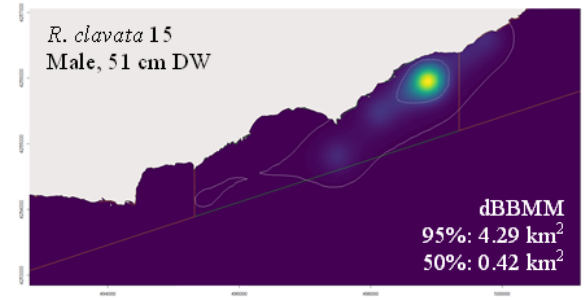
R. clavata 15
Male, 51 cm DW
dBBMM
95%: 4.29 km²
50%: 0.42 km²

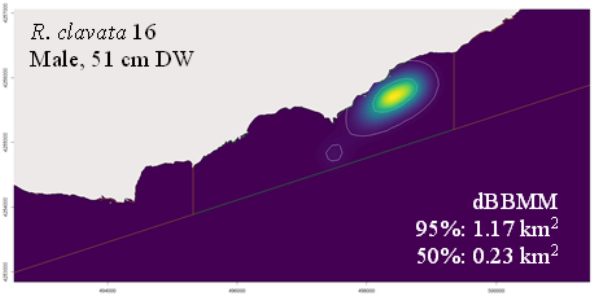
R. clavata 16
Male, 51 cm DW
dBBMM
95%: 1.17 km²
50%: 0.23 km²

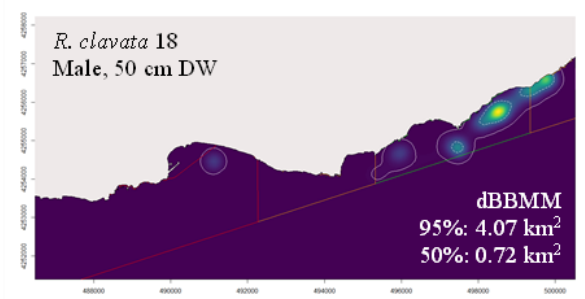
R. clavata 18
Male, 50 cm DW
dBBMM
95%: 4.07 km²
50%: 0.72 km²

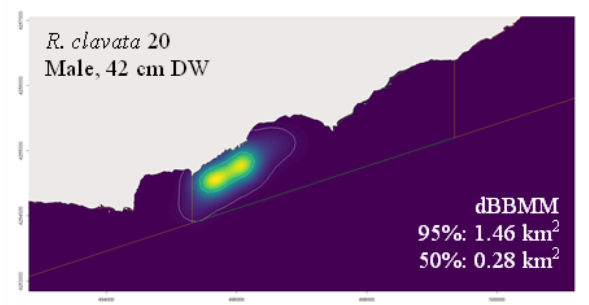
R. clavata 20
Male, 42 cm DW
dBBMM
95%: 1.46 km²
50%: 0.28 km²

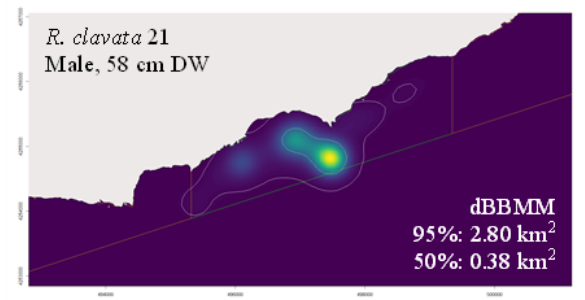
R. clavata 21
Male, 58 cm DW
dBBMM
95%: 2.80 km²
50%: 0.38 km²

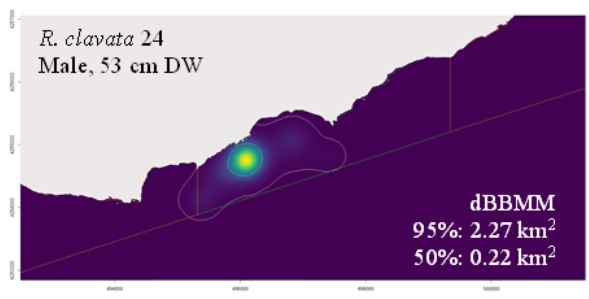
R. clavata 24
Male, 53 cm DW
dBBMM
95%: 2.27 km²
50%: 0.22 km²

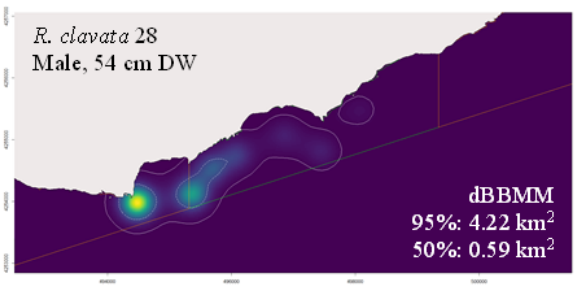
R. clavata 28
Male, 54 cm DW
dBBMM
95%: 4.22 km²
50%: 0.59 km²

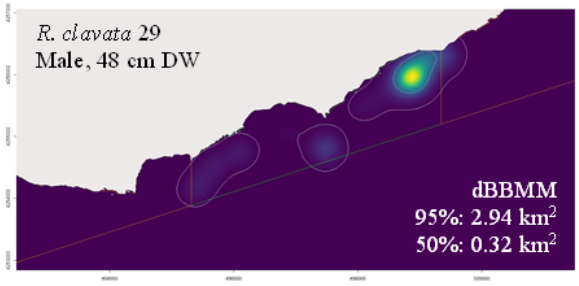
R. clavata 29
Male, 48 cm DW
dBBMM
95%: 2.94 km²
50%: 0.32 km²

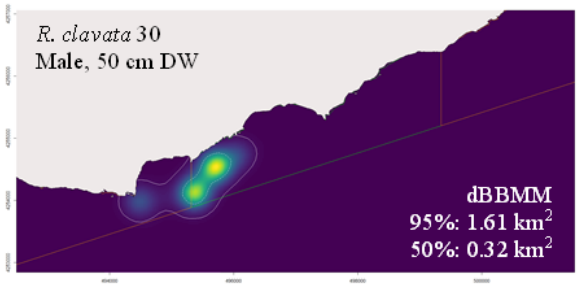
R. clavata 30
Male, 50 cm DW
dBBMM
95%: 1.61 km²
50%: 0.32 km²

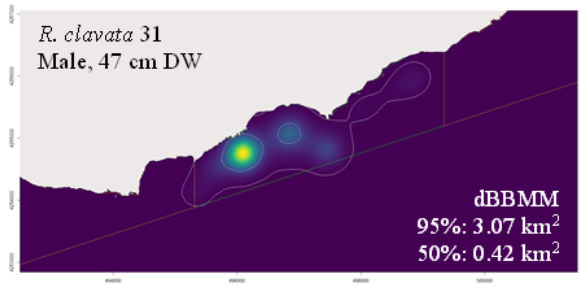
R. clavata 31
Male, 47 cm DW
dBBMM
95%: 3.07 km²
50%: 0.42 km²

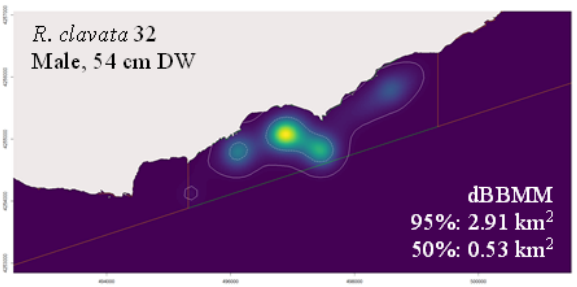
R. clavata 32
Male, 54 cm DW
dBBMM
95%: 2.91 km²
50%: 0.53 km²

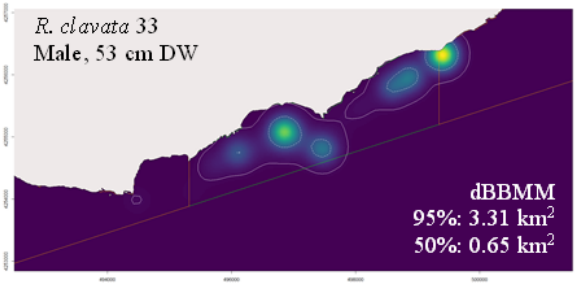
R. clavata 33
Male, 53 cm DW
dBBMM
95%: 3.31 km²
50%: 0.65 km²

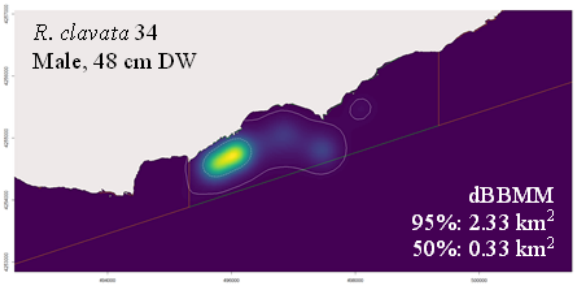
R. clavata 34
Male, 48 cm DW
dBBMM
95%: 2.33 km²
50%: 0.33 km²

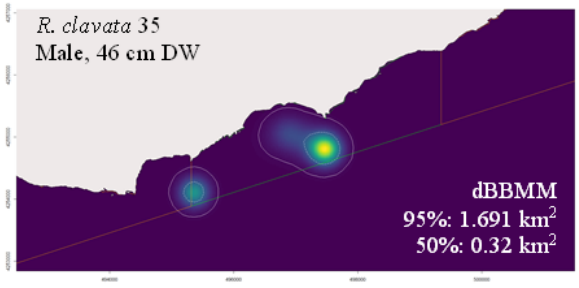
R. clavata 35
Male, 46 cm DW
dBBMM
95%: 1.691 km²
50%: 0.32 km²

Chapter 6

Exploration of co-occurrence and gregariousness in *Dasyatis pastinaca* using social network analysis

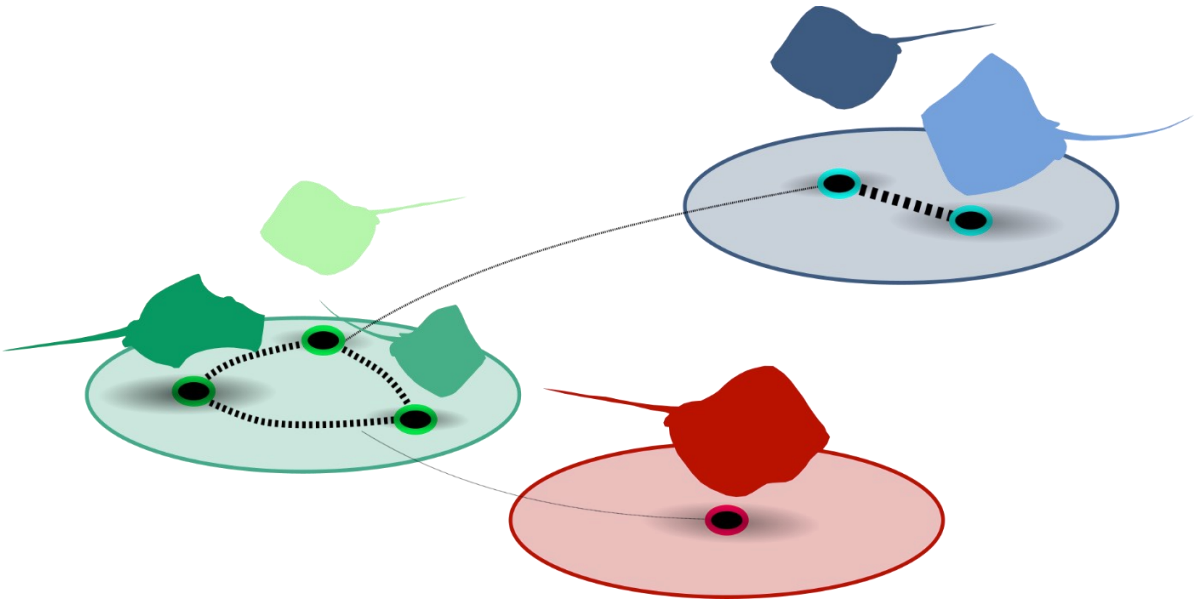

Representation of a social network of Dasyatis pastinaca

Chapter published as:

Kraft S., Winkler, A. C., Abecasis, D. & Mourier, J. Long-term co-occurrence and gregariousness in the migratory common stingray using network analysis. Marine Biology 171, 176. https://doi.org/10.1007/s00227-024-04498-z

Abstract

Aggregations and social interactions play an important role in the movement ecology of many animals, including elasmobranchs. Several species have shown the capability of complex social behaviours, and the importance of sociality in this taxon is being realized. Although social network analysis is a growing field of study for elasmobranchs, information to better understand these processes is still missing for most species, especially to support management and conservation policies. In this study, we analysed a long-term acoustic telemetry dataset collected on *Dasyatis pastinaca* in a coastal marine protected area, a species that performs seasonal migrations to a nearby estuary. Social network analysis was used to investigate preferential associations among individuals, revealing non-random associations. The analysis revealed a few strong and consistent associations that were maintained across inter-migratory periods, also suggesting temporal stability. Individuals also had similar average positions and a generally high overlap of space use between both periods, indicating some level of fine-scale site fidelity. Aggregations of up to 64% of tagged individuals were noted, particularly in the western side of the acoustic array. Despite our limited sample size that likely underestimated associations, these results show that, in addition to their large-scale movement pattern, *D. pastinaca* also presents active partner preference and spatial structure at a finer scale. The nature of such results is relevant to support the protection of these species.

Keywords:
Acoustic telemetry, aggregation, group formation, intra-specific association, sociality

6.1 Introduction

Aggregations, or the gathering of individuals in a specific location and time, are an important phenomenon undertaken by many marine animals, from zooplankton and crustaceans to fishes, birds, and marine mammals (Genin, 2004; Jermacz et al., 2017; Plötz et al., 1991). Aggregations can be passive processes driven by the distribution of suitable habitat or prey, attracting individuals to group in certain areas without social drivers. For example, animals in the pelagic zone, which is a typically unproductive environment, are drawn to patches of zooplankton and fish to feed (Genin, 2004). Aggregations can also be formed in response to the spatial distribution of shelter and the presence of predators (Jermacz et al., 2017). In some instances, the time and place of these events can also be predictable, such as the case of seasonal reproductive spawning aggregations in fishes (Domeier, 2012).

Aggregations are also important in that these may represent some of the most basic forms of social behaviour (Deneubourg et al., 2002). They are considered a prerequisite for social interactions (Graves and Duvall, 1995; Sims et al., 2000) and the development of social groups (Jacoby et al., 2012; Palacios et al., 2023). In this sense, the formation of aggregations may also be sociality-driven, with or without other environmental influences (Capello et al., 2011; Jermacz et al., 2017). In these cases, aggregations are based on active partner choice rather than the result of passive mechanisms.

Non-social aggregations and social interactions, even if different in nature, are also an important part of the movement ecology of species (Spiegel et al., 2017), thus understanding their structures and dynamics can be relevant to the development and improvement of conservation efforts behind many species (Jacoby et al., 2012; Mourier et al., 2018; Snijders et al., 2017). For example, aggregation areas may increase fishing vulnerability, so studying their distribution can lead to the development of fishery management strategies (Clark and O'Driscoll, 2003). Additionally, the environment plays a role in facilitating social interactions, so understanding where these occur can improve the performance of marine protected areas (Villegas-Ríos et al., 2022).

Animal interactions in the marine environment can be studied using a variety of tools. Under favourable circumstances, data can be collected by direct observation of animal interactions (Mourier et al., 2012; Perryman et al., 2019; Pini-Fitzsimmons et al., 2021). Visual surveys while SCUBA diving, from boats, or from the shore can provide detailed information on the interactions between individuals and on their directionality (Mourier et al., 2012; Pini-Fitzsimmons et al., 2021). However, this can be a demanding task, influenced by visual factors

(i.e., night-time, high turbidity or currents, complex environments, study area accessibility), requiring the identification of each individual (e.g., photo-ID), and constrained to fuel availability and diving capacities, so continuous monitoring is generally difficult.

On the other hand, automated monitoring systems like passive acoustic telemetry have been used in recent years to study sociality in many aquatic animals (Jacoby et al., 2016). Telemetry data does not have the same resolution and detail on the nature of the interactions as direct observation, although data at very fine temporal (seconds) and spatial scales (sub-meter) have been obtained in some cases (e.g., Aspillaga et al., 2021; Baktoft et al., 2017). However, passive acoustic telemetry systems present advantages like unaffected survey capacities in low light or dark conditions and in most environmental conditions, and the uninterrupted and long-term monitoring of tagged individuals (Krause et al., 2011). Social network analysis is an increasingly applied method in studies on elasmobranchs from acoustic telemetry data (Mourier et al., 2018). It has proven to be a powerful and adaptable method that can be used to answer a variety of questions about social systems (Farine and Whitehead, 2015; Krause et al., 2009; Sosa et al., 2021), particularly in species that do not evidently display social preference or that are hard to study (Snijders et al., 2017). Considering these advantages, marine systems are particularly fitting environments to apply this approach as these have been historically challenging to study (Hussey et al., 2015).

Compared to taxa like birds and mammals, the study of sociality in fishes is a more recent topic. Most work has been conducted on collective behaviour and structure, and the mechanisms driving individual interactions (Katz et al., 2011). Fishes have shown to present socially intricate interactions, some as complex as cooperative breeding (i.e., where breeding animals are assisted by other individuals, increasing the reproductive success of the former) (Tanaka et al., 2018). Similarly, the study of social interactions and aggregations in elasmobranchs is an even newer endeavour (Jacoby et al., 2012). Aggregative behaviour has been reported in a variety of species and habitats (McInturf et al., 2023), and a wide array of social behaviours like social grouping, forming and maintaining social structures, dominance hierarchies, leadership, and non-random associations between individuals have also been demonstrated (Jacoby et al., 2012; Jacoby et al., 2016; Mourier et al., 2012; Palacios et al., 2023). Among batoids (superorder Batoidea), perhaps the best known example are mobulids (Palacios et al., 2023), which can display individual preference and associations that last for weeks or months as in dynamic fission-fusion societies (Perryman et al., 2019). But other species have shown evidence of complex and structured social behaviour such as *Bathytoshia brevicaudata* (Pini-Fitzsimmons et al., 2021) or *Himantura fai* (Furst, 2011). However, despite

these recent advances, the study of aggregations and associations in elasmobranchs is still in development and more research is needed (Mourier et al., 2018).

In this study, we focused on *Dasyatis pastinaca*, a medium-sized stingray found in the northeastern Atlantic, from the British Isles to Mauritania, and the Mediterranean (Last et al., 2016). This is a viviparous stingray of conservation interest, as it is currently catalogued as Vulnerable by the IUCN Red List (IUCN, 2020). To study this species, we used a long-term acoustic telemetry data set collected in the Professor Luís Saldanha Marine Park (LSMP), a coastal marine protected area off Portugal, to evaluate if *D. pastinaca* forms aggregations at specific locations and if so, whether they represent passive gathering or non-random socially driven associations. This species is seasonally present in the LSMP, migrating to the nearby Sado estuary to spend spring and summer (Chapter 3, Kraft et al., 2023), which allowed us to compare inter-migratory periods to test the stability of associations over time and the repeatability in space use. Finally, these results were discussed in the context of the conservation of this species in coastal MPAs like the LSMP.

6.2 Materials and methods

6.2.1 Study area

The LSMP covers 53 km^2 over 38 km of coastline and is organised into three different protection levels: a total protection area or marine reserve of 4.3 km^2, four partial protection areas that cover a total of 21 km^2 and three complementary protection areas or buffer areas of a combined 28 km^2 (Figure 6.1). Entrance and any kind of fishing are prohibited in the total protection area. In the partial protection areas octopus traps and jigs are allowed beyond 200 m from the coastline, while in the buffer areas only local licensed fishing boats under 7 m can operate (Figure 6.1).

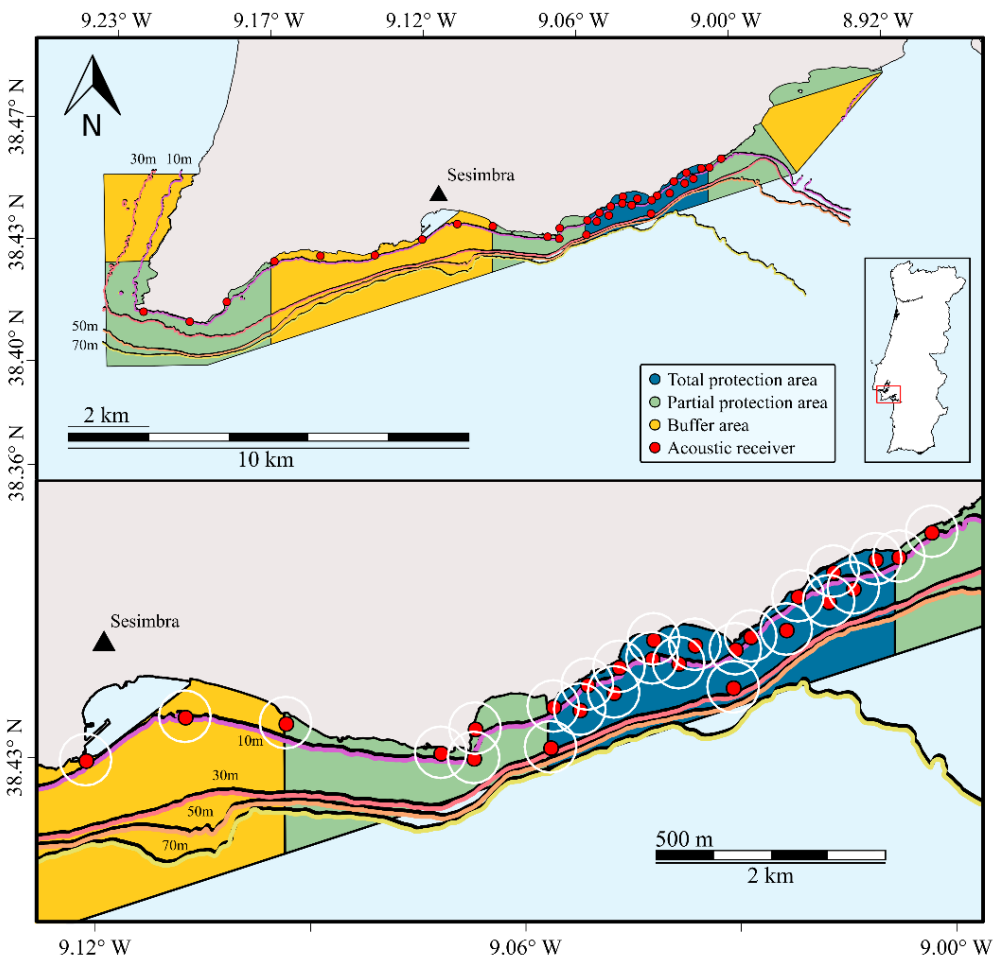

Figure 6.1: Top panel: Overview of the Professor Luis Saldanha Marine Park, its three different protection levels, and placement of acoustic receivers (red). Bottom panel: zoom-in to the denser portion of the acoustic array, centred in the total protection area. Detection range of 200 m indicated by white circles; isobaths are colour coded.

6.2.2 Terminology

In the context of this study, we defined co-occurrence as "the incidental or deliberate presence of at least-two individuals within the same spatial and temporal boundaries" and aggregations as "the co-occurrence of two or more individuals in space and time due to the deliberate use of a common driver" (McInturf et al., 2023). Following this definition, a driver can be social (i.e., interactions with other individuals) and non-social (i.e., environmental factors like resources, habitats, and other abiotic conditions) (McInturf et al., 2023). Co-occurrences to investigate aggregations were obtained from the co-detection of two or more individuals at the same receiver during the same time window. For the social network analysis, we used a gambit-of-the-group approach, i.e., we assumed that all individuals in a group are associated (Whitehead and Dufault, 1999). We used the term "association" to refer to the co-

detection of individuals in the context of social network analysis, and “dyads” to refer to the pair of individuals.

These definitions (co-occurrence, aggregation, association, dyad) do not necessarily represent socialization because we lacked the resolution and type of data required to confidently assess this. Although social interactions underlie some aggregations, and could still be a possibility in this case, elasmobranch aggregations are also frequently driven by asocial factors like habitat or resource availability, predator avoidance, resting habits, or synchronized patterns of activity (Jacoby et al., 2012; Palacios et al., 2023). Similarly, because of the less mobile and benthic nature of the study species, establishing a direct equivalency between simultaneous detection and social interaction greatly increases the chances of false positive interactions (Mourier et al 2017).

6.2.3 Tagging and tracking

Individuals were captured using trammel nets in 2019. The monofilament trammel nets were 500 m in length and 1.6 m in height, with 100 mm inner panels of stretched mesh and outer panels of 600 mm. The fishing gear was deployed at depths between 5-40 m, mostly inside the fully protected area and additionally in the partially protected area. Deployments were always in the morning and soaking time was around 24h. We brought individuals on board and placed them into a container filled with seawater that was changed after every individual. First, a hydrophone was used to detect previously tagged individuals. We used a measuring tape to obtain total length (TL), disc width (DW), and clasper length for males. We made a 2 cm incision in the peritoneal cavity using a scalpel to insert the tags and closed the incision using absorbable suture. We used three types of Innovasea 69 kHz acoustic tags: V9, V13, and V9P with pressure sensor. Respective expected battery lifetimes were 651, 1,317, and 404 days according to the manufacturer. We deployed tags based on animal size and tag availability. Additionally, individuals were fitted with a disc tag (www.floytags.com) with a unique ID number and contact information.

Capture, handling, and tagging was done under permits of the Portuguese Institute for Nature Conservation and Forests (permits n°145/2019/CAPT; 13/2020/CAPT; 70/2021/CAPT) and the Veterinary General Directorate (permit n° 2018-08-29 015730). Tagging procedures were also approved by the Animal Welfare Committee of the Centro de Ciências do Mar (CCMAR - ORBEA). The monitoring array was composed of Innovasea VR2W acoustic receivers deployed throughout the LSMP (Figure 6.1). Receivers were deployed on a variety of bottom types, which are distributed in patches throughout the area. Most receivers were on

medium-grained sand (the largest patches), followed by fine-grained sand, coarse-grained sand, and mixed sand, which stretched over the outer limit of the array. Other habitats within detection range of the receivers were nearshore reefs, algae on rocks, and muddy sands. Receivers were at depths that ranged between 5-17 meters. Previous studies showed code detection efficiency of 0.54 at 250 m (Abecasis, 2013) and no major variation in detection efficiency were found from environmental variables and/or background noises, so it was assumed to be constant across the receiver array (Abecasis et al., 2014). Based on this, a conservative detection range of 200 m was adopted.

6.2.4 Data analysis

For this study, a subset of a larger acoustic telemetry dataset on *Dasyatis pastinaca* was used (between 23/10/2019 to 04/12/2020) to ensure that all included individuals had the same probability of being detected throughout the analysed period (full detection plot in supplementary material 6.1). This avoids biases from individuals entering later into the studied group. The first 24 hours of detections of individual were deleted to remove possible anomalies induced by the fishing and tagging processes. To answer our research questions, the data was organized in three sets: the first set contained the complete dataset with all detections from the LSMP and Sado; the second set included the detections obtained in the LSMP during the period before migrating to Sado (LSMP period 1); and the third dataset contained the detections obtained in the LSMP during the period after returning from Sado (LSMP period 2). We used these datasets to study aggregations and social network analysis. The detections from Sado were not considered because of the sparsity of the array.

6.2.4.1 Aggregations

We used the number of individuals co-detected at the same receiver every 15 minutes as a proxy to study aggregations. Co-detected individuals will be referred to as “groups”. The spatio-temporal changes in aggregations were also studied. To assess the spatial distribution of group sizes in the LSMP and Sado, the cumulative number of individuals co-detected per hour per receiver were calculated for the study duration and plotted to characterize the distribution of the different group sizes and their cumulative frequencies. To investigate the variation of co-detections over time, the daily maximum number of co-occurring individuals at any receiver was obtained. The variation of group size per diel phase was investigated with a Generalized Linear Mixed-Effects Model as implemented in the R package *lme4* (Bates et al., 2015). Diel phase (daytime, night, and twilight) was used as fixed effect and receiver as random effect.

6.2.4.2 Social Network Analysis

Social networks were created using the R package *asnipe* (Farine, 2013). Considering the 200 m detection range defined for the VR2W receivers, two or more individuals were determined to be co-occurring (i.e., associated) if they were detected within this range in the same 15-minute window. Although in isolation the detection range is too large to confidently determine if two individuals were actually associated, this is offset by the numerous receivers in the array and the long-term data set, i.e., individuals actively moving together through the array should be detected. Network edges were weighted using the simple ratio index (SRI), which calculates the probability that A and B are observed together given that at least one has been detected (Cairns and Schwager, 1987). This index is estimated by dividing the number of times individuals A and B were detected together at the same receiver (x) by the sum of x, the times A was detected, and B was not (y_A), B was detected and A was not (y_A), and when A and B were both detected but not associated, i.e., A and B were at different receivers (y_{A+B}). The formula is: $x/(x + y_A + y_B + y_{A+B})$.

Next, a randomization process was done to test whether the observed network is a result of individuals randomly associating or if it reflects true preferred associations among individuals. For this process, the observed association matrix was randomized 10 000 times, and to account for space (i.e., if individuals were randomly occurring at the same sites), randomizations were done among individuals co-detected at the same receiver (therefore, no individuals were randomly shuffled as the structure of the data was conserved). Similarly, because there are two distinct periods in the LSMP with different group sizes, which changes the association probabilities in each period, a temporal limitation was added to randomize only within periods. Then, the standard deviation (SD) of each matrix was calculated. SD is used to detect non-random associations in networks because if preferred associations are present, these usually have a higher association value than expected for a random association (Farine and Whitehead, 2015). In turn, a network with these characteristics will have a higher SD compared to that of a network with only random associations (i.e., with a small SD). A p-value was calculated as the proportion of randomized SDs equal or greater than the observed SD at a significance level of 0.05.

To explore the persistence of associations between dyads before and after migration, separate networks were created for the LSMP periods 1 and 2. To investigate changes in associations during the day, networks were created for daytime, night, and twilight by separating detections according to diel phase using the R package *suncalc* (Thieurmel and

Elmarhraoui, 2019). The time between sunrise and sunset (appearance and disappearance of the sun over the horizon) was considered as “daytime”, morning and evening twilight collectively as “twilight”, and the period between evening twilight and morning twilight as “night”. A Mantel test was performed among networks for each period and diel phase to evaluate if the observed associations are similar among them using the R package *vegan* (Oksanen et al., 2022).

6.2.4.3 Reuse of space

To assess if the *D. pastinaca* used the same areas before and after returning from the Sado estuary (in LSMP periods 1 and 2), we calculated individual kernel utilization distributions (KUD) using the R package adehabitatHR (Calenge, 2006) and a fixed bandwidth of 200. Because these results will be compared with the associations, centers of activity (Simpfendorfer et al., 2002b) were calculated using the same time window of 15 min. Separate KUDs were calculated for the 7 *D. pastinaca* that were present in both LSMP periods. Then an index of reuse (IOR) was defined as the overlap (intersect) between both areas divided by the cumulative area occupied during both periods, following Morrissey and Gruber (1993).

6.3 Results

The study period spanned between 23/10/2019 and 04/12/2020 (409 days) and included 14 individuals (9 males and 5 females). This subset of the data was skewed towards males, but the full dataset was not (n = 31 individuals, 17 males and 14 females). Of these, *D. pastinaca* (Dp) 19 (female) was the only one to never be co-detected with other individuals as it was detected only a few times and promptly left the study area. The detection plot of the data shows the two periods in the LSMP (Figure 6.2).

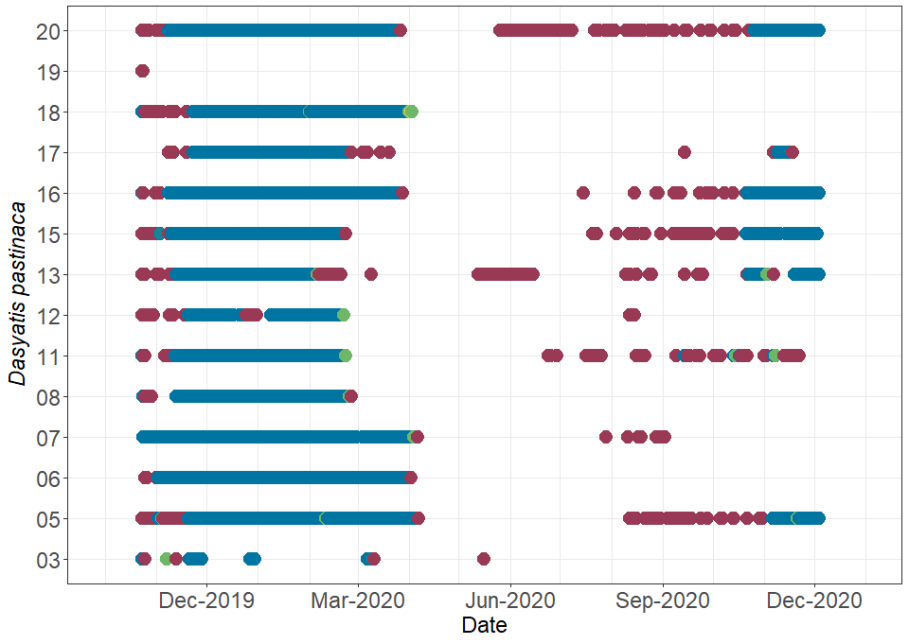

Figure 6.2: Abacus plot of the *Dasyatis pastinaca* individuals used in the present study, between October 23rd, 2019, and December 4th, 2020. Individuals Dp 03 to Dp 08 were tagged earlier in 2019, and individuals Dp 11 to Dp 20 were tagged at the beginning of the time window used in this study. Detections are colour-coded per receiver location: those in the fully protected area are blue, in the partially protected area green, in the buffer area yellow, and red in Sado.

6.3.1 Aggregations

Because of the low number of individuals that were detected after their migration to Sado (n = 7, 50% of total), aggregations were only assessed for the period before migrating to the Sado estuary. Throughout this period, aggregations of up to 9 individuals were detected at the same receiver. Group sizes of 2-4 were relatively evenly distributed across the array, and more frequently to its western half. As the group size class increased, their distribution became increasingly more skewed towards the west of the array (Figure 6.3). A similar pattern was also noted in the number of times each group size was detected, i.e., a same group size tended to be more frequently detected by receivers more to the west side of the fully protected area.

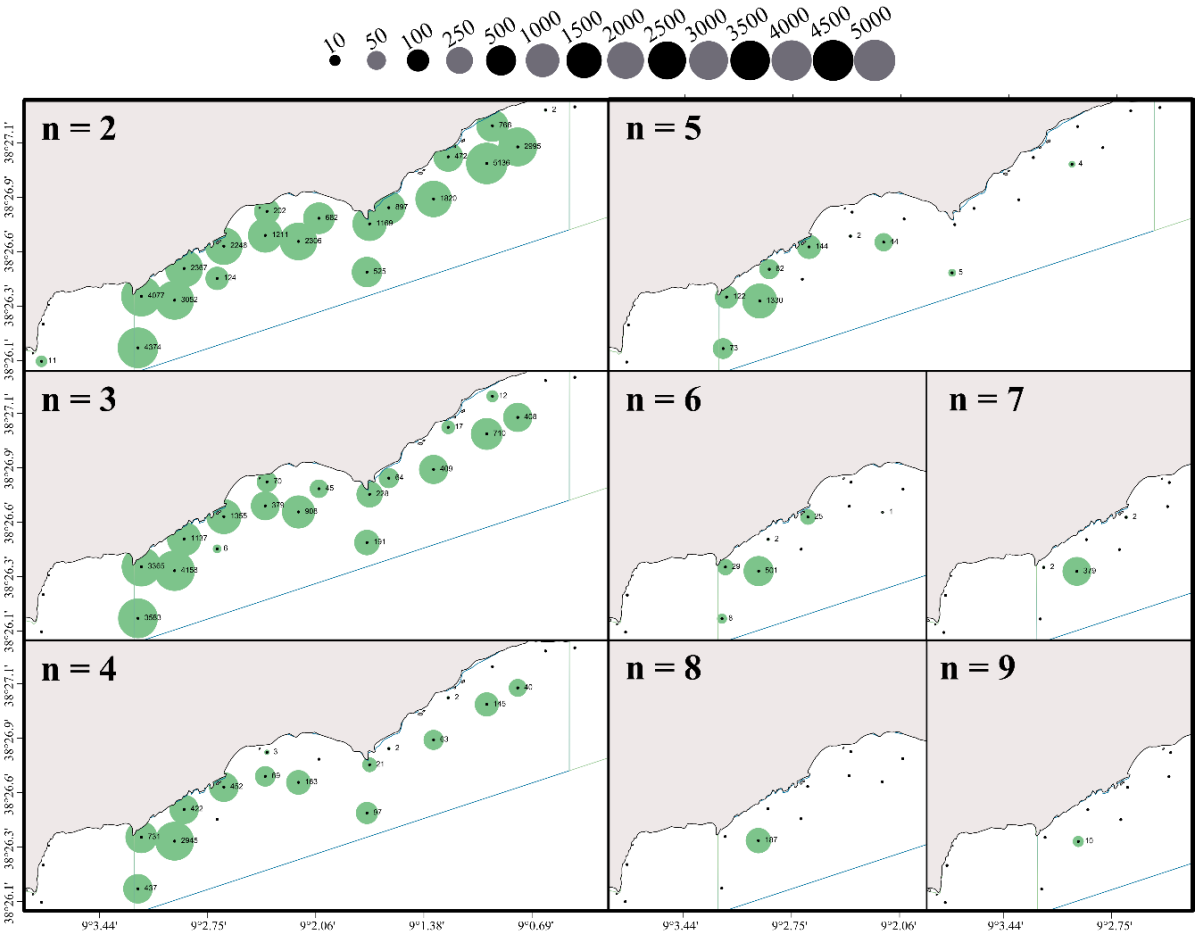

Figure 6.3: Cumulative co-detections of *Dasyatis pastinaca* individuals per receiver throughout the first period in the Luiz Saldanha Marine Park (first and last detections between 23/10/2019 and 07/04/2020). Circle size is proportional to the number of observations and plotted in logarithmic scale for illustration purposes (scale values are not transformed). For group sizes 6 to 9 only the western side of the fully protected area is shown, where these were detected. Black dots indicate the positions of receivers.

All group size classes were detected in all diel phases (daytime, night, and twilight). The Generalized Linear Mixed-Effects Model found statistically significant differences in group size among diel phases. Group size was larger during daytime than at night, although by a small difference (diff. 3.2%, $p<0.001$), but not compared to twilight (diff. 0.9%, $p=0.19$) (supplementary material 6.2). The daily maximum number of co-detected individuals varied over time, from 1 to 9 (Figure 6.4). Daily maximum group size was equal or larger than 50% of the daily available individuals (i.e., individuals that were detected at least once on a given day) 64.5% of the time (Figure 6.4). Maximum daily group sizes of 0 (no detections) were only obtained after the departure to Sado.

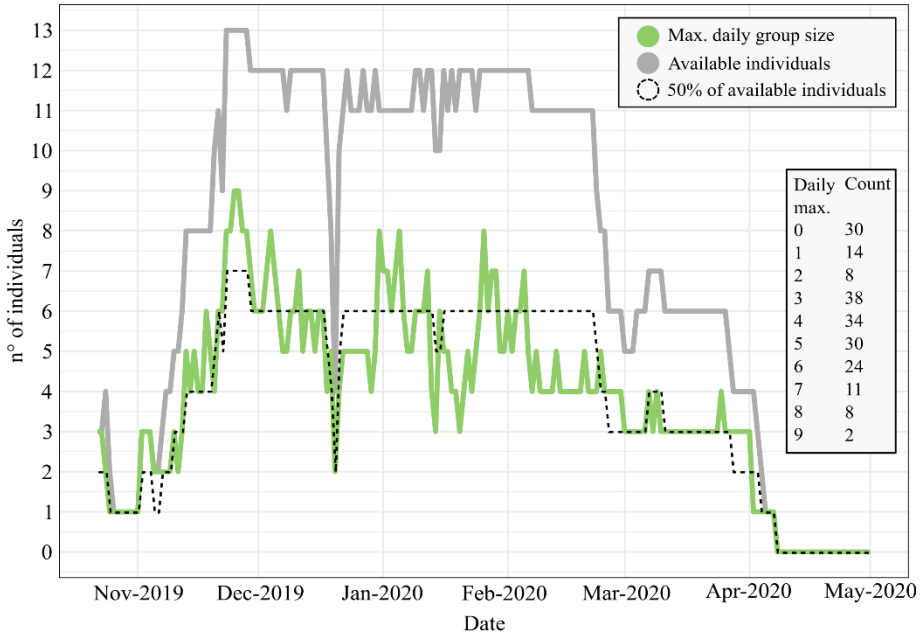

Figure 6.4: Daily maximum number of co-detected *Dasyatis pastinaca* individuals in the Luiz Saldanha Marine Park (green line) before the migration to the Sado estuary. The grey line indicates the daily maximum number of available individuals in the marine park (i.e., total number of tags detected in the array each day), and the dashed line indicates 50% of this value (rounded up to only have integers). This did not affect the estimated percentage of daily maximum group size greater than 50% of the available tags.

6.3.2 Social network

The resulting network of the complete dataset was composed of 13 connected individuals, 9 males and 4 females, representing 13 vertices and 75 edges (Figure 6.5a). SRI values averaged 0.062 ± 0.082 and ranged from 0.0001 to 0.4035. Significantly higher mean SD of association indices (SD_{obs} = 0.0797; mean random SD = 0.0794; range 0.0792 - 0.0797; p = 0.017) indicates that preferred associations are present in the observed network (supplementary material 6.3). For the networks per diel phase, average SRI per diel phase was 0.065 ± 0.085 for daytime, 0.064 ± 0.085 for twilight and 0.060 ± 0.080 for night, and the associations were positively correlated among all diel phases (Mantel statistic r: 0.985-0.996, all $p < 0.001$ after 1000 permutations), suggesting that associations were consistent across diel phases.

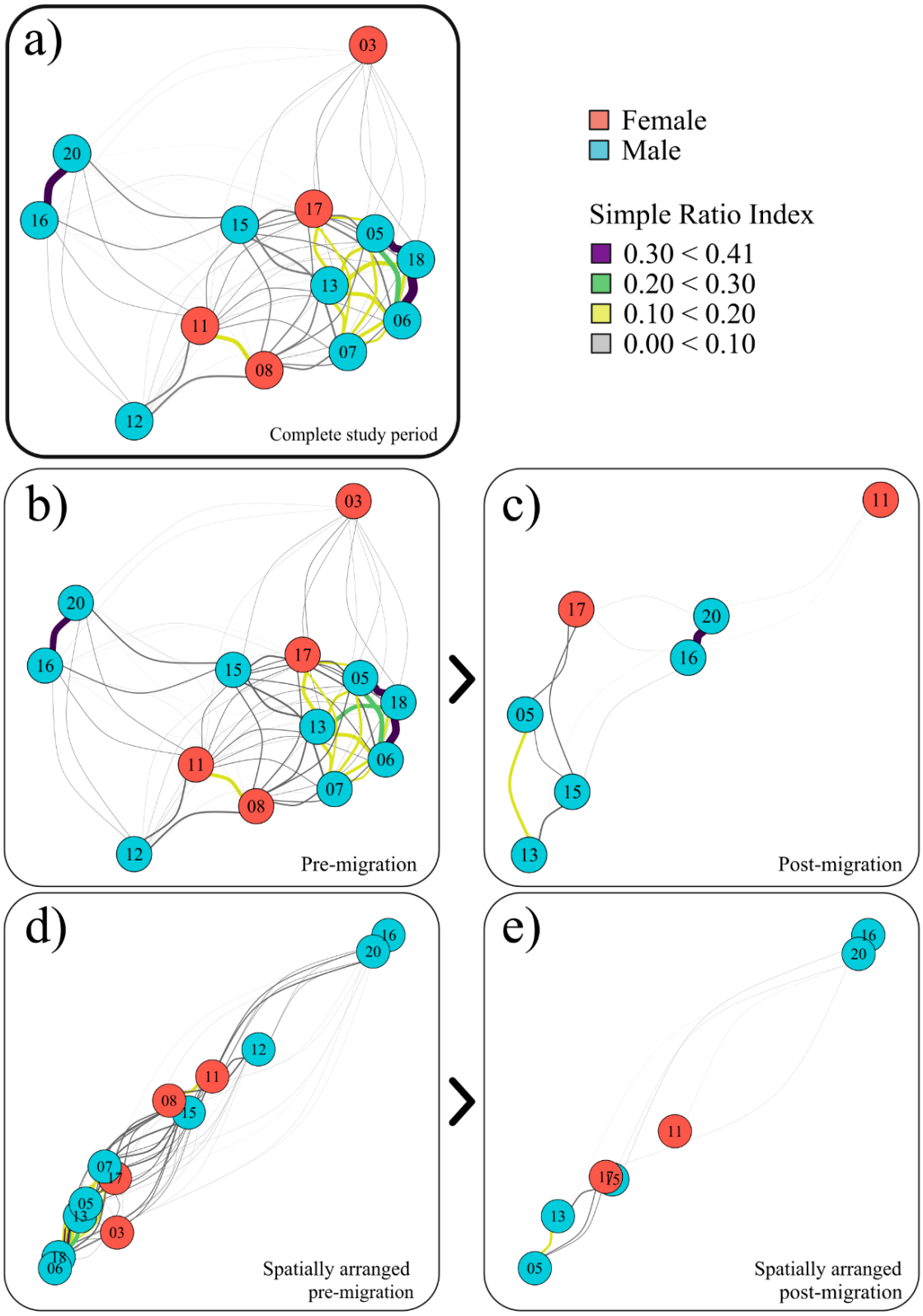

Figure 6.5: Social networks of *Dasyatis pastinaca* for a) the complete study period, b) Luiz Saldanha Marine Park (LSMP) before the migration to Sado and c) LSMP after the return from Sado; d) and e) show the same networks (b and c, respectively), but spatially organized based on the average centre of activity position of each individual per period. Dp 19 left quickly after tagging and is not shown.

The network for the first period (Figure 6.5b) had more nodes than the network of the second period in the LSMP (Figure 6.5c) because some individuals progressively stopped being detected over the study period, likely because of dispersal. Nevertheless, some similarities stand out, like the high association strength of the Dp16-Dp20 dyad and their relative isolation from the rest of the detected individuals in both periods. To compare the networks of each period in the LSMP, the 7 individuals that were detected in both subsets of the data were selected. A Mantel test found a statistically significant and positive correlation among associations (Mantel statistic r: 0.867, p= 0.007). In fact, the spatial distribution also appears to be similar between the two periods, as shown by the respective networks arranged by average position per individual (Figure 6.5d and e). In these, the Dp16-Dp20 dyad is spatially segregated from the rest of the network, and the position of individuals relative to each other is generally similar between both periods. The period in Sado was not included because a smaller acoustic array was used, precluding direct comparisons.

Considering that some dyads maintained a high level of association after migration, the co-detections of Dp13-Dp15 and Dp16-Dp20, two of the dyads with highest association values in both LSMP periods, were plotted to describe their area use and to illustrate two contrasting situations (Figure 6.6). First, the area use of each dyad was calculated to illustrate the full extent of the space each individual used (i.e., merged 95% KUD of the individuals in each dyad). This resulted in a large area for Dp13-Dp15 that extended throughout most of the array, and a small area for Dp16-Dp20 which was restricted to the east of the array. Regarding the co-detections of the individuals in each dyad, the co-detections of Dp13-Dp15 concentrated on the western end of their combined KUD area, while those of Dp16-Dp20 were noted throughout their combined KUD area. A few co-detections of the two dyads were noted in the middle of the array during the first period, but Dp13-Dp15 was scarcely detected here. Similar scenarios were observed during both inter-migratory periods, suggesting consistency in their space use and areas of co-detection. The dyad-level IOR were 55% for Dp13-Dp15 and 72% for Dp16-Dp20. The lower value of the former occurred because of the smaller 95% KUD registered in the second period.

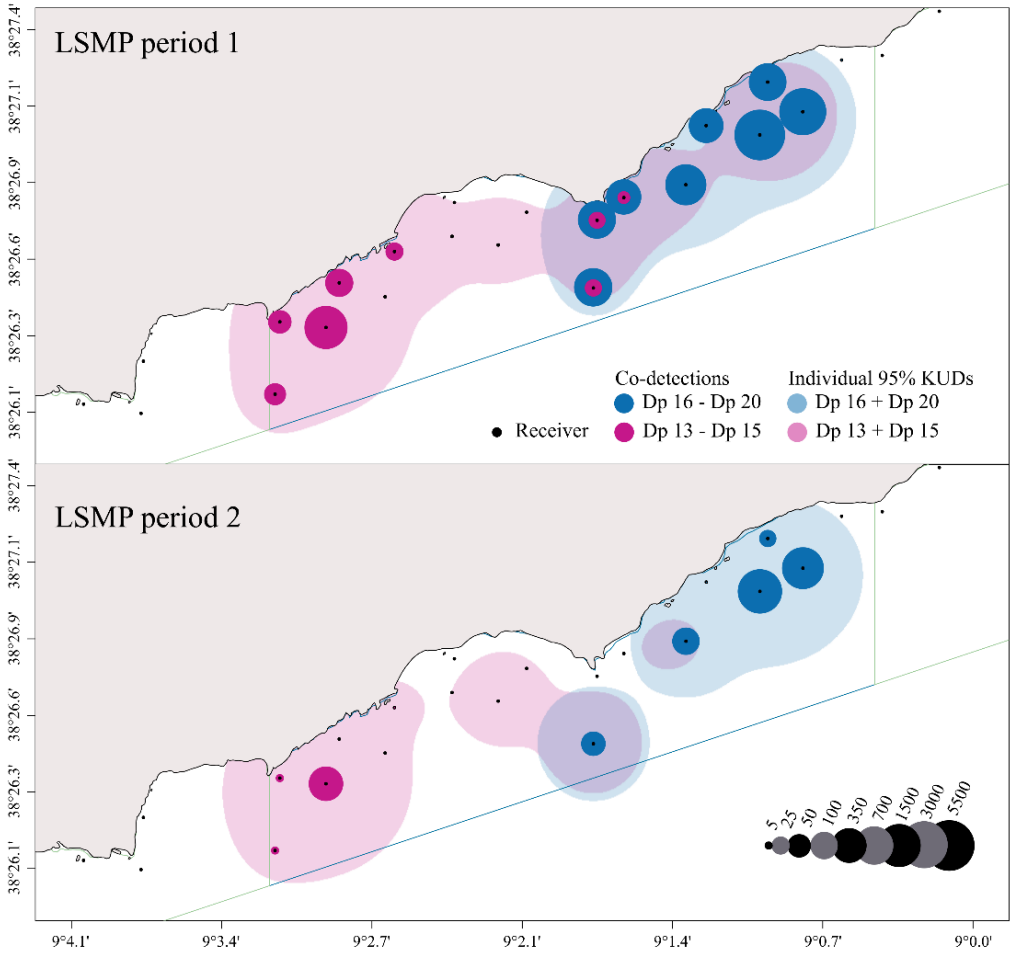

Figure 6.6: Receivers at which the *Dasyatis pastinaca* dyads Dp13-Dp15 and Dp16-Dp20 were detected in the Luiz Saldanha Marine Park during the period before migrating to the Sado estuary (LSMP period 1) and after returning (LSMP period 2). The combined 95% Kernel Utilization Distribution areas of the individuals in each dyad are also shown to display the total area covered. Circle size is proportional to the number of observations and plotted in logarithmic scale for illustration purposes (scale values are not transformed).

6.3.3 Reuse of space

After the initial period in the LSMP, seven individuals (50%) were detected returning, therefore an index or reuse between both periods was possible to calculate for these individuals (Table 6.1). A wide range of values was obtained, the lowest being 18%, but in general the area of reuse was high, averaging an overlap of 54 ± 21% for the 50% KUDs and 64 ± 11% for the 95% KUD.

Table 6.1: Index of reuse (IOR) for each *Dasyatis pastinaca* that was detected in both periods in the Luiz Saldanha Marine Park, before and after their migration to Sado. Kernel Utilisation Distribution (KUD) at the 50% and 95% levels, their area of overlap, and the area of their combined surfaces are also shown. All units are in km^2 except IOR which is in percentage.

	50% KUD (km2)					95% KUD (km2)				
Individual	Period 1	Period 2	Total	Overlap	IOR (%)	Period 1	Period 2	Total	Overlap	IOR (%)
Dp 05	0.38	0.27	0.46	0.20	44	1.92	1.30	2.17	1.05	48
Dp 11	0.73	0.93	1.40	0.26	18	3.04	4.99	5.21	2.82	54
Dp 13	0.21	0.21	0.23	0.19	83	1.24	1.18	1.36	1.06	78
Dp 15	0.81	0.35	0.81	0.35	43	3.82	2.69	4.06	2.45	60
Dp 16	0.40	0.29	0.40	0.29	71	1.99	1.72	2.12	1.58	74
Dp 17	0.50	0.37	0.53	0.34	65	2.94	3.27	3.83	2.38	62
Dp 20	0.50	0.32	0.53	0.29	54	1.96	1.84	2.26	1.55	69
Mean	0.51	0.40	0.64	0.27	54	2.41	2.43	3.00	1.84	64
SD	0.21	0.24	0.38	0.06	21	0.88	1.36	1.38	0.71	11

6.4 Discussion

In this study, we expanded on previous findings that described the seasonal philopatry of *D. pastinaca* to this area (Chapter 3, Kraft et al., 2023) to explore the finer-scale dynamics of aggregations and associations among individuals of this species. These two aspects were investigated and compared across years, allowing to examine their long-term stability (i.e., across migrations). Although the acoustic telemetry system that was used is not optimal for researching social interactions (Mourier et al., 2017), the longevity of the acoustic telemetry dataset allowed to obtain interesting insights into the social and spatial patterns of *D. pastinaca*.

6.4.1 Aggregations and associations

The first objective of this study focused on identifying and characterizing spatiotemporal patterns of aggregations. Although a low number of tagged individuals was used for this purpose (n=14), a clear aggregation site was detected to the west of the array. Here, up to nine *D. pastinaca* were co-detected at the same receiver, representing 64% of tagged individuals or 69% of available individuals on the day of occurrence. Half or more of the daily available individuals were co-detected at least once in 67% of days, indicating that *D. pastinaca* formed larger aggregations with some regularity. An important factor for the interpretation of these results is the presence of untagged individuals, therefore the true aggregation size is unknown and may encompass more individuals. Similarly, the existence of other aggregation sites is also unknown. For this, future studies on the fine-scale spatial fidelity of individuals in both inter-migratory periods may show some clues. For example, considering

the presence of unaccounted-for individuals, the spatially isolated Dp16-Dp20 dyad may be part of another spatially separated aggregation.

The second objective of this study was to evaluate whether non-random (i.e., social) associations are formed between individuals within these aggregations, and the social network analysis suggested the existence of preferred associations. Considering the low number of tagged individuals, it is noteworthy that strong associations were noted among the generally low SRI values. The co-detection of pairs of individuals at receivers throughout the acoustic array also reflects this, which can be interpreted as a signal of synchronous movement of actively associating individuals. The observed associations were also stable across inter-migratory periods, as shown by the Mantel test. Whether these associations are maintained during their reproductive season or are resumed after returning to the LSMP remains to be evaluated. Regardless of this, these results indicate that the extended seasonal migration this species undergoes (Chapter 3, Kraft et al., 2023) did not disrupt the associations detected in the present study.

Other species in the family Dasyatidae have also been observed forming non-random associations, at least under specific conditions at provisioning sites (Furst, 2011; Pini-Fitzsimmons et al., 2021). In these situations, individuals displayed complex behaviours in the form of different kinds of interactions and social structures akin to despotic societies or size-based social structures (Furst, 2011; Pini-Fitzsimmons et al., 2021).

These results complement previous findings on the migratory movement pattern of *D. pastinaca* (Chapter 3, Kraft et al., 2023) by using a different approach to characterize their fine-scale movements and the social drivers behind them. In combination, these results illustrate the intricacy and stratification of their spatial ecology. Future studies could use a more suitable approach to study the association patterns among individuals in this species, for example proximity loggers or receivers with a shorter detection range (Mourier et al., 2017). Considering that aggregations are a prerequisite for social interactions (Jacoby et al., 2012; Palacios et al., 2023), the site where *D. pastinaca* was observed to aggregate in large numbers could be a candidate to start this study.

6.4.2 Ecological interpretation of aggregations

Elasmobranchs are known to aggregate across a variety of habitats (McInturf et al., 2023), and several factors can underlie this process. They can passively aggregate as an outcome of the distribution of suitable habitats or prey or as the result of synchronized diel or seasonal movements (Jacoby et al., 2012). An example of the latter is the migration of *D. pastinaca* to the Sado estuary, likely as a response to environmental cues such as temperature (Chapter 3, Kraft et al., 2023). Variables like currents, temperature, and visibility can also play a role in the formation of aggregations, gathering individuals as these seek sites to rest or to accelerate gestation (Jirik and Lowe, 2012; Meese and Lowe, 2019; Semeniuk and Dill, 2005).

Despite the statistically significant difference in *D. pastinaca* group size per diel phase, the estimated variation (0.9-3.2%) is likely not biologically significant. Although visibility can have an influence in group formation, such as through changes in turbidity and environmental light conditions (Semeniuk and Dill, 2005), this may not always be enough to increase group size to large numbers. A study on *Pastinachus sephen* showed that it is more prone to form groups in low visibility conditions, but these groups were of around 3 individuals (Semeniuk and Dill, 2005). Drawbacks also exist in the formation of large aggregations, such as increased conspicuousness and interference among individuals (Semeniuk and Dill, 2005), which may explain why large groups were rarer. However, this could also be an artifact of the study design. In another example, *Triakis semifasciata* and juvenile *Carcharhinus melanopterus* mostly aggregate during the day, but with the exception of June for the latter, when it occurs at night as well (Heupel and Simpfendorfer, 2005; Nosal et al., 2014).

In the present study, the seafloor where the largest aggregations of *D. pastinaca* were seen is mostly covered in fine, medium, and mixed sand, which are also among the most common bottom types in the LSMP (Henriques et al., 2015) (supplementary material 6.4). Similarly, most receivers were deployed at depths of around 5-10 meters (supplementary material 6.4), making significant depth-related temperature differences unlikely. This suggests that if the availability of suitable habitat has an effect, it may not be the sole driver of their spatial distribution.

Social factors can also drive group formation in elasmobranchs. Some species engage in active social associations during specific events of their life cycle, like reproduction (Sims et al., 2000). Indeed, *D. pastinaca* has been reported to form breeding aggregations in which behaviours like courtship have been documented (Chaikin et al., 2020; Morey et al., 2006). In

the present study area, reproduction likely occurs in the nearby Sado estuary (Chapter 3, Kraft et al., 2023), therefore the observed social aggregations are not for reproductive purposes.

An important function of group formation is predator avoidance (e.g., Heupel and Simpfendorfer, 2005). This can be particularly important for stingrays when resting, and grouping allows them to reduce risk by engaging in protective formations, obtain early warning signs and coordinate their escape (Semeniuk and Dill, 2005). Although the anti-predator advantages of grouping greatly rely on the dilution effect of gathering in large numbers, which as previously mentioned can occur in non-social situations, in some cases preferential associations can also direct anti-predator behaviour. For example, *P. sephen* can actively choose to rest near individuals of *Himantura uarnak* because of the latter's faster escape response to predators (Semeniuk and Dill, 2006). This indicates an active neighbour choice when deciding on a resting site.

Another important role of social grouping is the transfer of information among group members, an ability that stingrays are likely to possess. Laboratory experiments on *Potamotrygon falkneri* (Potamotrygonidae) have shown this species is capable of social learning and imitation (Thonhauser et al., 2013), which in wild stingrays could mediate the transfer of information in the form of local enhancement (discovery of food patches by observing other group members, Thorpe [1965]). This has been shown for spatially-organized social communities of *Carcharhinus amblyrhynchos*¸ which socially transfer information in the form of local enhancement (Papastamatiou et al., 2020).

In conjunction with the previous drivers, social factors can also mediate the distribution of individuals and aggregations in space. Elasmobranchs are capable of organizing into spatially delimited communities that can arise from non-social factors but also active partner choice, for example as seen in *Mobula alfredi* (Perryman et al., 2022) and in *Carcharhinus melanopterus* (Mourier et al., 2012). Stingrays also display at least some form of spatial memory and can construct spatial maps of their surroundings (Schluessel and Bleckmann, 2005), which would enable them to identify spaces and return to known sites after traveling to other areas. This is supported by the similar average positions and generally high IOR values observed in the two inter-migratory periods, reflecting that some level of fine-scale spatial fidelity was maintained that may organize individuals into separate communities (Chapman et al., 2015).

6.4.3 Conservation and management

Although *D. pastinaca* is not a targeted species in this region, they are captured as bycatch in fishing operations targeting other species like flatfishes (Baeta et al., 2010; Batista et al., 2009). In relation to the LSMP, the aggregations formed by *D. pastinaca* were detected by interior receivers in the full protection area, suggesting this aggregation site may be protected from fishing. The neighbouring partial protection areas provide similar protection, as the activities allowed in them do not represent a risk to this species. However, the actual distribution of the individuals in these aggregations and their closeness to the marine park's border remains to be better assessed, as the current study design only confirms that they were inside the detection range of a receiver. This is relevant to clarify because the distribution of elasmobranchs can directly influence their susceptibility to fishing (Mucientes et al., 2009; Wearmouth and Sims, 2008), which is important information for MPA management.

Susceptibility increases at aggregation sites because the concentration of individuals inside a delimited area facilitates their capture in larger numbers (Palacios et al., 2023), and the closeness of individuals to an MPA's border may exacerbate the aggregation's exposure to risk (Villegas-Ríos et al., 2021). In turn, removing individuals in large numbers can have detrimental effects on the social processes of a population beyond the reduction in numbers. Social learning relies on the structure of social groups, and the disturbance of this structure can reduce the social information available in a population, affecting its adaptability and survival (Wilson and Giske, 2023). Excessive harvesting can lead, for example, to the loss of social nodes through which relevant information travels, such as related to feeding or migration routes, and even to the disruption of the general social structure (Villegas-Ríos et al., 2022). Therefore, to avoid irreversible changes in the social processes of populations, and the consequences this can have, understanding the dynamics of aggregations and associations is needed to push for improvements in their management and conservation (Villegas-Ríos et al., 2022).

6.5 References

Abecasis, D., 2013. Multispecies spatial dynamics under different protection levels: an evaluation of the effects and optimal design of the Luiz Saldanha Marine Park (Ph.D. Thesis). Universidade do Algarve, Faro, Portugal.

Abecasis, D., Afonso, P., Erzini, K., 2014. Can small MPAs protect local populations of a coastal flatfish, *Solea senegalensis*? Fisheries Management and Ecology 21, 175–185. https://doi.org/10.1111/fme.12061

Aspillaga, E., Arlinghaus, R., Martorell-Barceló, M., Follana-Berná, G., Lana, A., Campos-Candela, A., Alós, J., 2021. Performance of a novel system for high-resolution tracking of marine fish societies. Animal Biotelemetry 9, 1. https://doi.org/10.1186/s40317-020-00224-w

Baeta, F., Batista, M., Maia, A., Costa, M.J., Cabral, H., 2010. Elasmobranch bycatch in a trammel net fishery in the Portuguese west coast. Fisheries Research 102, 123–129. https://doi.org/10.1016/j.fishres.2009.10.016

Baktoft, H., Gjelland, K.Ø., Økland, F., Thygesen, U.H., 2017. Positioning of aquatic animals based on time-of-arrival and random walk models using YAPS (Yet Another Positioning Solver). Scientific Reports 7, 14294. https://doi.org/10.1038/s41598-017-14278-z

Bates, D., Mächler, M., Bolker, B., Walker, S., 2015. Fitting Linear Mixed-Effects Models Using lme4. Journal of Statistical Software 67. https://doi.org/10.18637/jss.v067.i01

Batista, M.I., Teixeira, C.M., Cabral, H.N., 2009. Catches of target species and bycatches of an artisanal fishery: The case study of a trammel net fishery in the Portuguese coast. Fisheries Research 100, 167–177. https://doi.org/10.1016/j.fishres.2009.07.007

Cairns, S.J., Schwager, S.J., 1987. A comparison of association indices. Animal Behaviour 35, 1454–1469. https://doi.org/10.1016/S0003-3472(87)80018-0

Calenge, C., 2006. The package "adehabitat" for the R software: A tool for the analysis of space and habitat use by animals. Ecological Modelling 197, 516–519. https://doi.org/10.1016/j.ecolmodel.2006.03.017

Capello, M., Soria, M., Cotel, P., Deneubourg, J.-L., Dagorn, L., 2011. Quantifying the Interplay between Environmental and Social Effects on Aggregated-Fish Dynamics. PLoS ONE 6, e28109. https://doi.org/10.1371/journal.pone.0028109

Chaikin, S., Belmaker, J., Barash, A., 2020. Coastal breeding aggregations of threatened stingrays and guitarfish in the Levant. Aquatic Conservation: Marine and Freshwater Ecosystems 30, 1160–1171. https://doi.org/10.1002/aqc.3305

Chapman, D.D., Feldheim, K.A., Papastamatiou, Y.P., Hueter, R.E., 2015. There and Back Again: A Review of Residency and Return Migrations in Sharks, with Implications for Population Structure and Management. Annual Review of Marine Science 7, 547–570. https://doi.org/10.1146/annurev-marine-010814-015730

Clark, M., O'Driscoll, R., 2003. Deepwater Fisheries and Aspects of Their Impact on Seamount Habitat in New Zealand. Journal of Northwest Atlantic Fishery Science 31, 441–458. https://doi.org/10.2960/J.v31.a34

Deneubourg, J.L., Lioni, A., Detrain, C., 2002. Dynamics of Aggregation and Emergence of Cooperation. The Biological Bulletin 202, 262–267. https://doi.org/10.2307/1543477

Domeier, M.L., 2012. Revisiting Spawning Aggregations: Definitions and Challenges, in: Sadovy De Mitcheson, Y., Colin, P.L. (Eds.), Reef Fish Spawning Aggregations: Biology, Research and Management. Springer Netherlands, 1–20. https://doi.org/10.1007/978-94-007-1980-4_1

Farine, D.R., 2013. Animal social network inference and permutations for ecologists in R using asnipe. Methods in Ecology and Evolution 4, 1187–1194. https://doi.org/10.1111/2041-210X.12121

Farine, D.R., Whitehead, H., 2015. Constructing, conducting and interpreting animal social network analysis. Journal of Animal Ecology 84, 1144–1163. https://doi.org/10.1111/1365-2656.12418

Furst, E.A., 2011. Network Analysis of the Tahitian Ray (Himantura fai): Is There Social Structure to the Feeding Frenzy? UC Berkeley: UCB Moorea Class: Biology and Geomorphology of Tropical Islands. Retrieved from https://escholarship.org/uc/item/56n206sn.

Genin, A., 2004. Bio-physical coupling in the formation of zooplankton and fish aggregations over abrupt topographies. Journal of Marine Systems 50, 3–20. https://doi.org/10.1016/j.jmarsys.2003.10.008

Graves, B.M., Duvall, D., 1995. Aggregation of Squamate Reptiles Associated with Gestation, Oviposition, and Parturition. Herpetological Monographs 9, 102. https://doi.org/10.2307/1466999

Henriques, V., Guerra, M.T., Mendes, B., Gaudêncio, M.J., Fonseca, P., 2015. Benthic habitat mapping in a Portuguese Marine Protected Area using EUNIS: An integrated approach. Journal of Sea Research 100, 77–90. https://doi.org/10.1016/j.seares.2014.10.007

Heupel, M.R., Simpfendorfer, C.A. 2005. Quantitative analysis of aggregation behavior in juvenile blacktip sharks. Marine Biology 147, 1239-1249. https://doi.org/10.1007/s00227-005-0004-7

Hussey, N.E., Kessel, S.T., Aarestrup, K., Cooke, S.J., Cowley, P.D., Fisk, A.T., Harcourt, R.G., Holland, K.N., Iverson, S.J., Kocik, J.F., Mills Flemming, J.E., Whoriskey, F.G., 2015. Aquatic animal telemetry: A panoramic window into the underwater world. Science 348, 1255642–1255642. https://doi.org/10.1126/science.1255642

IUCN, 2020. *Dasyatis pastinaca*: Jabado, R.W., Chartrain, E., De Bruyne, G., Derrick, D., Dia, M., Diop, M., Doherty, P., Leurs, G.H.L., Metcalfe, K., Pacoureau, N., Pires, J.D., Ratão, S., Seidu, I., Serena, F., Soares, A.-L., Tamo, A., VanderWright, W.J. & Williams, A.B.: The IUCN Red List of Threatened Species 2021: e.T161453A124488102. https://doi.org/10.2305/IUCN.UK.2021-2.RLTS.T161453A124488102.en

Jacoby, D.M.P., Croft, D.P., Sims, D.W., 2012. Social behaviour in sharks and rays: analysis, patterns and implications for conservation: Shark social behaviour. Fish and Fisheries 13, 399–417. https://doi.org/10.1111/j.1467-2979.2011.00436.x

Jacoby, D.M.P., Papastamatiou, Y.P., Freeman, R., 2016. Inferring animal social networks and leadership: applications for passive monitoring arrays. Journal of The Royal Society Interface 13, 20160676. https://doi.org/10.1098/rsif.2016.0676

Jermacz, Ł., Andrzejczak, J., Arczyńska, E., Zielska, J., Kobak, J., 2017. An enemy of your enemy is your friend: Impact of predators on aggregation behavior of gammarids. Ethology 123, 627–639. https://doi.org/10.1111/eth.12635

Jirik, K.E., Lowe, C.G., 2012. An elasmobranch maternity ward: female round stingrays *Urobatis halleri* use warm, restored estuarine habitat during gestation. Journal of Fish Biology 80, 1227–1245. https://doi.org/10.1111/j.1095-8649.2011.03208.x

Katz, Y., Tunstrøm, K., Ioannou, C.C., Huepe, C., Couzin, I.D., 2011. Inferring the structure and dynamics of interactions in schooling fish. Proceedings of the National Academy of Sciences 108, 18720–18725. https://doi.org/10.1073/pnas.1107583108

Kraft, S., Winkler, A.C., Abecasis, D., 2023. Small coastal marine protected areas offer recurring, seasonal protection to the common stingray (*Dasyatis pastinaca*). Ocean & Coastal Management 246, 106891. https://doi.org/10.1016/j.ocecoaman.2023.106891

Krause, J., Lusseau, D., James, R., 2009. Animal social networks: an introduction. Behavioral Ecology and Sociobiology 63, 967–973. https://doi.org/10.1007/s00265-009-0747-0

Krause, J., Wilson, A.D.M., Croft, D.P., 2011. New technology facilitates the study of social networks. Trends in Ecology & Evolution 26, 5–6. https://doi.org/10.1016/j.tree.2010.10.004

Last, P.R., Manjaji-Matsumoto, B.M., Naylor, G.J.P., White, W.T., 2016. Stingrays, family Dasyatidae, in: Last, P.R., White, William Toby, de Carvalho, M.R., Séret, B., Stehmann, M., Naylor, Gavin J. P., Marshall, L. (Eds.), Rays of the World. CSIRO Publishing, Clayton South VIC, pp. 522–618.

McInturf, A.G., Bowman, J., Schulte, J.M., Newton, K.C., Vigil, B., Honig, M., Pelletier, S., Cox, N., Lester, O., Cantor, M., Chapple, T.K., 2023. A unified paradigm for defining elasmobranch aggregations. ICES Journal of Marine Science 80, 1551–1566. https://doi.org/10.1093/icesjms/fsad099

Meese, E.N., Lowe, C.G., 2019. Finding a Resting Place: How Environmental Conditions Influence the Habitat Selection of Resting Batoids. Bulletin, Southern California Academy of Sciences 118, 87. https://doi.org/10.3160/0038-3872-118.2.87

Morey, G., Moranta, J., Riera, F., Grau, A.M., Morales-Nin, B., 2006. Elasmobranchs in trammel net fishery associated to marine reserves in the Balearic Islands (NW Mediterranean). Cybium 30, 125–132. https://doi.org/10.26028/cybium/2006-304supp-017

Morrissey, J.F., Gruber, S.H., 1993. Home Range of Juvenile Lemon Sharks, *Negaprion brevirostris*. Copeia 1993, 425. https://doi.org/10.2307/1447141

Mourier, J., Bass, N.C., Guttridge, T.L., Day, J., Brown, C., 2017. Does detection range matter for inferring social networks in a benthic shark using acoustic telemetry? Royal Society Open Science 4, 170485. https://doi.org/10.1098/rsos.170485

Mourier, J., Lédée, E., Guttridge, T., Jacoby, D.M.P., 2018. Network Analysis and Theory in Shark Ecology - Methods and Applications, in: Carrier, J., Heithaus, M., Simpfendorfer, C. (Eds.), Shark Research: Emerging Technologies and Applications for the Field and Laboratory. CRC Press, Boca Raton, USA, pp. 337–356.

Mourier, J., Vercelloni, J., Planes, S., 2012. Evidence of social communities in a spatially structured network of a free-ranging shark species. Animal Behaviour 83, 389–401. https://doi.org/10.1016/j.anbehav.2011.11.008

Mucientes, G.R., Queiroz, N., Sousa, L.L., Tarroso, P., Sims, D.W., 2009. Sexual segregation of pelagic sharks and the potential threat from fisheries. Biology Letters 5, 156–159. https://doi.org/10.1098/rsbl.2008.0761

Nosal, A., Caillat, A., Kisfaludy, E., Royer, M., Wegner, N., 2014. Aggregation behavior and seasonal philopatry in male and female leopard sharks *Triakis semifasciata* along the open coast of southern California, USA. Marine Ecology Progress Series 499, 157–175. https://doi.org/10.3354/meps10632

Oksanen, J., Simpson, G.L., Blanchet, F.G., Kindt, R., Legendre, P., Minchin, P.R., O'Hara, R.B., Solymos, P., Stevens, M.H.H., Szoecs, E., Wagner, H., Barbour, M., Bedward, M., Bolker, B., Borcard, D., Carvalho, G., Chirico, M., Caceres, M.D., Durand, S., Evangelista, H.B.A., FitzJohn, R., Friendly, M., Furneaux, B., Hannigan, G., Hill, M.O., Lahti, L., McGlinn, D., Ouellette, M.-H., Cunha, E.R., Smith, T., Stier, A., Braak, C.J.F.T., Weedon, J., 2022. vegan: Community Ecology Package.

Palacios, M.D., Stewart, J.D., Croll, D.A., Cronin, M.R., Trejo-Ramírez, A., Stevens, G.M.W., Lezama-Ochoa, N., Zilliacus, K.M., González−Armas, R., Notarbartolo Di Sciara, G., Galván−Magaña, F., 2023. Manta and devil ray aggregations: conservation challenges and developments in the field. Frontiers in Marine Science 10, 1148234. https://doi.org/10.3389/fmars.2023.1148234

Papastamatiou, Y.P., Bodey, T.W., Caselle, J.E., Bradley, D., Freeman, R., Friedlander, A.M., Jacoby, D.M.P., 2020. Multiyear social stability and social information use in reef sharks with diel fission–fusion dynamics. Proceedings of the Royal Society B: Biological Sciences 287, 20201063. https://doi.org/10.1098/rspb.2020.1063

Perryman, R.J.Y., Mourier, J., Venables, S.K., Tapilatu, R.F., Setyawan, E., Brown, C., 2022. Reef manta ray social dynamics depend on individual differences in behaviour. Animal Behaviour 191, 43–55. https://doi.org/10.1016/j.anbehav.2022.06.010

Perryman, R.J.Y., Venables, S.K., Tapilatu, R.F., Marshall, A.D., Brown, C., Franks, D.W., 2019. Social preferences and network structure in a population of reef manta rays. Behavioral Ecology and Sociobiology 73, 114. https://doi.org/10.1007/s00265-019-2720-x

Pini-Fitzsimmons, J., Knott, N.A., Brown, C., 2021. Heterarchy Reveals Social Organization of a Smooth Stingray (*Bathytoshia brevicaudata*) Population in a Provisioned Food Context. Frontiers in Marine Science 8, 641761. https://doi.org/10.3389/fmars.2021.641761

Plötz, J., Weidel, H., Bersch, M., 1991. Winter aggregations of marine mammals and birds in the north-eastern Weddell Sea pack ice. Polar Biology 11. https://doi.org/10.1007/BF00239022

Schluessel, V., Bleckmann, H., 2005. Spatial memory and orientation strategies in the elasmobranch *Potamotrygon motoro*. Journal of Comparative Physiology A 191, 695–706. https://doi.org/10.1007/s00359-005-0625-9

Semeniuk, C.A.D., Dill, L.M., 2006. Anti-Predator Benefits of Mixed-Species Groups of Cowtail Stingrays (*Pastinachus sephen*) and Whiprays (*Himantura uarnak*) at Rest. Ethology 112, 33–43. https://doi.org/10.1111/j.1439-0310.2006.01108.x

Semeniuk, C.A.D., Dill, L.M., 2005. Cost/benefit analysis of group and solitary resting in the cowtail stingray, *Pastinachus sephen*. Behavioral Ecology 16, 417–426. https://doi.org/10.1093/beheco/ari005

Simpfendorfer, C.A., Heupel, M.R., Hueter, R.E., 2002. Estimation of short-term centers of activity from an array of omnidirectional hydrophones and its use in studying animal movements. Canadian Journal of Fisheries and Aquatic Sciences 59, 23–32. https://doi.org/10.1139/f01-191

Sims, D.W., Southall, E.J., Quayle, V.A., Fox, A.M., 2000. Annual social behaviour of basking sharks associated with coastal front areas. Proceedings of the Royal Society B: Biological Sciences 267, 1897–1904. https://doi.org/10.1098/rspb.2000.1227

Snijders, L., Blumstein, D.T., Stanley, C.R., Franks, D.W., 2017. Animal Social Network Theory Can Help Wildlife Conservation. Trends in Ecology & Evolution 32, 567–577. https://doi.org/10.1016/j.tree.2017.05.005

Sosa, S., Sueur, C., Puga-Gonzalez, I., 2021. Network measures in animal social network analysis: Their strengths, limits, interpretations and uses. Methods in Ecology and Evolution 12, 10–21. https://doi.org/10.1111/2041-210X.13366

Spiegel, O., Leu, S.T., Bull, C.M., Sih, A., 2017. What's your move? Movement as a link between personality and spatial dynamics in animal populations. Ecological Letters 20, 3–18. https://doi.org/10.1111/ele.12708

Tanaka, H., Kohda, M., Frommen, J.G., 2018. Helpers increase the reproductive success of breeders in the cooperatively breeding cichlid *Neolamprologus obscurus*. Behavioral Ecology and Sociobiology 72, 152. https://doi.org/10.1007/s00265-018-2566-7

Thieurmel, B., Elmarhraoui, A., 2019. R Package "suncalc": compute sun position, sunlight phases, moon position and lunar phase.

Thonhauser, K.E., Gutnick, T., Byrne, R.A., Kral, K., Burghardt, G.M., Kuba, M.J., 2013. Social learning in Cartilaginous fish (stingrays *Potamotrygon falkneri*). Animal Cogniton 16, 927–932. https://doi.org/10.1007/s10071-013-0625-z

Thorpe, W.H., 1965. Learning and instinct in animals. Harvard University Press.

Villegas-Ríos, D., Claudet, J., Freitas, C., Moland, E., Thorbjørnsen, S.H., Alonso-Fernández, A., Olsen, E.M., 2021. Time at risk: Individual spatial behaviour drives effectiveness of marine protected areas and fitness. Biological Conservation 263, 109333. https://doi.org/10.1016/j.biocon.2021.109333

Villegas-Ríos, D., Jacoby, D.M.P., Mourier, J., 2022. Social networks and the conservation of fish. Communications Biology 5, 178. https://doi.org/10.1038/s42003-022-03138-w

Wearmouth, V.J., Sims, D.W., 2008. Chapter 2 Sexual Segregation in Marine Fish, Reptiles, Birds and Mammals, in: Advances in Marine Biology. Elsevier, pp. 107–170. https://doi.org/10.1016/S0065-2881(08)00002-3

Whitehead, H., Dufault, S., 1999. Techniques for analyzing vertebrate social structure using identified individuals: review and recommendations. Advances in the study of behavior 28, 33–74.

Wilson, J.A., Giske, J., 2023. Does fishing dismantle fish culture and ecosystem structure? Questions about the implications of social learning among fish and fishers. Fish and Fisheries 24, 889–895. https://doi.org/10.1111/faf.12755

6.6 Supplementary material

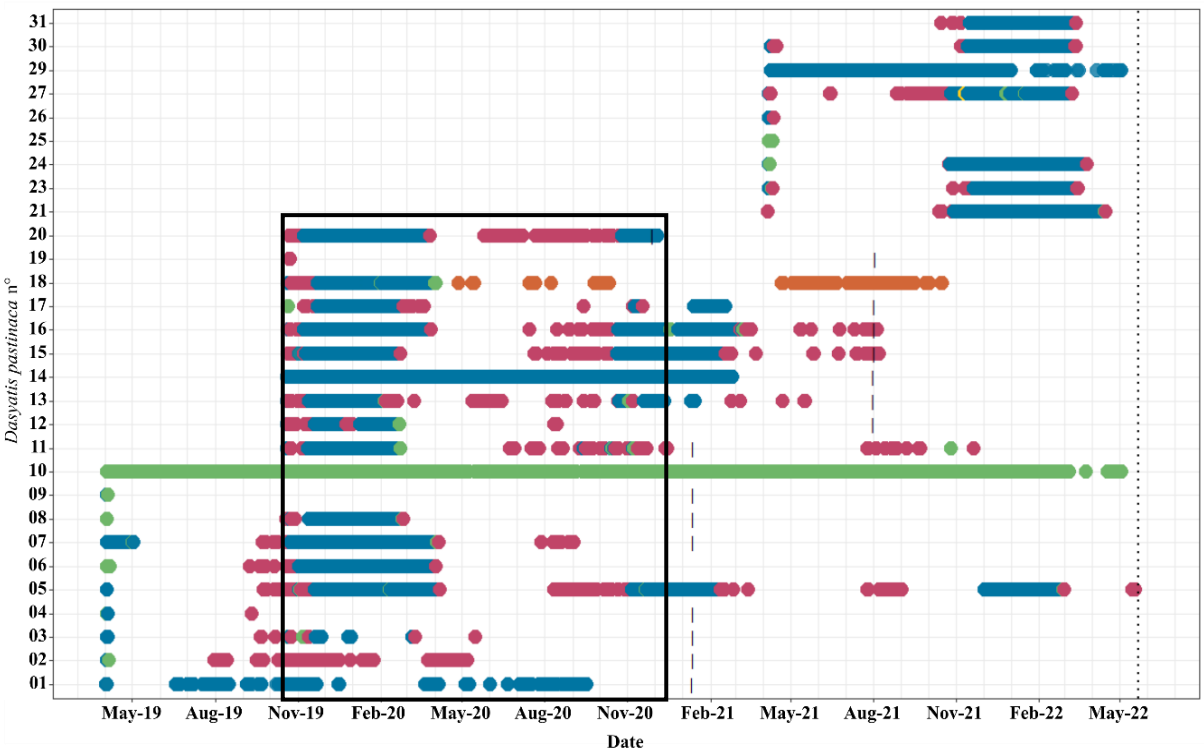

Supplementary material 6.1: Full detection plot of *Dasyatis pastinaca* used by Kraft et al. (2023) from which the data subset was extracted (black rectangle). Detections are colour coded: full protection area in blue, partial protection areas in green, buffer area in yellow, Sado estuary in red, and Tejo estuary in orange. Vertical lines indicate tag expiration dates, and the vertical dotted line indicates the end of the study. Dp 01, 02, 10 and 14 were not included because they died during the study.

Supplementary material 6.2: Results of the Generalized Linear Mixed-Effects Model evaluating the variation of *Dasyatis pastinaca* group size with diel phase, with receiver as random effect.

Generalized Linear Mixed-Effects model fit by maximum likelihood
(Laplace Approximation)
Family: poisson (log)
Formula: group_size ~ dielphase + (1 | receiver)

Random effects:

Group Name	Variance	Std.Dev.
Receiver (Intercept)	0.07343	0.271

Number of obs: 119167; groups: Receiver, 27

Fixed effects:

	Estimate	Std. Error	z value	p(>|z|)
Daytime (Intercept)	0.366494	0.056848	6.447	1.14E-10
Night	-0.03236	0.004593	-7.047	1.83E-12
Twilight	-0.00877	0.006818	-1.287	0.198

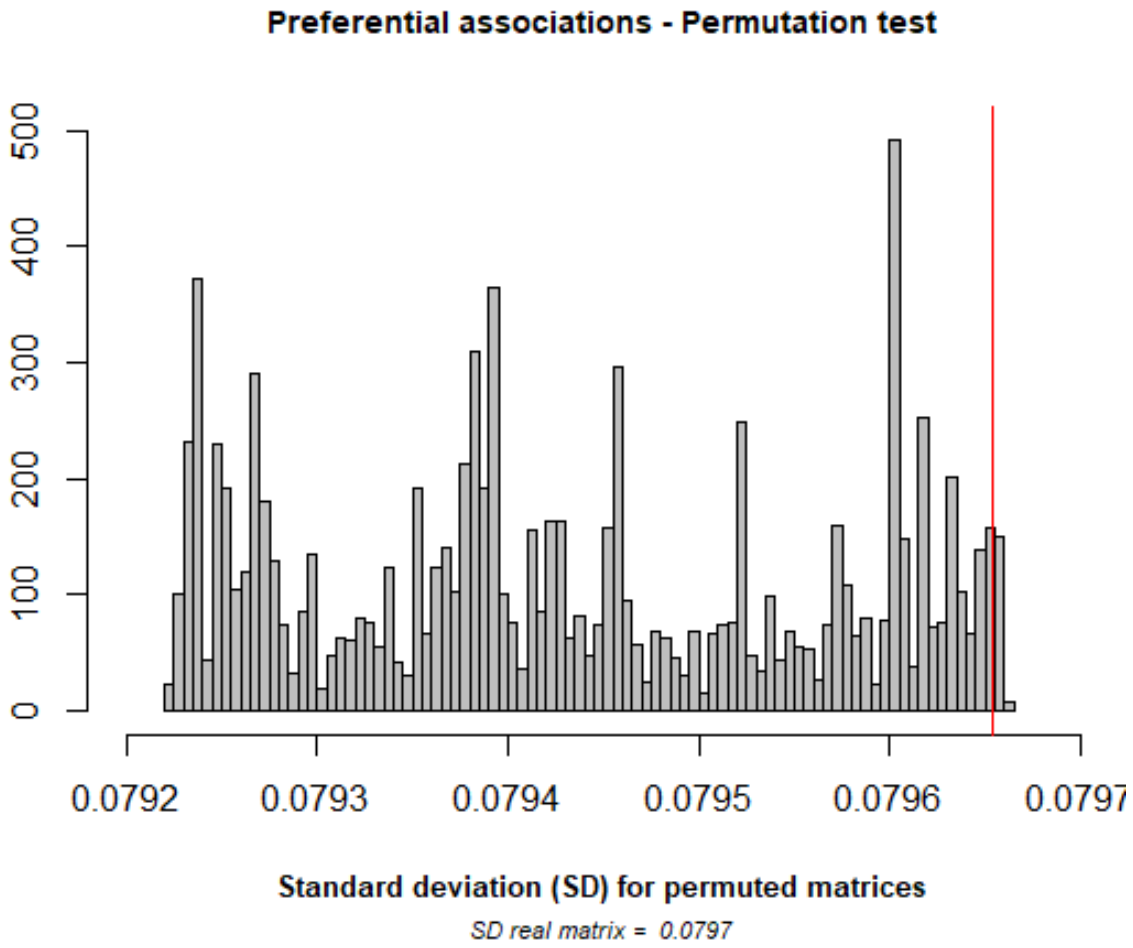

Supplementary material 6.3: Histogram showing the distribution of the standard deviation for the 10000 randomized association matrices (grey bars) and the observed association matrix (red line).

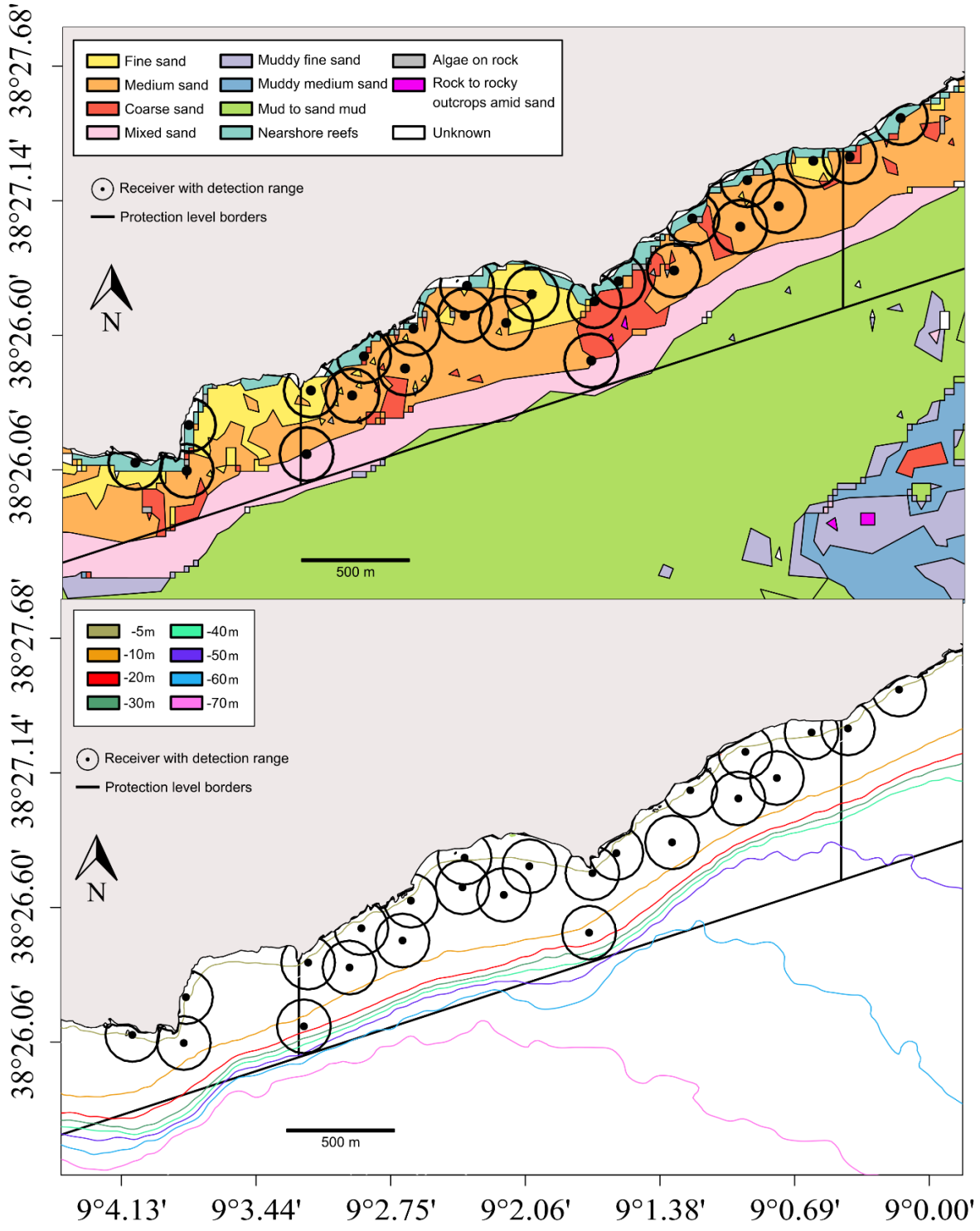

Supplementary material 6.4: Habitat types (top panel) and bathymetry (bottom panel) in the full protection area and adjacent partial protection areas of the Luíz Saldanha Marine Park. Habitat types and isobaths are colour-coded, and the receivers, their detection range (200 m), and each protection level's borders are also indicated.

Chapter 7

General discussion

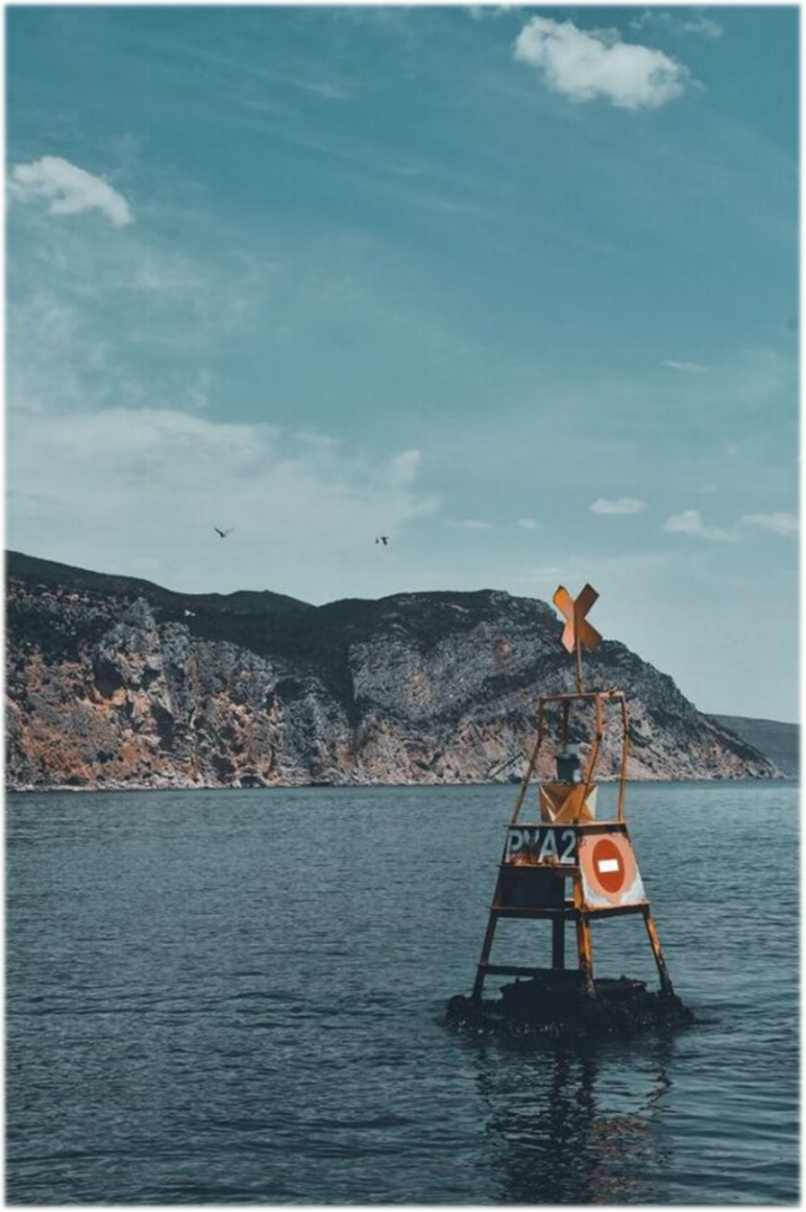

PNA2, limit of the Luíz Saldanha Marine Park
© Kim Birnie-Gauvin

7.1 General discussion

Understanding the movement ecology of elasmobranchs is key to improve the effectiveness of spatial conservation and management strategies like MPAs (Allen and Singh, 2016). However, the significance of this data is in stark contrast with its availability for such ends (Hyde et al., 2022; Siskey et al., 2019). In light of this, this study used acoustic telemetry data sets on batoids, with some individuals tracked for up to three-years, to contribute to the general understanding of their spatial ecology. Thanks to the long-term monitoring of the species, important aspects of their movements were characterized, like yearly seasonal return migrations and long-term residencies in the LSMP, and the contribution of coastal MPAs to their protection was evaluated. Other highlights of this study include the production of a guide to the use of residence and space use estimators, the first results on the large- and small-scale movements of the viviparous *D. pastinaca* and non-random associations among individuals of this species using social network analysis, the expansion of the limited knowledge on the spatial ecology of the Critically Endangered *Rostroraja alba*, and contribution with new information for southern Europe on the movement patterns of the globally heavily exploited *Raja clavata*. This also responds to the pressing need for more region-specific movement data on elasmobranchs to guide their protection efforts under MPAs (van Zinnicq Bergmann et al., 2022).

7.1.1 Space use

In general terms, one of the most noticeable species-level differences was the low average residency of *D. pastinaca*, attributed to its seasonal variation in presence. This contrasted with the higher and more stable residencies of *Raja clavata* and *Rostroraja alba*. However, the latter two species displayed important demographic differences that were not as prevalent in *D. pastinaca*. Although the males of *D. pastinaca* presented higher residencies than females, both sexes were evenly represented in the sample and conducted similar movement patterns. On the other hand, important sex-based differences were noted in *Raja clavata*, which likely reflects overarching differences in the distribution of each sex in this species. In the case of *Rostroraja alba*, because immature individuals composed almost the entire sample, the LSMP likely provides greater protection to this segment of the population, suggesting a potential nursery area role.

The presence of resident and migrant individuals throughout all species was also an interesting finding. This kind of variability in migratory patterns is known as partial migration

and, while it is commonplace among fishes, has been historically seldomly investigated in elasmobranchs (Chapman et al., 2012, 2015). Other movement patterns were common to most individuals of the three species. This includes the diel changes in activity and area of use, which were greater during the night and twilight hours and subsided during the day, and the vertical migration pattern noted in individuals for which depth data was available. These activity patterns are observed in other elasmobranchs as well, and are associated to their predatory habits while also serving as a predator avoidance strategy (Hammerschlag et al., 2016; Humphries et al., 2017).

The residency and depth results of this thesis, along with other studies, e.g., (Humphries et al., 2016; Hunter et al., 2006; Thorburn et al., 2021), provide evidence that challenges the misconception of skates as chiefly deep-water species. These studies have shown how several species of this group inhabit shallow coastal areas either seasonally or year-round for various purposes such as reproduction and as nursery areas. This highlights coastal MPAs as a tool that may be providing skates with more protection than initially assumed, especially in cases when MPAs are in areas that are key to their life cycle. To further explore this, tagging studies could be conducted in unevaluated coastal MPAs to incorporate them into local conservation efforts.

Finally, the use of long-term data to study the aggregations and associations of *Dasyatis pastinaca* revealed that species can present spatial patterns at several levels, coupling seasonal, long-range migration patterns with small-scale spatial organization and active partner choice. Although evidence of sociality in elasmobranchs is rising, this is still a growing area of research (Jacoby et al., 2012).

7.1.2 Conservation and management

7.1.2.1 Diversity in movement patterns

Studying the spatial ecology of multiple species allows to obtain a fuller picture of the existing variability in movement patterns, which in turn can be used to better develop protection efforts (Abecasis et al., 2014). One of the most common protection indicators used is time spent within an MPA (Kramer and Chapman, 1999), calculated here as a residency index. While the average species-level residency indices of *Raja clavata* and *Rostroraja alba* suggest they receive more protection than *D. pastinaca*, the previously mentioned intra-specific variations in *Raja clavata* and *Rostroraja alba* indicate that important demographic differences in protection are also present in each species. The sex-based differences noted in *Raja clavata* indicate protection in the LSMP may be biased towards males, while for *Rostroraja alba* this

appeared to be the case for immature individuals. Considering that few females of *Raja clavata* and adults of *Rostroraja alba* were captured, these could be found in deeper areas. If future studies investigating their space use indicate this to be the case, an expansion of the protection area or the creation of new ones to cover deeper sites can be proposed (expanded in section 7.1.3 Limitations and future directions). This would likely improve the contribution of the marine park to the protection of these less sheltered demographic segments and the overall effect of the LSMP for elasmobranch conservation. Additionally, in the particular case of *D. pastinaca*, this species would benefit from a protected corridor connecting the LSMP and Sado because of their seasonal and predictable exposure during migration (discussed further ahead).

The study of aggregations and associations showed that individual risk can also hinge on the finer-scale distribution of individuals in a population, which can be driven by social and asocial factors. This study showed that some *D. pastinaca* individuals appear to actively associate and do not randomly distribute in space, which is important to incorporate into management and conservation decisions. In populations with such dynamics, the effects of excessive extraction are not limited to the reduction of the number of individuals, but also to the loss of important components that contain and propagate relevant information for the survival and adaptability of a population, such as migration routes, hunting strategies, and location of food patches (Villegas-Ríos et al., 2022; Wilson and Giske, 2023).

In addition to studying multiple species, understanding the intra-species variability in movement is also key to improve protection (Chin et al., 2022; Villegas-Ríos et al., 2021). For example, if individuals of a species are under uneven protection scenarios, it can lead to selective fishing pressures on a population (Andersen et al., 2018) and even have evolutionary repercussions (Villegas-Ríos et al., 2017). In the case of passive fishing gear, which is commonly used in this area and other coastal regions in the form of trammel nets and longlines, it may bias captures towards more mobile individuals (Andersen et al., 2018). In this sense, the presence of resident and migrant individuals is also relevant to assess because the former will generally receive more protection than migratory individuals when centred inside an MPA (Villegas-Ríos et al., 2021).

Finally, the diel changes in activity and area of use that were detected in all species (Figure 7.1) can result in increased encounter rates with passive fishing gear during the hours of lower light conditions (Hammerschlag et al., 2016; Uusiheikkila et al., 2008). This, in turn, highlights the time windows during which elasmobranchs in general have a potentially greater risk exposure to fishing.

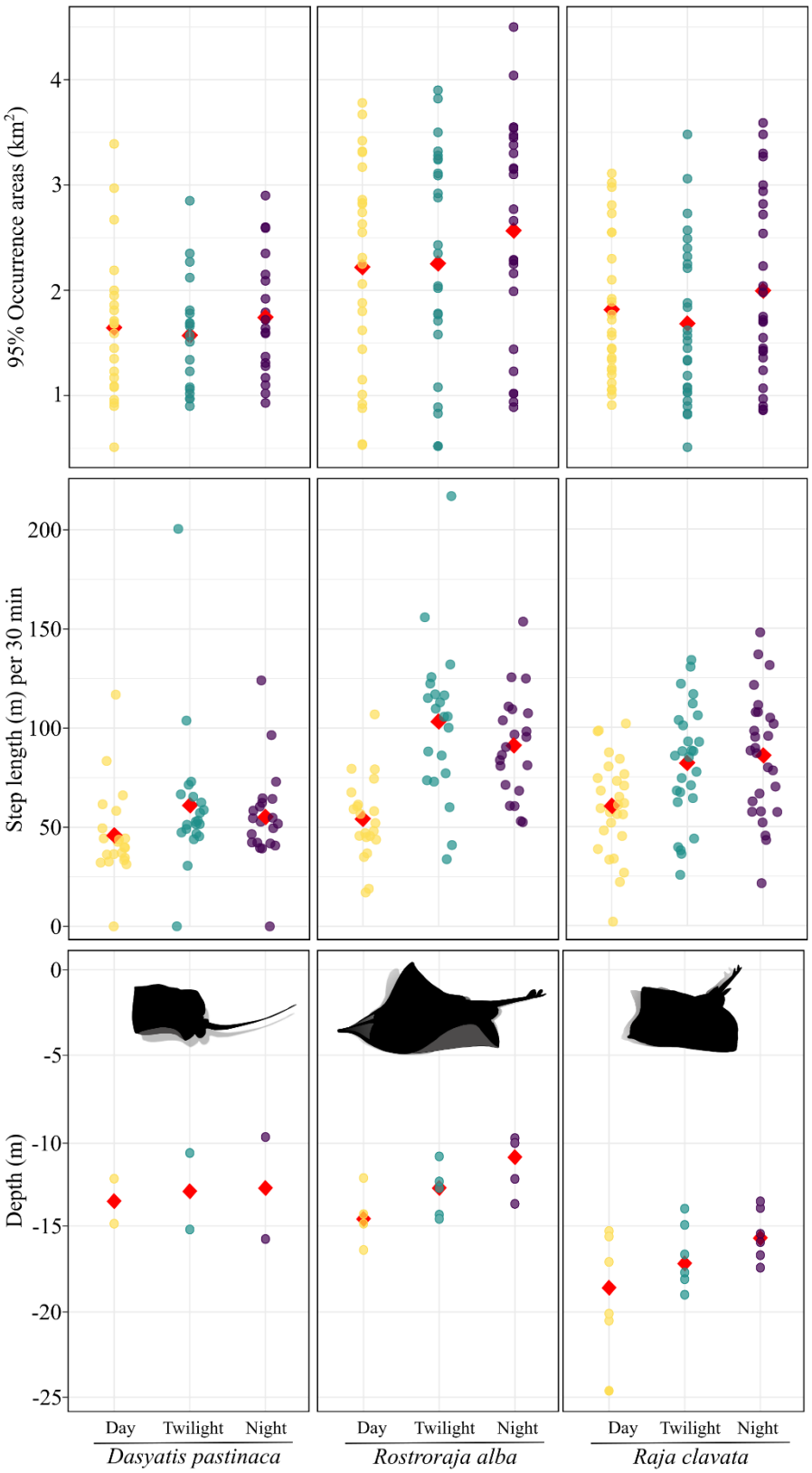

Figure 7.1: Summary of the diel patterns detected in 95% occurrence areas (top panels), activity (center panels) and depth (lower panels) for all studied individuals of the three batoid species. Red diamonds indicate averages per species per diel phase: daytime (yellow), twilight (green) and night (purple).

7.1.2.2 Human aspects of elasmobranch conservation

Understanding how humans interact with elasmobranchs also helps to improve their protection, to secure the livelihoods of local people (Simpfendorfer et al., 2011), and to increase the effectiveness of MPAs, as proper management of its biological and social factors is central (MacKeracher et al., 2019). Among the important aspects to monitor are the changes in fishing practices that arise after the establishment of an MPA. This is particularly relevant when important ports occur nearby, which in the case of the LSMP corresponds to two of the most important landing sites of elasmobranchs in Portugal, Sesimbra and Setúbal (Baeta et al., 2010; Figueiredo et al., 2020). The reaction of a fishery to the implementation of an MPA will depend on its characteristics; the target species can be changed, fishing can be moved to another area if the former fishing grounds are now protected, and even illegal fishing can be adopted as a mean to maintain income (Batista et al., 2011; Horta e Costa et al., 2013). A practice that usually occurs after the establishment of an MPA is to fish close to its border (i.e., "fishing the line"), which has been reported in the LSMP (Horta e Costa et al., 2013). On the other hand, illegal fishing is also known to occur, as illegal fishing gear has been confiscated (Cunha et al., 2011), and is considered a management problem by local fishers (Martínez-Ramírez et al., 2021; Pita et al., 2020). Overlaying these activities with the results of spatial ecology studies such as this can help in identifying areas and times where their probability of interaction is greatest, allowing management strategies to be adapted accordingly.

In addition to fishing, the values and attitudes people hold towards elasmobranchs can also be significant points of action for the protection of these species, as these perceptions can tangibly affect conservation efforts (Simpfendorfer et al., 2011). The group of people that interact the most with elasmobranchs are fishers, whether industrial, artisanal, or recreational, and therefore are vital to consider in this regard. A study that interviewed fishers in the port of Sesimbra reported an apparent lack of awareness about certain aspects of the biology and conservation of elasmobranchs, like their reproductive seasons and state of populations, and closing this knowledge gap could improve current conservation efforts (Silva et al., 2021). For example, changes in attitudes towards elasmobranch conservation after the inclusion of fishers into research projects have been noted in other areas, which increased their willingness to report incidental catches, follow regulations (landing animals whole, release animals that are landed alive), and improve their communication with researchers (Giareta et al., 2021). These factors, combined with an improved understanding of the spatial ecology of elasmobranchs, are

important to consider for the success of the LSMP's conservation goals and of that of any MPA that is used to protect elasmobranchs.

7.1.2.3 Connectivity of protected areas

Beyond the borders of a marine park, one important consideration is connectivity with other sites. In the case of the LSMP, the ubiquitous seasonal movement of *D. pastinaca*, and to a lesser degree *Raja clavata* (one individual), showed a strong link of the LSMP with the Sado estuary (Figure 7.1). This migratory route is not exclusive to elasmobranchs, as *Sepia officinalis* performs a similar seasonal reproductive migration (Abecasis et al., 2013), as their abundance increases during spring and summer when they reproduce, and almost completely depart the estuary in winter (Batista et al., 2009; Neves et al., 2009). A natural reserve is in place in this estuary, the Reserva Natural do Estuário do Sado, therefore future protection efforts could focus on establishing seasonal protected corridors. The importance of the Tejo estuary was lower in comparison, likely because of its distance from the LSMP. However, it was shown that at least one *D. pastinaca* travelled and relocated to this area, suggesting some level of connectivity.

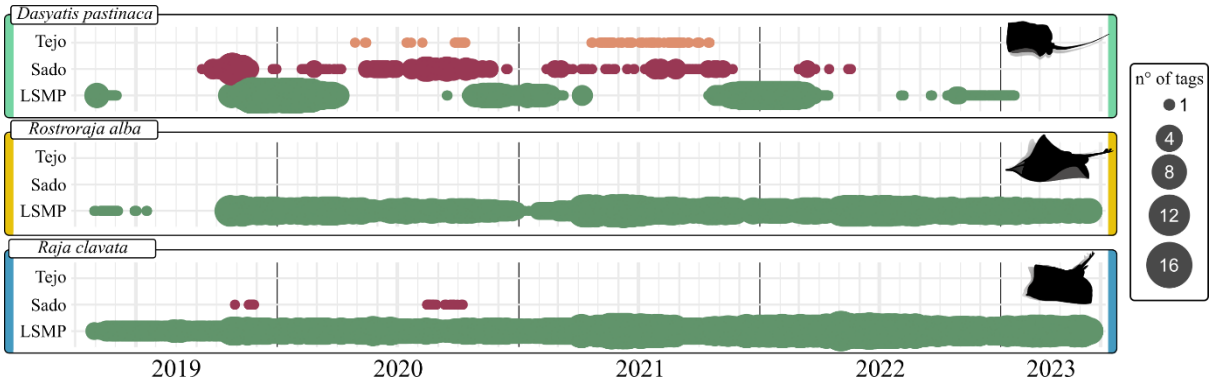

Figure 7.2: Study-wide detections of all individuals of the three batoid species across the three surveyed areas: Luiz Saldanha Marine Park (green), Sado estuary (red) and Tejo estuary (orange). Circle size is proportional to the number of individuals (tags) detected each day.

The effectiveness of MPAs generally improves when they operate as a network instead of in isolation, especially when protecting species of high vagility like many elasmobranchs (Heupel et al., 2015). Prime examples of the benefits of marine reserve networks have been long produced in the Australian Great Barrier Reef, benefitting species and ecosystem health alike (McCook et al., 2010). Similar proposals to extend MPA boundaries and connecting MPAs into networks to safeguard more of a species' movements and habitats have been made

elsewhere, some with successful implementation (Espinoza et al., 2015; Lea et al., 2016). In turn, the results of the present study further emphasize the significance of surveying for key areas nearby MPAs and to consider these for the improvement of species protection. This is particularly important for coastal MPAs, as these are usually placed in areas of great anthropogenic activity. Coastal areas concentrate most of the human population (Small and Nicholls, 2003) which has resulted in intensive coastal development, habitat degradation and destruction, resource exploitation and pollution (Halpern et al., 2008; Lloret et al., 2018).

7.1.2.4 Application of new data

Newly acquired information on spatial ecology can be included into the management practices of MPAs, to improve its performance using an adaptive management process (Bunnell et al., 2009). This is a fundamental component of the long-term success of MPAs (Allen and Singh, 2016; Grafton and Kompas, 2005). As previously done with data on commercially important species of cuttlefish and bony fishes (Abecasis et al., 2014), the information here presented can further contribute to the marine park's goals using this new data on three elasmobranch species. To contextualize this, the framework developed by Chin et al., (2022) can be followed to identify the stages at which this data is useful. This framework uses the financial concept of portfolio risk to describe four categories in this process: assessment context, asset portfolio, portfolio risk, and insurance and mitigation, and acoustic telemetry can provide valuable information for the latter three. In this context, the assets are the species and its attributes, like their spatial and behavioural characteristics, reproductive traits, conservation status, and others. In this thesis, the spatial characteristics of three assets of the LSMP were explored, their residency, occurrence areas, activity, and some depth, and how these changed over time. Portfolio risk describes the exposure and sensitivity of species to the identified threats (like fishing), for which acoustic telemetry can also be useful. Finally, insurance and mitigation describe the effects of management interventions, like establishing an MPA. In this part, acoustic telemetry can measure the overlap of the protected area with the distribution and movements of the local human population.

Spatial management instruments such as MPAs also are an important complement to traditional fishing management approaches. While the former focus on a defined area, the latter are implemented on a larger scale as they set regulations on the fishing activity as a whole, for example through size limits, species bans or temporal bans. MPAs provide advantages that are missed by traditional fishing management. They have an ecosystemic approach, meaning that their implementation not only protects species but also the habitats found inside their protected

boundaries. Secondly, MPAs can protect important environments (such as reproduction or feeding areas) and greatly reduce illegal or unreported activities if properly enforced, which is more difficult to control in other contexts, such as a vessel capturing a prohibited species or size class in an unprotected area, but which is discarded and unreported when returning to port.

7.1.3 Limitations and future directions

One of the main constraints of most acoustic telemetry studies is the limitation of tracking capabilities of the array. The array used in the present study has changed in shape since its establishment in 2010, as it was expanded by the inclusion of new receivers and reduced by the removal of others, therefore the present shape of the array is a result of several factors. Some receivers were removed because few to no detections were obtained, indicating that not all areas in this marine park are equally used. Receivers have also been lost to environmental factors and human activities. For example, the external portion of the LSMP is a sandy area exposed to strong currents where some receivers have been quickly buried, reducing their listening power, and even resulting in their loss. Other receivers have been lost to illegal fishing activities, as these can get tangled in fishing gear inside the protected area (Abecasis et al., 2013).

Therefore, although the most relevant area of the LSMP was well covered and the data needed to answer the research questions was gathered, these results are still tied to the areas that were under receiver coverage. This is especially important to consider for the depth results, as the study species are known to occur much deeper than the range of the array. Although the depth readings were mostly concentrated in shallower waters, some individuals reached depths close to the tag's depth limit. The low number of deeper occurrences could be from genuine depth preferences (Humphries et al., 2016), but it could also be an outcome of a lower coverage at deeper sites. To address some of the gaps in the current knowledge and obtain a fuller understanding of the depth preferences of these species, complementary approaches can be suggested. For example, acoustic receivers with remote release systems could be deployed at deeper sites, as these do not require researchers to physically reach the receivers to retrieve it. Alternatively, data-loggers such as data storage tags (DSTs) could be employed, as it has been successfully done on batoids (Humphries et al., 2017, 2016; Hunter et al., 2006, 2005). DSTs are programmed to record depth and temperature at a predefined interval and enclosed in a buoyant case which is externally attached to an individual. Another alternative for larger individuals could be the use of pop-up satellite archival tags (PSATs), which are anchored into the muscle tissue and can be programmed to release and float to the surface. These tags can

collect data on depth, temperature, and light conditions, which can be used as a proxy of geographic position. Once at the surface, information summaries start to be emitted via satellite. PSATs have also been used to track the movements and depth preferences of large sized batoids (Farrugia et al., 2016; Le Port et al., 2008). Although these tags need to be recovered to access the data, they are not tethered to the detection range of an acoustic array and could therefore more confidently reflect true depth preferences. Additionally, other meaningful information can be obtained, like temperature to study the thermal preferences.

Future efforts could be focused on specifically targeting some of the less protected demographic segments of *Rostroraja alba* and *Raja clavata* that were not well covered (adults and females, respectively). For this, some improvements to the fishing process could be introduced to reduce the mortality rate. In the present study, the trammel nets that were used depended on the availability and expertise of a local fisherman, yet this method may not be the best fit for a study of these characteristics. On the other hand, because of field work related limitations (weather conditions, availability of personnel, equipment and boat), longline deployments and acoustic receiver servicing were scheduled together. If the conditions can be met, these tasks could be separated in the future to reduce the soaking time of the fishing gear and retrieve it in good light conditions (i.e., not having to wait until the next day). Individuals that are not large enough to carry PSATs could be fitted with DSTs. The latter type of tag is also an option to use in combination with PSATs considering their higher price. The use of DSTs can also be particularly insightful to study the temperature preferences of *D. pastinaca*, a species of small to medium size and with a marked seasonal migration. Because temperature can have a major influence in the gestation process and the movements of stingrays during reproduction (Jirik and Lowe, 2012), studying their thermal preferences could improve our understanding of their reproduction cycle, coupled with surveys for pregnant *D. pastinaca* and neonate or juvenile stingrays. Similarly, since all individuals included in this thesis were tagged in the LSMP, and mostly showed fidelity to this area, expanding the tagging efforts to include other sites, such as the Sado estuary, could reveal whether individuals of these species also show fidelity to other areas.

Finally, another effective way of addressing the geographical limitations of acoustic telemetry studies is by establishing large-scale networks through collaborations among researchers from different groups (Abecasis et al., 2018; Ellis et al., 2019). The integration of geographically separated arrays into one interconnected network greatly expands the reach of studies, increasing the likelihood of detecting long-distance movements of tagged individuals and other important sites to protect. An example of such an effort is the European Tracking

Network (ETN[11]), through which the detections from the Tejo estuary were obtained. Similarly, analogous initiatives exist around the world, indicating that the advantages of large scale collaborations are increasingly being recognized in recent years (Cooke et al., 2011; Cowley et al., 2017; Currier et al., 2015; Steckenreuter et al., 2017).

7.2 General conclusions

The use of acoustic telemetry has allowed a greater understanding of the inter- and intra-specific differences in spatial ecology and the complex fine scales that batoids can present (Mourier et al., 2012; Perryman et al., 2022; Siskey et al., 2019). This is a growing field, not only in the study of animal movement, but also as a tool to design, evaluate, and improve the MPAs used to secure the existence of many marine species and habitats. With this thesis, contributions were made in the form of a methodological review on the use of acoustic telemetry data to estimate space use and residency metrics (Kraft et al., 2023a), space use of three species of batoids (Kraft et al., 2023; Kraft et al., 2024a; Kraft et al., 2024b) and the exploratory application of social network analysis (Kraft et al., 2024c), a field that can still be considered as novel in the study of elasmobranchs. The methodological review presented in the second chapter of this thesis will contribute greatly to the field, to new and more experienced researchers that look for possible ways to use this kind of data to answer their research questions, while the results presented on *D. pastinaca*, *R. clavata* and *R. alba* will serve to better understand the variety and patterns of movements in this important group, and to improve the LSMP's mission in protecting marine species and environments. This information was collected for over three years, providing a robust overlook on the spatial ecology of these species, which proves key to support conservation and management plans in the LSMP and other coastal MPAs where these species occur.

[11] https://www.europeantrackingnetwork.org/en

7.3 References

Abecasis, D., Afonso, P., Erzini, K., 2014. Combining multispecies home range and distribution models aids assessment of MPA effectiveness. Marine Ecology Progress Series 513, 155–169. https://doi.org/10.3354/meps10987

Abecasis, D., Afonso, P., O'Dor, R.K., Erzini, K., 2013. Small MPAs do not protect cuttlefish (*Sepia officinalis*). Fisheries Research 147, 196–201. https://doi.org/10.1016/j.fishres.2013.05.004

Abecasis, D., Steckenreuter, A., Reubens, J., Aarestrup, K., Alós, J., Badalamenti, F., Bajona, L., Boylan, P., Deneudt, K., Greenberg, L., Brevé, N., Hernández, F., Humphries, N., Meyer, C., Sims, D., Thorstad, E.B., Walker, A.M., Whoriskey, F., Afonso, P., 2018. A review of acoustic telemetry in Europe and the need for a regional aquatic telemetry network. Animal Biotelemetry 6, 12. https://doi.org/10.1186/s40317-018-0156-0

Allen, A.M., Singh, N.J., 2016. Linking Movement Ecology with Wildlife Management and Conservation. Frontiers in Ecology and Evolution 3, 155. https://doi.org/10.3389/fevo.2015.00155

Andersen, K.H., Marty, L., Arlinghaus, R., 2018. Evolution of boldness and life history in response to selective harvesting. Canadian Journal of Fisheries and Aquatic Sciences 75, 271–281. https://doi.org/10.1139/cjfas-2016-0350

Baeta, F., Batista, M., Maia, A., Costa, M.J., Cabral, H., 2010. Elasmobranch bycatch in a trammel net fishery in the Portuguese west coast. Fisheries Research 102, 123–129. https://doi.org/10.1016/j.fishres.2009.10.016

Batista, M.I., Baeta, F., Costa, M.J., Cabral, H.N., 2011. MPA as management tools for small-scale fisheries: The case study of Arrábida Marine Protected Area (Portugal). Ocean & Coastal Management 54, 137–147. https://doi.org/10.1016/j.ocecoaman.2010.10.032

Batista, M.I., Teixeira, C.M., Cabral, H.N., 2009. Catches of target species and bycatches of an artisanal fishery: The case study of a trammel net fishery in the Portuguese coast. Fisheries Research 100, 167–177. https://doi.org/10.1016/j.fishres.2009.07.007

Bunnell, F.L., Dunsworth, G.B., Huggard, D.J., Kremsater, L.L., 2009. The problem, in: Forestry and Biodiversity: Learning How to Sustain Biodiversity in Managed Forests. University of British Columbia Press, Vancouver, BC.

Chapman, B.B., Skov, C., Hulthén, K., Brodersen, J., Nilsson, P.A., Hansson, L. -A., Brönmark, C., 2012. Partial migration in fishes: definitions, methodologies and taxonomic distribution. Journal of Fish Biology 81, 479–499. https://doi.org/10.1111/j.1095-8649.2012.03349.x

Chapman, D.D., Feldheim, K.A., Papastamatiou, Y.P., Hueter, R.E., 2015. There and Back Again: A Review of Residency and Return Migrations in Sharks, with Implications for Population Structure and Management. Annual Review of Marine Science 7, 547–570. https://doi.org/10.1146/annurev-marine-010814-015730

Chin, A., Molloy, F.J., Cameron, D., Day, J.C., Cramp, J., Gerhardt, K.G., Heupel, M.R., Read, M., Simpfendorfer, C.A., 2022. Conceptual frameworks and key questions for assessing the contribution of marine protected areas to shark and ray conservation. Conservation Biology cobi.13917. https://doi.org/10.1111/cobi.13917

Cooke, S.J., Iverson, S.J., Stokesbury, M.J.W., Hinch, S.G., Fisk, A.T., VanderZwaag, D.L., Apostle, R., Whoriskey, F., 2011. Ocean Tracking Network Canada: A Network Approach to Addressing Critical Issues in Fisheries and Resource Management with Implications for Ocean Governance. Fisheries 36, 583–592. https://doi.org/10.1080/03632415.2011.633464

Cowley, P., Bennett, R., Childs, A.-R., Murray, T., 2017. Reflection on the first five years of South Africa's Acoustic Tracking Array Platform (ATAP): status, challenges and opportunities. African Journal of Marine Science 39, 363–372. https://doi.org/10.2989/1814232X.2017.1399927

Currier, R., Kirkpatrick, B., Simoniello, C., Lowerre-Barbieri, S., Bickford, J., 2015. iTAG: Developing a cloud based, collaborative animal tracking network in the Gulf of Mexico, in: OCEANS 2015 - MTS/IEEE Washington. IEEE, Washington, DC, pp. 1–3. https://doi.org/10.23919/OCEANS.2015.7401864

Ellis, R.D., Flaherty-Walia, K.E., Collins, A.B., Bickford, J.W., Boucek, R., Walters Burnsed, S.L., Lowerre-Barbieri, S.K., 2019. Acoustic telemetry array evolution: From species- and project-specific designs to large-scale, multispecies, cooperative networks. Fisheries Research 209, 186–195. https://doi.org/10.1016/j.fishres.2018.09.015

Espinoza, M., Lédée, E.J.I., Simpfendorfer, C.A., Tobin, A.J., Heupel, M.R., 2015. Contrasting movements and connectivity of reef-associated sharks using acoustic telemetry: implications for management. Ecological Applications 25, 2101–2118. https://doi.org/10.1890/14-2293.1

Farrugia, T., Goldman, K., Tribuzio, C., Seitz, A., 2016. First use of satellite tags to examine movement and habitat use of big skates *Beringraja binoculata* in the Gulf of Alaska. Marine Ecology Progress Series 556, 209–221. https://doi.org/10.3354/meps11842

Figueiredo, I., Maia, C., Lagarto, N., Serra-Pereira, B., 2020. Bycatch estimation of Rajiformes in multispecies and multigear fisheries. Fisheries Research 232, 105727. https://doi.org/10.1016/j.fishres.2020.105727

Giareta, E.P., Prado, A.C., Leite, R.D., Padilha, É., Santos, I.H.D., Wosiak, C.D.C.D.L., Wosnick, N., 2021. Fishermen's participation in research and conservation of coastal elasmobranchs. Ocean & Coastal Management 199, 105421. https://doi.org/10.1016/j.ocecoaman.2020.105421

Grafton, R.Q., Kompas, T., 2005. Uncertainty and the active adaptive management of marine reserves. Marine Policy 29, 471–479. https://doi.org/10.1016/j.marpol.2004.07.006

Halpern, B.S., Walbridge, S., Selkoe, K.A., Kappel, C.V., Micheli, F., D'Agrosa, C., Bruno, J.F., Casey, K.S., Ebert, C., Fox, H.E., Fujita, R., Heinemann, D., Lenihan, H.S., Madin, E.M.P., Perry, M.T., Selig, E.R., Spalding, M., Steneck, R., Watson, R., 2008. A Global Map of Human Impact on Marine Ecosystems. Science 319, 948–952. https://doi.org/10.1126/science.1149345

Hammerschlag, N., Skubel, R.A., Calich, H., Nelson, E.R., Shiffman, D.S., Wester, J., Macdonald, C.C., Cain, S., Jennings, L., Enchelmaier, A., Gallagher, A.J., 2016. Nocturnal and crepuscular behavior in elasmobranchs: a review of movement, habitat use, foraging, and reproduction in the dark. Bulletin of Marine Science 93, 355–374. https://doi.org/10.5343/bms.2016.1046

Heupel, M.R., Simpfendorfer, C.A., Espinoza, M., Smoothey, A.F., Tobin, A., Peddemors, V., 2015. Conservation challenges of sharks with continental scale migrations. Frontiers in Marine Science 2. https://doi.org/10.3389/fmars.2015.00012

Horta e Costa, B., Batista, M.I., Gonçalves, L., Erzini, K., Caselle, J.E., Cabral, H.N., Gonçalves, E.J., 2013. Fishers' Behaviour in Response to the Implementation of a Marine Protected Area. PLoS ONE 8, e65057. https://doi.org/10.1371/journal.pone.0065057

Humphries, N., Simpson, S., Sims, D., 2017. Diel vertical migration and central place foraging in benthic predators. Marine Ecology Progress Series 582, 163–180. https://doi.org/10.3354/meps12324

Humphries, N., Simpson, S., Wearmouth, V., Sims, D., 2016. Two's company, three's a crowd: fine-scale habitat partitioning by depth among sympatric species of marine mesopredator. Marine Ecology Progress Series 561, 173–187. https://doi.org/10.3354/meps11937

Hunter, E., Berry, F., Buckley, A.A., Stewart, C., Metcalfe, J.D., 2006. Seasonal migration of thornback rays and implications for closure management: Ray migration and closure management. Journal of Applied Ecology 43, 710–720. https://doi.org/10.1111/j.1365-2664.2006.01194.x

Hunter, E., Buckley, A.A., Stewart, C., Metcalfe, J.D., 2005. Repeated seasonal migration by a thornback ray in the southern North Sea. Journal of the Marine Biological Association UK 85, 1199–1200. https://doi.org/10.1017/S0025315405012300

Hyde, C.A., Notarbartolo di Sciara, G., Sorrentino, L., Boyd, C., Finucci, B., Fowler, S.L., Kyne, P.M., Leurs, G., Simpfendorfer, C.A., Tetley, M.J., Womersley, F., Jabado, R.W., 2022. Putting sharks on the map: A global standard for improving shark area-based conservation. Frontiers in Marine Science 9, 968853. https://doi.org/10.3389/fmars.2022.968853

Jacoby, D.M.P., Croft, D.P., Sims, D.W., 2012. Social behaviour in sharks and rays: analysis, patterns and implications for conservation: Shark social behaviour. Fish and Fisheries 13, 399–417. https://doi.org/10.1111/j.1467-2979.2011.00436.x

Jirik, K.E., Lowe, C.G., 2012. An elasmobranch maternity ward: female round stingrays *Urobatis halleri* use warm, restored estuarine habitat during gestation. Journal of Fish Biology 80, 1227–1245. https://doi.org/10.1111/j.1095-8649.2011.03208.x

Kraft, S., Gandra, M., Lennox, R.J., Mourier, J., Winkler, A.C., Abecasis, D., 2023a. Residency and space use estimation methods based on passive acoustic telemetry data. Movement Ecology 11, 12. https://doi.org/10.1186/s40462-022-00364-z

Kraft, S., Winkler, A.C., Abecasis, D., 2023b. Small coastal marine protected areas offer recurring, seasonal protection to the common stingray (*Dasyatis pastinaca*). Ocean & Coastal Management 246, 106891. https://doi.org/10.1016/j.ocecoaman.2023.106891

Kraft, S., Winkler, A.C., Abecasis, D., 2024a. Horizontal and vertical movements of the critically endangered *Rostroraja alba* in a coastal marine protected area. Aquatic Conservation: Aquatic Conservation: Marine and Freshwater Ecosystems 34, e4204. https://doi.org/10.1002/aqc.4204

Kraft, S., Winkler, A.C., Abecasis, D., 2024b. Seasonal movement dynamics of the commercially important thornback ray (*Raja clavata*) in a coastal marine protected area. Ocean & Coastal Management 254, 107210. https://doi.org/10.1016/j.ocecoaman.2024.107210

Kraft, S., Winkler, A.C., Abecasis, D., Mourier, J., 2024c. Long-term co-occurrence and gregariousness in the migratory common stingray using network analysis. Marine Biology 171, 176. https://doi.org/10.1007/s00227-024-04498-z

Kramer, D.L., Chapman, M.R., 1999. Implications of fish home range size and relocation for marine reserve function. Environmental Biology of Fishes 55, 65–79. https://doi.org/10.1023/A:1007481206399

Le Port, A., Sippel, T., Montgomery, J.C., 2008. Observations of mesoscale movements in the short-tailed stingray, *Dasyatis brevicaudata* from New Zealand using a novel PSAT tag attachment method Journal of Experimental Marine Biology and Ecology 359, 110–117. https://doi.org/10.1016/j.jembe.2008.02.024

Lea, J.S.E., Humphries, N.E., von Brandis, R.G., Clarke, C.R., Sims, D.W., 2016. Acoustic telemetry and network analysis reveal the space use of multiple reef predators and enhance marine protected area design. Proceedings of the Royal Society B: Biological Sciences 283, 20160717. https://doi.org/10.1098/rspb.2016.0717

Lloret, J., Cowx, I.G., Cabral, H., Castro, M., Font, T., Gonçalves, J.M.S., Gordoa, A., Hoefnagel, E., Matić-Skoko, S., Mikkelsen, E., Morales-Nin, B., Moutopoulos, D.K., Muñoz, M., Dos Santos, M.N., Pintassilgo, P., Pita, C., Stergiou, K.I., Ünal, V., Veiga, P., Erzini, K., 2018. Small-scale coastal fisheries in European Seas are not what they were: Ecological, social and economic changes. Marine Policy 98, 176–186. https://doi.org/10.1016/j.marpol.2016.11.007

MacKeracher, T., Diedrich, A., Simpfendorfer, C.A., 2019. Sharks, rays and marine protected areas: A critical evaluation of current perspectives. Fish and Fisheries 20, 255–267. https://doi.org/10.1111/faf.12337

Martínez-Ramírez, L., Priester, C.R., Sousa, I., Erzini, K., Abecasis, D., 2021. Reserve effect of a small North-East Atlantic marine protected area (Arrábida, Portugal) on soft-sediment fish species. Aquatic Conservation: Marine and Freshwater Ecosystems 31, 1584–1595. https://doi.org/10.1002/aqc.3577

McCook, L.J., Ayling, T., Cappo, M., Choat, J.H., Evans, R.D., De Freitas, D.M., Heupel, M., Hughes, T.P., Jones, G.P., Mapstone, B., Marsh, H., Mills, M., Molloy, F.J., Pitcher, C.R., Pressey, R.L., Russ, G.R., Sutton, S., Sweatman, H., Tobin, R., Wachenfeld, D.R., Williamson, D.H., 2010. Adaptive management of the Great Barrier Reef: A globally significant demonstration of the benefits of networks of marine reserves. Proceedings of the National Academy of Sciences 107, 18278–18285. https://doi.org/10.1073/pnas.0909335107

Mourier, J., Vercelloni, J., Planes, S., 2012. Evidence of social communities in a spatially structured network of a free-ranging shark species. Animal Behaviour 83, 389–401. https://doi.org/10.1016/j.anbehav.2011.11.008

Neves, A., Cabral, H., Sequeira, V., Figueiredo, I., Moura, T., Gordo, L.S., 2009. Distribution patterns and reproduction of the cuttlefish, *Sepia officinalis* in the Sado estuary (Portugal). Journal of the Marine Biological Association UK 89, 579–584. https://doi.org/10.1017/S0025315409002677

Perryman, R.J.Y., Mourier, J., Venables, S.K., Tapilatu, R.F., Setyawan, E., Brown, C., 2022. Reef manta ray social dynamics depend on individual differences in behaviour. Animal Behaviour 191, 43–55. https://doi.org/10.1016/j.anbehav.2022.06.010

Pita, C., Horta E Costa, B., Franco, G., Coelho, R., Sousa, I., Gonçalves, E.J., Gonçalves, J.M.S., Erzini, K., 2020. Fisher's perceptions about a marine protected area over time. Aquaculture and Fisheries 5, 273–281. https://doi.org/10.1016/j.aaf.2020.01.005

Simpfendorfer, C.A., Heupel, M.R., White, W.T., Dulvy, N.K., 2011. The importance of research and public opinion to conservation management of sharks and rays: a synthesis. Marine and Freshwater Research 62, 518. https://doi.org/10.1071/MF11086

Siskey, M.R., Shipley, O.N., Frisk, M.G., 2019. Skating on thin ice: Identifying the need for species-specific data and defined migration ecology of Rajidae spp. Fish and Fisheries 20, 286–302. https://doi.org/10.1111/faf.12340

Small, C., Nicholls, R.J., 2003. A Global Analysis of Human Settlement in Coastal Zones. Journal of Coastal Research 19, 584–599. https://www.jstor.org/stable/4299200

Steckenreuter, A., Hoenner, X., Huveneers, C., Simpfendorfer, C., Buscot, M.J., Tattersall, K., Babcock, R., Heupel, M., Meekan, M., van den Broek, J., McDowall, P., Peddemors, V., Harcourt, R., 2017. Optimising the design of large-scale acoustic telemetry curtains. Marine and Freshwater Research 68, 1403. https://doi.org/10.1071/MF16126

Uusiheikkila, S., Wolter, C., Klefoth, T., Arlinghaus, R., 2008. A behavioral perspective on fishing-induced evolution. Trends in Ecology & Evolution 23, 419–421. https://doi.org/10.1016/j.tree.2008.04.006

van Zinnicq Bergmann, M.P.M., Guttridge, T.L., Smukall, M.J., Adams, V.M., Bond, M.E., Burke, P.J., Fuentes, M.M.P.B., Heinrich, D.D.U., Huveneers, C., Gruber, S.H., Papastamatiou, Y.P., 2022. Using movement models and systematic conservation planning to inform marine protected area design for a multi-species predator community. Biological Conservation 266, 109469. https://doi.org/10.1016/j.biocon.2022.109469

Villegas-Ríos, D., Claudet, J., Freitas, C., Moland, E., Thorbjørnsen, S.H., Alonso-Fernández, A., Olsen, E.M., 2021. Time at risk: Individual spatial behaviour drives effectiveness of marine protected areas and fitness. Biological Conservation 263, 109333. https://doi.org/10.1016/j.biocon.2021.109333

Villegas-Ríos, D., Jacoby, D.M.P., Mourier, J., 2022. Social networks and the conservation of fish. Communications Biology 5, 178. https://doi.org/10.1038/s42003-022-03138-w

Villegas-Ríos, D., Moland, E., Olsen, E.M., 2017. Potential of contemporary evolution to erode fishery benefits from marine reserves. Fish and Fisheries 18, 571–577. https://doi.org/10.1111/faf.12188

Wilson, J.A., Giske, J., 2023. Does fishing dismantle fish culture and ecosystem structure? Questions about the implications of social learning among fish and fishers. Fish and Fisheries 24, 889–895. https://doi.org/10.1111/faf.12755